

NOVEL FUNCTIONS AND PHYSIOLOGICAL SIGNIFICANCE  
OF RAL INTERACTING PROTEIN - RLIP76  
IN *IN VITRO* AND *IN VIVO* MODELS

by

EWA ZAJAC

Presented to the Faculty of the Graduate School of  
The University of Texas at Arlington in Partial Fulfillment  
of the Requirements  
for the Degree of

DOCTOR OF PHILOSOPHY

THE UNIVERSITY OF TEXAS AT ARLINGTON

December 2006

Copyright © by Ewa Zajac 2006

All Rights Reserved

## ACKNOWLEDGEMENTS

I would like to thank my supervising professor Dr. Sanjay Awasthi for his invaluable scientific advice, technical help, and encouragement through my research. He has shaped me into the scientist that I am today.

I would like to thank my committee, Drs. Sanjay Awasthi, Edward Bellion, Frederick MacDonnell, Carl J. Lovely, and Subhrangsu S Mandal, for providing support and advice for this project.

I also thank Dr. Sushma Yadav an excellent investigator who is highly regarded in her field and has been an inspiration to me for years. She was never too busy to explain the nuances of molecular biology and always happy to discuss new ideas and to solve incoming problems.

I was fortunate enough to work with Dr. Sharad Singhal who introduced me to protein chemistry and invested countless hours in my training, always showing me nothing but patience and encouragement. Special thanks go to Mrs. Jyotsana Singhal, tissue culture expert who spent hours teaching me all the techniques required for proper cell line maintenance.

I thank them all for their guidance, patience and expertise.

I would like give my special thanks to my friends Dilki Wikramarachchi, Kenneth Drake and Aalok Nadkar who share with me the badge of honor of being

involved in the Awasthi lab. They have all contributed to my research and will forever be remembered and respected.

I want to thank all the staff of the Chemistry and Biochemistry department for their support and for being the great people they are.

Financial support from National Institute of Health and the University of Texas at Arlington are gratefully acknowledged.

I also owe so much to my family for their support. Especially my husband who always encouraged me to continue my education and has always had faith in me; none of this would have been possible without him.

September 19, 2006

ABSTRACT

NOVEL FUNCTIONS AND PHYSIOLOGICAL SIGNIFICANCE  
OF RAL INTERACTING PROTEIN - RLIP76  
IN *IN VITRO* AND *IN VIVO* MODELS

Publication No. \_\_\_\_\_

Ewa Zajac, PhD.

The University of Texas at Arlington, 2006

Supervising Professor: Sanjay Awasthi

This dissertation is divided into four parts. The first part is an introduction of energy dependent xenobiotic transporters and their relevance in multidrug resistance. However, the main focus is the description of RLIP76 protein, non-ABC transporter, which is the most efficient transporter of glutathione conjugates and anti-cancer drugs.

The second part describes materials and methods that were used in two investigated projects.

The third part explains the correlation of RLIP76 with signaling protein POB1 and an involvement of these two proteins in apoptosis of lung cancer cells. The effect of recombinant POB1 and its deletion mutant POB1<sup>1-512</sup>, on transport activity of RLIP76 towards doxorubicin and dinitrophenyl-glutathione were studied. The results demonstrated that, along with an increased POB1/RLIP76 ratio, the transport of doxorubicin and dinitrophenyl-glutathione by RLIP76 decreased. Incubation of cancer cells with recombinant POB1 led to an arrest of their cell cycle. Augmentation of cellular POB1 caused increasing intracellular doxorubicin accumulation as well as a decreasing rate of doxorubicin efflux from cells. These results showed for the first time that augmented POB1 inhibits RLIP76 transport function, leading to apoptosis of cancer cells through the accumulation of endogenously formed GSH-conjugates.

In the fourth part, it was demonstrated, that RLIP76, through participation in ligand-receptor complex endocytosis, can mediate insulin-resistance. Insulin sensitivity tests demonstrated that administration of increasing doses of recombinant RLIP76 resulted in development of insulin resistance in RLIP76 wild type (WT) mice. Double administration of insulin to RLIP76 knockout (KO) animals caused a dramatic increase of insulin sensitivity. Distribution of hydrocortisone, into RLIP76 KO animals did not have any effect on glucose level. Lack of RLIP76 in KO animals did not change an expression of phosphoenolpyruvate carboxykinase and fructose 1,6-bisphosphatase but specific activities of these enzymes were diminished. Cell culture studies showed that inhibition of RLIP76 resulted in increased glucose uptake, Akt1 phosphorylation,

FOXO1 inactivation, and a reduction of endocytosis of insulin and epidermal growth factor. Augmenting RLIP76 by cell transfection caused an opposite effect. These studies demonstrated that RLIP76 antagonizes the effect of insulin, and link oxidative stress with the mechanisms which function to terminate insulin-signaling through ligand-receptor complexes endocytosis.

## TABLE OF CONTENTS

ACKNOWLEDGEMENTS.....	iii
ABSTRACT.....	v
LIST OF ILLUSTRATIONS.....	xvii
LIST OF TABLES.....	xxiv
Chapter	
1 INTRODUCTION.....	1
1.1 General principle of the detoxification system.....	1
1.2 Biotransformation of xenobiotics.....	2
1.2.1 Phase I of biotransformation.....	3
1.2.2 Phase II of biotransformation.....	5
1.2.3 Phase III of biotransformation.....	9
1.2.3.1 ATP-binding cassette transporters.....	10
1.2.3.1.1 P-Glycoprotein.....	11
1.2.3.1.2 Multidrug resistance associated protein.....	15
1.2.3.1.3 Breast cancer resistance protein (BCRP)....	19
1.2.3.2 Non-ABC transporter family.....	23
1.2.3.2.1 Major vault protein (MVP).....	23
1.2.3.2.2 Ral Interacting Protein 1 (RLIP76).....	27
2 METHODS.....	39
2.1 Preparation of GSH-Sepharose affinity resin.....	39



2.1.1 Materials .....	39
2.1.2 Methods .....	41
2.2 Purification of Glutathione S-Transferases (GSTs) from mouse liver .....	41
2.2.1 Materials .....	42
2.2.2 Methods .....	43
2.3 Glutathione S-Transferases activity assay .....	43
2.3.1 Materials .....	44
2.3.2 Methods .....	44
2.4 Determination of protein concentration .....	45
2.4.1 Materials .....	45
2.4.2 Methods .....	46
2.5 Synthesis of Dinitrophenyl S-Glutathione (DNP-SG) .....	48
2.5.1 Materials .....	48
2.5.2 Methods .....	49
2.6 Preparation of DNP-SG, cyanogen bromide (CNBr) activated sepharose 4B resin .....	50
2.6.1 Materials .....	51
2.6.2 Methods .....	52
2.7 Molecular cloning .....	53
2.7.1 Materials .....	53
2.8 Preparation of competent cells ( <i>E. coli</i> DH5 $\alpha$ ) for plasmid transformation .....	57
2.9 <i>E. coli</i> transformation with prokaryotic expression vector .....	58

2.10 Purification of plasmid DNA from overnight culture of E.Coli DH5 $\alpha$ in LB medium.....	58
2.10.1 Materials .....	58
2.10.2 Methods .....	59
2.11 Restriction endonucleases digestion of DNA.....	60
2.11.1 Materials .....	60
2.11.2 Methods .....	60
2.12 Ligation of fragment DNA into a plasmid .....	61
2.12.1 Materials .....	61
2.12.2 Methods .....	61
2.13 Prokaryotic expression of RLIP76 .....	62
2.14 Bacterial stock preparation.....	64
2.15 Purification of recombinant RLIP76 from <i>E. coli</i> .....	64
2.15.1 Materials .....	64
2.15.2 Methods .....	67
2.16 Sodium Dodecyl Sulfate Polyacrylamide Gel Electrophoresis (SDS-PAGE).....	68
2.16.1 Materials .....	68
2.16.2 Methods .....	70
2.16.3 Sample preparation.....	72
2.16.4 Electrophoresis.....	72
2.16.5 Protein visualization .....	72
2.17 Western blot analysis.....	72

2.17.1 Materials .....	73
2.17.2 Methods .....	74
2.18 Reconstitution of purified recombinant protein into proteoliposomes .....	75
2.18.1 Materials .....	75
2.18.2 Methods .....	76
2.19 Mammalian cell transfection.....	76
2.19.1 Cloning into the eukaryotic expression vectors .....	77
2.19.1.1 pcDNA3.1(+). .....	77
2.19.1.2 Ecdysone inducible vector.....	78
2.19.2 Stable cell transfection.....	80
2.19.2.1 Method.....	80
2.19.3 Transient cell transfection.....	82
2.20 MTT Doxorubicin sensitivity assay .....	82
2.20.1 Materials .....	83
2.20.2 Methods .....	83
2.21 Isolation of RNA by TRIZOL method .....	85
2.21.1 Materials .....	85
2.21.2 Methods .....	86
2.22 Agarose gel electrophoresis of RNA.....	87
2.22.1 Materials .....	87
2.22.2 Methods .....	88
2.23 Reverse transcription polymerase chain reaction (RT-PCR) .....	88

2.23.1 Materials .....	89
2.23.2 Methods .....	90
2.24 Agarose gel electrophoresis of DNA.....	90
2.24.1 Materials .....	91
2.24.2 Methods .....	92
2.25 Prokaryotic expression of POB1 and POB1 <sup>1-512</sup> .....	92
2.25.1 Cloning of POB1 and POB <sup>1-512</sup> into a prokaryotic expression vector pET30a(+)	92
2.26 Purification of recombinant POB1 and POB <sup>1-512</sup> from E.Coli BL21(DE3).....	95
2.26.1 Materials .....	95
2.26.2 Methods .....	97
2.27 Anti-POB1 Immunoglobulin G production.....	98
2.27.1 Materials .....	98
2.27.2 Methods .....	99
2.28 Anti-POB1 antibody purification .....	100
2.28.1 Materials .....	101
2.28.2 Methods .....	102
2.29 Effect of full length POB1 and POB1 <sup>1-512</sup> on cancer cell apoptosis by TUNEL assay.....	103
2.29.1 Materials .....	103
2.29.2 Methods .....	104
2.30 Transport of <sup>14</sup> C-DOX and <sup>3</sup> H-DNP-SG in proteoliposomes reconstituted with RLIP76 along with POB1 and POB1 <sup>1-512</sup> .....	105

2.30.1 Materials .....	105
2.30.2 Methods .....	106
2.31 Effect of POB1-liposomes on <sup>14</sup> C-DOX accumulation in lung cancer cell .....	107
2.31.1 Materials .....	107
2.31.2 Methods .....	107
2.32 <sup>14</sup> C-DOX efflux studies .....	108
2.32.1 Materials .....	108
2.32.2 Methods .....	108
2.33 Genotyping of transgenic mice by PCR method .....	109
2.33.1 Materials .....	109
2.33.2 Methods .....	110
2.34 Quantifying insulin and glucose level in wild type and RLIP76 knockout mice after augmenting RLIP76 level .....	113
2.34.1 Materials .....	113
2.34.2 Methods .....	113
2.35 Quantifying glucose level in wild type and RLIP76 knockout mice after administration hydrocortisone .....	114
2.35.1 Materials .....	114
2.35.2 Methods .....	114
2.36 Effect of anti-RLIP76 IgG on <sup>14</sup> C-glucose uptake by lung cancer cells.....	114
2.36.1 Materials .....	114
2.36.2 Methods .....	115

2.37 EGF binding and internalization assay.....	115
2.37.1 Materials .....	115
2.37.2 Methods .....	116
2.38 Effect of anti-RLIP76 IgG on FITC-conjugated insulin binding and internalization.....	116
2.38.1 Materials .....	116
2.38.2 Methods .....	117
2.39 TransAM FKHR (FOXO1) Assay .....	117
2.39.1 Materials .....	118
2.39.2 Methods .....	119
2.40 Insulin-stimulated phosphorylation of Akt-1 .....	120
2.40.1 Materials .....	120
2.40.2 Methods .....	121
2.41 Phosphoenolpyruvate carboxykinase activity assay.....	122
2.42 Fructose 1,6-bisphosphatase enzyme activity assay.....	123
<b>3 APOPTOSIS OF LUNG CANCER CELLS AS AN EFFECT OF INHIBITION OF RLIP76 ACTIVITY .....</b>	<b>125</b>
3.1 Introduction.....	125
3.2 Results .....	130
3.2.1 Purification of Glutathione-S Transferases from mouse liver.....	130
3.2.2 Synthesis of 2,4-Dinitrophenyl S-Glutathione.....	133
3.2.3 Prokaryotic expression and purification of RLIP76 .....	136

3.2.4 Mammalian transient cell transfection with Partner of RalBP1 (POB1) cloned into pcDNA 3.1 .....	140
3.3 Amplification of pVgRXR and pIND vectors.....	141
3.3.1 Polymerase chain reaction of LacZ.....	145
3.3.2 Co-transfection of pVgRXR stably transfected NSCLC H358 with pIND/LacZ.....	148
3.3.3 Polymerase chain reaction of POB1 .....	149
3.4 Prokaryotic expression and purification of POB1 and POB1 <sup>1-512</sup> .....	153
3.5 Doxorubicin and DNP-SG transport inhibition by POB1 in RLIP76 proteoliposomes.....	156
3.6 DOX sensitivity assay in NSCLC H358 after augmentation of POB1 level.....	158
3.7 Apoptosis of cancer cells as a result of overexpression of POB1 .....	160
3.8 Accumulation and efflux of <sup>14</sup> C-DOX in H358 lung cancer cell treated with POB1.....	161
3.9 Discussion .....	164
4 THE ROLE OF RLIP76 IN A DEVELOPMENT OF INSULIN RESISTANCE .....	166
4.1 Introduction.....	166
4.2 Effect of RLIP76 on insulin and blood glucose level in mice.....	171
4.3 Glucose level in WT and RLIP76 KO animals in response to hydrocortisone.....	184
4.4 Expression and activity of phosphoenol pyruvate carboxykinase and fructose 1,6 bis phosphatase in liver of WT and RLIP76 KO mice.....	186
4.5 Mammalian cell transfection with pcDNA 3.1/RLIP76.....	191
4.5.1 Cloning of RLIP76 into the eukaryotic expression vector pcDNA3.1 .....	192

4.5.2 RT-PCR analysis of RLIP76 mRNA .....	196
4.5.3 Western Blot analysis of RLIP76 expression in cancer cell lines H1618 and H358 .....	197
4.6 RLIP76 antagonizes glucose uptake by cells in culture .....	200
4.7 Insulin signaling of Akt1 and FOXO1 in cancer cell lines .....	203
4.8 Effect of RLIP76 on endocytosis of insulin-insulin receptor and EGF-epidermal growth factor receptor .....	209
4.9 Discussion .....	215
 Appendix	
A. NUCLEOTIDE SEQUENCES OF INVESTIGATED GENES .....	222
REFERENCES .....	232
BIOGRAPHICAL INFORMATION.....	253



## LIST OF ILLUSTRATIONS

### Figure

1.1	Detoxification reactions catalyzed by Oxidase in Phase I of xenobiotcbiotransformation (Yan et al., 2001) .....	3
1.2	Detoxification reactions catalyzed by Monooxygenase in Phase I of xenobiotc biotransformation (Yan et al., 2001) .....	4
1.3	Detoxification reactions catalyzed by Reductase in Phase I xenobioticbiotransformation (Yan et al., 2001) .....	5
1.4	Reaction of electrophilic metabolites with glutathione (Douglas, 1987).....	8
1.5	Mercapturic acid biosynthesis (Hinchman et al., 1994).....	9
1.6	Phylogenetic tree of the ABC transporters involved in cancer MDR (Allen et al., 1999).....	11
1.7	Topology of P-glycoprotein (MDR1), (Higgins et al., 2001) .....	12
1.8	Two-dimensional membrane topology for MRP1 and MRP5, (Borst et al., 2000).....	17
1.9	Membrane topology of ABCG2, (Higgins et al., 2001).....	20
1.10	Structure of vault. ....	25
1.11	RLIP76 signaling pathway .....	34
1.12	Localization of RLIP76 on the cell surface.....	35
1.13	RLIP76 binding domains.....	37
2.1	Synthesis of Dinitrophenyl S-Glutathione (DNP-SG) .....	44
2.2	BSA standard curve.....	47

2.3	Synthesis of dinitrophenyl S- glutathione (DNP-SG) .....	48
2.4	The PCR cycles for RLIP76 amplification.....	63
2.5	pcDNA3.1 vector map (Invitrogen) .....	78
2.6	Maps of pVgRXR and pIND vectors which form the ecdysone inducible system (Invitrogen).....	79
2.7	Temperature cycle profile for RT-PCR.....	90
2.8	Temperature cycle profile for PCR of POB1 and POB <sup>1-512</sup> .....	94
2.9	Agarose gel of DNA samples from RLIP76 KO and WT animals. ....	110
2.10	The PCR cycles for mice genotyping. ....	112
2.11	PCR amplification of a region of the inserted gene. ....	112
3.1	Sequence and domain analysis of RLIP76 by NCI-BLAST against all protein databases (Awasthi et al., 2003).....	126
3.2	Linear map of full length of POB1 (Ikeda et al., 1998). ....	127
3.3	Homogeneity of GSTs purified from mouse liver. ....	133
3.4	DNP-SG absorbance spectrum. ....	135
3.5	Agarose gel electrophoresis of native pET30 a(+) with RLIP76 (A) and digested pET30 a(+) with RLIP76 with BamHI and XhoI restriction enzymes (B).....	137
3.6	Purification of recombinant RLIP76 from <i>E. coli</i> BL21 (DE3).....	138
3.7	RT-PCR analysis of POB1 mRNA isolated from NSCLC H226 (Panel A) and NSCLC H358 (Panel B) transfected with vector pcDNA3.1 containing POB1 gene .....	140
3.8	1% agarose gel electrophoresis of native pVgRXR vector (Panel A) and native pIND vector (Panel B). ....	142
3.9	Nucleotide sequence recognized by EcoRI.....	143

3.10	1% agarose gel electrophoresis of pVgRXR plasmid digested with EcoRI.....	143
3.11	Nucleotide sequence recognized by NheI and XhoI.....	144
3.12	1% agarose gel electrophoresis of pIND plasmid digested with NheI and XhoI. ....	144
3.13	LacZ gene amplified by PCR method .....	146
3.14	1% agarose gel electrophoresis of native pIND/POB1, 7.0 kb band.....	147
3.15	1% agarose gel electrophoresis of pIND/LacZ plasmid digested with NheI and XhoI, where 5.0 kb band represents pIND plasmid and 2.0 kb band represents the LacZ gene. ....	147
3.16	Microscopic image of transient co-transfection of pVgRXR transfected NSCLC H358 cells with pIND/LacZ after $\beta$ -Galactosidase staining. Panel A, B, C demonstrate three different clones. ....	149
3.17	1% agarose gel of pcDNA/POB1 recombinant plasmid, digested with KpnI and XhoI. 5.0 kb band represents a vector, 2.0 kb band POB1 gene. ....	150
3.18	1 % agarose gel of PCR product, POB1 gene, which is represented by 2.0 kb band. ....	151
3.19	1% agarose gel of digested PCR product, POB1 gene, with NheI and XhoI, 2.0 kb band represents POB1 gene. ....	152
3.20	1% Agarose gel of native recombinant plasmid pET30a(+)/POB1 .....	154
3.21	1% Agarose gel of recombinant plasmid pET30a(+)/POB1. ....	154
3.22	SDS-PAGE of Ni-NTA super flow resin purified recombinant POB1.....	155
3.23	Western Blot of purified recombinant POB1 (A) and POB1 <sup>1-512</sup> (B). ....	156
3.24	The transport activity of RLIP76 towards DOX (red symbols) and DNP-SG (blue symbols) measured in artificial liposomes reconstituted with purified recombinant RLIP76 along with varied amount of POB1 (triangles), POB1 <sup>1-512</sup> (square) or bovine-serum albumin (diamond). (Yadav and Zajac 2005) .....	157

3.25	The effect of increased POB1 on DOX-cytotoxicity in NSCLC H358. IC <sub>50</sub> of DOX measured after incubating cells with proteoliposomes containing either POB1 (triangle), POB1 <sup>1-512</sup> (square) or albumin (diamond) (Yadav and Zajac et al., 2005).....	159
3.26	The effect of POB1-overloading on H358 cells apoptosis (TUNEL assay).....	161
3.27	The cellular accumulation of DOX in H358 cells treated with 40 µg/ml control liposomes (diamond), purified rec-POB1 <sup>1-512</sup> liposomes(square), and purified rec-POB1 liposomes (triangle). The values of DOX uptake are presented in terms of pmol/1x 10 <sup>6</sup> cells (Yadav and Zajac et al., 2005).....	162
3.28	The back-added curves of cellular residual DOX vs. time in H358 cells treated with control liposomes (diamond), purified rec-POB1 <sup>1-512</sup> liposomes(square), and purified rec-POB1 liposomes (triangle) and incubated with <sup>14</sup> C-DOX. (Yadav and Zajac et. al., 2005).....	163
4.1	Blood glucose level in wild type (WT) and RLIP76 knockout mice (KO), male and female. ....	172
4.2	Insulin level in RLIP76 wild type (WT) and RLIP76 knockout (KO) mice, male and female.....	172
4.3	Blood glucose level in WT male and female, treated with 200µg and 500µg of RLIP76 encapsulated in liposomes.....	173
4.4	Insulin level in WT male and female, treated with 200µg and 500µg of RLIP76 encapsulated in liposomes.....	173
4.5	Western blot of 100 µg of crude membrane fraction of male liver and heart. ....	175
4.6	Densitometry scans of Western blots of 100 µg of crude membrane fraction of WT male and female liver treated with RLIP76 liposomes. ....	176
4.7	Densitometry scans of Western blots of 100 µg of crude membrane fraction of WT male and female heart, treated with RLIP76 liposomes.....	176
4.8	Blood glucose/Insulin ratio in WT and RLIP76 knockout mice, male and female .....	179

4.9	QUICKI test of insulin resistance in WT and RLIP76 knockout mice, male and female.....	179
4.10	HOMA test of insulin resistance in WT and RLIP76 knockout mice, male and female.....	180
4.11	Blood Glucose/Insulin ratio in WT and RLIP knockout mice, male and female, treated with recombinant RLIP76 delivered in proteoliposomes.....	180
4.12	QUICKI test of insulin resistance in WT and RLIP knockout mice, male and female, treated with recombinant RLIP76 delivered in liposomes.....	181
4.13	HOMA test of insulin resistance in WT and RLIP76 knockout mice, male and female, treated with recombinant RLIP76 delivered in liposomes.....	181
4.14	Blood glucose level in WT and RLIP76 knockout animals after administration of 0.02 U/ml of insulin. ....	183
4.15	Blood glucose level in WT and RLIP76 knockout animals after second administration of 0.02U/ml of insulin. ....	183
4.16	Blood glucose level in WT and RLIP76 knockout animals after IP administration of 30 mg of hydrocortisone .....	185
4.17	Panel A: Western blot of PEPCK WT and KO from crude liver homogenate, Panel B: western blot of FBPase WT and KO from crude liver homogenate. 100 µg of protein was loaded in both cases.....	188
4.18	RT-PCR of PEPCK and FBPase. 2 µg of DNA was loaded to each well.....	189
4.19	Specific activity of phosphoenolpyruvate carboxy kinase and fructose 1.6,- bisphosphatase from WT and RLIP76 KO mice liver. ....	190
4.20	1% agarose gel DNA. Panel A represents native recombinant plasmid pcDNA with RLI76, Panel B represents pcDNA3.1/RLIP76 plasmid digested with BamHI and XhoI .....	193
4.21	Gel electrophoresis of RNA isolated from SCLC H1618 (Panel A) and NSCLC H358 (Panel B) transfected with vector pcDNA3.1	

	alone and vector containing RLIP76 gene (4 stable clones from each cell line were isolated after transfection). .....	195
4.22	RT-PCR results of RLIP76 mRNA isolated from SCLC H1618 (Panel A) and NSCLC H358 (Panel B) transfected with vector pcDNA3.1 alone or vector containing RLIP76 gene (4 stable clones from each cell line were isolated after transfection). .....	196
4.23	Transfection of RLIP76 in SCLC H1618 and NSCLC H358. Western Blot of RLIP76 expression in cancer cell lines H1618 (Panel A) and H358 (Panel B) transfected with pcDNA3.1 alone or pcDNA3.1 containing RLIP76. $\beta$ Actin was used as an internal control (Singhal et al., 2005).....	198
4.24	The graph is a representation of the level of expression of RLIP76 in H1618 cancer cell line after transfection with pcDNA3.1 alone or pcDNA3.1 containing RLIP76 gene. ....	199
4.25	The graph is a representation of the level of expression of RLIP76 in H358 cancer cell line after transfection with pcDNA3.1 alone or pcDNA3.1 containing RLIP76 gene. ....	199
4.26	Effect of anti-RLIP76 IgG and insulin on glucose uptake in SCLC H1618. ....	201
4.27	Effect of anti-RLIP76 IgG and insulin on glucose uptake in NSCLC H358 .....	201
4.28	Effect of anti-RLIP76 IgG and insulin on glucose uptake in hepatoma cells HepG2.....	202
4.29	FOXO1 DNA binding activity in NSCLC H358 .....	206
4.30	FOXO1 DNA binding activity in hepatoma HepG2 cell line .....	206
4.31	FOXO1 DNA binding activity in SCLC H1618 .....	207
4.32	Phospho-Akt1 expression in SCLC H1618.....	207
4.33	Phospho-Akt1 expression in NSCLC H358 .....	208
4.34	Phospho-Akt1 expression in HepG2 hepatoma cell line .....	208

4.35	Effect of RLIP76 on EGF receptor internalization in NSCLC H358.....	210
4.36	Effect of RLIP76 on insulin receptor internalization in NSCLC H358 .....	211
4.37	Effect of RLIP76 on clathrin mediated endocytosis of insulin receptor in MEF WT and MEF KO cells after suppression of EPS15 with siRNA.....	212
4.38	Effect of RLIP76 on clathrin mediated endocytosis of epidermal growth factor receptor in MEF WT and MEF KO cells after suppression of EPS15 with siRNA.....	213

## LIST OF TABLES

### Table

1.1	Cofactors crucial for Phase II of detoxification (Yan et al., 2001) .....	6
1.2	Substrate drugs of P-glycoprotein (Kerb et al., 2001).....	13
1.3	Substrates transported by MRP1 (Deeley et al., 2006) .....	18
1.4	Substrate specificity of RLIP76 .....	28
2.1	GSTs activity assay, composition per 1 ml of reaction mixture.....	45
2.2	Dilution of BSA solutions .....	46
2.3	Absorbance of BSA solutions measured at 595 nm.....	47
2.4	The concentration of antibiotic required to select resistant bacteria transformants .....	56
2.5	Denaturing 12.5% resolving gel solution.....	71
2.6	Denaturing 7% stacking gel solution.....	71
2.7	Conditions for stable cell transfection using Lipofectamine 2000 (Invitrogen).....	81
2.8	Doxorubicin stock solution preparation for IC50 measurments.....	84
2.9	Procedure for anti-POB1 IgG production .....	100
2.10	PEPCK enzyme activity assay, composition of 1ml of reaction mixture.....	123
2.11	PEPCK enzyme activity assay, composition of 1 ml of reaction mixture.....	124
3.1	Purification of GSTs isoenzymes from mouse, male, liver tissue.....	131
3.2	Advanced Reads Report of DNP-SG Absorbance. ....	135
3.3	Purification table of RLIP76 from 300 ml of <i>E. coli</i> culture.....	139



# CHAPTER 1

## INTRODUCTION

### 1.1 General principle of the detoxification system

Cells are constantly exposed to numerous xenobiotics during the course of their lifetime. Many of these compounds may cause damage to proteins, RNA, and DNA within the cell. To defend against xenobiotics, cells have developed several, equally important systems for detoxifying these foreign compounds. This detoxification system is analogous to an intracellular chemical immune system, extensive, highly complex, and influenced by several regulatory mechanisms. It works to diminish the rate of damage from xenobiotics, thus it is necessary for maintaining the normal life span of cells. Xenobiotics are created not only through man-made processes (pharmaceuticals, pesticides, or pollutants) but they also naturally occur naturally as plant metabolites, or toxins produced by molds, plants, and animals. These compounds are divided into two groups: hydrophilic and lipophilic. Hydrophilic toxins are generally not well absorbed in the intestine, but relatively easily in bile or urine. Lipophilic xenobiotics, however, because of the high affinity towards fat, tend to accumulate in the body unless they are converted to hydrophilic or amphiphilic compounds that could be excreted in bile or urine. Most xenobiotics, however, are fat soluble (lipophilic), therefore, the act of detoxification involves making fat soluble substances water soluble.

## 1.2 Biotransformation of xenobiotics

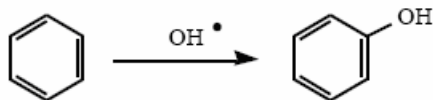
Tecwyn R. Williams was the first to propose that biotransformation of toxins is performed in two stages. In the first, reactions such as oxidation, reduction or hydrolysis take place in order to introduce functional groups such as -OH, -NH<sub>2</sub>, -SH, or -COOH in to the foreign compound. This causes only a small increase in the hydrophilicity of lipophilic toxins. In the second stage of biotransformation, xenobiotic hydrophilicity is largely increased by attaching water-soluble groups to its reactive site. These two step conjugation reactions are termed Phase I and Phase II detoxification, respectively (Williams, 1959). The enzymes involved in xenobiotic biotransformation are widely distributed through the body and are present in a variety of cellular organelles. This distribution differs from tissue to tissue. The highest expression of these enzymes is in the liver, where most of the detoxification processes take place. However, they are also located in the skin, lung, nasal mucosa, eye, and gastrointestinal tract – parts of the body which are major routes of exposure to xenobiotics as well as variety of other organs including kidney, adrenal, pancreas, spleen, heart, brain, testis, ovary, placenta, and aorta (Graham et al., 1980, Krishna et al., 1994). Within a cell, Phase I detoxification enzymes are mainly found in the endoplasmic reticulum (microsomes) or the soluble fraction of the cytoplasm, and with lesser amounts in mitochondria, nuclei and lysosomes. Phase II enzymes, such as glutathione-transferases, are found in both, cytoplasm and microsomal fractions.

### 1.2.1 Phase I of biotransformation

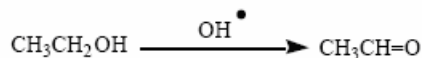
Phase I is the initial enzymatic defense against foreign compounds, where the group of enzymes such as cytochromes P450, epoxide hydrolases, esterases, and amidases activate xenobiotics by introducing or exposing reactive groups (OH, NH<sub>2</sub>, SH, COOH). In Phase I all enzymatic reactions result in only a small augmentation in the hydrophilicity of xenobiotics by performing reactions of hydrolysis, reduction and oxidation using oxygen, NADPH, and NAD<sup>+</sup> as cofactors (Guengerich et al., 1999). Examples of Phase I reactions are shown below (Fig.1.1-1.3).

#### *Oxidase Activity*

- **Aromatic Hydroxylation**



- **Ethanol Oxidation**



- **Catechol Oxidation**

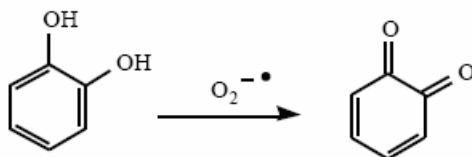
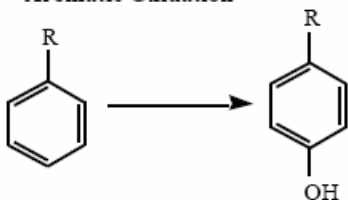


Figure 1.1 Detoxification reactions catalyzed by Oxidase in Phase I of xenobiotcbiotransformation (Yan et al., 2001)

**Monoxygenase Activity (Oxidation)**

- **Aromatic Oxidation**



- **Aliphatic Oxidation**



- **Epoxidation**



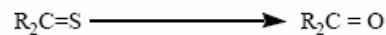
- **N-Oxidation**



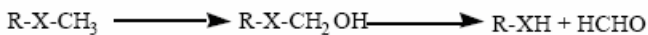
- **S-Oxidation**



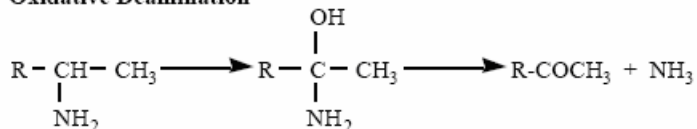
- **Desulfuration**



- **Dealkylation**



- **Oxidative Deamination**



- **N-Hydroxylation**

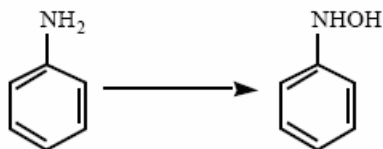
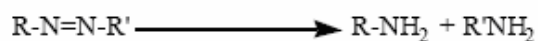


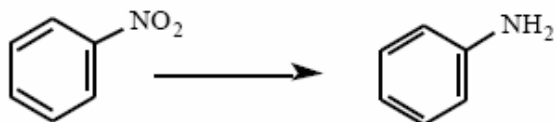
Figure 1.2 Detoxification reactions catalyzed by Monoxygenase in Phase I of xenobiotic biotransformation (Yan et al., 2001)

*Reductase Activity (Reduction)*

- **Azo Reduction**



- **Nitro Reduction**



- **Reductive dehalogenation**

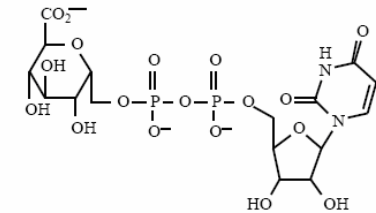
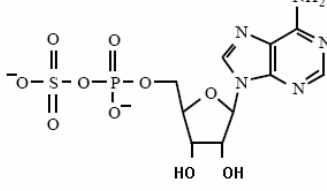
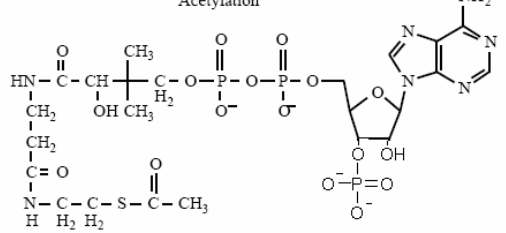
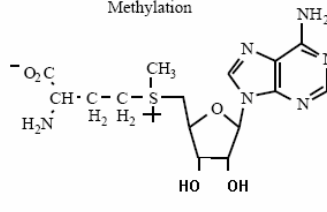
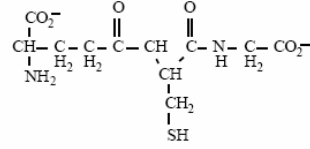
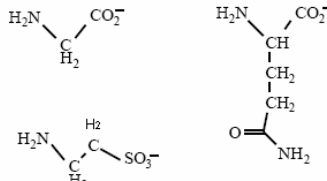


Figure 1.3 Detoxification reactions catalyzed by Reductase in Phase I xenobiotic biotransformation (Yan et al., 2001)

### *1.2.2 Phase II of biotransformation*

Phase II conjugation reactions which generally follow Phase I activation, result in a large increase of xenobiotic hydrophilicity. Phase II enzymatic reactions include glucuronidation, sulfonation, acetylation, methylation, conjugation with glutathione, and conjugation with amino acids (such as glycine, taurine, and glutamic acid) (Paulson et al., 1986). The structures of cofactors for these reactions are shown in Table 1.1.

Table 1.1 Cofactors crucial for Phase II of detoxification (Yan et al., 2001)

<p style="text-align: center;">Glucuronidation</p>  <p style="text-align: center;">Uridine 5'-diphospho-α-D-glucuronic acid (UDP-GA)</p>	<p style="text-align: center;">Sulfation</p>  <p style="text-align: center;">3'-Phosphoadenosine-5'-phosphosulfate (PAPS)</p>
<p style="text-align: center;">Acetylation</p>  <p style="text-align: center;">Acetyl coenzyme A</p>	<p style="text-align: center;">Methylation</p>  <p style="text-align: center;">S-Adenosylmethionine</p>
<p style="text-align: center;">Glutathione Conjugation</p>  <p style="text-align: center;">Glutathione</p>	<p style="text-align: center;">Amino Acid Conjugation</p> 

Phase II enzymes are generally transferases, and are responsible for conjugating a drug or its Phase I metabolites with hydrophilic compounds. The most important of these enzymes are glutathione S-transferases (GST), sulfotransferases (ST), N-acetyl transferases (NAT), and UDP-glycosyltransferases (UDPGT) (Dalhoff et al., 2005). Among all these enzymes glutathione S-transferases have become the most extensively studied because of their cellular abundance and high concentration of their substrate glutathione, within a cell (~ 2-5 mM). The GST family consists of numerous isoenzymes, which can constitute up to 10% of the cytosolic proteins in some mammalian organs (Boyer, 1989; Hayes et al., 1995). Mammalian GSTs have been

subdivided into eight classes (alpha, mu, pi, theta, sigma, omega, kappa and epsilon) based on chemical and physical properties, sequence homologies, and subunit assembly patterns. Individual classes of GSTs assemble in homo- or hetero-dimeric combinations, and exhibit overlapping but distinct substrate and ligand-binding specificities. Genetic polymorphisms of mammalian GSTs have been correlated with individual variations in susceptibility to carcinogenesis and to differences in response to drugs (McIlwain et al., 2006; Hayes et al., 2005).

GSTs catalyze the conjugation reaction of reduced glutathione (Fig 1.4) to electrophilic centers on a wide variety of substrates such as 1,2-dichloro-4-nitrobenzene, 1-chloro-2,4-dinitrobenzene, 4-nitropyridine-N-oxide, p-nitrobenzyl chloride, and 1,2-naphthalene oxide (Habig et al., 1974). Moreover, the activity of GST towards electrophiles is useful in the detoxification of endogenous compounds, such as oxidized membrane lipids, created during oxidative stress, as well as the metabolism of xenobiotics (Hayes et al., 1995).

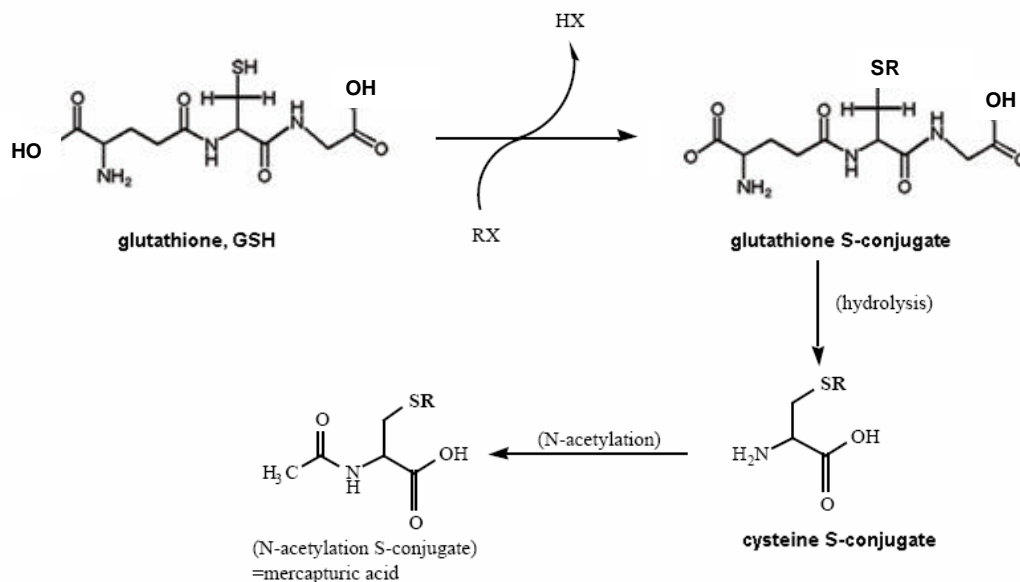


Figure 1.4 Reaction of electrophilic metabolites with glutathione (Douglas, 1987)

The glutathione S-conjugates thus formed are transported out of cells for further metabolism by gamma-glutamyltransferase and dipeptidases, ectoproteins that catalyze the sequential removal of the glutamyl and glycyl moieties, to form the cysteinyl glycine and cysteine S-conjugates respectively (Hinchman et al., 1994), followed by transport of the cysteine S-conjugate back into the cells. Mercapturic acid is formed by acetylation of these conjugates in the reaction, catalyzed by intracellular N-acetyltransferases. (Hinchman et al., 1991). Mercapturic acid is then released into the bloodstream and transported to the kidney for excretion in urine. (Fig 1.5).



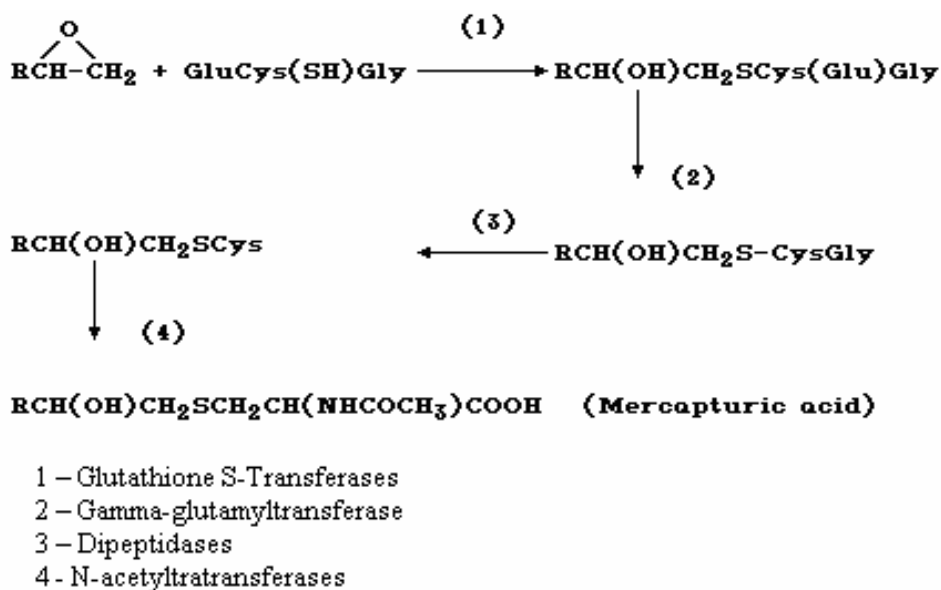


Figure 1.5 Mercapturic acid biosynthesis (Hinchman et al., 1994)

Accumulation of glutathione conjugates within cells causes an inhibition of the enzymes responsible for biotransformation; which lead to the cell death. Therefore, the cell has evolved a transport mechanism for the exclusion of these toxic metabolites from the cellular environment. The transport mechanisms involved in the efflux of these compounds have been designated as Phase III of the detoxification processes (Ishikawa, 1992).

### 1.2.3 Phase III of biotransformation

Since the discovery of proteins involved in multidrug resistance, Phase III of detoxification has attracted a great deal of interest. The question of how the body can handle such wide range of xenobiotics and their conjugates has led to considerable

study in an attempt to understand the role of transporter proteins in a biotransformants cellular efflux.

In eukaryotes and prokaryotes, two major classes of proteins involved in plasma membrane trafficking of xenobiotics are distinguished on the basis of their sequence homology, molecular mechanism and structure: (1) ATP-binding cassette (ABC) transporters (Allikments et al., 1996) and (2) non-ABC transporters. These efflux pumps require energy from ATP hydrolysis in order to transport toxins from the cellular environment against a substrate concentration gradient.

#### 1.2.3.1 ATP-binding cassette transporters

The ATP-binding cassette (ABC) transporters represent one of the largest families of trafficking proteins in living organisms (Dean et al., 2005; Sharma et al., 2003; Gottesman et al., 2001). The recent annotation of the human genome sequence revealed 48 genes for ABC transporters (Dean et al., 2001; Szakács et al., 2004). Some ABC proteins facilitate the transport of inorganic ions, whereas others pump various organic compounds like peptides, sugars, lipids, chemotherapeutic agents and their metabolites across the cell membrane using ATP as an energy source (Higgins, 2001; Kipp et al., 2002; Leslie et al., 2001). Mutations in ABC transporters' genes have been linked to several human diseases, including cystic fibrosis, persistent hyperinsulinemic hypoglycemia of infancy, the Dubin-Johnson syndrome, Stargardt's disease, and Tangier disease (Higgins, 2001; Ambudkar et al., 2006). The transport activity of ABC proteins plays an important role in chemotherapy, by modulating the absorption, distribution and excretion of numerous anticancer agents. Clinical studies have shown

that the multi-drug resistance phenotype in tumors is frequently associated with the over-expression of certain ABC transporters, termed MDR proteins (Ejendal et al., 2002). These mechanisms present a major limitation to cancer chemotherapeutic efficiency. Cells which over-expressed MDR proteins also frequently exhibit additional properties, including genome instability and loss of checkpoint control, which complicate further therapy. Three ABC genes appear to account for nearly all of the MDR tumor cells in both human and rodent cells. These are ABCB1 (PGP/MDR1), ABCC1 (MRP1), and ABCG2 (MXR/BCRP) (Allen et al, 1999). The phylogenetic tree of the ABC transporters involved in cancer MDR is presented in Figure 1.6.

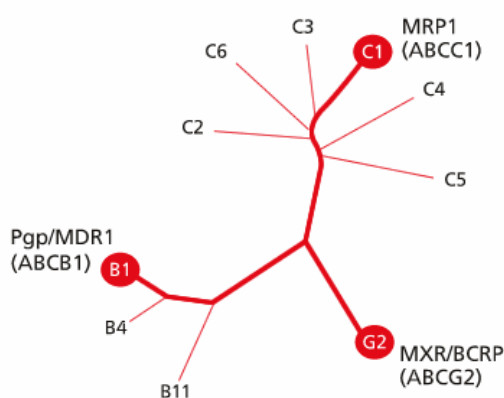


Figure 1.6 Phylogenetic tree of the ABC transporters involved in cancer MDR (Allen et al., 1999)

#### 1.2.3.1.1 P-Glycoprotein

The P-glycoprotein (Pgp, MDR1, ABCB1) mediated multi-drug resistance was first discovered in Chinese hamster ovary cell line (Juliano et al., 1976). This 170 kDa protein has two trans-membrane domains, each containing six trans-membrane

segments and two ATP binding sites (NBD- nucleotide binding domain), which includes the highly conserved Walker A and B motifs, the ABC signature domain and the Q, D, and H loops (Fig 1.7) (Holland et al., 1999; Borst et al., 2002; Higgins et al., 2001).

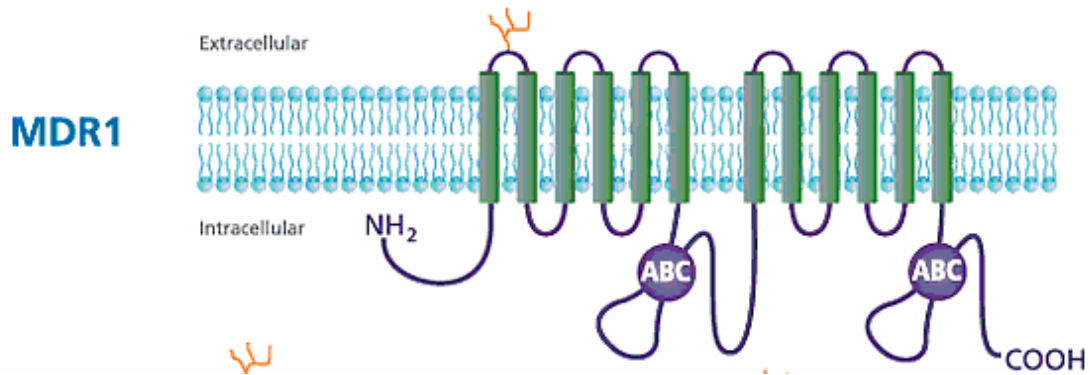


Figure 1.7 Topology of P-glycoprotein (MDR1), (Higgins et al., 2001)

Besides the over-expression of Pgp in cancer cells, this protein is naturally present at varying levels in several mammalian tissues, including renal epithelium, intestinal epithelium, liver, vascular endothelium of brain, testis, and placenta, pancreatic ductules, biliary canaliculi, adrenal cortex, and bone marrow stem cells, where they serve to provide a natural barrier against toxins (Thiebaut et al., 1987; Gottesman et al., 1996). It has been shown that Pgp knockout mice, lacking functional *mdr* genes, appear to have two defects: first, the rate of transport of P-glycoprotein substrates into bile and urine is diminished in liver and kidney, and second, increased accumulation of certain drugs (vinblastine, ivermectin, cyclosporin A, dexamethasone, and digoxin) in the brain, testis, ovaries and adrenal gland compared with wild-type mice. (Schinkel et al., 1995). This finding indicates that P-glycoprotein prevents

cytotoxic compounds from entering the most important organs in the body and eliminates them by secretion into a bile and urine. Even though the crystal structure of Pgp is known, the mechanism by which MDR1 pumps drugs has been difficult to explain because of a variety of Pgp substrates which can simultaneously bind to the different regions of the protein (Table 1.2).

Table 1.2 Substrate drugs of P-glycoprotein (Kerb et al., 2001)

<b>Category</b>	<b>Drug</b>
Anti-cancer drugs	daunorubicin, doxorubicin, doxetaxel, irinotecan, mitomycin C, mitoxantrone, paclitaxel, tamoxifen, tenoposide, topotecan, vinblastine, vincristine
Antibiotics	cefazolin, cefoperazon, erythromycin, levofloxacin
Antiemetics	domperidon,
Cardiac drugs	amiodaron, digitoxin, digoxin, propafenon, quinidine,
Calcium channels blockers	diltiazem, mibefradil, nicardipine, verapamil,
Others $\beta$ -blockers	losartan, bunitrolol, celiprolol, talinolol
CNS drugs	perphenazin, phenoxazine, phenytoin
Antihistamine	fexofenadine, terfenadine, cimetidine, ranitidine
HIV Protease inhibitor	amprenavir, indinavir, nelfinavir, ritonavir
Immuno-supressant	cyclosporin, tacrolimus
Lipid-lowering drug	atorvastatin, simvastatin
Morphins	morphine, loperamide
Steroids	aldosterone, dexamethasone, hydrocortisone

Methods including immunological characterization (Bruggemann et al., 1989; Bruggemann et al., 1992), site-directed mutagenesis (Ambudkar et al., 1999), photoaffinity labeling (Sauna et al., 2001), chemical cross-linking (Pleban et al., 2005),

and MALDI-MS (Ecker et al., 2002) have been used to localize the drug –interacting regions of Pgp. Several groups (Loo et al., 2001a; Lugo et al., 2005; Sauna et al., 2004) have proposed a drug binding domain of P-glycoprotein located in the trans-membrane, cysteine-rich domain, shaped like a funnel, with the narrow ending facing the cytoplasmic side. The funnel has been called the drug binding pocket because it is large enough to accommodate at least two and possibly several different substrates at the same time. Although, the structure of Pgp seems to be resolved, the suggested mechanisms of drug transportation through the membrane remain controversial. Currently there are two competing models for the mechanism of transport by Pgp. In the first model the drug binds to a high affinity binding site in the trans membrane domain of P-glycoprotein reducing the activation energy needed for ATP binding and increasing the affinity for ATP simultaneously (Higgins et al., 2004). This causes a dimerization of the two nucleotide binding domains (NBDs) with two ATPs strongly attached to the NBDs interface. This dimerization leads to conformational changes of the protein which forces the drug to move to a low affinity extracellular location from where it is released. Then, the ATPs, undergo hydrolysis one by one which provides enough energy to rupture the nucleotide dimer-ATP sandwich and to reset the Pgp to its ground state.

In the second model, both a drug and ATP bind to the drug binding domain and NBDs respectively (Sauna et al., 2001). Next, one ATP undergoes hydrolysis which causes the change in protein conformation, lowering the affinity towards the drug, and leading to the release of the drug. At this stage, the phosphate group is discharged and

ADP makes the NBDs accessible to ATP, however, but the drug binding site maintains the low-affinity conformation which prevents binding of drug-substrate molecules. Then, the second hydrolysis of ATP takes place, providing energy to return Pgp to ground state where it can again bind both a nucleotide and a drug.

The development of a single model of Pgp transport mechanism to resolve the disparate proposals remains a challenge and may be resolved by structural studies of Pgp at various stages of the catalytic cycle.

#### 1.2.3.1.2 Multidrug resistance associated protein

In 1992, a second type of drug pump in MDR cancer cells, the multidrug resistance associated protein (MRP) was discovered (Cole et al., 1992). This C subfamily of the ABC family consists of 13 characterized members (MRP1 through MRP13, also named ABCC1 through ABCC13, respectively) (Borst et al., 2000). However, among all MRP proteins MRP1 is the most studied and several substrates and inhibitors for this protein have been identified. The protein is expressed in most tissues, including kidney, liver, placenta, testis, pancreas, breast, ovary, intestine, lungs, and prostate (Gottesman et al., 2002). Depending on the tissue type, this 190 kDa protein is located in either the plasma or intracellular membranes (Kruh et al., 1995; Kuwano et al., 1999; Nies et al., 2004). Like Pgp1, MRP utilizes energy from ATP hydrolysis to transport a wide variety of structurally and functionally unrelated compounds across the plasma membrane. The natural function of MRP is protection of cells against toxins. However, over-expression of the protein leads to resistance of anticancer drugs, including anthracyclines, plant alkaloids and antifolates because the protein transports

them out of cells. It has been shown that mutations in few genes encoding ABCC cause major pathological conditions in humans with varying severity. Hence, mutations in MRP2 (ABCC2) cause a mild conjugated hyperbilirubinemia, known as Dubin-Johnson Syndrome (Machida et al., 2005; Mor-Cohen et al., 2001), mutations in ABCC6 (PXE, MRP6) are responsible for a connective tissue disorder known as pseudoxanthoma elasticum (Schulz et al., 2005; Hu et al., 2004), mutations in ABCC7, the cAMP-regulated cystic fibrosis transmembrane conductance regulator (CFTR), cause cystic fibrosis (Feldmann et al., 2001; Audrezet et al., 2004; McGinniss et al., 2005); and mutations in the sulfonylurea receptor SUR1 (ABCC8), which regulates the K<sup>+</sup> channel Kir6.2, cause persistent hyperinsulinemic hypoglycemia of infancy (PHHI) (Darendeliler et al., 2002). MRP1 is a 190 kDa ATP transporter present in either the plasma or intracellular membranes (Kuwano et al., 1999; Nies et al., 2004). Both sequence analyses and biochemical studies predict that the core structures of MRP4, MRP5, and MRP8 consist of two nucleotide-binding domains located between a membrane spanning domain. Each membrane spanning domain consists of six trans membrane segments. The two ATP binding domains are situated on the cytosolic face of the membrane (Haimeur et al., 2004). Five members of the ABCC family (MRP1, as well as MRPs 2, 3, 6, and 7) are characterized by a three membrane-bound domains. These include two trans membrane domains containing six transmembrane subunits and an additional N-terminal polypeptide region of about 280 amino acids, forming a membrane-bound domain (TMD<sub>0</sub>), which consists of five transmembrane subunits and a cytoplasmic loop, L<sub>0</sub>. TMD<sub>0</sub> is not found in MRP5 (Bakos et al., 1998) (Fig 1.8).



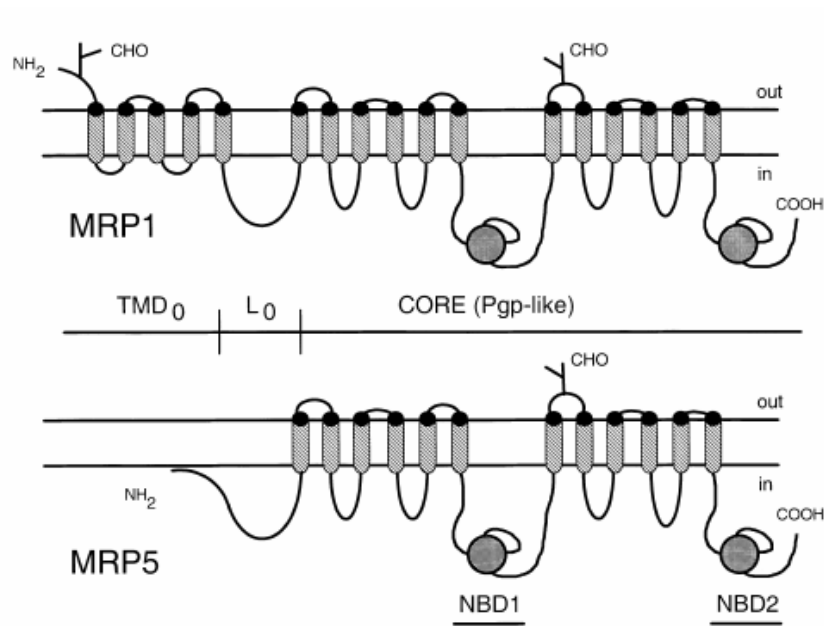


Figure 1.8 Two-dimensional membrane topology for MRP1 and MRP5, (Borst et al., 2000)

Unlike Pgp, which has a low affinity for anionic compounds, preferred substrates for MRP1 are organic anions, such as drugs conjugated to glucuronate, sulfate or glutathione (GSH), as well as the GSH conjugates leukotriene C<sub>4</sub> (LTC<sub>4</sub>) and prostaglandin A<sub>2</sub> (Jedlitschky et al., 1996; Evers et al., 1997; Leier et al., 1996). Hence, MRP1 functions as a glutathione-conjugate efflux pump, exporting xenobiotics including chemotherapeutic drugs from cancer cells after conjugation with glutathione (Leier et al., 1994; Muller et al., 1994). In addition, GSH appears necessary for keeping the MRP1 structure in an active conformational state in order for it to transport unmodified drugs such as vincristine and daunorubicin (Renes et al., 1999; Loe et al., 1998; Broxterman et al., 1996). The table below (Table 1.3) summarizes the current knowledge of the substrate specificity of MRP1.

Table 1.3 Substrates transported by MRP1 (Deeley et al., 2006)

Category	Class	Examples
Drugs /Xenobiotics/	Antineoplastics	methotrexate, eadtrexate, doxorubicin, epitubicin, daunorubicin, vincristin, vinblastine, etoposide
	Antivirals	saquinavir, ritonavir
	Antibiotics	difloxacin, grepafloxacin
	Metalloids	sodium arsenite, sodium arsenate, potassium antimonite
	Fluorescent probes	calcein, fluo-3
	Toxicants	aflatoxinB1, methoxychlor, chlorpropham
Drug/Xenobiotic conjugates	GSH conjugates	2,4-dinitrophenyl-SG, bimane-SG
	Glucuronide conjugates	etoposide-Gluc
Naturally occur metabolites	GSH conjugates	leukotriene C4, prostaglandin A2-SG, hydroxynonenal-SG
	Glucuronide conjugates	17 $\beta$ -estradiol-17- $\beta$ -D-gluc, glucuronosylbilirubin
	Folates	folic acid, L-leucovorin
	Peptides	GSH, GSSG

The position of a substrate binding site in MRP1 depends on the substrate structure and function. Several methods were used in order to identify regions responsible for binding, such as site directed mutagenesis, UV cross linking studies with photoactivated substrates and other ligands, partial proteolysis, and MALDI-TOF. In general, the major sites appear to involve the 10<sup>th</sup> and 11<sup>th</sup> trans membrane helices,

located on MSD1 and the 16<sup>th</sup> and 17<sup>th</sup> transmembrane helices located on MSD2 (Ito et al., 2001; Campbell et al., 2004; Ren et al., 2003; Koike et al., 2002; Situ et al. 2004; Zhang et al., 2002).

The general transport mechanism of MRP proteins has been summarized by Deleey (Deleey et al., 2006). First, the substrate binds to a high affinity site on the cytosolic side of the membrane. Next, this substrate binding site is reoriented to the extracellular region of the membrane where the binding affinity is diminished so that the substrate may be released. The last step of the mechanism is the return of the binding site to its initial high affinity state. Nonetheless, the detailed transport mechanism of MRP1 has not yet been established.

#### 1.2.3.1.3 Breast cancer resistance protein (BCRP)

The alternative drug transporter which belongs to ABCG subfamily of the ABC family, is a breast cancer resistance protein (BCRP) known as ABCG2, a half transporter that confers resistance to several anti-cancer drugs such as doxorubicin and daunorubicin (Doyle et al., 1998), mitoxantrone (Miyake et al., 1999; Hazlehurst et al., 1999; Kawabata et al., 2001), irinotecan (Maliepaard et al., 1999) and topotecan (Yang et al., 2000; Honjo et al., 2001). BCRP was first identified and isolated from breast cancer cell line by Doyle (Doyle et al., 1998). This 663 amino acid, 72 kDa protein exhibits an ATP dependent efflux of anthracyclines from the intracellular matrix.

The G subfamily has a reverse domain arrangement as compared with other ABC efflux pumps. Its nucleotide binding side is located toward the N terminus of the polypeptide

chain (Krishnamurthy et al., 2006). There is only one transmembrane domain which contains six transmembrane segments (Fig 1.9).

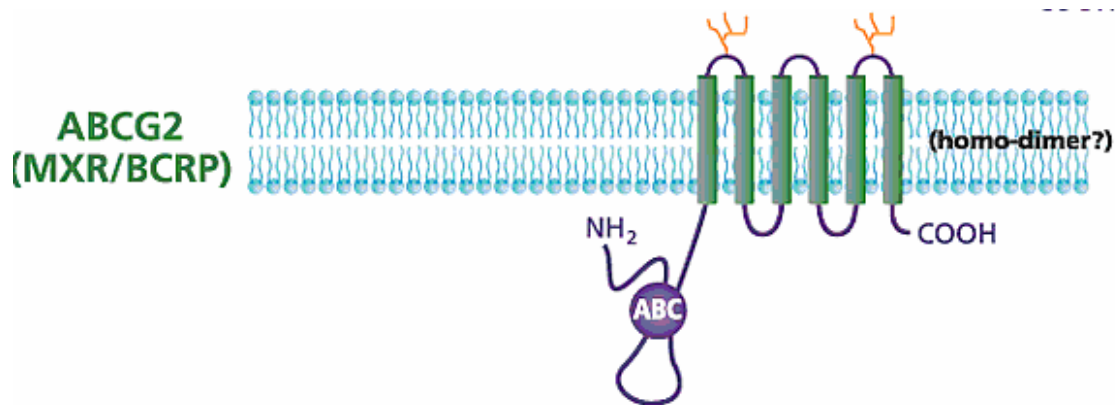


Figure 1.9 Membrane topology of ABCG2, (Higgins et al., 2001)

Immunohistochemical and confocal microscopy studies have demonstrated that ABCG2 is mainly present in the plasma membrane rather than in a membrane of subcellular organelle like mitochondrion, endoplasmic reticulum, or peroxisome. So far, 4 genes encoding human members of the G subfamily, ABCG1, ABCG2, ABCG5, and ABCG8, have been identified (Qingcheng et al., 2005). ABCG1 is involved in regulation of cellular lipid homeostasis in macrophages through facilitating efflux of cellular lipids including cholesterol and phospholipids (Klucken et al., 2000). ABCG5 and ABCG8 have also been shown to efflux cholesterol and plant sterols (Yu et al., 2004; Graf et al., 2003; Yu et al., 2002). ABCG5 and ABCG8 are highly expressed in the apical membranes of the small intestine and the canalicular membranes in the liver. They are involved in lipid transportation by regulating the absorption of dietary sterols

(Qingcheng' et al., 2005). There is increasing evidence to suggest that ABCG proteins may operate as either homodimers or heterodimers (Graf et al., 2003).

Recent studies have shown that ABCG2 is expressed in heart, lung, skeletal muscle, kidney, pancreas, spleen, thymus, brain, and placenta (Doyle et al., 2003) and it functions as a xenobiotic transporter preventing the accumulation of toxins in cells. In addition, the protein is highly expressed in hematopoietic stem cells, which gives it a unique function to maintain progenitor cells in an undifferentiated state (Schuetz et al., 2001). This discovery was explained by suggesting that ABCG2 causes the efflux of substances important not only for differentiation, but also for growth or survival of stem cells. BCRP expression has also been observed in stem cells from a variety of other tissues such as the interstitial spaces of mammalian skeletal muscle (Tamaki et al., 2002), human pancreas islets (Lechner et al., 2002), the human liver (Shimano et al., 2003) and the developing and adult heart (Martin et al., 2004). Hence, BCRP is a natural determinant of the SP phenotype and can be used as a marker for selection of stem cells.

Several studies have also demonstrated that BCRP protein and its mRNA have been present in numerous types of human cancers, including lymphoblastic leukemia, acute myeloid leukemia, melanoma, carcinomas of the digestive tract, osteosarcomas of the bladder, neuroblastomas, small and non small cell lung cancer (Krishnamurthy et al., 2006). Functional characterization of BCRP has demonstrated that it can transport a wide range of substrates ranging from chemotherapeutic agents to organic anion conjugates. Some of them overlap with substrates for Pgp and MRP1 (daunomycin,

daunorubicin, epirubicin, etoposide, imatinib, topotecan) but the majority are specific only for ABCG2 (bisantrone, diflomotecan, 9-aminocamptothecin, flavopiridol, irinotecan, mitoxantrone, quinazoline, teniposide, lamivudine, zidovudine) (Krishnamurthy et al., 2006). This protein recognizes differences in substrate structure; for instance, when one of the nucleophilic groups of camptothecin was exchanged to the more polar substituent (amino group for nitro group), the accumulation of the drug inside the cell was reduced (Yoshikawa et al., 2004).

At the present time, the mechanism by which BCRP transports drugs is still poorly understood. Recent mutational analyses have begun to address the importance of certain amino acids associated with a plasma membrane in determining substrate selectivity by BCRP. However, additional studies are necessary for a clear understanding of the molecular mechanism of this important drug transporter.

Significant progress has been made since discovery of p-glycoprotein in 1976 by Juliano and Ling (Juliano and Ling, 1976) in understanding the function and structure of ABC transporters in both prokaryotes and eukaryotes. The largest attractions for scientists are ABC transporters which are involved in multidrug resistance in human tumor chemotherapy, like Pgp, BCRP and MRP1, whereas little is known about the function of ABC transporters in other families, like those in ABCE and ABCF family.

In addition to the association of ABC transporters with multidrug resistance, most of ABC transporters studied thus far in humans are connected with various severe, genetic disorders such as Dubin-Johnson syndrome (DJS), Zellweger syndrome, Cystic

Fibrosis (CF), Persistent Hyperinsulinemic Hypoglycemia of Infancy (PHHI) (Higgins et al., 2001; Ambudkar et al., 2006).

It has been shown that ABC transporters are commonly duplicated locally and arranged as a dimer in order to functionally complement each other. They may also work as functional redundancy to make sure that cells stay alive during adverse circumstances when some of ABC transporters cannot work well.

Apparently, all ABC proteins will be identified with the completion of the Human Genome Project. However, the determination of corresponding function to them will be very difficult and time consuming because of the broad substrate specificity of some ABC transporters and existence of local duplicates which may have comparable functions.

#### 1.2.3.2 Non-ABC transporter family

Another group of proteins which are also involved in multidrug resistance are non-ABC transporters. These proteins do not have structural elements typical for ABC transporters, such as trans membrane domains, each containing six subunits and characteristic cytoplasmic nucleotide binding sites called Walker motifs. However, they have the required structure and specific domains which allow these proteins to transport toxins, peptides, and chemotherapeutic agents from the cells, keeping them alive (Awasthi et al., 2003; Sharma et al., 2003).

##### 1.2.3.2.1 Major vault protein (MVP)

The first non-ABC transporter known as major vault protein (MVP) or lung resistance associated protein (LRP), was discovered in 1993 by R. J. Scheper (Scheper

et al., 1993) in non - small cell lung cancer cell line selected for doxorubicin resistance but did not express P-glycoprotein. Studies in humans have shown that the expression of MVP is tissue-dependent. LRP is distributed in both normal and cancer cells with different patterns. It is highly expressed in normal tissues such as bronchus, digestive tract, renal proximal tubules, keratinocytes, macrophages, and adrenal cortex. In addition, LRP was detected in many cancer cell lines but its expression depended on the exposure of these cells to xenobiotics. For example, low levels of LRP were seen in testicular cancer, neuroblastoma, chronic myeloid leukemia (CML), and acute myeloid leukemia. Intermediate levels were seen in ovarian cancer and melanoma, and high levels occurred in colon, renal, and pancreatic carcinomas, epithelial, gastrointestinal, and lung cells (Izquierdo et al., 1995; Schadendorf et al., 1995; List et al., 1996; Dingemans et al., 1996; Shimamoto et al., 2006) In these cell lines, the expression of LRP was associated with intrinsic resistance to doxorubicin,, mitoxantrone, etoposide and cis-platinum (II) diamine dichloride.

MVP/LRP is a 110 kDa protein which contributes 70% to the composition of vaults (Scheffer et al., 1995). Vaults are large ribonucleoprotein particles, originally identified in preparations of clathrin coated vesicles (Kedersha N L., et al., 1986), Rome Let al., 1991, Kickhoefer, VA., et al., 1996). Vaults are composed in majority with MVP and in minority with two high-molecular weight proteins 240 kDa telomerase-associated protein 1 and 193 kDa poly(ADP-ribose) polymerase which surrounds a small 140 nucleotides RNA molecules. These structures are arranged into a typical hollow, barrel-like organelle with a waist and two overhanging caps (Fig 1.10).



Vaults are broadly distributed throughout diverse eukaryotic species, ranging from humans to *Dictyostelium discoideum*, and their morphology is highly conserved among them (Kedersha et al., 1990). About 5% of vaults are associated with the nuclear membrane and nuclear pore complex, but the majority of them are located in the cytoplasm where they are associated with cytoskeletal elements (Van Zon et al., 2003).

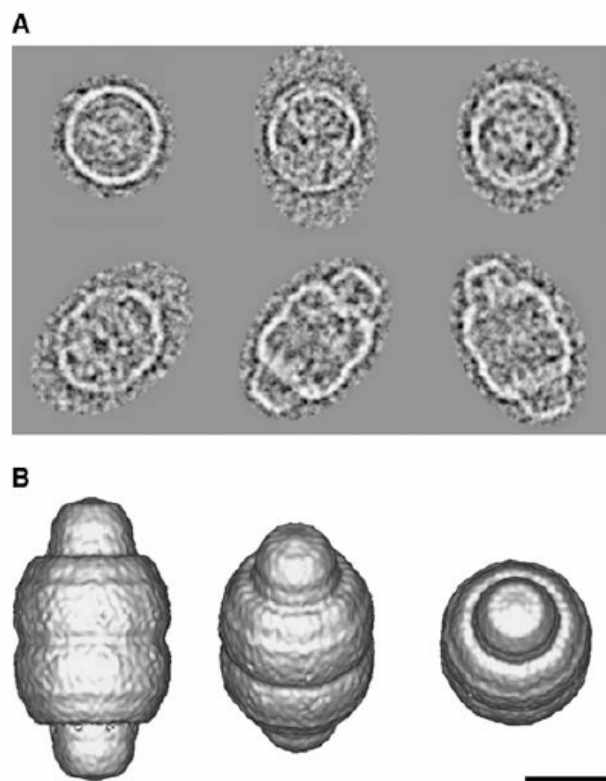


Figure 1.10 Structure of vault.

A Cryoelectron microscopy images showing individual vault particles in different orientation.

B Three-dimensional model of the vault complex. Bar correspondes to 100Å. (Kong et al., 1999)

In addition to resistance to chemotherapeutic agents, it has been shown by Shimamoto that MVP level is elevated after treatment with UV radiation. These

findings suggested that DNA damage caused by UV radiation enhances MVP promoter activity which leads to a considerable increase in the level of MVP (Shimamoto et al., 2006). Other investigators have shown that vaults are very sensitive to low temperature. Incubation at 21 °C for one hour resulted in the formation of distinct tube-like structures in the cytoplasm. Raising the temperature up to 37 °C reverses this process (Van Zon et al., 2003), but, at present, the function of these vault tubes remains unknown.

In contrast to the previous published results, two independent groups of investigators have shown that LRP did not participate in chemoresistance in non-small cell lung carcinoma cells. It is over-expressed after exposure to doxorubicin but it does not contribute to its transport from the nucleus. Redistribution of doxorubicin from the nucleus into distinct vesicular structures in the cytoplasm was not accompanied by changes in the intracellular localization of vaults. These results indicate that vaults are not directly involved in the sequestration of anthracyclines in vesicles or in their efflux from the nucleus (Van Zon et al., 2004; Huffman et al., 2005). These data suggest the need for further study in order to link regulation of vaults and malignancy.

The wide distribution of vaults in the eukaryotic cells and their remarkable structure conservation suggest an important function in cellular activities. However, no specific function has been assigned to these complexes. Transport of anticancer agents carried out by vaults is questionable. It has been suggested that vault might support the protein folding or protein complex assembly and that this assistance becomes important when cells are challenged by adverse changes in their environment (Shimamoto et al., 2006; Steiner et al., 2006).

#### 1.2.3.2.2 Ral Interacting Protein 1 (RLIP76)

The second distinct member of the ABC transporters was discovered by Yogesh Awasthi's lab as a dinitrophenyl S-glutathione (DNP-SG) ATPase (LaBelle et al., 1988). This protein was identified and purified from human erythrocyte membrane as a glutathione conjugate binding ATPase. Subsequently, stimulation of ATPase activity was demonstrated for other compounds including those which are also substrates for ABC transporters (La Belle et al., 1988; Awasthi et al., 1994, 1998a, 1998b; Sharma et al., 1990; Singhal et al., 1991; Awasthi et al., 2000; Awasthi et al., 2003 I, II, III; Stuckler et al., 2004). Cloning of DNP-SG ATPase was accomplished using an antibody against purified protein (Awasthi et al., 2000). Immuno-screening of human bone marrow cDNA library  $\lambda$ gt11 led to the demonstration of identity of DNP-SG ATPase to a protein previously described as Ral Interacting Protein 76 (RLIP76) (Jullien-Flores et al., 1995), known also as Ral Binding Protein 1 (RalBP1) (Cantor S., et al., 1995) or RIP1 (Park S.H., et al., 1995) which corresponds to human, rat or mouse orthologs, respectively (Awasthi et al., 2000). The recombinant protein could be purified to the parent homogenate by the same DNP-SG affinity method used to initially purify DNP-SG ATPase. Immunological identity of DNP-SG ATPase and RLIP76 was also established (Awasthi et al., 2000). Reconstitution of this recombinant protein in artificial liposomes was the unique opportunity to study the transport kinetics and properties in a completely isolated system (Awasthi et al., 2000; Awasthi et al., 2001; Yadav et al., 2004). The filtration method used for transport studies in artificial liposomes yielded high precision and accuracy (Awasthi et al., 1994; 2000; 2001a).

A large number of substrates has been studied in the isolated system to yield an unquestionable proof of RLIP76 transport properties (Table 1.4).

Table 1.4 Substrate specificity of RLIP76

<b>Class</b>	<b>Example</b>
Drugs/xenobiotics	doxorubicin, doxorubicinone, dihydrodoxorubicinone, dihydrodoxorubicin
Glutathione conjugates	S-(methyl)glutathione, S-(n-propyl) glutathione, S-(n-pentyl)glutathione, S-(n-decyl) glutathione, S-(p-chlorophenacyl)glutathione, S-(p-nitrobenzyl) glutathione, and the GSH conjugate of 9,10-epoxystearic acid, 2,4-dinitrophenyl-SG, melphelan-SG (Sharma R, et al., 1990, Awasthi S., et al., 1994).
Antineoplastic agents	daunorubicin, vinblastin (Awasthi et al., 1994), vincristine (Awasthi et al., 2003), colchicine (Awasthi et al., 1999), navelbine (Stuckler et al., 2005),
Naturally occurring metabolites	Leucotriene C <sub>4</sub> , hydroxynonenal-SG, prostaglandin

It was demonstrated that the transport of these compounds against a concentration gradient was saturable with respect to the substrate, temperature-dependent, sensitive to the osmolarity of the assay medium, and ATP dependent (Awasthi et al., 1998).

These transport studies were performed also in inside-out plasma membrane vesicles (IOV) in a variety of cancer cells with or without RLIP76 transfection (Awasthi et al., 2005; Singhal et al., 2005). An overall contribution of RLIP76 versus eleven other ABC transporters was evaluated using immunoprecipitation methods in these crude membrane IOVs (Awasthi et al., 2002). Interestingly, RLIP76 was found to be a predominant transporter of doxorubicin as well as glutathione conjugates, representing about 2/3 of the transport capacity in lung cancer (Awasthi et al., 2003a, Singhal et al., 2003b, Awasthi et al., 2003c). The remainder of the transport activity is contributed by MRP and Pgp. In contrast, in breast cancer, MRP1 or BCRB1 represent predominant transporters of glutathione conjugates and doxorubicin. These results were confirmed by studies on mice embryo fibroblasts isolated from RLIP76 knockout mice (MEF KO) as well as crude membrane vesicles prepared from RLIP76 knockout mice tissues, where the total transport activity for doxorubicin (DOX) and GSH conjugates was diminished (Awasthi et al., 2005). These studies demonstrated that RLIP76 was indeed a predominant transporter of xenobiotics and GSH conjugates.

Endogenous lipid derived alkynals such as 4-hydroxynonenal (4-HNE), potent apoptotic inducers which are metabolized primarily to GSH conjugates were shown to be effluxed from cells predominately by RLIP76 (Cheng et al., 2001). We reasoned that loss of RLIP76 should result in the increase in cellular accumulation of these conjugates, as well as lipid hydroperoxides (LOOH) and 2-thiobarbituric-acid-reactive substances (TBARS). This was demonstrated by a 2-9 fold increase in LOOH as well as TBARS concentration in the tissues from RLIP76 knockout animals (RLIP76 KO)

(Awasthi et al., 2005). Since hydroperoxides are a necessary product of oxidative stress and are obligate intermediates generated as a result of radiation, it was hypothesized that RLIP76 KO mice should be radiation sensitive. A marked increase in radiation sensitivity was demonstrated in the RLIP76 KO animals and RLIP76 KO animals with recombinant RLIP76 delivered in proteoliposomes, completely abolished radiation sensitivity (Awasthi et al., 2005). The protective effect of RLIP76 augmentation has been demonstrated not only in animals but also in cultured cells. Its protective effect extends to the toxicity of hydrogen peroxide, X-radiation, UV light, several natural products, alkylating agents, and platinum compounds (Singhal et al., 2006). These studies demonstrated that increased sensitivity of the RLIP76 KO animals to noxious agents was due to the lack of RLIP76.

The marked increase in the tendency towards apoptosis caused by radiation or chemicals found in cells and in RLIP76 KO animals, suggested that RLIP76 is an important anti-apoptotic agent. Moreover, it may create a generalized stress protection mechanism since lipid oxidation is a common obligate intermediate of chemical as well as radiant stress. These findings were supported also by other investigators who showed that RLIP76 mediates its activity through heat shock proteins such as HSF1, HSP1, and HSP90 (Hu et al., 2003). This finding was echoed in results from RLIP76 KO animals which show a marked increase in the level of heat shock proteins.

Since stress protective mechanisms are known to be active in cancer cells and are known to play a role in resistance to radiation and chemotherapy, it was proposed that RLIP76 was a key component in stress defense which may be important for

survival of cancer cells (Awasthi et al., 2003). Gene expression studies have demonstrated an increased RLIP76 expression in lung cancer, melanoma, and leukemia cells (Singhal et al., 2006). Inhibition of RLIP76, using antibodies that recognized specific cell surface epitope of RLIP76, caused apoptosis in cancer cells as demonstrated by both DNA laddering, TUNEL assay and assays of caspase activation and part cleavage (Awasthi et al., 2002; Awasthi et al., 2003 II, III; Singhal et al., 2003; Awasthi et al., 2003; Yadav et al., 2005). Stress caused by inhibition by RLIP76 was evident from finding increased JNK activation and AP1 binding. The findings were reproducible in thirteen cancer cell lines such as lung cancer, melanoma, prostate cancer, and ovarian cancer cells (Singhal et al., 2006, Singhal et al., 2006). The specificity of these antibodies has been demonstrated by double immuno-diffusion assay (Awasthi et al., 2002). Depletion of RLIP76 by specific siRNA also caused apoptosis, confirming that the antibody effect was specifically due to loss of RLIP76 activity (Yadav et al., 2004). This finding clearly demonstrated that inhibition of RLIP76 by siRNA or antiRLIP76 IgG, caused apoptosis in malignant cells, such as lung cancer, melanoma, prostate cancer, and ovarian cancer cells (Singhal et al., 2006, Singhal et al., 2006). Remarkably unaffected were breast cancer and hepato cellular carcinoma which contain little RLIP76 activity (Singhal et al., 2006). These results indicate that the physiological GSH-conjugate transporting activity of RLIP76 is a crucial determinant of apoptosis.

A novel role for GSH-conjugate transport activity of RLIP76 became evident when these findings were viewed in context of studies by other investigators showing

that it is a crucial component of endocytotic pathways, particularly, clathrin dependent endocytosis (Nakashima et al., 1999; Jullien-Flores et al., 2000; Matsuzaki et al., 2002; Rosse et al., 2003). Proteins including POB1, AP2, Src, and GRB2, have been linked with RLIP76 and clathrin-dependent endocytosis, mostly in the context of insulin signaling and its regulation by Ral-GTPase pathways which regulate membrane plasticity (Nakashima et al., 1999; Jullien-Flores et al., 2000).

Ral proteins are members of the Ras superfamily of GTPases. These small proteins function as molecular switches that cycle between the active GTP-bound and inactive GDP-bound states (Urano et al., 1996). Ras proteins can activate Ral-GTPases by binding to a set of Ral-GEFs (Ral-specific guanine nucleotide exchange factors) that contain Ras-binding domains at their C-terminal (Urano et al., 1996; Wolthuis et al., 1997). Ral-GTPases are activated in response to several mitogenic signals which placed this protein as a contributing factor to oncogenic Ras-induced cellular transformation (Urano et al., 1996; Reuther et al., 2000; Chien et al., 2003). Ral-GEF stimulates Ral proteins (Ral-GEFs), by promoting GDP release from Ral and allowing GTP binding. Active Ral proteins participate, and at the same time influence a variety of cellular regulation processes, and can affect several mitogenic regulatory cascades through the interaction with Src (Goi et al., 2000), phospholipase D1 (Luo et al., 1998) and nuclear factor  $\kappa$ B (Henry et al., 2000), Jnk kinase (de Ruiter et al., 2000), cyclin D (Gille et al., 1999, Henry et al., 2000), and the forkhead transcription factor (Kops et al., 1999)

Several recent studies have implicated a role of Ral in receptor-mediated endocytosis (Nakashima et al., 1999; Jullien-Flores et al., 2000; Matsuzaki et al., 2002).



Ral, localized in the plasma membrane, contributes to the regulation of the clathrin-dependent endocytosis of a variety of ligands-receptor complexes, for example: transferrin, activin, insulin, and epidermal growth factor (EGF) receptors. This process is possible through the recruitment of Ral interacting protein (RLIP76), which in turn binds to the  $\mu$ -adaptin subunit of the heterotetrameric adaptor protein-2 (AP2) adaptor complex, EPS15 and Epsin required for clathrin-mediated endocytosis (Nakashima et al., 1999; Jullien-Flores et al., 2000; Matsuzaki et al., 2002, Feig, et al., 2003).

The data from literature suggests a signaling model of RLIP76 activation. After receptor tyrosine kinase activation, Ras protein activated by Ras GAP interacts with active form of RalGDS, which in turn causes activation of Ral by binding of GTP. This GTP bound form of Ral binds to RLIP76 and makes it active (Wolthuis et al., 1998b). This process triggers the cascade of cellular processes which involve the interaction of RLIP76 with a variety of its downstream proteins such as POB1 (Ikeda et al. 1998; Nakashima et al., 1999), Hsf1 (Hu et al., 2003), AP2 (Jullien-Flores et al., 2000), and Rac/CDC42 (Jullien-Flores et al., 1995) (Fig 1.11).

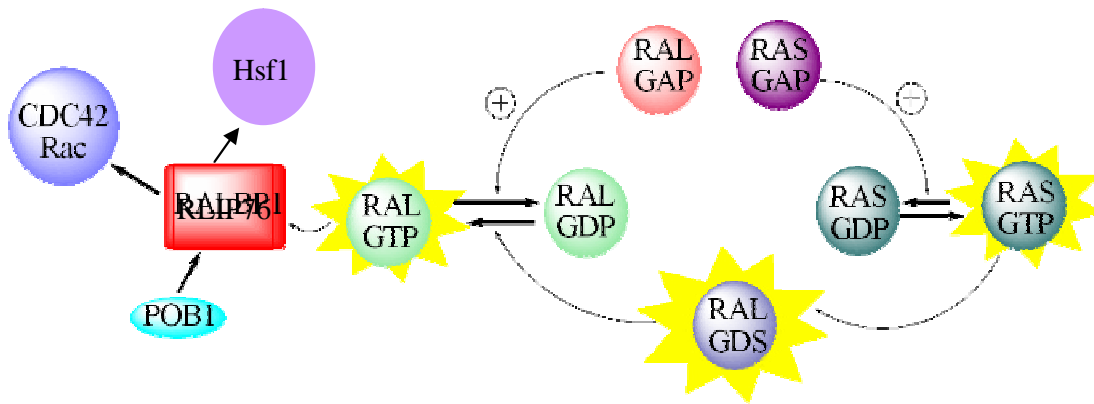


Figure 1.11 RLIP76 signaling pathway

Because of the broad specificity towards interacting proteins, RLIP76 participates in the following processes: endocytosis of insulin and epidermal growth factor receptors (Ikeda et al., 1998; Nakashima et al., 1999; Jullien- Flores et al., 2000; Matsuzaki et al., 2002), cell mitosis and filopodia formation (Ohta et al., 1999; Rossé et al., 2003; Shingo et al., 2006), stress response (Hu et al., 2003), and control of actin cytoskeleton dynamics (Kozma et al., 1995; Lebreton et al., 2004).

RLIP76 is ubiquitously expressed in most tissues in the body including liver, lung, placenta, muscles, kidneys, erythrocytes, leucocytes, intestine, pancreas, spleen, and brain (LaBelle et al., 1988; Rajendra et al., 1990; Singhal et al., 1991; Saxena et al., 1992; Awasthi et al., 1994, 1998 a,b, 2005). According to the RLIP76 amino acid sequence, the majority of the protein should be located in the cytoplasm because of the lack of classical trans-membrane domains in its structure. However, immunohistochemical studies on live, unfixed lung cancer cells, utilizing anti-RLIP76 IgG as the primary antibody raised against full-length RLIP76, demonstrated that RLIP76 is associated with the cell membrane. (Fig 1.12) (Yadav et al., 2004). In order

to support this finding, other experiments such as flow cytometry studies were performed. The results also showed that a significant percentage of cells was detected by anti-RLIP76 IgG, indicating that some domains of RLIP76 recognized by these specific antibodies are present at the cell surface (Awasthi et al., 2003c). In addition, the fact that the full length protein can be purified only when an anionic detergent is present in the lysis buffer signifies that the protein has to be associated with the cell membrane (Awasthi et al., 2000).

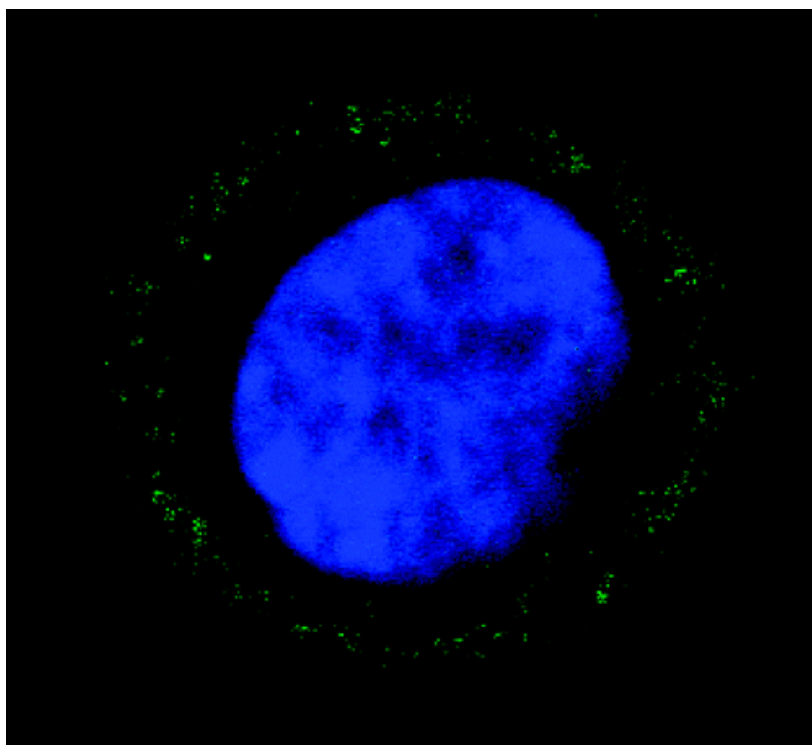


Figure 1.12 Localization of RLIP76 on the cell surface. Green staining indicates RLIP76 on the cell membrane, blue staining shows a nucleus. (Yadav et al., 2004).

RLIP76 is classified as a non-ABC transporter because besides the fact that it does not have typical trans-membrane domains and also lacks Walker motifs where

ATP binding sites are located. However, preliminary studies have shown that transport of glutathione conjugates and anti-cancer drugs by RLIP76 is ATP dependent, therefore the ATP binding sites have to be present in its structure. Analysis of the sequence of the N and C terminal of RLIP76 resulted in identification of two domains which are similar to Walker motifs of ABC transporters (<sup>69</sup>GKKKKGK<sup>74</sup> comparing to GXXXXGK – Walker A motif) and phosphoglycerate kinases ATP binding site (<sup>418</sup>GGIKDLSK<sup>425</sup> comparing to GGXKVXXK). In order to confirm this supposition, site directed mutagenesis experiments were carried out replacing two amino acids, one on the N-terminus and the second at the C-terminus of RLIP76. When lysine K<sup>74</sup> was replaced with methionine on the N-terminus of RLIP76, ATPase activity dropped significantly for this 367 amino acid long peptide. Likewise, when lysine K<sup>425</sup> was substituted with methionine on the C-terminus of RLIP76, most of ATPase activity of this peptide was lost. These results strongly suggest that two fragments <sup>69</sup>GKKKKGK<sup>74</sup> and <sup>418</sup>GGIKDLSK<sup>425</sup> located on RLIP76 N- and C-termini respectively are responsible for ATP binding (Awasthi et al., 2001). Surprisingly, even though both terminals show ATPase activity, they are not able to mediate the ATP dependent transport of DOX or colchicines when they are separately reconstituted into proteoliposomes. The situation changes when the N- and C-termini are reconstituted together in proteoliposomes. These two fragments can reassemble to form a complex capable of catalyzing the transport of xenobiotics (Awasthi et al., 2001b).

The primary structure of RLIP76 reveals many interesting features. This 655 amino acid protein has four major protein/protein binding domains (Fig 1.13).

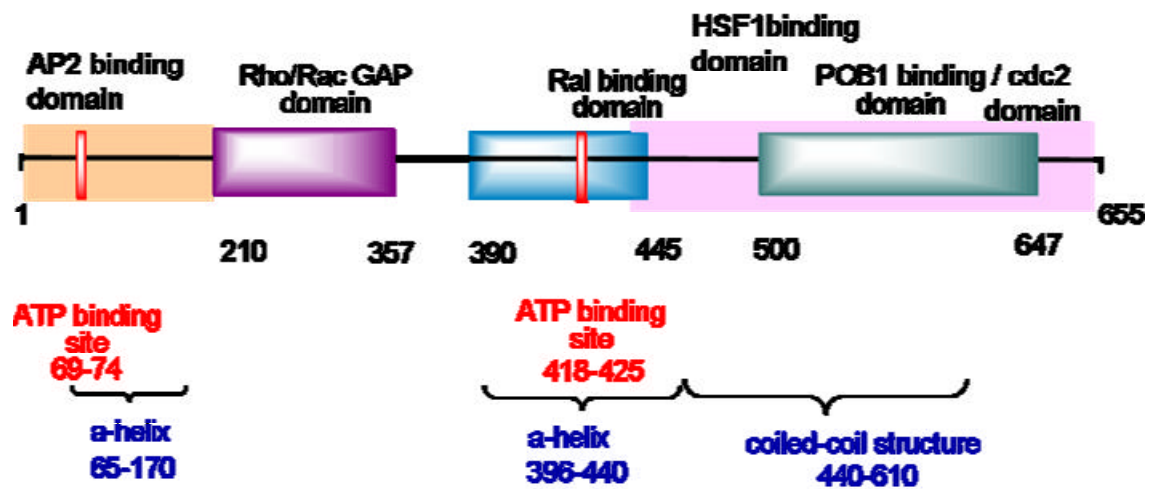


Figure 1.13 RLIP76 binding domains

Three distinct central domains are distinguished carrying Rho/Rac GAP activity (aa 210-357), Ral binding domain (aa 391-499), POB1/REPS2 domain (aa 500-647) (Jullien-Flores et al.,1995; Ikeda et al., 1998), and an additional domain located on the C-terminus overlapping POB1 binding site, HSF1 binding site (aa 440-655) (Hu et al., 2003). In addition, the amino acid sequence of RLIP76 indicates the presence of N-glycosylation site (aa 341-344), ATP binding sites (aa 69-74, 418-425), cAMP (aa113-116), cGMP-dependent protein kinase phosphorylation sites (aa 650-653), tyrosine kinase phosphorylation site (aa 308-315), N-myristoylation sites (aa 21-26, 40-45, 191-196), leucine zipper pattern (aa 547-578), and protein kinase C  $\alpha$  sites (aa 118-120, 297-299, 353-355, 509-511) (Awasthi et al., 2002). The tremendous variety of all these motifs in the primary structure of RLIP76 potentially provides this protein with multiple

functions and may bring it into the collection of significant proteins involved in cell signaling and drug efflux in a living cell.

Based on these findings, it is proposed that GSH-conjugates transport activity of RLIP6 is an important determinant of glycemic regulation and through its effects insulin signaling. Specifically, it is proposed that ATP hydrolysis driven GSH conjugate efflux is coupled with endocytosis such that this transport is the driving force and the rate determining mechanism for endocytosis. If this were true, increased RLIP76 should accelerate the rate of insulin-insulin receptor endocytosis and confirm conditions resembling insulin resistance. Depletion of RLIP76 should prolong the effects of insulin because of slowed endocytosis of insulin-receptor complex. The present thesis addresses this hypothesis at an animal, tissue, cellular, biochemical, and chemical level.

## CHAPTER 2

### METHODS

#### 2.1 Preparation of GSH-Sepharose affinity resin

Glutathione (GSH) affinity resin was prepared in order to purify isoenzymes of Glutathione S-Transferases (GSTs) from mouse liver using an affinity chromatography method. This process of bioselective adsorption allows for the highly specific and efficient purification of GSTs. The enzyme has very high affinity towards GSH, therefore, this ligand was immobilized on a beaded and porous matrix of Sepharose 6B resin. The resin exists in lyophilized powder and has the ability to swell from 1g of powder to 3 ml of gel.

##### *2.1.1 Materials*

The following solutions were prepared and stored at 4 °C:

1. 1 M  $K_2HPO_4$  500 ml

The solution was prepared by dissolving 87.1 g of  $K_2HPO_4$  in distilled water.

2. 1 M  $KH_2PO_4$  500 ml

The solution was prepared by dissolving 68.0 g of  $KH_2PO_4$  in distilled water.

3. 1 M  $Na_2HPO_4$  50 ml

The solution was prepared by dissolving 71.0g of  $\text{Na}_2\text{HPO}_4$  in distilled water.

4. Epoxy-activated sepharose 6B resin (Sigma) 1.5 g

5. Linking buffer (44 mM  $\text{Na}_2\text{HPO}_4/\text{KH}_2\text{PO}_4$ ), pH 7 50 ml

The buffer was prepared by mixing 0.8 ml of 1 M  $\text{KH}_2\text{PO}_4$  with 1.4 ml of 1 M  $\text{Na}_2\text{HPO}_4$  and diluting with distilled water to the final volume of 50 ml.

6. Glutathione (GSH) solution

150 mg of GSH was dissolved in 1.5 ml of linking buffer. The pH was adjusted to 7 with 5 M NaOH.

7. 1 M Ethanolamine pH 8 (Sigma)

8. 0.1 M Sodium Acetate buffer, pH 4 1000 mL

The buffer was prepared by dissolving 5.1 g of acetic acid monohydrate with 2.05 g sodium acetate dehydrate in 1000 mL of water.

9. 0.5 M KCl in 0.1 M Sodium Acetate buffer, pH 4 500 ml

The buffer was prepared by dissolving 18.6 g KCl in 500 ml of sodium acetate buffer, pH 4.

10. 0.1 M Sodium Borate buffer, pH 8 1000 mL

The buffer was prepared by dissolving 20.3 g of sodium tetraborate in 800 ml of distilled water and when pH adjusted with boric acid reached 8 the total volume was filled up to 1000 mL.

11. 0.5 M KCl in 0.1 M Sodium Borate buffer, pH 8

The buffer was prepared by dissolving 18.6 g of KCl in 500 ml of 0.1 M sodium borate buffer, pH 8.



12. Affinity buffer

200 ml

This buffer was prepared by adding  $\beta$ -Mercaptoethanol ( $\beta$ -ME) to 22 mM potassium phosphate buffer, pH 7, to the final concentration of 1.4 mM.

### *2.1.2 Methods*

About 1.5 g of epoxy-activated sepharose 6B resin was placed into 10 ml of deionized (DI) water and left on the orbital shaker at 4 °C for half an hour. When the beads increased their volume to 3.5 times (1 g of dry bead became 3-3.5 ml), the resin was collected after centrifugation at 4000 g, for 4 min, at 4 °C. Then, the resin was washed twice with a linking buffer and nitrogen was passed through it for 3 min. After an addition of 1.5 ml of glutathione solution to the resin, nitrogen was passed again. Next, the resin was incubated with gentle shaking at 37 °C for 12 hours, followed by washing with DI water. The unreacted epoxy groups were blocked by incubating the resin with 5 ml of 1 M ethanolamine, pH 8.0 for 3 hours at room temperature with gentle shaking. After washing the resin with water it was incubated separately with three buffers in the following order: KCl/CH<sub>3</sub>COONa, KCl/Na<sub>3</sub>BO<sub>3</sub> and affinity buffer. The resin was stored at 4 °C in affinity buffer for future usage.

### 2.2 Purification of Glutathione S-Transferases (GSTs) from mouse liver

According to the literature, liver is the organ which has the highest concentration of GSTs compared to other organs (Hayes et al., 2005). Therefore, liver tissue was used to purify GSTs according to the procedure of Singhal (Singhal et al.,

1992). All purification steps were carried out at 4 °C. The solutions listed below were prepared as follows:

### 2.2.1 Materials

1. Liver from mouse, male 235 mg

2. 1 M Phosphate buffer (KH<sub>2</sub>PO<sub>4</sub>/ K<sub>2</sub>HPO<sub>4</sub>), pH 7 155 ml

The buffer was prepared by mixing 100 ml of 1 M KH<sub>2</sub>PO<sub>4</sub> with 55 ml of 1 M K<sub>2</sub>HPO<sub>4</sub>

3. Buffer A (10 mM KH<sub>2</sub>PO<sub>4</sub>/ K<sub>2</sub>HPO<sub>4</sub>, pH 7 containing 1.4 mM β-ME) 1000 mL

10 ml of 1 M KH<sub>2</sub>PO<sub>4</sub>/ K<sub>2</sub>HPO<sub>4</sub>, pH 7, was diluted in 990 ml of distilled water and 96.5 μl of 14.5 M β-mercaptoethanol was added to the final concentration of 1.4 mM.

4. Affinity buffer 1 L

22 mM KH<sub>2</sub>PO<sub>4</sub>/ K<sub>2</sub>HPO<sub>4</sub>, pH 7, containing 1.4 mM β-mercaptoethanol (β-ME)

22 ml of 1 M KH<sub>2</sub>PO<sub>4</sub>/ K<sub>2</sub>HPO<sub>4</sub>, pH 7, was diluted in 978 ml of DI water and 96.5 μl of 14.5 M β-ME was added to the final concentration of 1.4 mM

5. Elution buffer: 4 ml

The buffer was prepared by dissolving 12.3 mg of glutathione in 50 mM Tris(hydroxymethyl)amino methane (Tris-HCl), pH 9.6 containing 1.4 mM β-ME to the final concentration of 10 mM.

### *2.2.2 Methods*

235 mg of mouse liver tissue, previously stored at -80 °C, were placed into the corex tube and washed twice with 1 ml PBS. Next, 2.35 ml of buffer A was added in order to make 10% homogenate and the tissue was blended for 20 sec using a tissuemizer (Tekmar Company). Then, after centrifugation at 28000 g for 45 min, the supernatant was dialyzed overnight against buffer A. The next day, 2.3 ml of the aliquot was centrifuged again at 28000 g for 30 min. The collected fraction was applied to GSH-sepharose affinity resin and left on an orbital shaker overnight at 4 °C. The following day, the resin was centrifuged at 4500 g for 4 min at 4 °C and an unabsorbed fraction was collected in order to determine protein activity. Next, the resin was washed with Buffer B until the optical density, measured at 280 nm wavelength, reached 0. The protein was eluted with 4 ml of eluting buffer, in two fractions (2 times for 2 ml) and the mixed extract was dialyzed against buffer A all night at 4 °C. Finally, the activity and protein concentration were established.

### 2.3 Glutathione S-Transferases activity assay

Enzyme activity with 1-chloro-2,4-dinitrobenzene (CDNB) was determined according to the method described by Habig (Habig et al., 1974). The absorbance of the mixture of GST substrates with the presence of enzyme was measured in dual beam spectrophotometer (Varian 300) at 340 nm. This assay is based on the GST-catalyzed reaction between 1-chloro-2,4-dinitrobenzene (CDNB) and GSH. Following addition of GST to the reaction cuvette CDNB and GSH combined to form a dinitrophenyl thioether chromophore and a chloride ion.

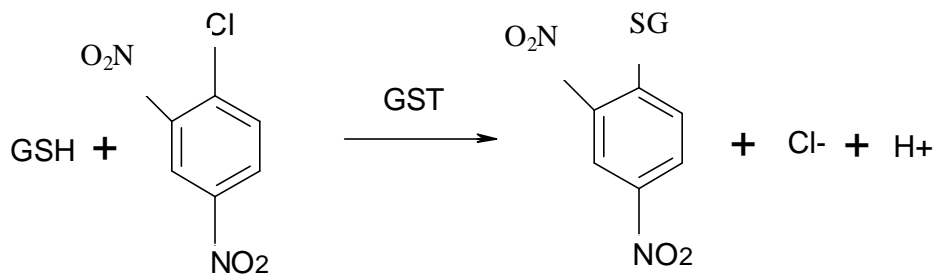


Figure 2.1 Synthesis of Dinitrophenyl S-Glutathione (DNP-SG)

### 2.3.1 Materials

1. Assay buffer: 100 mM  $\text{KH}_2\text{PO}_4/\text{K}_2\text{HPO}_4$ , pH 6.5 1000 mL  
 100 ml of 1 M  $\text{KH}_2\text{PO}_4/\text{K}_2\text{HPO}_4$ , pH 6.5, was diluted in 900 ml of distilled water.
2. 20 mM 1-chloro-2,4-dinitrobenzene (CDNB) in absolute ethanol 10 ml  
 40.5 mg of CDNB was dissolved in 10 ml of ethanol.
3. 10 mM Glutathione solution in assay buffer 2 ml  
 6.1 mg of GSH was dissolved in 2 ml of assay buffer.

### 2.3.2 Methods

The following components were added to the reaction cuvette in the following order: 830  $\mu\text{l}$  of GST assay buffer, 50  $\mu\text{l}$  of CDNB solution, 100  $\mu\text{l}$  of GSH solution and 20  $\mu\text{l}$  of diluted enzyme. The cuvette was then sealed with parafilm and gently rocked by hand, followed by immediate measurements in the spectrophotometer.

As a control, 20  $\mu\text{l}$  of enzyme was replaced with 20  $\mu\text{l}$  of  $\text{KH}_2\text{PO}_4/\text{K}_2\text{HPO}_4$  buffer. The table 2.1 summarizes the conditions for the GSTs activity assay.

Table 2.1 GSTs activity assay, composition per 1 ml of reaction mixture

<b>Components</b>	<b>Blank [ml]</b>	<b>Experimental 1 [ml]</b>	<b>Experimental 2 [ml]</b>	<b>Experimental 3 [ml]</b>
GST Assay Buffer	850	830	830	830
10 mM GSH	100	100	100	100
Enzyme 1:10 dilution	-	20	20	20
20 mM CDNB	50	50	50	50

The assay was performed at 340 nm wavelength. The extinction coefficient of DNP-SG conjugate at 340 nm is  $9.6 \text{ mM}^{-1} \cdot \text{cm}^{-1}$ .

#### 2.4 Determination of protein concentration

The concentration of protein was estimated by the method of Bradford (Bradford 1976). The Bradford assay is based on the equilibrium between two forms of Coomassie Brilliant Blue G-250. Under strongly acid conditions, the dye is most stable as a doubly-protonated red form, reaching a maximum absorbance at 470 nm. Upon binding to protein, however, the maximum absorbance of the acidic solution of Coomassie Blue is shifted from 465 nm to 595 nm due to the hydrophobic and ionic interactions which stabilize the anionic form of the dye, causing a visible color change from red to blue. The protein concentration can be easily calculated from the Beer's Law, where the absorbance is proportional to the amount of protein present in the sample.

##### *2.4.1 Materials*

1. Bradford reagent	500 ml
Composition: Coomassie Brilliant Blue G-250	50 mg

Ethanol (95%)	25 ml
Phosphoric acid (85%)	50 ml
Distilled water	425 ml

The solution was filtered a few times with Whatman No 2 filter paper and stored in an amber bottle at room temperature.

2. 1 mg/ml BSA solution in water 1 ml

#### 2.4.2 Methods

The standard curve was prepared according to the manufacturer's description.

BSA standard solutions were prepared by a serial dilution of 1 mg/ml BSA protein standard in Bradford reagent in the following concentration (Table 2.2):

Table 2.2 Dilution of BSA solutions

No	BSA standard solution [mg/ml]	Bradford reagent [ml]
1	0.002	1
2	0.005	1
3	0.010	1
4	0.015	1
5	0.020	1

The dye – protein mixtures were vortexed gently followed by incubation at room temperature for 10 min. Next, the samples were transferred into the cuvettes and the

absorbance was measured at 595 nm (Table 2.3). The absorbance was plotted against the protein concentration of each standard (Fig 2.1).

Table 2.3 Absorbance of BSA solutions measured at 595 nm

No	BSA standard solution [mg/ml]	Absorbance reading at 595 nm
1	0.000	0.00
2	0.002	0.01
3	0.005	0.13
4	0.010	0.23
5	0.015	0.34
6	0.020	0.55

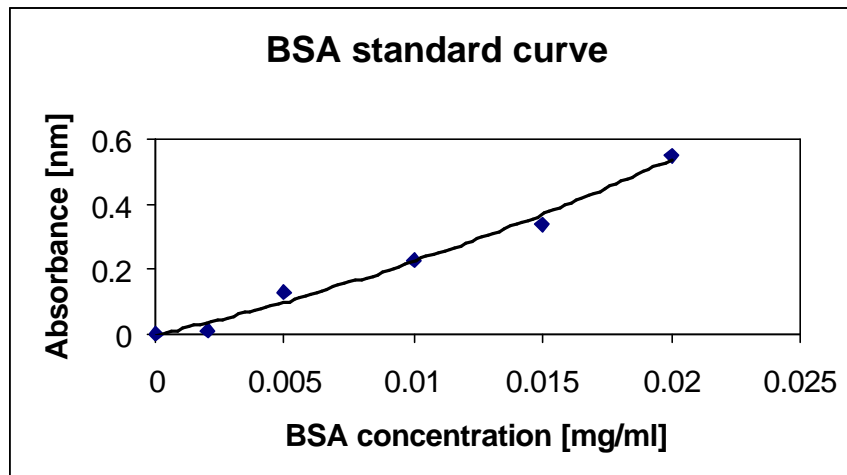


Figure 2.2 BSA standard curve.

The unknown protein total volume of the sample was 100  $\mu$ l, while the amount of Bradford reagent remained constant 1 ml for a total volume of 1.1 ml. The absorbance of the protein solution was measured against the Bradford reagent, used as a

blank. The unknown protein concentration was determined by comparison of the absorbance values versus the BSA standard curve.

### 2.5 Synthesis of Dinitrophenyl S-Glutathione (DNP-SG)

Dinitrophenyl S-glutathione (DNP-SG) was synthesized under the catalytic power of glutathione S-transferases purified from mouse liver. The compound was later used to prepare, cyanogen bromide CDBN activated sepharose 4B resin for the purification of recombinant RLIP76 from *E. coli*. The following equation summarizes the reaction between glutathione and 1-Chloro-2,4-dinitrobenzene.

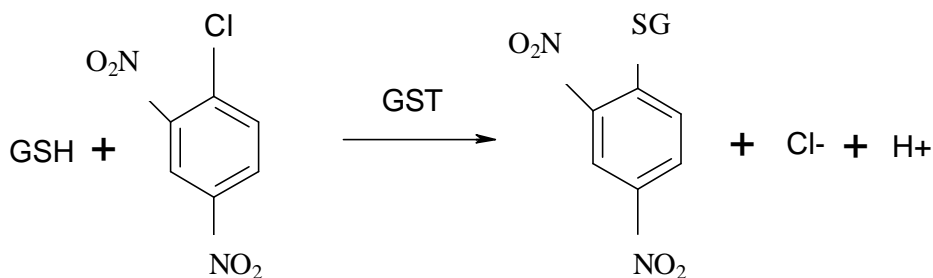


Figure 2.3 Synthesis of dinitrophenyl S-glutathione (DNP-SG)

#### 2.5.1 Materials

1. 1 M  $\text{KH}_2\text{PO}_4$  100 ml

The solution was prepared by dissolving 13.61 g of  $\text{KH}_2\text{PO}_4$  in 100 ml of distilled water resulting in pH 4.5.

2. 1 M  $\text{K}_2\text{HPO}_4$  100 ml

The solution was prepared by dissolving 17.42 g of  $\text{K}_2\text{HPO}_4$  in 100 ml of distilled water resulting in pH 9.5.

3. 100 mM  $\text{KH}_2\text{PO}_4/\text{K}_2\text{HPO}_4$  (Assay buffer) 1000 mL



The assay buffer was prepared by mixing 67.2 ml of 1 M  $\text{KH}_2\text{PO}_4$ , pH 4.5, with 32.4 ml of 1 M  $\text{K}_2\text{HPO}_4$  to the final pH of 6.5, followed by dilution with distilled water to the final volume of 1000 ml.

4. 400 mM 1-chloro-2,4-dinitrobenzene (CDNB) 2.5 ml

The solution was prepared by dissolving 202.6 mg of CDNB in 2.5 ml of absolute ethanol.

5. 15 mM glutathione 50 ml

The solution was prepared by dissolving 230 mg glutathione in 50 ml of assay buffer and the pH was adjusted to 7 with 5 M NaOH

6. Glutathione S-transferases (GSTs) 6 U

Enzyme was purified as described previously.

7. Acetonitrile (Sigma-Aldrich) 100 ml

### *2.5.2 Methods*

15 mM glutathione solution in assay buffer was placed into an Erlenmeyer flask covered with aluminum foil. Nitrogen was passed through the solution for 3 min to remove existing air from the flask, Next, 6 U of glutathione S-transferases was added to the flask, and the solution was mixed with a magnetic stirrer for 10 min at room temperature. 400 mM CDNB solution was added drop wise for the next 30 min. After mixing all components, nitrogen was passed for 3 min through the solution and the flask was covered with parafilm. The reaction mixture was left overnight with continuous stirring. The next day the bright yellow solution was separated into 4 glass tubes and freeze dried for 5 hours in a Jouan RC 10.10 lyophilizer. The remaining pellet was later

washed two times with ethanol in order to remove excess of CDNB. Then, all four pellets were collected into one tube and 2 ml of DI water was added. Because DNP-SG is soluble in water, the yellow supernatant containing DNP-SG was collected after centrifugation.

Thin layer chromatography was carried out in order to separate DNP-SG from unreacted GSH or GSSG. The TLC chamber was saturated with acetonitrile and water in a 7:2 volume ratio. Meanwhile, 20 cm x 20 cm, .25 mm thick silica gel TLC plates were spotted with the yellow supernatant 1.5 cm from the bottom. After drying out the second layer of DNP-SG solution was loaded. Next, the TLC plates were placed to the saturated chamber. The solvents were allowed to migrate for 3 hours to approximately 1 cm from the top of the plates. Then, the plates were removed from the chamber and allowed to dry overnight.

DNP-SG was located as a lower, yellow layer on the TLC plate. The upper, light yellow spots were GSH or GSSG. After scraping DNP-SG from the plate, the product was resuspended in 3 ml of DI water and left on the orbital shaker for 1 hour at 4 °C. The supernatant, pure DNP-SG, was collected after centrifugation at 3000 rpm for 10 min. For the concentration determination, a 1:100 fold dilution of DNP-SG was prepared and both the spectra (200-500 nm) and O.D. at 340 nm against water were measured.

#### 2.6 Preparation of DNP-SG, cyanogen bromide (CNBr) activated sepharose 4B resin

DNP-SG affinity resin was prepared in order to purify recombinant protein RLIP76 from *E. coli* using affinity chromatography. RLIP76 is an ATPase which has

ability to transport DNP-SG across the cell's membrane. The enzyme has very high affinity towards DNP-SG, therefore, this ligand was immobilized on a beaded and porous matrix of sepharose 4B resin.

### 2.6.1 Materials

1. CNBr activated sepharose 4B resin (Sigma-Aldrich) 1.0 g
2. 1 mM HCl, 100 ml  
8.3  $\mu$ l of 12 M HCl was diluted with distilled water to the final volume of 100 ml.
3. 1 M NaHCO<sub>3</sub> 100 ml  
8.4 g of NaHCO<sub>3</sub> were dissolved in 100 ml of distilled water.
4. 5 M NaCl 100 ml  
29.25 g of NaCl was dissolved in 100 ml of distilled water.
5. Coupling buffer 100 ml  
The buffer was prepared by mixing 10 ml of 1 M NaHCO<sub>3</sub> with 25 ml of 5 M NaCl. The solution was adjusted to pH 7.9 with 12 M hydrochloric acid and brought to a final volume of 100 ml.
6. 5 M KCl 100 ml  
37.2 g of KCl was dissolved in 100 ml of distilled water.
7. 1 M CH<sub>3</sub>COONa 100ml  
8.2 g of CH<sub>3</sub>COONa was dissolved in 100 ml of distilled water.
8. 0.5 M KCl in 0.1 M CH<sub>3</sub>COONa 100 ml

The buffer was prepared by mixing 10 ml of 1 M CH<sub>3</sub>COONa with 10 ml of 5 M KCl. The solution was adjusted to pH 4 with concentrated acetic acid and brought to a final volume of 100 ml.

9. 1 M Na<sub>3</sub>BO<sub>3</sub>, 100 ml

38.1 g of Na<sub>3</sub>BO<sub>3</sub> was dissolved in 100 ml of distilled water.

10. 0.5 M KCl in 0.1 M Na<sub>3</sub>BO<sub>3</sub>, 100 ml

The buffer was prepared by mixing 10 ml of 1 M Na<sub>3</sub>BO<sub>3</sub> with 10 ml of 5 M KCl. The solution was adjusted to pH 8 with boric acid and brought to a final volume of 100 ml

11. 1 M Ethanolamine (Sigma-Aldrich) 20 ml

The solution was prepared by dilution of 1.25 ml of 16 M ethanolamine (Sigma) in 18.75 ml of distilled water

12. 25.9 mM DNP-SG

DNP-SG was synthesized as described previously and the concentration was established using spectrophotometric methods

### *2.6.2 Methods*

1.0 g of CNBr-activated sepharose 4B resin was equilibrated twice with 12 ml of 1 mM HCl. The mixture was placed into the tube covered with aluminum foil and left on the orbital shaker at 4 °C for half an hour. After centrifugation at 2000 g for 4 min, at 4 °C the resin was collected and washed twice with coupling buffer. The supernatant was discarded and 1 ml of fresh coupling buffer was added to the resin to make a total volume of 5.5 ml (4.5 ml resin and 1 ml buffer). Next, 0.63 ml of DNP-SG was added

to the resin to obtain the final concentration of 3mM and the resin was left on an orbital shaker for 12 hours at 4 °C. Then, the excess DNP-SG was washed from the resin with 20 ml of coupling buffer, followed by incubation in ethanolamine for 4 hours at room temperature in order to block the unreacted epoxy groups. Three buffers in the following order were used to wash the resin:

- 0.5 M KCl in 0.1 M sodium acetate buffer, pH 4
- 0.5 M KCl in 0.1 M sodium borate buffer, pH 8
- coupling buffer

In the last step, the resin was collected after centrifugation at 2000 g for 5 min and stored at 4 °C in 10 ml of coupling buffer in a tube covered with aluminum foil.

1 g of CNBr 4B resin affords 3 ml of affinity resin.

## 2.7 Molecular cloning

The following molecular biology manipulation methods were used to clone the fragment of DNA gene encoding targeted protein into the prokaryotic plasmid and transform it into the *E. coli* cells, which later expressed the protein after induction with isopropyl β-D-thiogalacto-pyranoside (IPTG).

### *2.7.1 Materials*

1. Working solution	500 ml
60 mM CaCl <sub>2</sub>	3.3 g
10 mM 4-(2-hydroxyethyl)-1-piperazineethanesulfonic acid (HEPES)	1.2 g

The solution was filtered using Wattmann filter paper, followed by addition of 75 ml of glycerol (15%). The final volume was brought to 500 ml with distilled water, and stored at 4 °C for further usage.

2. Luria-Berani (LB) for Kanamycin selection	1000 mL
Trypton	10 g
NaCl	5.0 g
Yeast extract	10 g

Total volume was brought to 1000 mL with distilled water and pH was adjusted to 7 with 5 M NaOH

3. Luria-Berani (LB) for Zeocin selection	1000 mL
Trypton	10 g
NaCl	5.0 g
Yeast extract	5.0 g

Total volume brought to 1000 mL with distilled water and pH 7.5 was adjusted with 1 M NaOH. The dry reagents were combined and DI water was added to the required volume. Next, the medium was autoclaved at 15 psi and 121 °C for 45 min. Antibiotic was added after the medium cooled to 55 °C.

4. SOB medium	1000 mL
Trypton	20 g
NaCl	0.5 g
Yeast extract	5.0 g
1 M MgCl <sub>2</sub>	10 ml

1 M MgSO <sub>4</sub>	10 ml
-----------------------	-------

Total volume was brought to 1000 mL liter with water and pH was adjusted to 7 with 5 M NaOH. The dry reagents were combined and DI water was added to the required volume. Next, the medium was autoclaved at 15 psi and 121 °C for 45 min. After the medium cooled to 55 °C, 1 M MgCl<sub>2</sub> and 1 M MgSO<sub>4</sub> were added to it. The medium was stored at 4 °C for further usage.

5. SOC medium	1000 mL
---------------	---------

Trypton	20 g
---------	------

NaCl	0.5 g
------	-------

Yeast extract	5.0 g
---------------	-------

1 M MgCl <sub>2</sub>	10 ml
-----------------------	-------

1 M MgSO <sub>4</sub>	10 ml
-----------------------	-------

2 M Glucose	10 ml
-------------	-------

Total volume was brought to 1000 mL liter with water and pH 7 was adjusted with 5 M NaOH. The dry reagents were combined and DI water was added to the required volume. Next, the medium was autoclaved at 15 psi and 121 °C for 45 min. After the medium cooled to 55 °C, 1 M MgCl<sub>2</sub> and 1 M MgSO<sub>4</sub>, and 2 M glucose were added to it. The medium was stored at 4 °C for further usage.

6. Agar plates for kanamycin or ampicilin selection	1000 mL
---	---------

Agar	20 g
------	------

NaCl	10 g
------	------

Tryptone	10 g
----------	------

Yeast extract 5.0 g

Total volume brought to 1000 mL liter with distilled water and pH was adjusted to 7 with 5 M NaOH.

7. Agar plates for zeocin selection 1000 mL

Agar 15 g

NaCl 10 g

Tryptone 10 g

Yeast extract 5.0 g

Total volume was brought to 1000 mL liter with distilled water and pH was adjusted to 7 with 1 M NaOH.

Table 2.4 The concentration of antibiotic required to select resistant bacteria transformants

<b>Antibiotic</b>	<b>Concentration mg/ml</b>
kanamycin	35
ampicilin	70
zeocin	40

300 ml of agar medium was autoclaved at 15 psi and 121 °C for 45 min and after cooling (temp. about 50 °C). The appropriate antibiotic was added (Table 2.4). Next, the medium was gently swirled in order to mix the antibiotic without creating any air bubbles. After storing at room temperature for 5 minutes, agar medium was poured into 12 Petri dish plates to about half the plate volume.



Plates were kept at room temperature for 2 hours to solidify and stored upside down at 4 °C up to 2 weeks.

### 2.8 Preparation of competent cells (*E. coli* DH5 $\alpha$ ) for plasmid transformation

A single colony of *E. coli* DH5 $\alpha$  (Novagen) was inoculated in 5 ml of SOB medium and incubated at 37 °C with shaking at 227 rpm overnight. The next day, an aliquot of the overnight culture was aseptically transferred into a 1000 ml culture flask containing 200 ml of previously autoclaved SOC medium. The culture was incubated at 37 °C with shaking until the optical density, measured at 600 nm, reached a value of 0.6, which indicating mid-log phase of the cell growth. After incubation, cells were placed on ice for 20 min, followed by centrifugation for 10 min at 3000 rpm at 4 °C in four sterile centrifuge tubes. Next, the supernatant was decanted and the obtained pellet was resuspended in 25 ml of ice cold 50mM CaCl<sub>2</sub>/15% glycerol using a Pasteur pipette. Then, cells were placed on ice for 20 min and pelleted again. Cells were transferred into two tubes, centrifuged again and resuspended in CaCl<sub>2</sub>/HEPES/15% glycerol solution followed by incubation on ice for 20 min. This procedure was repeated 2 times resulting in only one tube containing competent cells. The last pellet's resuspension in 5 ml of working solution was performed very gently because of the fragile nature of competent cells.

Only 200  $\mu$ l of cells was used for DNA transformation. The remaining 4.8 ml of competent cells was transferred in 200  $\mu$ l aliquots into the Eppendorf tubes and stored for up to 6 months at -80 °C.

## 2.9 *E. coli* transformation with prokaryotic expression vector

*E. coli* DH5 $\alpha$  was used for DNA transformation. About 0.4  $\mu$ g of a plasmid DNA (1  $\mu$ l) was added to 200  $\mu$ l of fresh competent cells. After incubation on ice for 20 min the cells were subjected to the heat shock procedure by placing them at 42 °C for 60 sec. Next, they were kept on ice for 5 min, followed by inoculation in 1 ml of SOC medium. Cells were incubated at 37 °C for 60 min. with gentle shaking. Next, 25 ml, 50 ml, and 100 ml aliquots were streaked onto agar plates containing appropriate antibiotic (kanamycin 35 mg/ml, ampicilin 70 mg/ml) using a flame sterilized spreader. Plates were incubated for 5 min at room temperature and later placed upside down at 37 °C and incubated overnight. The next day, one colony was picked from the agar plates using a sterile, wooden stick and inoculated in 10 ml of LB medium containing antibiotic. The cells were incubated at 37 °C with shaking at 227 rpm. The following day, the plasmid DNA was purified using a Qiagen QIAprep Spin Miniprep Kit.

## 2.10 Purification of plasmid DNA from overnight culture of *E.Coli* DH5 $\alpha$ in LB medium

Plasmid DNA was purified according to the manual of Qiagen QIAprep Spin Miniprep Kit. The exact concentration of Qiagen buffers is not available.

### *2.10.1 Materials*

1. Buffer P1 250  $\mu$ l

Composition: 10 mM Tris HCl, EDTA, RNase A, pH 8.

2. Buffer P2 250  $\mu$ l

Composition: NaOH, Sodium Dodecyl Sulfate (SDS).

3. Buffer N3 350 µl

Composition: acidic potassium acetate.

4. Buffer PE 750µl

Composition: guanidinium chloride, propan 2-ol.

5. Buffer EB 50 µl

Composition: 10 mM Tris HCl, pH 8.5.

### *2.10.2 Methods*

10 ml of the aliquots of a bacterial culture were pelleted for 5 min in a microcentrifuge at room temperature at 14000 g. Next, the harvested bacterial cells were resuspended in 250 µl of P1 buffer, followed by the addition of 250 µl of P2 buffer. The cells were lysed by gently inverting the tube for 4–6 times. After 5 min of incubation at room temperature, 350 µl of N3 bufer was added and the tube was inverted a few times. The cocktail was centrifuged for 20 min at 14000 g at room temperature. Next, the supernatant was applied to the QIAprep spin column by decanting it and the column was subjected to centrifugation for 1 minute at 14000 g. The flow-through was discarded and the membrane was washed with 750 µl of PE buffer. The flow-through was discarded again and the column was centrifuge for an additional 1 min to remove residual wash buffer. The last step was the elution of plasmid DNA from the membrane by pipetting 50 µl of EB buffer to the center of the membrane followed by centrifugation for 1 min in a clean Eppendorf tube.

## 2.11 Restriction endonucleases digestion of DNA

In order to create a recombinant plasmid DNA, a gene and a vector were first digested using restriction endonucleases. Digestion of DNA is the first step in many gene manipulation projects. Restriction endonucleases are bacterial enzymes that cleave the DNA at a specific target sequence yielding DNA fragments of a convenient size for downstream manipulation.

### *2.11.1 Materials*

1. Ne 2 Buffer (New England Biolabs)	2 $\mu$ l
2. 100 x BSA (New England Biolabs)	0.2 $\mu$ l
3. Enzyme 1 (New England Biolabs)	2 U
4. Enzyme 2 (New England Biolabs)	2 U
5. DNA (0.4 $\mu$ g/ $\mu$ l)	5 $\mu$ l
6. DI Water	up to 20 $\mu$ l

### *2.11.2 Methods*

In order to prepare the digestion mixture, all ingredients were added to the tube in the following order: water, Ne 2 buffer, BSA, DNA and enzymes. Then, the tube was centrifuged for 10 seconds and left in a 37 °C water bath for 2 hours. If the digestion was not complete after 2 hours, the tube was incubated for 12 hours at 37 °C.

## 2.12 Ligation of fragment DNA into a plasmid

In order to insert a targeted gene into a plasmid, both a vector and a gene were subjected to the restriction enzyme digestion followed by ligation at room temperature with a DNA ligase.

### *2.12.1 Materials*

1. 0.4 µg/µl digested plasmid vector	2 µl
2. 0.4 µg/µl DNA fragment digested with the same enzymes as plasmid	8 µl
3. Takara Solution 1 (enzyme mixture)	10 µl

### *2.12.2 Methods*

According to the TAKARA manual, the ligation procedure is as follows: vector DNA and the DNA fragment to be inserted were combined in a total volume of 10 µl. Recommended amounts of DNA are vector:insert = 50 ng:(50 ng-500 ng). Next, one volume (10 µl) of Solution 1 was added to the DNA cocktail and mixed thoroughly, followed by incubation at 16 °C for 30 min. 10 µl of the ligation mixture was applied to 100 µl of competent cells (transformation) and a remaining 10 µl was left in the water bath for overnight ligation and next day transformation. *E. coli* transformation was performed according to the procedure described previously. Recombinant plasmid was purified from an individual *E. coli* transformant of an overnight culture by miniprep procedure and its size was determined by restriction mapping.

### 2.13 Prokaryotic expression of RLIP76

- The coding sequence of RLIP76 was used as a template for Polymerase Chain Reaction (PCR) amplification. Two primers, upstream and downstream were designed in order to introduce BamHI and XhoI restriction enzymes sites.

- **Upstream primer**

5' GTT GGA TCC GAC TGA GTG CTT CCT GCCC 3'

T<sub>m</sub> = 82 °C

- **Downstream primer**

3' CCG CTC GAG TCA GAT GGA CGT CTC CTT CCT ATC CC 5'

T<sub>m</sub> = 86 °C

- The melting temperature was calculated using an equation listed below:
  - $T_m = 81.5 + 0.41 * (\%GC) - 675/N$
  - Note: N-number of nucleotides
- The BamHI restriction enzyme site was introduced immediately upstream of the initiator codon, while the XhoI site was immediately downstream of the stop codon of the RLIP76 open reading frame. PCR amplification was performed under following incubation conditions.

- 100 µl of PCR amplification mixture contains:

DNA template

500 ng

Forward primer (Biosynthesis)	30 pmol
Reverse primer (Biosynthesis)	30 pmol
dNTPmix (Applied Biosystems)	2.5 $\mu$ M
Thermopol buffer (New England Biolabs)	1 x
BSA (New England Biolabs)	1 x
Vent polymerase (New England Biolabs)	2.5 U

- PCR cycles were performed as follows: incubation at 94 °C for 5 min followed by 35 cycles of 94 °C for 30 sec, 60 °C for 30 sec, 72 °C for 1 min and a final extension at 72 °C for 7 min (Fig 2.3).

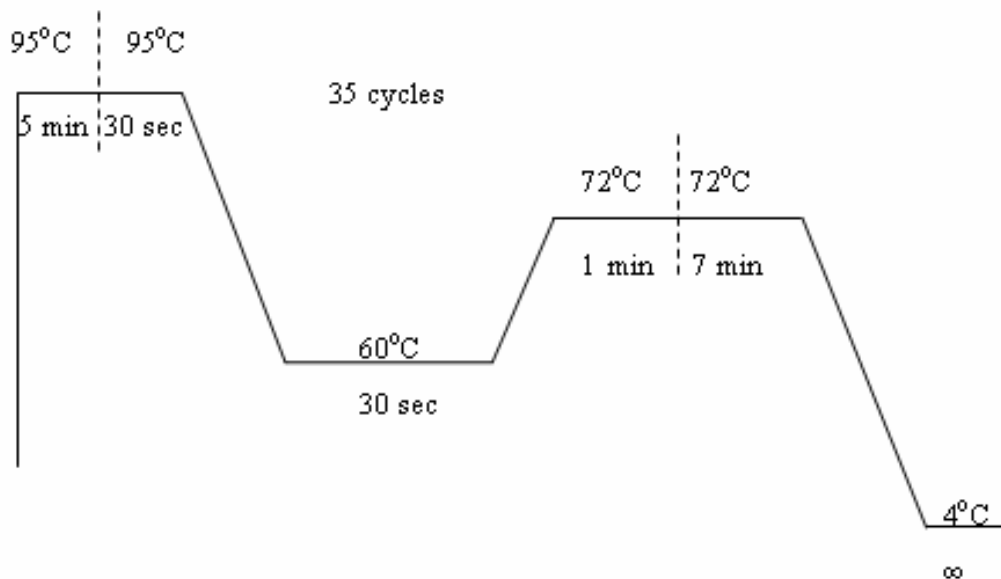


Figure 2.4 The PCR cycles for RLIP76 amplification

- PCR product was purified using a Qiagen PCR purification kit and digested with BamH1 and XhoI in order to create sticky ends, followed by ligation into the pET 30a (+) prokaryotic expression vector, previously digested with the same two enzymes.
- Next, the transformation of the recombinant plasmid into the DH5 $\alpha$  *E. coli* strain was carried out. The recombinant plasmid pET30a (+) with cloned RLIP76 was purified using a Qiagen plasmid purification kit from an overnight culture of a single colony. An identity of RLIP76 was confirmed by sequencing.

#### 2.14 Bacterial stock preparation

The single colony picked from an agar plate was inoculated into 50 ml of previously autoclaved LB media containing 50  $\mu$ g/ml kanamycin and incubated for 12 hours at 37 °C, and 225 rpm. Then, the pellet collected after centrifugation at 3000 rpm was re-suspended in 3 ml of LB medium containing 10% glycerol and stored at -80 °C in six Ependorff tubes for further use.

#### 2.15 Purification of recombinant RLIP76 from *E. coli*

Purification of recombinant RLIP76 from *E. coli* was done following the procedure developed by Awasthi (Awasthi et al., 2000).

##### *2.15.1 Materials*

1. Luria Bretain (LB) medium 300 ml

300 ml of the LB growth medium was prepared as described previously and 10.5 mg of kanamycin was added.



2. 0.4 mM Isopropyl- $\beta$ -D-thiogalactopyranoside (IPTG) 28 mg  
 28 mg of IPTG was used to obtain 300 ml of LB at a final concentration of 0.4 mM.

3. 0.5 M Phenylmethyl Sulfonyl Fluoride (PMSF) 10 ml  
 0.87 g of PMSF was dissolved in 10 ml of absolute ethanol.

4. 10% Polidocanol 10 ml  
 1 ml of 100% polidocanol was diluted in 9 ml of DI water.

5. 0.5 M ethylenediaminetetraacetic acid (EDTA) 100 ml  
 18.6 g of EDTA was dissolved in 100 ml of distilled water.

6. 0.5 M Butylated Hydroxytoluene (BHT) 10 ml  
 0.44 g of BHT was dissolved in 10 ml of absolute ethanol

7. Lysis buffer 1000 mL

Composition:	10 mM Tris (hydroxymethyl)aminomethane	1.2 g
	1.4 mM $\beta$ -Mercaptoethanol	0.1 ml of 14 M $\beta$ -ME
	100 $\mu$ M PMSF	0.2 ml of 0.5 M PMSF
	100 $\mu$ M EDTA	0.2 ml of 0.5 M EDTA
	50 $\mu$ M BHT	0.2 ml of 0.5 M BHT

The final volume was brought to 1000 mL with distilled water and the pH was adjusted to 7.4 with 12 M HCl

8. Washing buffer 1000 mL

Composition:	10 mM Tris (hydroxymethyl)aminomethane	1.2 g
	1.4 mM $\beta$ -Mercaptoethanol	0.1 ml of 14 M $\beta$ -ME

100 $\mu$ M PMSF	0.2 ml of 0.5 M PMSF
50 $\mu$ M BHT	0.2 ml of 0.5 M BHT
9.9 mM EDTA	19.8 ml of 0.5 M EDTA
150 mM NaCl	5.32 g
0.01% SDS	1 ml of 10% SDS

The final volume was brought to 1000 mL with distilled water and the pH was adjusted to 7.4 with 12 M HCl

9. Eluting buffer		8 ml
Composition:	Lysis buffer	6 ml
	10 mM $MgCl_2$	80 $\mu$ l of 1 M $MgCl_2$
	10 mM ATP	45.8 mg
	0.025% polidocanol	20 $\mu$ l of 10% polidocanol
	0.2 mM DNP-SG	54.2 $\mu$ l of 29.5 mM DNPSG

All ingredients were mixed with 6 ml of Lysis buffer and the pH was adjusted to 7.4 with 1 M NaOH. The final volume was brought to 8 ml with lysis buffer.

10. Dialysis buffer 2000 mL

20 ml of DE-52 resin along with 2 ml of 10% SDS solution was added to the 2000 mL of Lysis buffer.

### 2.15.2 Methods

300 ml of LB medium was sterilized by autoclaving for 45 min at 120 °C at 15 psi. Kanamycin was added after cooling, obtaining a final concentration of 50 µg/ml. Then, 10 µl of town *E. coli* BL21(DE3) expressing RLIP76 were inoculated into 3 ml of LB medium and incubated for 12 hours at 37°C, and 227 rpm. Then, the culture was diluted to the final volume of 300 ml and incubated at 37 °C, and 227 rpm. The protein expression was induced by adding 0.4 mM IPTG to the culture when its optical density read at 600 nm reached 0.6.

After 12 hours of incubation, *E. coli* was harvested by centrifugation at 14000 g for 15 min at 4°C. The pellet was resuspended in 10 ml of lysis buffer containing 100 µM PMSF, 1% Polidocanol and 2 mM EDTA followed by sonication in ice at 50 W for 30 sec. After 4 hours of incubation at 4 °C with gently shaking the mixture was centrifuged at 27000 g for 30 minutes at 4 °C and the pellet was discarded. The supernatant was subjected to affinity chromatography over a 1x10 cm column of DNP-SG coupled CNBr-activated Sepharose 4B resin, previously equilibrated with lysis buffer at a flow rate of 4 ml/hour; this flow rate was maintained throughout the affinity chromatography. The unbound proteins were removed with washing buffer and washing buffer containing 0.01% SDS until the absorbance at 280 nm was zero. RLIP76 was eluted with 8 ml of elution buffer. Next, the protein was dialyzed in 2 liters of fresh dialysis buffer at 4 °C for 3 days and lyophilized.

## 2.16 Sodium Dodecyl Sulfate Polyacrylamide Gel Electrophoresis (SDS-PAGE)

Denaturing gel electrophoresis was carried out according to the method of Laemmli (Laemmli et al., 1970).

### *2.16.1 Materials*

1. 60% acrylamide, bis-acrylamide (AB) 100 ml  
60 g acrylamide was mixed with 1.6 g bis-acrylamide and dissolved to the final volume of 100 ml with distilled water.
2. 3 M Tris (hydroxymethyl)aminomethane, pH 8.8 100 ml  
36.32 g of tris base was dissolved in 75 ml of DI water and the pH was adjusted to 8.8 with 12 M hydrochloric acid, followed by dilution to the final volume of 100 ml.
3. 0.5 M Tris (hydroxymethyl)aminomethane, pH 6.8 100 ml  
6.04 g of tris base was dissolved in 75 ml of DI water and the pH was adjusted to 6.8 with 12 M hydrochloric acid, followed by dilution to the final volume of 100 ml.
4. 10% (w/v) sodium dodecyl sulfate (SDS) 100 ml  
10 g of SDS was dissolved in 100 ml of DI water.
5. 5% (w/v) ammonium persulfate (APS) 1 ml  
50 mg of APS was dissolved in 1 ml of DI water. The solution was made fresh daily.
6. N,N,N',N',- tetramethylethylenediamine (TEMED)

This reagent was obtained from the manufacturer (Sigma-Aldrich) and used as received.

#### 7. 14.5 M $\beta$ -mercaptoethanol ( $\beta$ -ME)

This reagent was obtained from the manufacturer (Bio-Rad) and used as received.

8. Running buffer 1000 mL

Composition:	0.025 M Tris (hydroxymethyl)aminomethane	3.03 g
	0.192 M Glycine	14.4 g
	0.1% SDS	1.00 g

All ingredients were mixed together and diluted to the final volume of 1000 ml with DI water.

9. Sample buffer 3.1 ml

Composition:	0.5 M Tris (hydroxymethyl) aminomethane, pH 6.8	1.25 ml
	14.5 M $\beta$ -Mercaptoethanol	0.15 ml
	SDS	0.2 g
	0.1% Bromophenol Blue	0.2 ml
	Glycerol	1.5 ml

#### 10. Broad range molecular weight marker from Bio-Rad

Myosin	206 000 Daltons
$\beta$ -galactosidase	117 000 Daltons
Bovine serum albumin	79 000 Daltons
Ovalbumin	48 300 Daltons

Carbonic anhydrase	34 200 Daltons
Soybean trypsin inhibitor	29 300 Daltons
Lysozyme	21 300 Daltons
Aprotinin	7 300 Daltons

The standard solution was made according to the manufacturer's instructions

11. Staining solution		150 ml
Composition:	Coomassie Blue R	0.5 g
	Methanol	100 ml
	Acetic acid	50 ml
12. Destaining solution		100 ml
Composition:	Methanol	20 ml
	Acetic acid	10 ml
	Water	70 ml

SDS-PAGE was carried out on a 12.5% resolving gel and a 7% stacking gel. The compositions of the gels solutions are given in Table 2.5 and Table 2.6, respectively.

### *2.16.2 Methods*

All the components of the resolving gel, except APS and TEMED, were mixed and subjected to vacuum aspiration for 15 min. APS and TEMED were added with gentle swirling immediately prior to pouring the gel solution between two glass plates. After resolving, the stacking gel solution, prepared in a similar manner, was poured on

top of the resolving gel and 10 lane comb was inserted into the liquid prior to polymerization to facilitate the wells formation.

Table 2.5 Denaturing 12.5% resolving gel solution

<b>Components</b>	<b>2 Gels</b>	<b>4 Gels</b>
<i>Water</i>	7.25 ml	14.5 ml
<i>60% AB</i>	2.34 ml	4.48 ml
<i>10% SDS</i>	0.112 ml	0.225 ml
<i>14.5 M b-mercaptoethanol</i>	1.87 µl	3.75 µl
<i>3 M Tris-HCl, pH 8.8</i>	1.40 ml	2.81 ml
<i>5% APS</i>	0.112 ml	0.225 ml
<i>TEMED</i>	11.2 µl	22.5 µl

Table 2.6 Denaturing 7% stacking gel solution

<b>Components</b>	<b>2 Gels</b>	<b>4 Gels</b>
<i>Water</i>	3.07 ml	6.13 ml
<i>60% AB</i>	0.60 ml	1.2 ml
<i>10% SDS</i>	0.05 ml	0.1 ml
<i>0.5 M Tris-HCl, pH 6.8</i>	1.30 ml	2.6 ml
<i>5% APS</i>	50 µl	100 µl
<i>TEMED</i>	11.2 µl	22.5 µl

### *2.16.3 Sample preparation*

Lyophilized protein, about 2-3  $\mu\text{g}$ , was diluted in 20  $\mu\text{l}$  of denaturing sample buffer and placed in boiling water for 2 min in a sealed glass tube. Then, after removing the comb from the stacking gel, 3  $\mu\text{l}$  of the marker was loaded to the first well and the sample was applied to the next well upon cooling.

### *2.16.4 Electrophoresis*

SDS-PAGE was conducted at room temperature with a constant voltage of 200 V for 45 min, or until the bromophenol blue dye front reached the bottom of the resolving gel.

### *2.16.5 Protein visualization*

After electrophoresis, the gel was placed in a Petri dish with Coomassie Blue protein staining solution and incubated with moderate rocking for 3 hours at room temperature. Then, the staining solution was replaced with destaining solution. Five changes of destaining solution were needed over several hours in order to obtain a colorless gel, except for the protein's band which had stained dark blue.

## 2.17 Western blot analysis

Immunoblotting was performed according to the procedure of Towbin (Towbin et al., 1979), where protein identification is based on both antibody and antigens reactions.



### 2.17.1 Materials

1. Blotting buffer 2000 mL

Composition: methanol 400 ml  
25 mM Tris (hydroxymethyl) aminomethane 6.06 g  
192 mM Glycine 28.8 g

All ingredients were mixed together and diluted with DI water to a final volume of 2000 mL.

2. Tris-buffered saline (TBS) 2000 mL

Composition: NaCl 9.92 g  
Tris (hydroxymethyl) aminomethane 1.21 g

The above solution was diluted to a final volume of 2000 mL with DI water and pH was adjusted to 7.5 with 12 M HCl.

3. Blocking solution 100 ml

This solution was prepared by dissolving 5 g of non fat dried milk (NFDM) in 100 ml of TBS, pH 7.5.

4. Anti-protein primary antibody 20 µl/8ml of blocking buffer

Primary antibody was used at a 1:500 dilution for blots in which 5 mg of protein per well had been loaded on the corresponding gel

5. Secondary antibody solution 20 µl/8ml of blocking buffer

Goat horseradish peroxidase-conjugated antibody to rabbit IgG was used at 1:1000 dilutions.

6. Developing reagent

Color development solution was prepared by dissolving 60 mg 4-chloro1-naphthol in 20 ml of ice cold methanol and mixing it with 100 ml TBS containing 60  $\mu$ l of 30% H<sub>2</sub>O<sub>2</sub> immediately prior to use

#### *2.17.2 Methods*

Protein's fractions were first separated on a denaturing SDS polyacrylamide gel. Then, the gel was washed with blotting buffer for 30 min with gentle shaking. Previous to blotting, the gel was placed between a soak sponge pad containing whatman paper and a nitrocellulose membrane. Next, the cassette was assembled in a blotting chamber (Bio-Rad transblot cell) containing blotting buffer, and the blotting was performed under the constant current of 240 mA for 4 hours. Upon completion of blotting, the nitrocellulose membrane was removed from the cassette and washed with TBS containing 5% NFDm for 30 min at room temperature with gentle shaking. After that the membrane was removed from the milk and placed in a freshly made primary antibody solution for incubation overnight. The next day, the blot was washed four times in 10 min intervals with TBS containing 5% NFDm and eventually incubated with the secondary antibody solution for 4 hours. Then, the blot was washed with TBS followed by soaking in a color development solution to develop the color reaction, which resulted in identifying the antigen as a band. After the protein's band had reached a saturated blue-violet color, the blot was immediately placed in the DI water in order to terminate the color development reaction, and rinsed for 5 min before being dried out.

## 2.18 Reconstitution of purified recombinant protein into proteoliposomes

Reconstitution of purified recombinant proteins into proteoliposomes was performed by the method described by Awasthi (Awasthi et al., 1998).

### *2.18.1 Materials*

#### 1. Purified recombinant protein

2. Reconstitution buffer 2500 mL

Composition:	10 mM Tris-HCl, pH 7.4	25 ml of 1 M Tris-HCl, pH 7.4
	2 mM MgCl <sub>2</sub>	5 ml of 1 M MgCl <sub>2</sub>
	1 mM EGTA	0.95 g
	100 mM KCl	18.6 g
	40 mM sucrose	34.2 g
	2.8 mM $\beta$ Mercaptoethanol	0.48 ml of 14.5 M $\beta$ -ME
	0.05 mM BHT	0.25 ml of 0.5 M BHT
	0.025% polidocanol	6.25 ml of 10% polidocanol

All components were mixed and the final volume was brought to 2500 mL with DI water.

#### 3. Mixture of soybean lipids and cholesterol (4:1 ratio)

40 mg/ml Asolectin	62.0 mg
10 mg/ml Cholesterol	15.5 mg

The aqueous emulsion was prepared in 1.55 ml of reconstitution buffer by sonication at 50 W for 30 sec and left at 4 °C with gentle shaking for 4 hours.

#### 4. SM-2 Bio-beads

1 g

SM-2 Bio-beads were pre-equilibrated with 5 ml of reconstitution buffer without polidocanol for 6 hours.

#### *2.18.2 Methods*

Purified protein present in the elution buffer was dialyzed against reconstitution buffer overnight. Next, 100 µl of aqueous emulsion of soybean asolectin and cholesterol were added to 900 ml of purified protein and the mixture was sonicated at 50 W for 30 sec. In order to initiate a vesicle formation, 200 mg of SM-2 Bio-beads, pre-equilibrated in the reconstitution buffer was added to the protein mixture. Vesiculation was carried out for 4 hours at 4 °C, followed by removal of SM-2 Bio beads by centrifugation at 3620 g.

#### 2.19 Mammalian cell transfection

Cell transfection is a process of introduction of foreign genes into mammalian cells. The targeted DNA is delivered to the cell in the form of cationic lipoplexes through endocytosis. After escaping the endosomal pathway, complexes diffuse through the cytoplasm and enter the nucleus during mitosis, when the membrane is more permeable. In the nucleus, foreign DNA incorporates itself into the chromosomes, which lead to the targeted gene expression.

### 2.19.1 Cloning into the eukaryotic expression vectors

Eukaryotic expression vectors are used in order to perform transient, stable, or inducible cell transfection.

#### 2.19.1.1 pcDNA3.1(+)

This eukaryotic expression system is a 5.4 kb vector designed for high level stable and transient expression in mammalian hosts.

The vector contains the following elements:

- CMV promoter
- multiple cloning sites
- neomycin resistance gene for selection of stable cell lines
- ampicillin resistance gene for *E. coli* DH5 $\alpha$  transformants selection

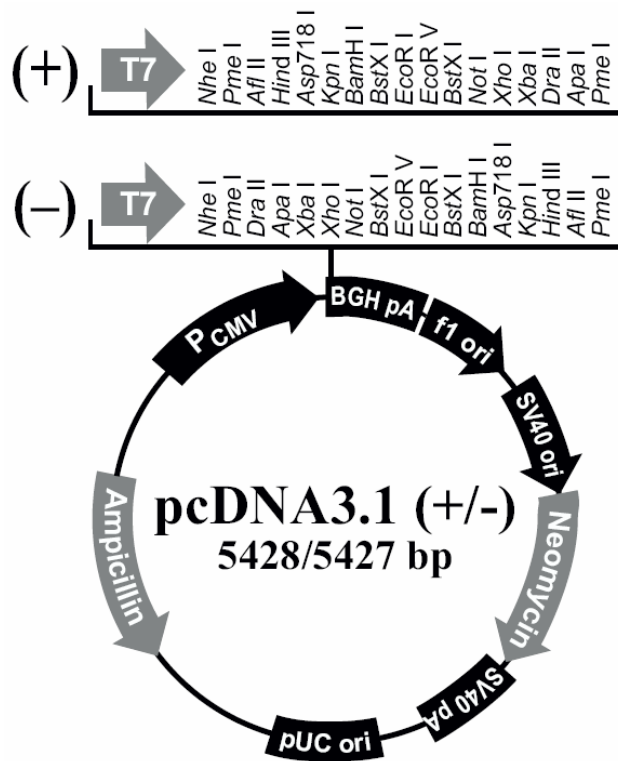


Figure 2.5 pcDNA3.1 vector map (Invitrogen)

Molecular manipulation experiments were performed in order to clone the targeted gene into pcDNA 3.1(+) expression vector and were based on the Molecular Cloning Manual by Sambrook and Russell (Sambrook and Russell, 1989). All solutions were prepared as described previously.

#### 2.19.1.2 Ecdysone inducible vector

Ecdysone inducible mammalian expression system is designed to provide the tightest control of expression available in mammalian cells. The system is based on a synthetic ecdysone-inducible receptor and a synthetic receptor recognition element that modulates expression of the gene of interest. Two plasmids, pVgRXR receptor vector

and pIND expression vector form the basics of the system. The pVgRXR plasmid contains an expression cassette from which the VgEcR and RXR protein are constitutively expressed. The pIND plasmid contains the muristeron A inducible cassette and multiple cloning sites for inserting the gene of interest. After addition of the inducer - muristeron A, a conformational change of the receptor subunits removes transcription repressors and recruits transcriptional machinery to activate transcription of targeted gene.

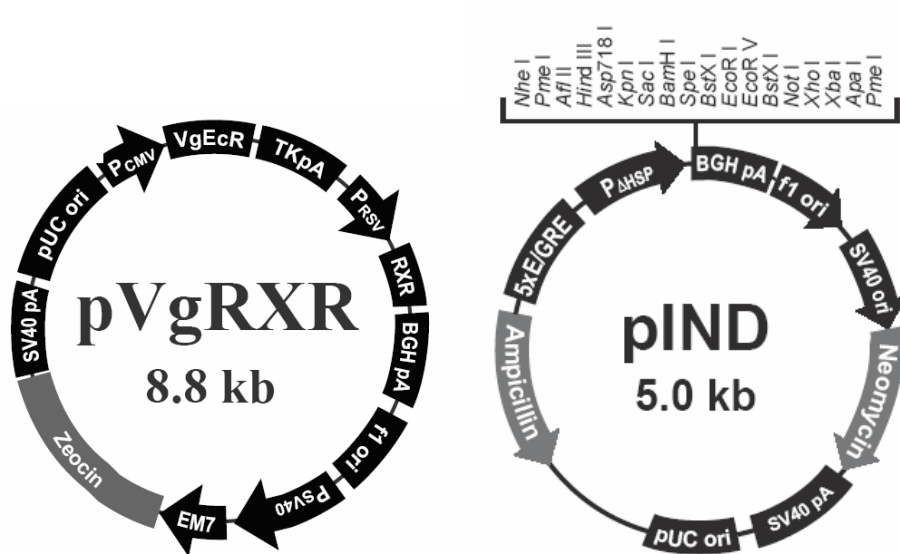


Figure 2.6 Maps of pVgRXR and pIND vectors which form the ecdysone inducible system (Invitrogen)

In this system double transfection of cells is required. First, the cells are stably transfected with pVgRXR. Next, Zeocin selected transfectants are transiently transfected with pIND containing targeted gene. The protein is expressed after addition of steroid.

### *2.19.2 Stable cell transfection*

Before starting, the cells' transfection antibiotic concentration, required to kill 100% of cell within 14 days, needs to be established. The concentration of this selective marker is essential to perform stable transfection.

In order to carry out the transfection, about  $1 \times 10^6$  cells were plated in six well plate and different concentrations of antibiotic were added to the medium, from 100  $\mu\text{g/ml}$  to 1  $\text{mg/ml}$ . After two weeks of cell monitoring, the lowest concentration of antibiotic which killed all of the cells was chosen as a selective marker. After cell transfection, only cells containing an antibiotic resistant gene survived in the RPMI medium containing antibiotic.

#### 2.19.2.1 Method

In a six well plate, approximately  $0.5 \times 10^6$  cells per well were seeded in 2 ml of the RPMI growth medium supplemented with 10% fetal bovine serum. The cells were incubated at 37 °C in a CO<sub>2</sub> incubator until the cells achieved 90% of confluence (24 hours). Next, the medium was siphoning off and the cells were washed with PBS. The following mixtures of lipofectamine, eukaryotic expression vector containing targeted gene, and Opti-MEM I medium were added in order to optimize transfection conditions (Table 2.7).



Table 2.7 Conditions for stable cell transfection using Lipofectamine 2000 (Invitrogen)

<b>Lipofectamine:DNA ratio</b>	<b>vector stock* [ml] and Opti-MEM I volume [ml]</b>	<b>Lipofectamine [ml] and Opti-MEM I volume [ml]</b>
1:0.5	4 in 250	2 in 248
1:1	4 in 250	4 in 246
1:1.5	4 in 250	6 in 244
1:2	4 in 250	8 in 242
1:3	4 in 250	12 in 238

Note: vector stock concentration 1 µg/µl

Then, the complexes were removed from the cells and the medium was changed after 24 hours of incubation in order to avoid a toxicity of the transfection mixture. The cells were incubated for another 24 hours with RPMI medium to allow them to recover. The following day, a selective marker antibiotic was added to the cells' medium with a previously determined concentration. The medium containing antibiotic was replaced every 3 days for next 14 days and few colonies of transfected cells were isolated. Each clone was transferred to a separate well of a 24 well tray and allowed to grow in the required antibiotic medium. When cells became confluent, clones were transferred to larger six well trays. Then, each colony grown from a single cell was tested for protein expression on the RNA and DNA level.

### *2.19.3 Transient cell transfection*

In the case of transient transfection, incubation of the cell with medium containing antibiotic is not required. The procedure is similar to the transient transfection described previously. Briefly, approximately  $0.5 \times 10^6$  cells were seeded in a 12 well plate containing the RPMI growth medium supplemented with 10% fetal bovine serum and 1% P/S. The cells were incubated at 37 °C in a CO<sub>2</sub> incubator until the cells achieved 90% of confluence (24 hours). Next, after pipetting out the medium, the cells were washed with PBS and the mixtures of different concentrations of lipofectamine and eukaryotic expression vector containing targeted gene and Opti-MEM I medium were added to the cells. After 3-4 hours, the complexes were removed from the cells and cells were incubated for another 24 hours in medium containing serum. Then, the protein expression was checked on the RNA and DNA level.

### 2.20 MTT Doxorubicin sensitivity assay

The MTT Cell Proliferation Assay first described by Mosmann in 1983 (Mosmann et al., 1983) is a colorimetric assay system which measures the reduction of a tetrazolium component (MTT) into an insoluble formazan salt by the mitochondria of viable cells. The samples are read using an ELISA plate reader at a wavelength of 570 nm. The amount of color produced is directly proportional to the number of viable cells.

### 2.20.1 Materials

1. Cells	2x10 <sup>6</sup> cells/ml
2. Doxorubicin stock	3.4 mM
3. Liposomes containing 40 µg/ml of POB1 or POB1 <sup>1-512</sup>	
4. RPMI-1640 medium containing 10% Fetal Bovine Serum and 1% P/S	
5. [3-(4,5-dimethylthiazol-2-yl)-2,5-diphenyltetrazolium bromide] MTT	5 mg/ml PBS
6. DMSO (Sigma-Aldrich)	10 ml

### 2.20.2 Methods

Cell density during the log phase was determined by counting trypan blue excluding cells in a hemocytometer. 20,000 cells present in 160 µl of RPMI-1640 medium were plated into 11 lanes of 96 well flat bottomed microtiter plates, leaving the first lane for 200 µl of medium without cells. After 24 hours of incubation, the cells were treated with 40 µl of control liposomes or liposomes containing recombinant full length POB1 or POB1<sup>1-512</sup>. Next, the cells were washed twice with PBS and 160 µl of medium followed by the addition of 40 µl of different concentrations of Doxorubicin stock solutions (Table 2.8). After 96 hours of cell incubation at 37 °C, and CO<sub>2</sub> atmosphere, 20 µl of MTT was added in each well and the incubation was continued for next 2 hours. After that, the medium was discarded by centrifugation and 100 µl of DMSO

was added into each well. The plate was again incubated for another 2 hours at room temperature with gentle shaking and read at 570nm in an ELISA plate reader.

Eight replicate wells were used for each point in each of three separate measurement of IC<sub>50</sub>.

Table 2.8 Doxorubicin stock solution preparation for IC<sub>50</sub> measurements

<b>Lane</b>	<b>Final DOX concentration</b>	<b>Composition of stock solutions</b>	<b>Stock concentration</b>
1	-	200 µl medium RPMI	-
2	-	20,000 cells + 40 µl medium	-
3	0.01 µM	25 µl of 1 µM DOX + 475 µl medium	0.05 µM
4	0.04 µM	100 µl of 1 µM DOX + 400 µl medium	0.2 µM
5	0.07 µM	17.5 µl of 10 µM DOX + 482.5 µl medium	0.35 µM
6	0.1 µM	25 µl of 10 µM DOX + 475 µl medium	0.5 µM
7	0.15 µM	37.5 µl of 1 µM DOX + 462.5 µl medium	0.75 µM
8	0.2 µM	50 µl of 10 µM DOX + 450 µl medium	1.0 µM
9	0.4 µM	100 µl of 10 µM DOX + 400 µl medium	2.0 µM
10	0.7 µM	17.5 µl of 100 µM DOX + 482.5 µl medium	3.5 µM
11	1 µM	25 µl of 100 µM DOX + 475 µl medium	5.0 µM
12	2 µM	50 µl of 1 µM DOX + 450 µl medium	10 µM

## 2.21 Isolation of RNA by TRIZOL method

RNA can be purified from both cells and tissues using the Trizol Reagent method of Sambrook (Sambrook, 1989). The method is fast, simple and gives very high yield in terms of RNA purification.

### *2.21.1 Materials*

1. $10 \times 10^6$ cells or 50 mg tissue	
2. Trizol reagent (Sigma)	1 ml per purification
3. Chloroform (Sigma)	0.2 ml
4. Isopropyl alcohol (Sigma)	0.5 ml
5. 75% ethanol (Sigma)	1 ml
6. TE buffer	10 ml
Composition:	10 mM Tris(hydroxymethyl)aminomethane 12.1 mg
	1mM EDTA, 2.9 mg

All ingredients were mixed together and 6 ml of sterile water was added. Then, the pH was adjusted to 7 with 12 M HCl and the final volume was brought to 10 ml with sterile water.

### *2.21.2 Methods*

Trizol reagent was added to PBS washed cells and mixed by repetitive pipetting in an Eppendorf tube. To isolate RNA, the tissue was cut into small pieces, Trizol reagent was added, and the mixture was homogenized at 4 °C in ice for not more than 30 sec at a low speed. Next, the samples were incubated for 5 min at room temperature to permit dissociation of nucleoprotein complexes followed by addition of chloroform and incubation for 5 min at room temperature after vigorous shaking for 15 sec. Then, the samples were centrifuged for 15 min at 12000 g at 4 °C. The resulting three layer mixture was carefully handled to make sure that all layers remained separated. The lower, red, phenol-chloroform phase contained proteins, the middle, white, interphase had DNA and the upper, colorless, aqueous phase contained RNA. The upper phase was collected in an Eppendorf tube and RNA was precipitated with isopropyl alcohol for 10 min at room temperature followed by centrifugation at 12000 g for 10 min at 4 °C. Supernatant fluid was removed from the tube and the resulting pellet was washed with ethanol at 12000 g for 10 min at 4 °C. After that, the pellet was dried under vacuum for 10 min and dissolved in 200 µl of TE buffer. The RNA concentration was determined by measuring the absorbance at 260 and 280 nm, using the following equation:

- $\text{O.D. at 260 nm} / \text{O.D. at 280 nm} = 40 \mu\text{g/ml of RNA.}$

In addition, the concentration of RNA was confirmed by running an RNA gel.

## 2.22 Agarose gel electrophoresis of RNA.

### *2.22.1 Materials*

1. Running buffer (25x) 1000 mL

#### Composition:

40 mM 3-(N-Morpholino)-propanesulfonic acid (MOPS)	8.3 g
10 mM Sodium Acetate	34.0 g
2 mM EDTA Sodium Salt	18.7 g

All ingredients were mixed together and brought to the final volume of 1000 mL with distilled water; pH was adjusted to 7 with 5 M NaOH. 1.5% of 12 M formaldehyde was added to the running buffer right before using.

2. RNA loading buffer

#### Composition:

Formamide	0.75 ml
5 x RNA running buffer	0.3 ml
12 M formaldehyde	0.24 ml
Glycerol	0.15 ml
1.2% bromophenol blue	0.05 ml

Ethidium bromide 10  $\mu$ l

All ingredients were mixed in an Eppendorff tube and stored at -20 °C.

3. 1% Agarose (Sigma) 0.4 g

Agarose was dissolved in 40 ml of RNA running buffer in order to make a 1% gel and heated in the microwave oven for 1 min. After cooling, 1 ml of 12 M formaldehyde was added. Next, the solution was poured into the gel casting tray and allowed to solidify for 30 min at room temperature.

#### *2.22.2 Methods*

Before running an RNA gel all glassware was washed with RNase Zap to remove impurities and possible RNAases. After the preparation of running buffer, RNA loading buffer, and gel solidifying, the sample of RNA was prepared as follows:. The same volumes of RNA and loading buffer (example 5  $\mu$ l of RNA and 5  $\mu$ l of sample buffer) were mixed together followed by incubation at 60 °C for 10 min in order to denature RNA. Then, the sample was removed from a water bath and cooled on ice for 5 min. The RNA ladder was prepared similarly with only one difference; the mixture contained 1  $\mu$ l of RNA ladder, 3  $\mu$ l of water and 3  $\mu$ l of RNA loading buffer. The gel was run at 70 V for 2 hours.

#### 2.23 Reverse transcription polymerase chain reaction (RT-PCR)

RT-PCR is a method used for amplifying data containing RNA by converting it into DNA, and then amplifying it. The RNA strand is first reverse transcribed into its



complementary DNA, followed by amplification of the resulting DNA using polymerase chain reaction (PCR). Qiagen OneStep RT-PCR kit was used.

### 2.23.1 Materials

RNA samples	3-15 $\mu$ l
dNTP mixture	0.5 $\mu$ l
Qiagen OneStep RT-PCR buffer (5x)	5 $\mu$ l
Forward primer	1 $\mu$ l
Reverse primer	1 $\mu$ l
RT – PCR enzymes mix	0.5 U

Note: RT-PCR enzymes mix contains:

- Omniscript reverse transcriptase
- Sensiscript reverse transcriptase
- HotStarTaq DNA polymerase

Total volume was diluted to 25  $\mu$ l with water (RNAse free).

### 2.23.2 Methods

The RT-PCR was carried out in a Applied Biosystem, Gene Amp, PCR system 2700 thermocycler using a temperature cycle profile with the following conditions (Fig 2.6):

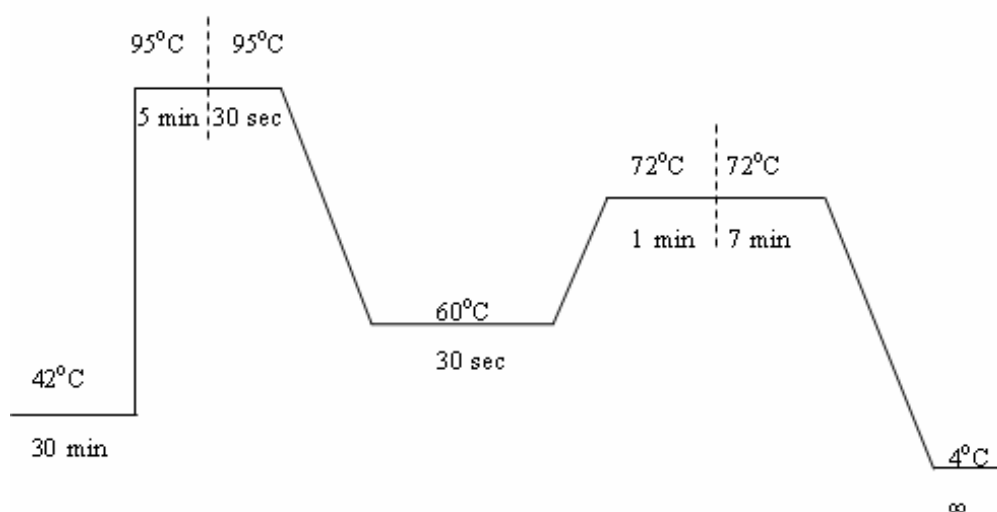


Figure 2.7 Temperature cycle profile for RT-PCR.

After completion of RT-PCR (about 4hours) the samples were stored at -20 °C. In order to run an agarose gel, only 5 µl of PCR mixture were used.

### 2.24 Agarose gel electrophoresis of DNA.

Agarose gel electrophoresis is the easiest and the most common way of separating and analyzing DNA. The purpose of the gel is to quantify DNA or to isolate

a particular band. The DNA is visualised in the gel by the addition of a fluorescent dye, ethidium bromide, which intercalates strongly between DNA bases.

#### 2.24.1 Materials

1. Tris-acetate-EDTA (TAE) buffer (50x) 1 L

Composition:

2 M Tris (hydroxymethyl)-aminomethane	242 g
Glacial acetic acid	57.1 ml
0.5 M EDTA (pH 8)	100 ml

All components were diluted to a final volume of 1000 mL with sterile, distilled water and kept at 4 °C for further usage. The pH 8.4 was adjusted with glacial acetic acid. The 1x working solution contained 40mM Tris-acetate and 1mM EDTA.

2. DNA loading buffer 10 ml

Composition:

Ficoll 400	20%
EDTA, pH 8	0.1 M
SDS	1%

Bromophenol Blue

0.25%

All components were mixed together and stored at room temperature in a tube covered with aluminum foil.

#### 2.24.2 Methods

Agarose powder was mixed with TAE buffer to the desired concentration, and then heated in a microwave oven until completely melted. After cooling the solution to about 60 °C, ethidium bromide is added to the gel (final concentration 0.5 µg/ml) to facilitate visualization of DNA after electrophoresis. Next, the gel is poured into a casting tray containing a sample comb and allowed to solidify at room temperature. To prepare the sample, DNA was combined with a DNA loading buffer in a 1:5 ratio and loaded into one well. In order to make bands visible on the gel, an optimum amount of DNA should be 1-2 µg. The 1% agarose gel was run at 80 V for 45 min.

### 2.25 Prokaryotic expression of POB1 and POB1<sup>1-512</sup>

All molecular manipulations were performed in a similar manner as described previously.

#### *2.25.1 Cloning of POB1 and POB<sup>1-512</sup> into a prokaryotic expression vector pET30a(+)*

The 2200 bp full length long version cDNA of POB1 was kindly provided by Prof. Leen J. Blok, Erasmus University, Rotterdam, Netherlands. The cDNA of POB1 was used as a template for PCR amplification of the POB1 full length and POB<sup>1-512</sup> deletion mutant coding sequence.

- The PCR mixture of 100  $\mu$ l consisted of the following ingredients:

DNA template	500 ng
Forward primer (Biosynthesis)	30 pmol
Reverse primer (Biosynthesis)	30 pmol
dNTPmix (Applied Biosystems)	2.5 $\mu$ M each
Thermopol buffer (New England Biolabs)	1 x
BSA (New England Biolabs)	1 x
Vent polymerase (New England Biolabs)	2.5 U

The PCR was carried out in a Applied Biosystem, Gene Amp, PCR system 2700 thermocycler using a temperature cycle profile of 95  $^{\circ}$ C for 5 minutes, 35 cycles of 95  $^{\circ}$ C for 30 sec, 60  $^{\circ}$ C for 60 sec, and 72  $^{\circ}$ C for 1 min followed by 72  $^{\circ}$ C for 7 minutes. The final holding temperature was 4  $^{\circ}$ C .( figure.2.7.)

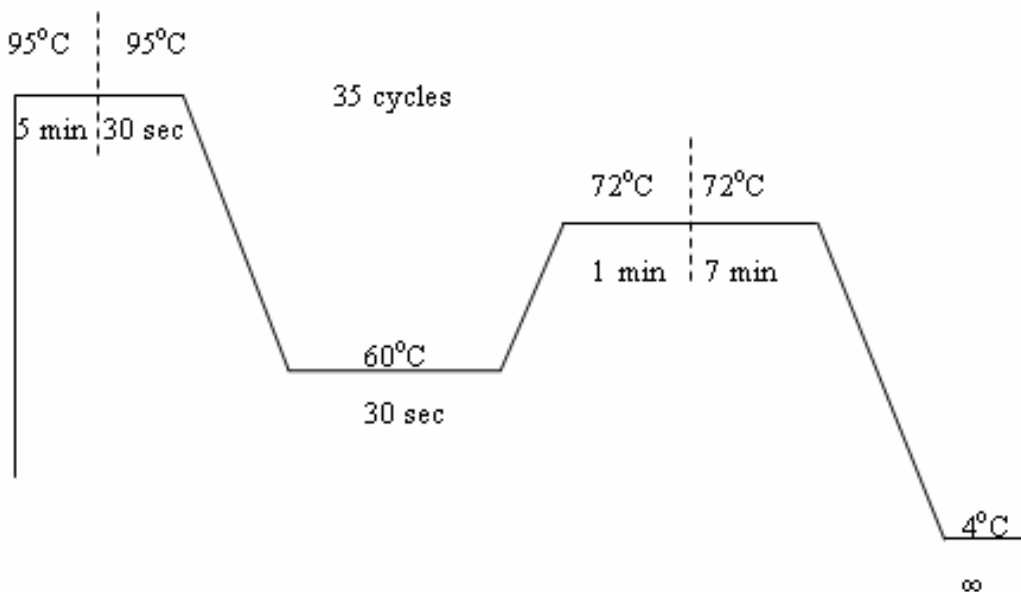


Figure 2.8 Temperature cycle profile for PCR of POB1 and POB<sup>1-512</sup>

The following primers, upstream and downstream, were designed to introduce a BamH1 restriction site (forward primer) immediately upstream of the initiator codon and a Xho I site (reverse primer) immediately downstream of the stop codon of the POB1 and POB<sup>1-512</sup> open reading frame.

- *POB1-BamH1 forward primer:*

5'GGCGGATCCATGGAGGCGGCAGCGGC 3'

T<sub>m</sub> = 87 °C

- *POB1-XhoI reverse primer:*

5'CCGCTCGAGTCACAACACAGTGACCGGAC 3'

T<sub>m</sub> = 84 °C

○ *POB<sup>1-512</sup>-XhoI reverse primer*

5'CCGCTCGAGGGTAACAATCCTGACTTGGTA 3'

T<sub>m</sub> = 82 °C

The PCR product was purified using a Qiagen PCR purification kit and digested with BamHI/XhoI restriction enzymes. The cleaved PCR product was ligated into pET30a (+), a prokaryotic expression vector, previously digested with the same restriction enzymes. After overnight ligation at room temperature, the products were expressed into the DH5a competent cells and plasmid DNA was purified from the overnight culture of a single colony using a Qiagen DNA purification kit. Following verification of the sequence of POB1, the pET30 a(+) plasmid containing the full-length POB1 was used to transform *E. coli* strain BL21(DE3), and protein was expressed in *E. coli* BL21(DE3).

#### 2.26 Purification of recombinant POB1 and POB<sup>1-512</sup> from E.Coli BL21(DE3).

POB1 and POB<sup>1-512</sup> were purified from *E. coli* over Ni-NTA super flow resin (Qiagen) thanks to the presence of 6 histidine residues at the C - terminal of the protein.

##### *2.26.1 Materials*

1. LB Medium 300 ml

LB medium was prepared as described previously.

2. Isopropyl-β-D-thiogalactopyranoside (IPTG) 27 mg

3. Ni-NTA superflow resin (QIAGEN) 1 ml
4. 1 M Tris (hydroxymethyl)-aminomethane (Tris-HCl) 100 ml
- 12.1 g of Tris base was dissolved in 80 ml of water and the pH was adjusted to 7.9 with 12 M HCl. The final volume was diluted to 100 ml with sterile water.

5. 0.5 M Phenylmethylsulphonylfluoride (PMSF) 10 ml
- 0.87 g of PMSF was dissolved in 10 ml of absolute ethanol

6. 1 M Imidazole 100 ml
- 6.8 mg of imidazole was dissolved in 100 ml of sterile water.

7. Lysis buffer 1000 mL

Composition:

20 mM Tris (hydroxymethyl)-aminomethane	2.4 g
250 mM NaCl	14.5 g
100 µM PMSF	200 µl of 0.5 M PMSF
5 mM imidazole	5 ml of 1 M Imidazole

All ingredients were mixed together, the pH was adjusted to 7.9 with 12 M HCl and the final volume was diluted to 1 L with sterile water

8. Washing buffer 1000 mL

Composition:

20 mM Tris (hydroxymethyl)-aminomethane	2.4 g
300 mM NaCl	17.4 g
20 mM imidazole	20 ml of 1 M Imidazole
100 µM PMSF	200 µl of 0.5 M PMSF



The pH was adjusted to 7.9 with 12 M HCl

9. Elution buffer 10 ml

Composition:

20 mM Tris (hydroxymethyl)-aminomethane	24 mg
500 mM NaCl	0.29 g of NaCl
400 mM imidazole	4 ml of 1 M Imidazole
100 $\mu$ M PMSF	2 $\mu$ l of 0.5 M PMSF

All ingredients were mixed together and remaining 5.8 ml of sterile water was added. The pH was adjusted to 7.4 with 5 M HCl.

10. Dialysis buffer 2000 mL

Composition:

10 mM Tris (hydroxymethyl)-aminomethane	24.22 g
100 $\mu$ M EDTA	58 mg
100 $\mu$ M PMSF	400 $\mu$ l of 0.5 M PMSF
0.025% polydocanol, (C <sub>12</sub> E <sub>9</sub> )	5 ml of 10% polidocanol

All ingredients were mixed together in 1500 mL of distilled water and the pH was adjusted to 7.4 with 12 M HCl, followed by dilution to a final volume of 2000 mL with DI water.

### 2.26.2 Methods

Rec-POB1 was purified by metal affinity chromatography over Ni-NTA superflow resin (Qiagen). The overnight culture of *E. coli* BL21(DE3) expressing POB1

was induced with 0.4 mM IPTG, collected as a pellet by centrifugation at 14000 g, and lysed in 8 ml of lysis buffer. Then, the pellet was sonicated on ice at 50 W for 30 sec. After 4 hours of incubation at 4 °C with gently shaking the mixture was centrifuged at 27000 g for 30 min at 4 °C and the pellet was discarded. The supernatant was mixed with Ni-NTA Superflow resin pre-equilibrated with the same buffer. The resin was incubated overnight at 4 °C with gentle shaking and washed with washing buffer until the optical density reached zero. Then, the protein was eluted from the resin with elution buffer and was dialyzed overnight in dialysis buffer.

Next, the protein was lyophilized and polyacrylamide gel electrophoresis and western blot analysis were performed.

### 2.27 Anti-POB1 Immunoglobulin G production

About 600 µg of POB1 protein was required for antibody production. Since, the purification yield of POB1 was very low, 10 protein purifications were carried out from 300 ml of bacterial culture.

#### *2.27.1 Materials*

- |  |        |
|--|--------|
| 1. Recombinant POB1 purified from <i>E. coli</i> | 600 µg |
| 2. New Zealand rabbit                            |        |
| 3. Complete Freund's adjuvant (Sigma)            | 1 ml   |
| 4. Incomplete Freund's adjuvant (Sigma)          | 1 ml   |

### *2.27.2 Methods*

A 3-4 month old New Zealand rabbit, weighing 6-8 lbs., was used to induce antibody production. New Zealand rabbit is the most widely used species for polyclonal antibody production. Rabbits are gentle and easy to handle. Blood sampling from the marginal ear veins is uncomplicated.

Prior to protein injection, the injection sites were shaved and cleaned with betadine solution to prevent abscess formation.

First pre-immune serum was prepared from the rabbit's blood prior to injection. Three days later approximately 0.1 mg of protein in a volume of 0.25 ml was emulsified with an equal volume of complete Freund's adjuvant and injected beneath the skin of the rabbit (subcutaneously) in the area around the shoulders and intra-muscularly into the large muscle of the rear legs. (About 1/4 of the antigen being used in each area). Complete Freund's adjuvant was used as an immunity –stimulating substance that in combination with antigen (purified POB1) enhances immunity levels.

Next, a second and third injection of 0.05 mg protein with incomplete Freund's adjuvant was performed in two weeks intervals. Blood was collected two weeks after from the central ear artery with a 19-gauge needle and allowed to clot and retract at 37 °C overnight. The clotted blood was then refrigerated for 24 hours before the serum was decanted and clarified by centrifugation at 2500 rpm for 20 min, at 5 °C, followed by inactivation at 56 °C for 2 hours.

Next, several booster injection and blood collection at intervals of two weeks were carried out (Table 2.9).

Table 2.9 Procedure for anti-POB1 IgG production

Day	Procedure
0	Pre-bleed (5 ml) to prepare pre-immune serum
3	Primary immunization (subcutaneously 0.05–0.1 ml volume, multiple sites)
17	Booster injection (subcutaneously 0.05–0.1 ml volume, multiple sites)
31	Booster injection (subcutaneously 0.05–0.1 ml volume, multiple sites)
45	Test bleed (2 ml)
59	Booster injection (subcutaneously 0.05–0.1 ml volume, multiple sites)
73	Test bleed (2 ml)
87	Booster injection (subcutaneously 0.05–0.1 ml volume, multiple sites)
101	Production bleed (10-20 ml)
115	Booster injection (subcutaneously 0.05–0.1 ml volume, multiple sites)
129	Production bleed (10-20 ml)
143	Production bleed (10-20 ml)
157	Final bleed (20 ml)

A total of 50 ml of crude serum was collected, and its sensitivity to POB1 antigen was checked by carrying out the western blot (as described previously) and western dot method.

#### 2.28 Anti-POB1 antibody purification

The IgG fractions were purified by DEAE-cellulose anion exchange column chromatography, followed by CNBr – Sepharose protein A column affinity chromatography. The method is widely used and works on the principle that IgG has a higher or more basic isoelectric point than most serum proteins. Therefore, if the pH is

kept below the isoelectric point of most antibodies, the immunoglobulins do not bind to an anion exchanger and are separated from the majority of serum proteins bound to the column matrix. The high capacity of DEAE-cellulose anion-exchange column allows for large-scale purification of IgG from serum.

The second step of purification is CNBr-Sepharose protein A chromatography. This method is based on the properties of protein A, a component of the cell wall of *Staphylococcus aureus*. This protein binds strongly to Fc portion on the heavy chain of immunoglobulin creating multimeric complexes. Next, IgG is eluted with low pH glycine solution after several washings.

#### 2.28.1 Materials

- |  |         |
|--|---------|
| 1. Heat inactivated serum                      | 3 ml    |
| 2. DEAE cellulose anion exchange resin (Sigma) | 1 g     |
| 3. 100 mM Tris (hydroxymethyl)-aminomethane    | 1000 mL |

12.1 g of Tris base was dissolved in 800 ml of distilled water and pH was adjusted to 7 with 12 M HCl. The final volume was brought to 1000 mL with sterile water.

- |   |         |
|---|---------|
| 4. CNBr-sepharose protein A –Sepharose      | 1 g     |
| 5. 100 mM Tris (hydroxymethyl)-aminomethane | 1000 mL |

12.1 g of Tris base was dissolved in 800 ml of distilled water and the pH was adjusted to 8 with 12 M HCl. The final volume was diluted to 1000 mL with sterile water.

- |  |         |
|--|---------|
| 6. 1 M Tris (hydroxymethyl)-aminomethane | 1000 mL |
|--|---------|

121 g of Tris base were dissolved in 800 ml of distilled water and pH was adjusted to 8 with 12 M HCl. The final volume was brought to 1000 mL with sterile water.

7. 10 mM Tris-HCl 100 ml

1.2 g of Tris base was dissolved in 80 ml of distilled water and the pH was adjusted to 7 with 1 M HCl. The final volume was brought to 100 ml with water.

8. 100 mM glycine 100 ml

The buffer was prepared by dissolving 0.75 g of glycine in 100 ml of distilled, sterile water; resulting in pH 3.

#### *2.28.2 Methods*

3 ml of the heat inactivated serum was passed over DEAE cellulose anion exchange column previously equilibrated with 100 mM Tris-HCl, (pH 7.0). The supernatant was collected after centrifugation for 10 min at 1500 g. Meanwhile, 1 ml of CNBr-Sepharose protein A –Sepharose was equilibrated in 100 mM Tris-HCl (pH 8.0) for 4 hours. Next, 0.1 column volume of 1 M Tris-HCl (pH 8.0) was added to the antibody and the mixture was loaded on the column. After overnight incubation at 4 °C on an orbital shaker the unabsorbed fraction was removed by centrifugation and the resin was washed with 10 column volumes of 100 mM Tris-HCl (pH 8.0) followed by 10 column volumes of 10 mM Tris-HCl (pH 8.0). The anti-POB1 IgG was eluted from the column using 1 ml of 100 mM glycine (pH 3.0). Total of 6 fractions were collected followed by measuring the absorbance at 280 nm, using an UV-VIS Spectrophotometer

(Varian 300). The concentrations of each fraction were calculated using the following equation:

$$1.33 \text{ O.D.}_{280} = 1 \text{ mg/ml of IgG.}$$

Next, the sensitivity of pure anti-POB1 IgG was tested by running a Western Blot.

### 2.29 Effect of full length POB1 and POB1<sup>1-512</sup> on cancer cell apoptosis by TUNEL assay

Promega's Apoptosis Detection System (TUNEL assay), based on the method of Gavrieli (Gavrieli et al., 1992) was used in order to detect and quantify apoptotic cells within a cell population consisting of both apoptotic and nonapoptotic cells. The assay is based on the fact that DNA of apoptotic cells undergoes fragmentation and these small fragments are labeled by catalytically incorporating fluorescein-12-dUTP at the 3'-hydroxyl ends of the fragmented DNA by the enzyme Terminal Deoxynucleotidyl Transferase (TdT). Such labeled DNA can be visualized by fluorescence microscopy.

#### *2.29.1 Materials*

1. Solutions provided by Promega:

Equilibration buffer	9.6 ml
Nucleotide Mix	300 $\mu$ l
Terminal Deoxynucleotidyl Transferase	20 $\mu$ l
SSC 20x	70 ml
Incubation buffer	50 $\mu$ l

Composition: 45  $\mu$ l of equilibration buffer + 5  $\mu$ l of dNTP Mix + 1  $\mu$ l of rTdT Enzyme

2. 4% methanol-free formaldehyde (Polyscience) solution in PBS 40 ml

3. 0.2% Triton X-100 solution in PBS	40 ml
4. Propidium iodide (Sigma) 1 µg/ml PBS	40 ml
5. PBS (Gibco)	200 ml

### 2.29.2 Methods

0.5 x 10<sup>6</sup> H358 cells were grown on the poly-L-lysine-coated glass slips. After 24 hours of incubation at 37 °C, in an CO<sub>2</sub> atmosphere, the cells were treated with equal amounts of liposomes reconstituted with 40 µg/ml (final concentration) recombinant full length POB1 and POB1<sup>1-512</sup> protein. The medium was removed after 24 hours, and cells were washed with PBS four times. Next, a TUNEL assay was performed using a Promega Fluorescence detection kit. Briefly, the cells were fixed by immersing slides in a freshly prepared 4% formaldehyde solution in a Coplin jar for 25 min at 4 °C. Then, the cells were washed twice with 1 ml of PBS for 5 minutes at room temperature and incubated for 5 min in 0.2% Triton X-100 solution in order to make the cells' membranes permeable. After an additional washing with PBS, 100 µl of equilibration buffer was pipetted on top of the cover slip followed by incubation for 10 min at room temperature. Next, the area around the equilibrated part was blotted with tissue paper and 50 µl of rTdT incubation buffer was applied on cells. To provide an even distribution of the reagent, the cells were covered with a plastic cover slip and placed in the humidified chamber wrapped with aluminum foil to protect from direct light. The cells were incubated at 37 °C for 60 min. After that, the plastic cover slip was removed and cells were immersed in 40 ml of 2 x SSC solution for 15 min to terminate the



reaction. Unincorporated fluorescein-12-dUTP the cells were removed by washing three times with PBS, followed by staining in 40 ml of propidium iodide solution for 15 min at room temperature in the dark. After washing cells with PBS, the samples were immediately analyzed using Zeiss LSM 510 META (Germany) laser scanning fluorescence microscope at 400 x magnification. Propidium iodide stains both apoptotic and alive cells red. Fluorescein-12-dUTP incorporation results in localized green fluorescence within the nucleus of apoptotic cells only. The following filters were used: 520 nm to view the green fluorescence of fluorescein and 620 nm to view red fluorescence of propidium iodide.

2.30 Transport of <sup>14</sup>C-DOX and <sup>3</sup>H-DNP-SG in proteoliposomes reconstituted with RLIP76 along with POB1 and POB1<sup>1-512</sup>

In this experiment, a fixed amount of purified rec-RLIP76 (20 µg) was reconstituted in proteoliposomes along with varying amounts (0-80 µg) of either POB1 or its deletion mutant (POB1<sup>1-512</sup>) as described previously. Transport of <sup>14</sup>C-DOX and <sup>3</sup>H-DNP-SG was measured in these proteoliposomes according to the method of Awasthi (Awasthi et al., 2000).

*2.30.1 Materials*

1. Transport buffer 250 ml

Composition:

10 mM Tris (hydroxymethyl)-aminomethane, pH 7.4	250ml
1 M Tris (hydroxymethyl)-aminomethane, pH 7.4	2.5 ml
2 mM MgCl <sub>2</sub>	0.5 ml of 1 M MgCl <sub>2</sub>

1 mM EGTA	95 mg
100 mM KCl	1.86 g
40 mM sucrose	3.42 g
2.8 mM $\beta$ Mercaptoethanol	50 $\mu$ l of 14.5 M $\beta$ ME
0.05 mM Butylated hydroxytoluene (BHT)	25 $\mu$ l of 0.5 M BHT

All components were mixed and the final volume was diluted to 250 ml with distilled, sterilized water.

2. [ $^3$ H]DNP-SG (Pharmacia Biotech)

Specific activity  $1.87 \times 10^4$  cpm/nmol

3. -[ $^{14}$ C]DOX (NEN Life Sciences)

Specific activity  $8.9 \times 10^4$  cpm/nmol

4. 40mM ATP in transport buffer 1 ml

20.3 g of ATP was dissolved in 1ml of transport buffer.

*2.30.2 Methods*

Proteoliposomes reconstituted with either RLIP76 and POB1 or RLIP76 and POB1<sup>1-512</sup> were diluted in 90  $\mu$ l of transport buffer containing either 100  $\mu$ M [ $^3$ H]DNP-SG ( $1.87 \times 10^4$  cpm/nmol) or 3.6  $\mu$ M 14-[ $^{14}$ C]DOX ( $8.9 \times 10^4$  cpm/nmol) and incubated for 15 min at 37 °C. Measurement of ATP-dependent transport was initiated by addition of 10  $\mu$ l of ATP prepared in transport buffer to the experimental group and 10  $\mu$ l of transport buffer alone to the control. The final concentration of ATP was 4mM. After incubation with ATP for 5 min, the reaction was terminated by placing the tubes on ice

and the aliquots of the reaction were filtered through a nitrocellulose membrane using a Millipore multiscreen 96 well plate vacuum filtration system. Next, the membranes were punched out from the plate and, after air drying, put individually in scintillation fluid. Radioactivity was counted with a liquid scintillation counter Beckman LS6500.

### 2.31 Effect of POB1-liposomes on <sup>14</sup>C-DOX accumulation in lung cancer cell

#### *2.31.1 Materials*

1. Lung cancer cells H358 5 x 10<sup>6</sup> cells/ml
2. RPMI-1640 medium containing 10% FBS + 1% P/S
3. Liposomes containing POB1 or POB1<sup>1-512</sup> 100 µg/ml
4. 14-[<sup>14</sup>C]-DOX (NEN Life Sciences, Boston, MA)

Final concentration 3.6 µM, specific activity 8.5 x 10<sup>4</sup> cpm/nmol

5. PBS (Gibco)
6. RPMI-1640 medium containing 10% of FBS and 1% P/S

#### *2.31.2 Methods*

NSCLC H358 cells were harvested and washed with PBS and aliquots containing 5 x 10<sup>6</sup> cells were inoculated into fresh medium. After overnight incubation, the cells were pelleted and 80 µl of RPMI medium containing 4 µg of either control, POB1 or POB1<sup>1-512</sup> liposomes was added, followed by incubation at 37 °C for 24 h. After that, 20 µl of 14-[<sup>14</sup>C]-DOX (final concentration 3.6 µM, specific activity 8.5 x 10<sup>4</sup> cpm/nmol) was added to the medium and the cells were incubated for 5, 10, 20, and 30 min at 37 °C. Drug uptake was terminated by rapid cooling on ice. Next, the cells

were centrifuged at 700 g for 5 min at 4 °C and the medium was decanted. Radioactivity was determined in the cell pellet after washing twice with ice-cold PBS.

### 2.32 <sup>14</sup>C-DOX efflux studies

#### *2.32.1 Materials*

1. Non Small Lung Cancer Cells H358 5 x 10<sup>6</sup> cells/ml
2. RPMI-1640 medium containing 10% FBS + 1% P/S
3. Liposomes containing POB1 or POB1<sup>1-512</sup> 100 µg/ml
4. 14-[<sup>14</sup>C]-DOX (NEN Life Sciences Boston, MA)  
Final concentration 3.6µM, specific activity 8.5 x 10<sup>4</sup> cpm/nmol
5. PBS (Gibco)
6. RPMI-1640 medium containing 10% of FBS and 1% P/S

#### *2.32.2 Methods*

5 x 10<sup>6</sup> of the NSCLC (H358) cells were grown in the culture flask at 37 °C, in fresh RPMI-1640 medium, and a CO<sub>2</sub> atmosphere. After overnight incubation, the cells were harvested, centrifuged in order to create a pellet, and washed two times with PBS. Then, 80 µl of medium containing 4 µg of either control, POB1 or POB1<sup>1-512</sup> liposomes was added and the cells were subjected to incubation at 37 °C for 24 h. After that, 20 µl of 14-[<sup>14</sup>C]-DOX (final concentration 3.6 µM, specific activity 8.5 x 10<sup>4</sup> cpm/nmol) was then added to the medium and incubated for 60 min at 37 °C. Next, the cells were centrifuged at 700 g for 5 min, after which the supernatant was removed completely and the cell pellet washed twice with PBS. The pellet was immediately resuspended in 1 ml

of PBS. The radioactivity was measured in 50 µl aliquots of clear supernatant in 1 min intervals. 15 samples were collected for radioactivity counting.

### 2.33 Genotyping of transgenic mice by PCR method

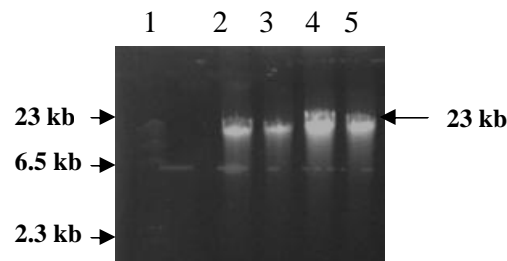
RLIP76 transgenic mice carry a segment of foreign DNA that has been incorporated into their genomes by a nonhomologous insertion method, such as pronuclear microinjection. The trapping cassette is inserted between 250 and 251 nucleotide of RLIP76 gene. The incorporated transgene is detected by genomic DNA isolation from a mice tail sample, followed by PCR amplification of a region of the inserted gene.

#### *2.33.1 Materials*

1. Mice tail	30 mg
2. ATL buffer	180 µl
3. Proteinase K	20 µl
4. AL buffer	200 µl
5. 96 % ethanol	200 µl
6. AW1 buffer	500 µl
7. AW2 buffer	500 µl
8. AE buffer	100 µl

### 2.33.2 Methods

The DNA samples were isolated using DNeasy tissue kit (Qiagen) from mice tail. About 1 cm of mice tail was cut into small pieces and placed in an Eppendorf tube. Then, ATL buffer was added along with Proteinase K. After vortexing, the mixture was incubated for 12 hours at 55 °C water bath followed by addition of AL buffer and incubation at 70 °C for 10 min. Next, absolute ethanol was mixed with the solution and the mixture was pipetted into the DNeasy spin column. Then, the column was washed twice with AW1 and AW2 buffers and centrifuged at 8000 rpm. In order to elute DNA from a column's membrane, AE buffer was applied. After incubation at room temperature for 1 min, the DNA sample was collected by centrifugation in an Eppendorf tube. The purity of samples was tested by running 0.8 % agarose gel.



- 1 - DNA marker (Fermentas,  $\lambda$  DNA HIND III)
- 2 - DNA from RLIP76 KO mouse (sample 1)
- 3 - DNA from RLIP76 KO mouse (sample 2)
- 4 - DNA from WT mouse (sample 1)
- 5 - DNA from WT mouse (sample 2)

Figure.2.9 Agarose gel of DNA samples from RLIP76 KO and WT animals.

The following three primers were used to determine the genotype of tested mice.

1. Primer A – upstream (121 – 140 nucleotides)

5' TCTTCTGCTCACTCGTCCCT 3'

2. Primer B – downstream (274 – 293 nucleotides)

5' GTTTCCCACTCAGCTTCCAG 3'

3. Primer C – Long Terminal Repeat (provided by Lexicon Genetics, Inc)

5' AAATGGCGTTACTTAAGCTAGCTTGC 3'

Master mix of reagents was prepared for PCR amplification

PCR buffer	2.5 µl
25mM MgCl <sub>2</sub>	1 µl
10mM dNTP	1 µl
Primer A	2 µl
Primer B	2 µl
Primer C	2 µl
Ampli Taq Gold (5 U/ µl)	0.25 µl
DNA template	1 µg (10 µl)
DI water	up to 25 µl

PCR was performed under the following conditions:

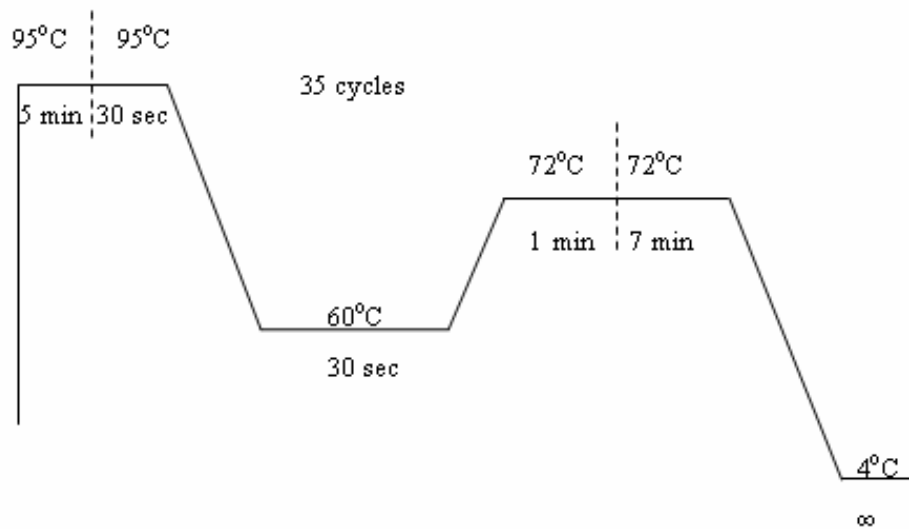
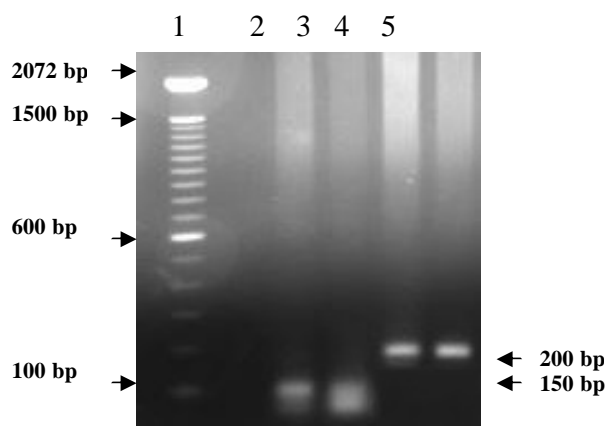


Figure 2.10 The PCR cycles for mice genotyping.

After PCR amplification, 10  $\mu$ l of a product was loaded into 1.5 % of agarose gel. The result is shown below:



- 1 - DNA marker (Invitrogen, 100bp)
- 2 - RLIP76 KO mouse (sample 1)
- 3 - RLIP76 KO mouse (sample 2)
- 4 - WT mouse (sample 1)
- 5 - WT mouse (sample 2)

Figure 2.11 PCR amplification of a region of the inserted gene.



The amplification of an investigated region of the knockout genomic sequence of RLIP76 with three primers: A, B, and C results in a product of approximately 150 bp (RLIP76 KO). Mice which do not containing the trapping cassette produced a 200 bp band upon amplification, denoted as a +/+ genotype (WT).

### 2.34 Quantifying insulin and glucose level in wild type and RLIP76 knockout mice after augmenting RLIP76 level

#### *2.34.1 Materials*

##### 1. Animals

Wild type mice RLIP76 (WT)

Homozygous mice RLIP76 (KO)

RLIP76 knockout mice were commissioned from Lexicon Genetics and were created using Cre-Lox technology.

2. Liposomes reconstituted with purified, recombinant RLIP76 1 g/ml

#### *2.34.2 Methods*

12 week old animals (WT, KO) were subjected to the single intra peritoneum (i.p.) injection of control or RLIP76-liposomes equivalent to 200 and 500  $\mu$ g of RLIP76 protein. After 24 hours, all animals were sacrificed and blood was collected for insulin and glucose level determination. These measurements were re-assayed and verified in the laboratory of Dr. Kent R. Refsal, Michigan State University, Michigan. In addition, liver and heart from wild type animals were collected in order to monitor the amount of RLIP76 in these tissues with or without administration of RLIP76 proteoliposomes. Uptake of RLIP76 by tissues was monitored by comparing the results of Western blots.

## 2.35 Quantifying glucose level in wild type and RLIP76 knockout mice after administration hydrocortisone

### *2.35.1 Materials*

#### 1. Animals

Wild type mice RLIP76 (WT)

Homozygous mice RLIP76 (KO)

2. Hydrocortisone (Solu-Cortef, Pharmacia) 50 mg/1ml of PBS

### *2.35.2 Methods*

12 weeks old animals (Wild type and Homozygous) were subjected to the single intra peritoneum (i.p.) injection of 60  $\mu$ l (3 mg) of hydrocortisone. The blood glucose level was measured using a free style blood glucose meter before injection and three times after injection on 30 min intervals from the mice tail.

## 2.36 Effect of anti-RLIP76 IgG on $^{14}$ C-glucose uptake by lung cancer cells

### *2.36.1 Materials*

1. Polyclonal anti-RLIP76 antibodies 40  $\mu$ g/ml
2. Insulin (GIBCO BRL Inc.) 0.02 U/100 $\mu$ l
3. SCLC (H1618) cell lines (control, pcDNA3.1, and RLIP76/pcDNA3.1. transfected)
4. NSCLC (H358) cell lines (control, pcDNA3.1, and RLIP76/pcDNA3.1. transfected)
5. Glucose D-[1- $^{14}$ C] (NEN life science) specific activity 55.4 mci/mmol
6. Hanks buffer (GIBCO BRL Inc.)
7. PBS (GIBCO BRL Inc.)

### 2.36.2 Methods

Two cell lines SCLC (H1618) and NSCLC (H358) were transfected with, vector (pcDNA3.1) alone and vector containing RLIP76 gene as described previously. Aliquots containing  $5 \times 10^6$  cells (in triplicate) were inoculated into Hanks buffer after washing with PBS and incubated for 4 hours at 37 °C in a CO<sub>2</sub> atmosphere. Next, the cells were pelleted by centrifugation and resuspended in fresh Hanks buffer containing anti-RLIP76-IgG. Such cocktail was incubated at 37 °C for another 60 min prior to addition of buffer without or with insulin. Then, <sup>14</sup>C-glucose (specific activity 93 cpm/pmol) was added to the medium and cells were incubated for additional 30 min at 37 °C. Finally, the pellet was collected, after centrifugation at 700 g at 4 °C, and medium was completely decanted. The cell pellet was washed twice with cold PBS followed by radioactivity measurements in a scintillation counter. Counts were normalized to the no-IgG control for the respective cell line.

### 2.37 EGF binding and internalization assay

#### 2.37.1 Materials

- |  |                              |
|--|------------------------------|
| 1. Non Small Lung Cancer Cells H358                      | 5 x 10 <sup>6</sup> cells/ml |
| 2. RPMI-1640 medium containing 10% FBS + 1% P/S          |                              |
| 3. 10 % goat serum (Sigma-Aldrich)                       |                              |
| 4. Pre-immune serum (Sigma-Aldrich)                      |                              |
| 5. Anti-RLIP76 IgG                                       | 40 µg/ml                     |
| 6. EGF-rhodamine solution (Molecular Probes, Eugene, OR) | 40 ng/ml                     |

Solution prepared in PBS containing 1% BSA)

7. PBS (Gibco)

8. 4% paraformaldehyde in PBS

### *2.37.2 Methods*

H358 cells ( $0.5 \times 10^6$  cells/ml) were grown on sterilized glass slides (18 mm size) in RPMI 1640 medium for 24 hours, at 37 °C, in a CO<sub>2</sub> atmosphere. After washing with PBS 4-5 times the cells were treated with 10% goat serum for 30 min at room temperature in order to reduce nonspecific binding of proteins to the cell membrane. Then, the cells were incubated with pre-immune serum as a negative control as well as with anti-RLIP76 IgG for 2 hrs at room temperature. After washing 4-5 times with PBS, 40 ng/ml EGF-rhodamine was pipetted on top of the slides followed by incubation for 60 min in ice (4 °C). After that, cells were placed in a humidified chamber and were incubated for 1, 5 or 10 min at 37 °C. Next, the cells were treated with 4% paraformaldehyde in PBS in order to fix the cells. Slides were analyzed using confocal laser scanning microscopy (Zeiss 510-meta system), with excitation at 555 nm and emission at 580 nm.

## 2.38 Effect of anti-RLIP76 IgG on FITC-conjugated insulin binding and internalization

### *2.38.1 Materials*

1. Non Small Lung Cancer Cells H358  $5 \times 10^6$  cells/ml
2. RPMI-1640 medium containing 10% FBS + 1% P/S
3. 10% goat serum (Sigma-Aldrich)

- |  |              |
|--|--------------|
| 4. Anti-RLIP76 IgG   | 40 µg/ml     |
| 5. FITC-conjugated insulin solution (Molecular Probes, Eugene, OR) | 100<br>ng/ml |
| Solution prepared in PBS containing 1% BSA)                        |              |
| 6. PBS (Gibco)   |              |
| 7. 4% paraformaldehyde in PBS                                      |              |

### *2.38.2 Methods*

About  $0.5 \times 10^6$  NSCLC H358 cells were grown on 18 mm sterilized glass cover slips in RPMI 1640 medium supplied in 10% FBS and 1% P/S. After overnight incubation at 37 °C and in a CO<sub>2</sub> atmosphere, anti-RLIP76 antibody was added to the medium followed by incubation for 20 min at 37 °C. Subsequently, cells were washed 4 times with PBS, and after addition of fresh RPMI 1640 medium, they were allowed to recover for 2 h at 37 °C, CO<sub>2</sub> incubator. Then, cells were washed with PBS and treated with 10% goat serum for 30 min at room temperature. After blocking nonspecific proteins binding, the cells were incubated with 100 ng/ml FITC-conjugated insulin for 60 min on ice. Next, cells were placed at 37 °C in a humidified chamber for 1, 5 or 10 min, followed by fixation with 4% paraformaldehyde in PBS at respective time. Slides were analyzed using confocal laser scanning microscopy (Zeiss 510-meta system), with excitation at 494 nm and emission at 518 nm.

### 2.39 TransAM FKHR (FOXO1) Assay

FKHR is a transcription factor (DNA-binding protein) that tightly regulates expression of gluconeogenic factors such as peroxisome proliferators-activated

receptor- $\gamma$  coactivator, glucose-6-phosphate and phosphoenolpyruvate carboxykinase (Daitoku et al., 2003; Schmoll et al., 2000; Ayala et al., 1999; Hall et al., 2000). In addition it plays a key role in insulin regulation of glucose level by controlling  $\beta$ -cell compensation for insulin resistance and glucose production in type 2 diabetes (Nakae et al., 2000) Moreover, FKHR have been shown to regulate catalase and superoxide dismutase gene expression which protects cells from oxidative stress (Nemoto et al., 2002; Kops et al., 2002). In this experiment the activity of FKHR was determined in two cancer cell lines (H1618, H358), control and RLIP76 transfected cells after treatment with anti-RLIP76 IgG, with or without insulin addition.

### 2.39.1 Materials

- |   |                              |
|---|------------------------------|
| 1. Non Small Lung Cancer Cells H358   | 5 x 10 <sup>6</sup> cells/ml |
| 2. Small cell lung cancer H358  | 5 x 10 <sup>6</sup> cells/ml |
| 3. RPMI-1640 medium containing 10% FBS + 1% P/S                               |                              |
| 4. PBS (Gibco)  |                              |
| 5. Anti-RLIP76 IgG  | 40 $\mu$ g/ml                |
| 6. Insulin (GIBCO BRL Inc)  | 0.02 U/100 $\mu$ l           |
| 7. TransAM FKHR (FOXO1), a DNA-binding ELISA kit (Active Motif, Carlsbad, CA) |                              |

Buffers provided by manufacturer (amounts used per 96 well plate):

- |  |            |
|--|------------|
| FKHR antibody                                  | 22 $\mu$ l |
| (1:500 dilution in 1x antibody binding buffer) |            |
| Anti-rabbit HRP-conjugated IgG                 | 11 $\mu$ l |

(1:1000 dilution in 1x antibody binding buffer)

1 M Dithiothreitol (DTT)	100 $\mu$ l
Protease Inhibitor Cocktail	100 $\mu$ l
1 $\mu$ g/ $\mu$ l Herring sperm DNA	100 $\mu$ l
Lysis buffer AM1	10 ml
Complete Lysis buffer	1.08 ml

(1.2  $\mu$ l of DTT, 10.8  $\mu$ l Protease Inhibitor Cocktail, 1.07 ml Lysis buffer AM1)

Binding buffer AM6	10 ml
Complete binding buffer	4.32 ml

(43.2  $\mu$ l Herring sperm DNA, 4.27 ml binding buffer AM6)

10 x Wash buffer AM2	22 ml
----------------------	-------

(1 x solution was prepared with distilled water)

10 x Antibody Binding buffer AM2	1.1 ml
----------------------------------	--------

(1 x solution was prepared with distilled water)

Developing solution	11 ml
Stop solution	11 ml

### 2.39.2 Methods

$5 \times 10^6$  cells (SCLC H1618 control, and RLIP76 transfected; NSCLC H358 control and RLIP76 transfected) were treated with anti-RLIP76 IgG (40  $\mu$ g/ml), in a RPMI-1680 medium with or without insulin. After 24 hours of incubation at 37 °C, in a CO<sub>2</sub> atmosphere, the cells were harvested and washed 4 times with PBS. Then, the

pellet was created by centrifugation and later lysed in lysis buffer by sonication (3 x 15 s at 50 W). The protein concentration of cell lysate was determined to be 50 µg/10µl of complete lysis buffer.

Meanwhile, 40 µl of complete binding buffer was added to each well used from a 96-well plate in which multiple copies of specific double-stranded oligonucleotides had been immobilized. Then, 10 µl of cell lysate was added to each well; for the blank, 10 µl of complete lysis buffer was added. The plate was sealed with the adhesive cover provided by the vendor and incubated for 1 hr at room temperature with mild rocking. Next, each well was washed three times with 200 µl of 1X wash buffer followed by the addition of 100 µl diluted FKHR primary antibody to each well. The plate was sealed again with a cover and incubated at room temperature for 1 hr without rocking. After that, the cells were washed 3 times with 200 µl 1X wash buffer followed by addition of 100µl diluted HRP-conjugated secondary antibody to each well. Next, the plate was incubated at room temperature for 1 hr without agitation. After washing 3 times with 200 µl of 1x washing buffer, 100 µl of developing solution was added to each well. The plate was incubated 2-10 min at room temperature, protected from light, until the wells turned medium to dark blue. The reaction was stopped by adding 100 µl stop solution and the absorbance was read at 450 nm in an ELISA plate reader.

## 2.40 Insulin-stimulated phosphorylation of Akt-1

### *2.40.1 Materials*

1. Non Small Cells Lung Cancer H358

5 x 10<sup>6</sup> cells/ml



- |   |   |
|---|---|
| 2. Small Cell Lung Cancer H358                              | 5 x 10 <sup>6</sup> cells/ml                    |
| 3. Hepatic carcinoma HepG2 cells                            | 5 x 10 <sup>6</sup> cells/ml                    |
| 4. RPMI-1640 medium containing 10% FBS + 1% P/S             |   |
| 5. Lysis buffer   |   |
| Composition:  | 10 mM Tris (hydroxymethyl)-aminomethane, pH 7.4 |
|   | 1.4 mM β-mercaptoethanol,                       |
|   | 1 mM EDTA                                       |
|   | 0.1 mM PMSF                                     |
|   | 0.05 mM BHT                                     |
|   | 0.5% polidocanol                                |
| 6. PBS (Gibco)  |   |
| 7. Anti-phospho-Akt1 IgG (Ser 473) (Upstate Cell Signaling) | 40 μg/ml  |
| 8. Anti-RLIP76 IgG  | 40 μg/ml  |
| 9. Insulin  | 0.02 U/100μl                                    |

#### 2.40.2 Methods

Three different cell lines: NSCLC (H358 control and RLIP76 transfected), SCLC (H1618 control and RLIP76 transfected), and Hepatic carcinoma HepG2 cells were incubated for 24 hours with anti-RLIP76 IgG (40 μg/ml) in the presence or absence of insulin in the RPMI medium. Next, after washing with PBS, the cells were pelleted and lysed in lysis buffer by sonication (3 x 15 s at 50 W). The cell lysate, containing 50 μg of protein, were subjected to SDS-PAGE in 12% gel. Western blot

analyses were performed using rabbit antibodies against human anti-phospho-Akt1 (Ser 473) as a primary antibody and peroxidase-conjugated goat anti-rabbit IgG as secondary antibodies.

#### 2.41 Phosphoenolpyruvate carboxykinase activity assay

Phosphoenolpyruvate carboxykinase is a key enzyme involved in gluconeogenesis. It converts oxaloacetate to phosphoenolpyruvate initiating the process of glucose production. The activity assay is based on the method of Opie and Newsholme (Opie et al., 1967). In vivo, oxaloacetate is formed by the oxidation of L-malate, catalysed by malate dehydrogenase. In gluconeogenesis, phosphoenolpyruvate is formed from the decarboxylation of oxaloacetate and hydrolysis of 1 GTP molecule. This reaction is catalyzed by the enzyme phosphoenolpyruvate carboxykinase (PEPCK), which is activated by  $Mn^{2+}$ .

PEP is then converted to Fructose1, 6-biphosphate in a series of steps involving oxidation of NADH to NAD. In this assay, the loss of NADH is determined by measuring absorbance at 340 nm (Table 2.10).

Table 2.10 PEPCCK enzyme activity assay, composition of 1ml of reaction mixture

<b>Stock solutions</b>	<b>Blank [ml]</b>	<b>Exp[ml]</b>	<b>Final Concentration</b>
Tris - HCl, pH 7.4, 1 M	66	66	66 mM
MnCl <sub>2</sub> , 55 mM	10	10	0.55 mM
PEP, 11 mM	100	100	1.1 mM
NADH <sub>2</sub> , 3.2 mM	25	25	0.08 mM
Inosine diphosphate (IDP), 30 mM	51.33	51.33	1.54 mM
NaHCO <sub>3</sub> , pH 7.5, 170 mM	-	100	17 mM
Malate dehydrogenase, 50 U/ml	20	20	1 U
10% tissue homogenate	-	20	
Water	727.67	607.67	

#### 2.42 Fructose 1,6-bisphosphatase enzyme activity assay

Fructose 1,6-bisphosphatase is an enzyme present in liver that converts fructose-1,6-bisphosphate (F16BP) to fructose-6-phosphate in order to produce glucose.

To detect FBPase activity a spectrophotometric coupled enzyme assay is used by a method of Taketa and Pogell (Taketa et al., 1965). FBPase activity is coupled with phosphoglucose isomerase (PGIase) and NADP dependent glucose 6-phosphate dehydrogenase (G6Pase), and NADPH formation is measured at 340 nm (Table 2.11).

Table 2.11 PEPCK enzyme activity assay, composition of 1 ml of reaction mixture

<b>Stock solutions</b>	<b>Blank [ml]</b>	<b>Exp[ml]</b>	<b>Final concentration</b>
Water	20	-	
Tris - HCl, pH 8, 120 mM	836	836	10 mM
MgCl <sub>2</sub> , 1 M	20	20	20 mM
β-mercaptoethanol, 1.4 M	14	14	20 mM
NADP <sup>+</sup> , 10 mM	40	40	0.4 mM
G6Pase, 20 U/ml	25	25	0.5 U
PGIase, 20 U/ml	25	25	0.5 U
10% tissue homogenate	-	20	

Incubate for 10 minutes at 30 °C

F16BP, 100 mM	20	20	2 mM
---------------	----	----	------

## CHAPTER 3

### APOPTOSIS OF LUNG CANCER CELLS AS AN EFFECT OF INHIBITION OF RLIP76 ACTIVITY

#### 3.1 Introduction

RLIP76 is a multifunctional Ral-binding effector protein which exhibits GAP activity towards a key pro-apoptotic G-protein, cdc42, and links the Ras signaling pathway to the Ral pathway. It has the ability to interact with a number of proteins which play a crucial role in cell homeostasis. RLIP76 regulates numerous cell processes by protein-protein interactions. It is able to transmit signals from its upstream effector-Ral to downstream partners such as Hsf1, cdc42/Rac, Ap2, and CDK1. The signal transducing properties of RLIP76 allow it to participate in processes such as endocytosis of insulin and epidermal growth factor receptors, cell mitosis and filopodia formation, stress response and control of actin cytoskeleton dynamics. Sequence homology comparisons of the translated amino-acid sequence of RLIP76, obtained from GenBank showed numerous domains and motifs which confirm incredible potential of this protein (Fig 3.1). In addition, it has been demonstrated that RLIP76 mediates ATP-dependent trans-membrane movement of anionic glutathione conjugates with electrophiles (GS-E) as well as weakly cationic anti-cancer drugs like for example Doxorubicin (DOX). Anti-RLIP76 antibodies have been shown to inhibit transport of

GS-E and DOX in lung cancer cells carried out by RLIP76. This significant reduction of transport activity of RLIP76 causes intracellular accumulation of the endogenously produced GS-E, 4-hydroxynonenal-S-glutathione (4HNE-SG), which leads to cancer cell apoptosis. Such multi-functionality of RLIP76 places this protein among the most significant proteins within a cell.

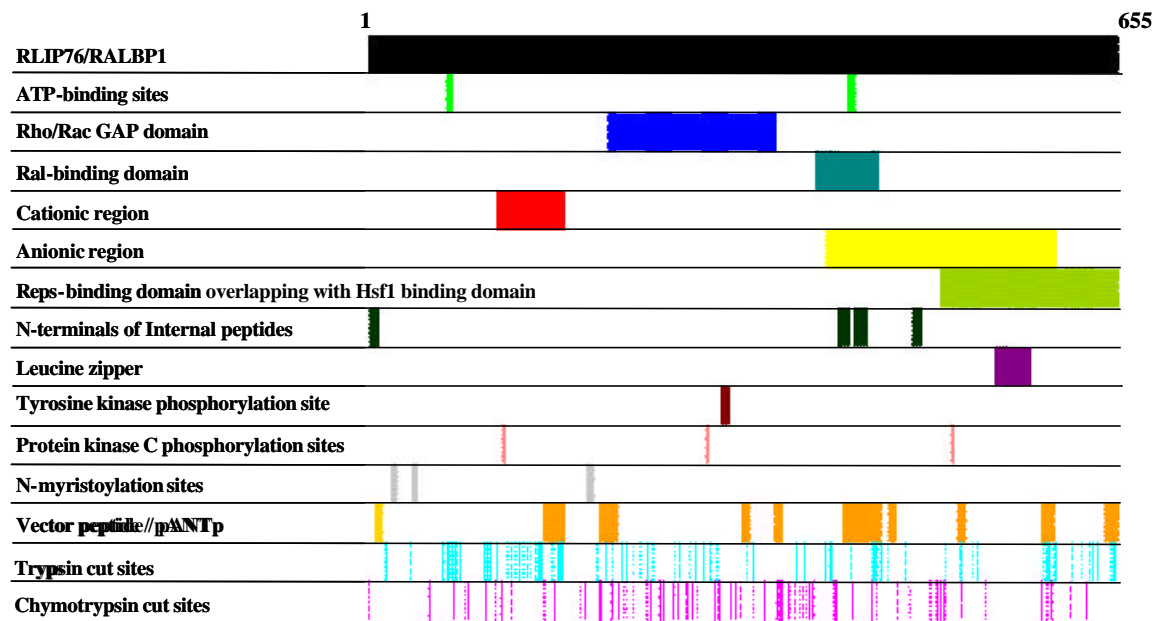


Figure 3.1 Sequence and domain analysis of RLIP76 by NCI-BLAST against all protein databases (Awasthi et al., 2003).

To gain more information about RLIP76, the protein has been used as bait in a yeast two-hybrid screen. This screening of mouse muscle cell cDNA library resulted in the isolation of a novel protein named POB1 (Partner of RalBP1) (Yamaguchi et al., 1997). POB1 has a single EPS15 homology (EH) domain on its N-terminal region, two proline-rich motifs and a coiled-coil structure in its C-terminal region (Fig 3.2) (Yamaguchi et al., 1997; Morinaka et al., 1999; Koshiba et al., 1999). The 2 proline rich

regions of POB1 are responsible for binding to the growth factor receptor adaptor protein Grb2, which regulates EGF and insulin receptor endocytosis (Ikeda et al., 1998; Kariya et al., 2000) and PAG2, which participates in cell migration (Oshiro et al, 2002). The C-terminal of the POB1 coiled-coil region is involved in RLIP76 binding (Yamaguchi et al., 1997). The coiled-coil structure is a common and important protein-protein interaction motif that consists of two or more  $\alpha$ -helices that wrap around each other with a super helical twist. The EH domain is a protein-binding domain that was first identified in the receptor tyrosine kinase substrate Eps15 and is conserved in evolution (Wong et al., 1995; Confalonieri et al., 2002). EH domains are about 100 amino acid long regions. Proteins that contain one or more of these domains are involved either in endocytosis, actin remodeling, or intracellular transduction of signals. The majority of EH domains have been shown to bind preferentially to proteins containing three amino acids Asn-Pro-Phe (NPF) which form a central part in EH domain-binding motif (Salcini et al., 1997; Kariya et al., 2000).

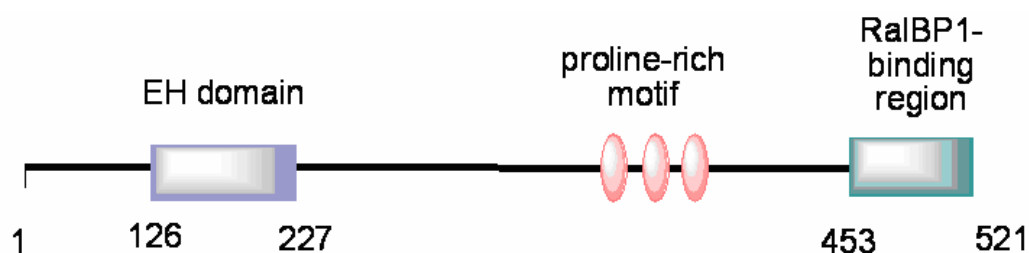


Figure 3.2 Linear map of full length of POB1 (Ikeda et al., 1998).

The Ral ( $\nu$ -ral simian leukemia viral oncogene homolog) signaling pathway in the regulation of endocytosis of the EGF and insulin receptors has been suggested by Nakashima (Nakashima et al., 1999). When a ligand binds to the EGF or Insulin receptors, Grb2 and SOS proteins directly interacting with these receptors undergo phosphorylation and activate Ras protein. Activated Ras recruits RalGDS to the plasma membrane, resulting in the activation of Ral. The activated form of Ral interacts with RLIP76, which forms a complex with POB1. Such dimer undergoes translocation to the plasma membrane and associates with Eps15 and Epsin, which bind to the AP2-clathrin complex, resulting in the formation of clathrin-coated vesicles with transmembrane receptors. This model was confirmed by Sugiyama (Sugiyama et al., 2004) showing that signaling from Ral to Eps15 and Epsin through RalBP1 and POB1 regulates receptor-mediated endocytosis of EGF and Insulin receptor.

Two forms of POB1 were identified by screening the mouse muscle cell cDNA library (Yamaguchi et al., 1997) and hypothalamus cDNA library (Oosterhoff et al., 2003): 521 and 659 amino acid proteins, respectively. Specific POB1 antibodies detected both forms of POB1 (78 kDa and 58 kDa) in prostate cancer cell lines (Oosterhoff et al., 2003). Recently, it has been shown that over-expression of POB1 in prostate cancer cells induces apoptosis in those cells (Oosterhoff et al., 2003, Penninkhof et al., 2004). Augmenting the level of mutant POB1 lacking RLIP76 binding site in prostate cancer cells showed a 50% decrease in apoptosis compared to full length POB1 (Oosterhoff et al., 2003). These results suggest that POB1 induced



apoptosis of prostate cancer cells could be due to inhibition of transport activity of RLIP76 by POB1 binding.

Based on this finding we have hypothesized that POB1 mediated apoptosis is due to inhibition of transport activity of RLIP76 and the consequential accumulation of Glutathione conjugates in the cell. The following experiments were performed to support our hypothesis.

## 3.2 Results

### *3.2.1 Purification of Glutathione-S Transferases from mouse liver*

GSTs isozymes were purified from mouse liver as described under experimental procedures. Three separate purifications of GST were carried out. Also, activities of GST towards CDNB were analyzed and a protein concentration was determined using the Bradford method. The data presented in Table 3.1 is a representation of one of these purifications. GST activity towards CDNB in the 28 000 g supernatant was found to be 126.5 U/g before dialysis and 126 U/g after dialysis against buffer A. The activity of the unabsorbed fraction is very low (1.6 U/g), which indicates strong binding of GST to the GSH-Sepharose Affinity Resin.

Table 3.1 Purification of GSTs isoenzymes from mouse, male, liver tissue

Fraction	GST activity towards CDNB			Protein			Specific activity	Yield
	U/ml	total act.	U/g tissue	mg/ml	mg/total volume	mg/g tissue	U/mg	%
<b>1. 28000g Supernatant</b>								
<b>A. Before Dialysis</b>	12.7	30.4	126.5	8.56	20.5	85.6	1.47	100
<b>B. After Dialysis</b>	12.6	30.2	126.0	8.20	19.7	82.0	1.53	99.6
<b>2. GST activity Unabsorbed fraction</b>								
	0.16	0.4	1.6	5.3	13.2	55.1	0.2	1.3
<b>3. GSH affinity chromatography</b>								
<b>A. B.D.</b>	3.00	13.2	54.8	0.12	0.54	2.27	24.1	43.3
<b>B. A.D.</b>	2.54	11.4	47.6	0.12	0.54	2.25	21.1	37.6

GSTs were purified to use as catalysts for the enzymatic synthesis of dinitrophenyl glutathione conjugate (DNP-SG), which is required for making DNP-SG sepharose affinity resin.

During the purification of GST by GSH – affinity column chromatography 37% of total GST activity was recovered. The protein concentration in 28000 g supernatant fluid was 85.6 mg/g tissue whereas after GSH-affinity chromatography column the concentration decreased to 2.25 mg/g tissue. The specific activity of the purified enzyme from mice liver was comparable with results reported by Igarashi (Igarashi et al., 1986).

The following equations were used in order to create a purification table:

1. Activity was calculated from a kinetics report

(Slope\*factor\*dilution\*homogenate percentage) [U/ml]

2. Specific activity  $\frac{\text{activity}[U / g]}{\text{protein}[mg / g]}$

3. Purification fold  $\frac{\text{Specific\_activity\_of\_pure\_protein}}{\text{Specific\_activity\_of\_crude\_fraction}}$

4. Yield  $\frac{\text{specific\_activity\_}[U / g]}{\text{activity\_of\_crude\_fraction\_}[U / g]} * 100\%$

5. Protein concentration per 1g of tissue  $\frac{\text{total\_protein\_in\_tissue\_}[mg]}{\text{mass\_of\_tissue\_}[g]} * 1000$

After final dialysis in buffer A, the protein present in the elution buffer was collected from the dialysis tube and lyophilized for 5 hours. Then, about 20 µg of protein was subjected to SDS-PAGE in order to check the purity of the sample. GSTs isozymes purified from mouse liver migrated on SDS-PAGE as three bands (Figure 3.3).

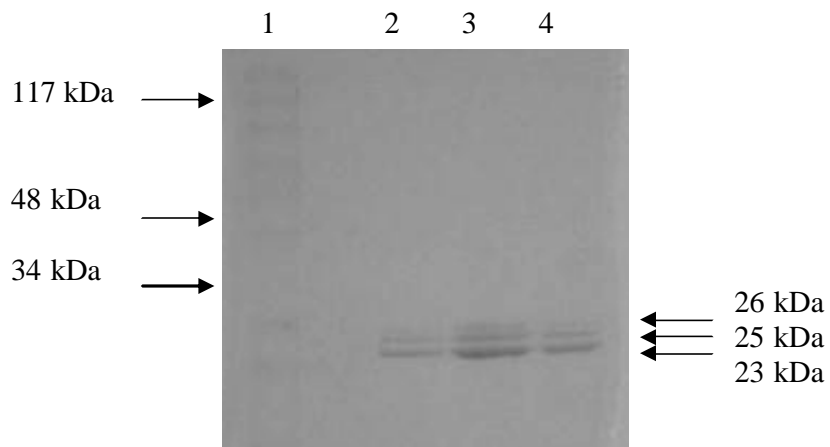


Figure 3.3 Homogeneity of GSTs purified from mouse liver. SDS-PAGE of the purified GSTs with standard protein marker (lane 1) and purified protein (lanes 2, 3, 4).

The purified enzyme showed three very clear bands in a Coomassie-stained denaturing SDS gel. First two minor bands at 26 and 25 kDa correspond to  $\mu$  and  $\alpha$  isozymes. The third band, the clearest one with a Mr value of 23 kDa, represents the  $\pi$  isozyme.

An excellent quality of the purified enzyme indicates lack of degradation during purification steps and very high affinity of GSTs towards glutathione.

### 3.2.2 Synthesis of 2,4-Dinitrophenyl S-Glutathione

2,4-Dinitrophenyl-S-glutathione (DNP-SG) was enzymatically synthesized with glutathione (GSH) and 1-chloro-2,4-dinitrobenzene (CDNB) using a homogenous preparation of Glutathione S-Transferase isolated from mouse liver, according to the method described by Awasthi (Awasthi et al., 1981). This compound is a result of the detoxification properties of GSTs which are utilized during Phase II of

biotransformation of toxins. It has been shown by Saxena (Saxena et al., 1992) that DNP-SG is an excellent substrate for purification of DNP-SG ATPase, known as RLIP76. The goal of this experiment was to synthesize DNP-SG in order to immobilize it on a sepharose resin as a ligand for purification of RLIP76, which has high affinity towards this substrate.

DNP-SG was purified using a thin layer chromatography method, and the concentration of this compound was determined by the Bradford method (as described under experimental section). First, the DNP-SG spectrum was taken from 500 nm to 200 nm using Cary 3.0 UV-VIS Spectrophotometer (Fig 3.4) followed by absorbance measurements at 340 nm (Table 3.2).

In order to perform an absorbance measurement the solution of DNP-SG was diluted 100 folds and 10  $\mu$ l of it was mixed with 990  $\mu$ l of water. As a control, 10  $\mu$ l of DNP-SG was replaced with water, so a total of 1 ml of water was used. The readings were performed on three samples in triplicates.

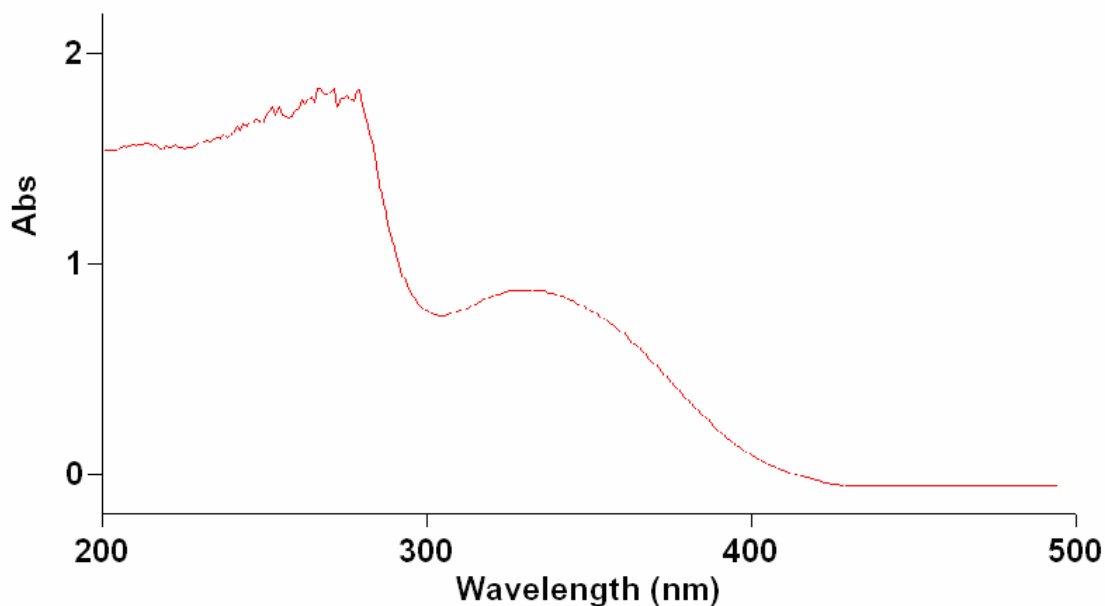


Figure 3.4 DNP-SG absorbance spectrum.

According to the literature, DNP-SG's maximum absorption occurs at 340 nm. This wavelength was chosen to determine the concentration of DNP-SG solution and calculated according to the Beer-Lambert law.

Table 3.2 Advanced Reads Report of DNP-SG Absorbance.

<b>Absorbance</b>	<b>Trial 1</b>	<b>Trial 2</b>	<b>Trial 3</b>
	0.91	0.87	0.95
	0.85	0.88	0.83
	0.80	0.90	0.90
<b>Average of each trial</b>	$0.85 \pm 0.05$	$0.88 \pm 0.01$	$0.89 \pm 0.06$
<b>Final average</b>	$0.87 \pm 0.04$		

The concentration was calculated using the following equation:

$$\frac{O.D. * dilution}{extinction\_coefficient} = concentration[mM]$$

1. Extinction coefficient of DNP-SG

$$9.6 \text{ [M}^{-1}\text{*cm}^{-1}\text{]}$$

2. The solution of DNP-SG was subjected to a 300 fold dilution

27.2 mM DNP-SG solution was used for the preparation of affinity chromatography for RLIP76 purification. The solution was distributed between several 1.5 ml Eppendorf tubes and stored at -20 °C.

*3.2.3 Prokaryotic expression and purification of RLIP76*

In this experiment RLIP76 was purified from *E. coli* BL21 after transformation of bacterial cells with the prokaryotic expression vector pET30 a(+) containing the RLIP76 gene, in order to reconstitute it into proteoliposomes for use in *in vitro* and *in vivo* studies.

DNA of RLIP76 was isolated from the RLIP76  $\lambda$ gt11 clone during immunoscreening of  $2.5 \times 10^7$  plaques from the human bone marrow cDNA library (Clontech) using polyclonal antibody against DNP-SG ATPase (Awasthi et al., 2000). The gene is located at the 18<sup>th</sup> chromosome 18p 11.3 and its open reading frame consists of 1968 bp. It has been shown that tumor suppressor genes, which may be involved in non-small cell lung cancer (NSCLC), brain tumors, and breast carcinomas, are located in this region on the short arm of chromosome 18<sup>th</sup> (Tran et al., 1998).

This gene was used as a template for PCR amplification under the conditions described in the methods section. The PCR product was purified from 1% agarose gel



and subjected to BamHI and XhoI enzymatic digestion for 12 hours at 37 °C.

Meanwhile, the vector pET30 a(+) (Invitrogen) was digested with the same two enzymes for 4 hours and the ligation of these two DNA fragments was performed. Next, the recombinant plasmid was transformed into *E. coli* DH5 $\alpha$  and purified from a single colony from the overnight culture.

After purification, the recombinant plasmid collected using Qiagen kit, pET30 a(+) with cloned gene of RLIP76, was subjected to enzymatic digestion with BamHI and XhoI followed by the 1% of DNA agarose gel electrophoresis (Fig 3.5).

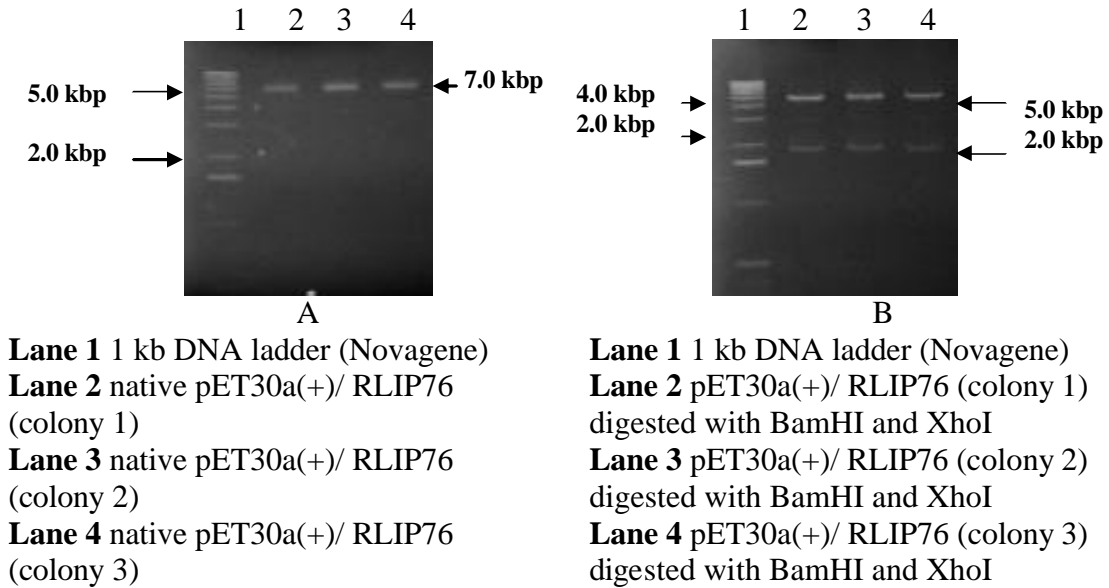


Figure 3.5 Agarose gel electrophoresis of native pET30 a(+) with RLIP76 (A) and digested pET30 a(+) with RLIP76 with BamHI and XhoI restriction enzymes (B)

The first picture (Figure 3.6, Panel A) shows one band at 7.0 kbp, which represents a native DNA (vector and a gene) in its circular form. The size of the recombinant plasmid is the sum of a gene (2.0 kbp) and a vector (5.0 kb). After restriction enzyme

digestion the recombinant plasmid is cut in two places, giving two linearized fragments, 5.0 kbp and 2.0 kbp which represent a vector and RLIP76 gene respectively (Figure 3.6, Panel B).

After confirmation of a successful ligation the recombinant plasmid was used to transform protein expression in bacterial strain *E. coli* BL21(DE3). In order to purify recombinant RLIP76, one colony was picked from the transformed cells grown on agar plates containing kanamycin.

RLIP76 was purified from 300 ml of bacterial culture by DNP-SG affinity chromatography as described in the experimental section. The purity of the sample was checked by SDS-PAGE and Western Blot analysis.

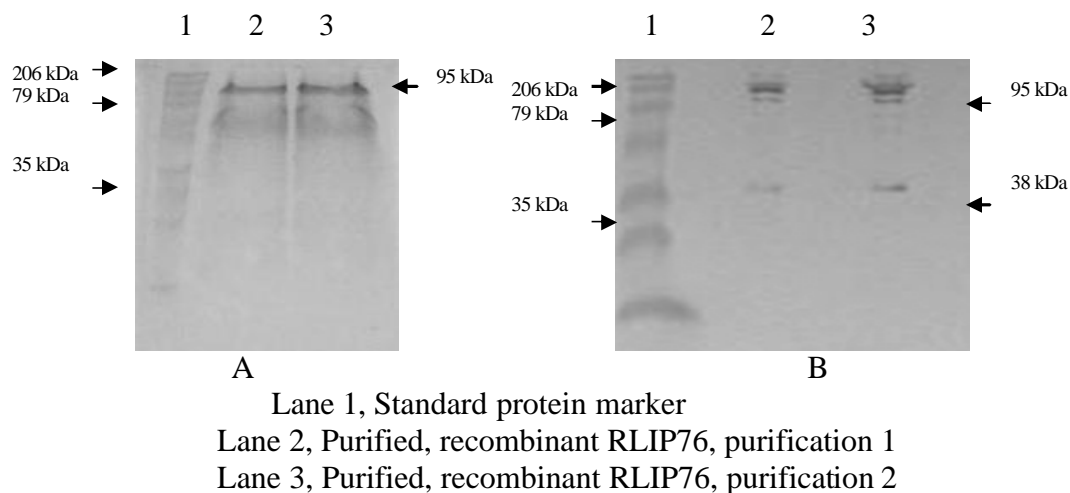


Figure 3.6 Purification of recombinant RLIP76 from *E. coli* BL21 (DE3). Panel A represents SDS-PAGE coomassie staining, Panel B Western Blot developed with 4-chloro1-naphtol/H<sub>2</sub>O<sub>2</sub> reagent.

RLIP76 protein expressed in *E. coli* migrated on SDS-PAGE as a 95 kDa band (Fig.3.6, Panel A), even though its theoretical molecular weight is 76 kDa. Anti-RLIP76 IgG recognized two dominant bands on the western blot, 95 kDa and 38 kDa (Fig 3.8, Panel B). This strange behavior of the protein was noticed before by Cantor (Cantor et al., 1995) and Awasthi (Awasthi et al., 2000) but it is not known why apparent molecular masses of full length RLIP76 and its fragments in SDS-PAGE are larger than expected from their sequences. The amino acid sequence analysis of bands present on SDS-PAGE confirmed the purity of recombinant RLIP76 and indicated that all fragments with molecular weight lower than 95 kDa originated from RLIP76 (Awasthi S., et al., 2000). RLIP76 is very susceptible to proteolytic degradation even in the presence of protease inhibitors in the purification buffers. That is why RLIP76 appears on the Western blot not as a single band but as a combination of few bands. In addition, the purification yield of RLIP76 was very low because it is a membrane associated protein and extraction of it from a membrane, even in a presence of a detergent (polidocanol), was not very efficient. Most of the protein remained attached to the bacterial membrane or was lost during the washing processes. Table 3.3 shows the concentration of proteins during the purification procedure.

Table 3.3 Purification table of RLIP76 from 300 ml of *E. coli* culture

<b>Fraction</b>	<b>Protein (mg/ml)</b>
Detergent extract	603 ± 25
Unabsorbed fraction	553 ± 38
DNP-SG Sepharose (before dialysis)	52 ± 16
DNP-SG Sepharose (after dialysis)	9.7 ± 0.5

3.2.4 Mammalian transient cell transfection with Partner of RalBP1 (POB1) cloned into pcDNA 3.1

Human cancer NSCLC cell line H358 and H226 were subjected to transformation with a eukaryotic expression vector pcDNA3.1 containing the POB1 gene using a Lipofectamine 2000 transfection kit (Invitrogen). The RT-PCR was performed utilizing the RNA purified from cell pellet by the TRIZOL method. The expression of POB1 mRNA in lung cancer cell lines was evaluated by RT-PCR analysis (Fig 3.7).

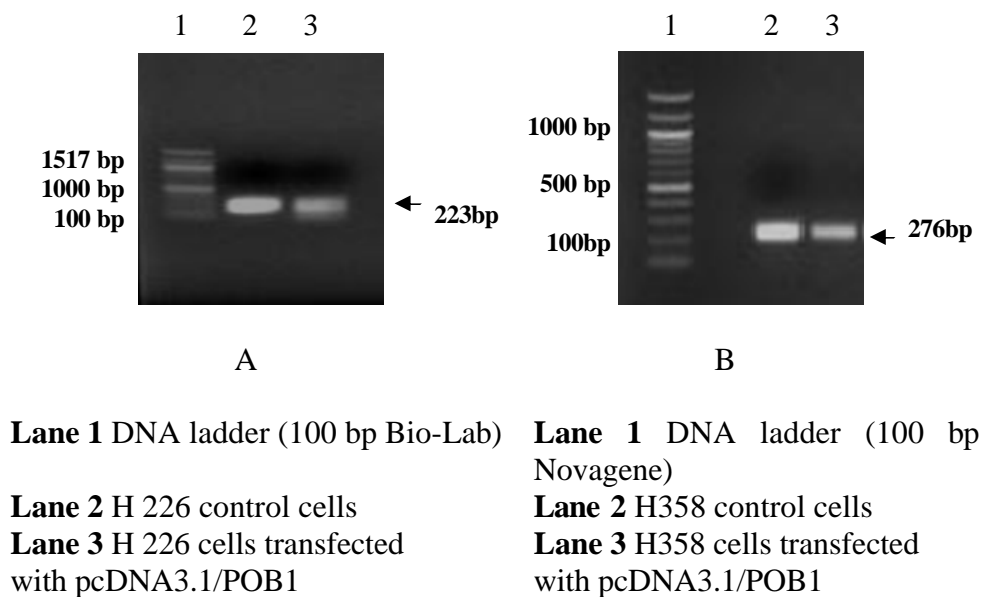


Figure 3.7 RT-PCR analysis of POB1 mRNA isolated from NSCLC H226 (Panel A) and NSCLC H358 (Panel B) transfected with vector pcDNA3.1 containing POB1 gene

Two lung cancer cell lines (H226 and H358) transiently transfected with pcDNA3.1/POB1 appeared to undergo apoptosis. The cells did not look healthy after

transfection compared to control cells. However, the RNA was isolated from the cell pellet and RT-PCR was performed. The final product of RT-PCR, a fragment of POB1 DNA, was subjected to 1% agarose gel and the intensity of the DNA bands visible under a UV light was analyzed. According to the densitometry analysis, there was a decrease of band intensity of POB1 transfected cell lines H226 and H358 by 50% as compared to the control. These results indicated that transient cell transfection with pcDNA 3.1/POB1 was not achieved. Therefore, a different transfection system was needed in order to augment the level of POB1 in cancer cells. The ecdysone inducible system (Invitrogen) was chosen (the description placed under experimental section).

### 3.3 Amplification of pVgRXR and pIND vectors.

The steroid inducible vector is a very convenient tool in in-vitro studies because it allows controlled protein expression in mammalian cells. However, applying such system into eukaryotic cells is difficult. NSLCS H358 cells were stably transfected with pVgRXR vector, using as a selective pressure 800 µg/ml of zeocin (Invitrogen). After 2 weeks, 20 clonal transfectants were established by sequential dilution into a 96-well plate, such that only a single cell was seeded in each well. The cells were maintained in medium containing 600 µg/ml of zeocin. Next, transient cotransfection with LacZ/pIND was performed in order to determine the best protein expressing clones after induction with Ponasteron A (Invitrogen). The colonies growing from such clones were used for cotransfection with pIND/POB1.

The two vectors, pVgRXR and pIND, were received as a generous gift from Prof. A.D. Sharrock from The Victoria University of Manchester, UK . The vectors

were amplified by transformation into the *E. coli* competent cells DH5 $\alpha$  and purified from the overnight culture of a single colony using Qiagen QIAprep Spin Miniprep Kit. DNA gel electrophoresis was performed to check the presence and the purity of these two plasmid DNAs (Fig 3.8).

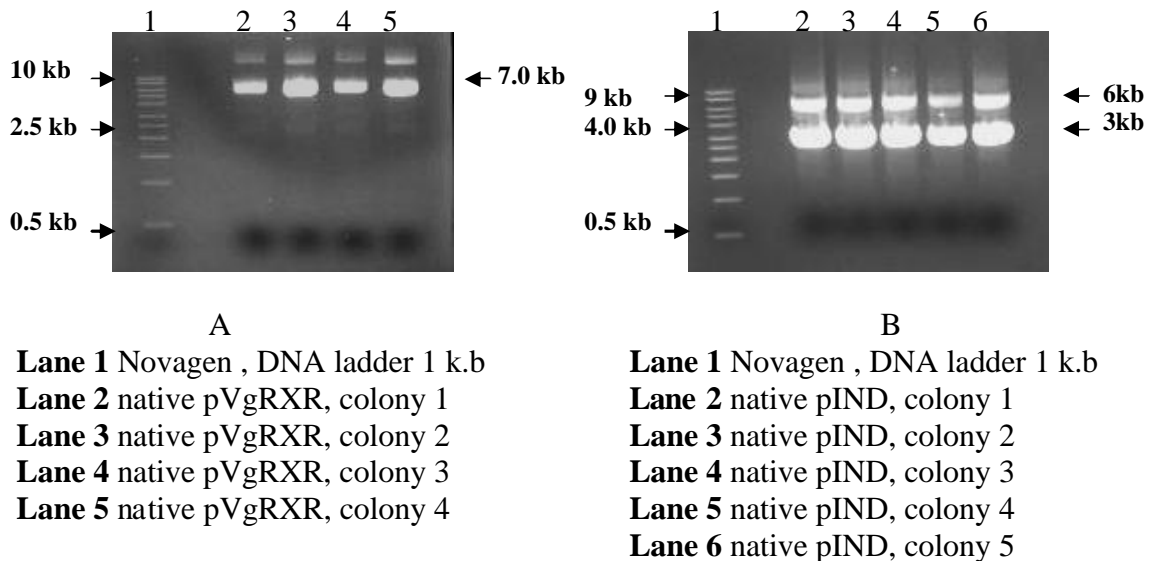


Figure 3.8 1% agarose gel electrophoresis of native pVgRXXR vector (Panel A) and native pIND vector (Panel B).

The theoretical size of the pVgRXXR vector is 8.8 kb. However, according to the agarose gel, the actual size is 7.0 kb (Fig 3.10, Panel A). The difference can be explained by the dissimilarity in migration speed on agarose gel of the different shaped of the plasmid DNA. The same pattern of DNA movement was noticed in the pIND vector. Each sample contained DNA of 3 kb and 6 kb (Fig 3.10, Panel B). Two bands indicate the different shapes of the DNA, the 3 kb band indicates a circular DNA, which travels faster under the current than the 6 kb, the super coiled plasmid DNA. In order to

confirm the actual size of pVgRXR and pIND, plasmids were subjected to restriction enzyme digestion. Endonuclease EcoRI cuts pVgRXR at two sites, 3014 and 6528 giving two fragments of DNA of 5.3kb and 3.5kb (Fig 3.10, Panel B). The enzyme recognized the following sequence of nucleotides (Fig 3.9):

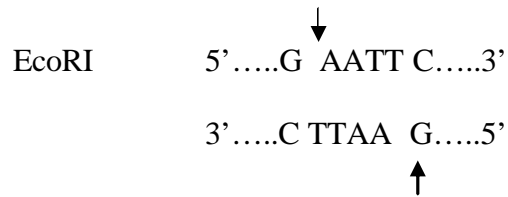
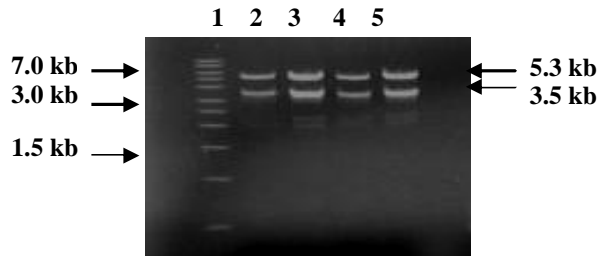


Figure 3.9 Nucleotide sequence recognized by EcoRI



- Lane 1** Novagen , DNA ladder 1 k.b
- Lane 2** pVgRXR, digested with EcoRI, colony 1
- Lane 3** pVgRXR, digested with EcoRI, colony 2
- Lane 4** pVgRXR, digested with EcoRI, colony 3
- Lane 5** pVgRXR, digested with EcoRI, colony 4

Figure 3.10 1% agarose gel electrophoresis of pVgRXR plasmid digested with EcoRI.

After the positive restriction mapping of pVgRXR, the vector was ready for NSCLC H358 cell line transfection, performed according to the procedure described in the experimental section.

The second plasmid, pIND, had a 700 bp gene inserted between the NheI and XhoI cloning sites. Therefore, the same restriction enzymes were used to cut out the gene and create sticky ends in the plasmid for ligation with POB1. Nhe I and XhoI cut at sites 477 and 567, respectively (Fig 3.11).

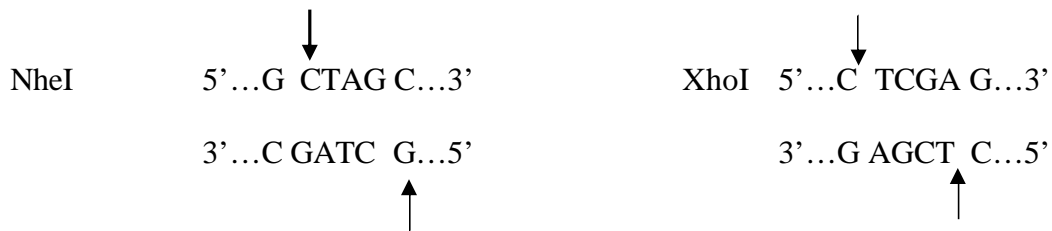
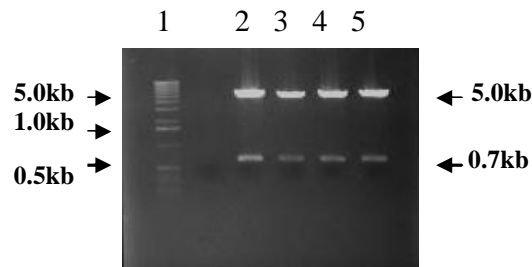


Figure 3.11 Nucleotide sequence recognized by NheI and XhoI

After overnight digestion of pIND/gene, DNA gel electrophoresis was carried out for 45 minutes at 80 V (Fig 3.12).



- Lane 1** Gibco , DNA ladder 1 k.b
- Lane 2** pIND, digested with NheI and XhoI, colony 1
- Lane 3** pIND, digested with NheI and XhoI, colony 2
- Lane 4** pIND, digested with NheI and XhoI, colony 3
- Lane 5** pIND, digested with NheI and XhoI, colony 4

Figure 3.12 1% agarose gel electrophoresis of pIND plasmid digested with NheI and XhoI.



The result showed that the actual size of the pIND vector is identical with the theoretical one and is equal to 5 kb. The 5 kb band was cut from an agarose gel and purified using a Qiagen plasmid purification kit. Digested pIND plasmid was ligated with the LacZ gene to use as a control and with POB1 to augment the level of this protein in mammalian cells.

### 3.3.1 Polymerase chain reaction of LacZ

The pcDNA/Lac Z (Invitrogen) was used as a template for PCR amplification of the LacZ coding sequence (3057 bp long). Two primers were designed to introduce the NheI restriction site (underlined) immediately upstream of initiator codon and the XhoI site (underlined) immediately downstream of the stop codon of the LacZ open reading frame.

- *LacZ-NheI forward primer:*

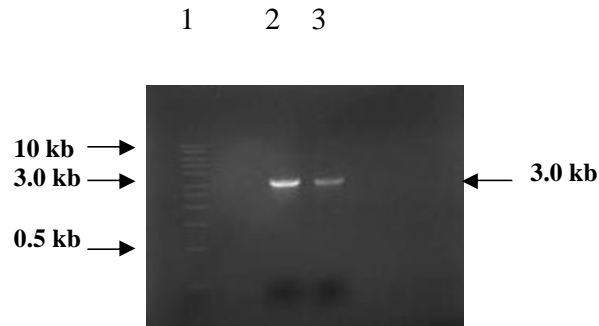
GGC GCT AGC ATG ACT GGT GGA CAG,      T<sub>m</sub> = 79 °C

- *LacZ-XhoI reverse primer:*

GGC CTC GAG TTA TTT TTG ACA CCA GA,      T<sub>m</sub> = 76 °C

The PCR conditions were used as described in the experimental section. Briefly, for the first 5 min. the Vent polymerase was activated at 95 °C followed by 35 cycles of 95 °C for 30 sec. for DNA dissociation, 60 °C for 30 sec. for primer annealing, and 1 min at 72 °C for DNA synthesis. The final extension was performed at 72 °C for 7 min.

The PCR product was purified using a Qiagen PCR purification kit and digested with two restriction endonucleases: NheI and XhoI (Fig 3.13).



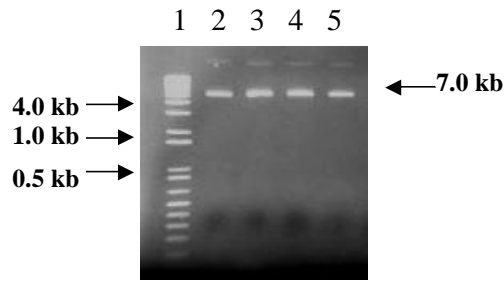
**Lane 1** Gibco , DNA ladder 1 k.b.

**Lane 2** LacZ gene amplified by PCR method,  
elution 1

**Lane 3** LacZ gene amplified by PCR method,  
elution 2

Figure 3.13 LacZ gene amplified by PCR method

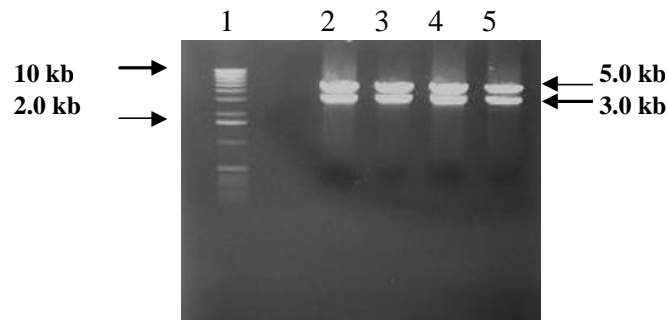
Next, the cleaved PCR product was ligated into the pIND vector previously digested with the same restriction enzymes and purified from a single colony of transformed DH5 $\alpha$  *E. coli* after an overnight incubation at 37 °C. The purity of native DNA was check by electrophoresis in 1% agarose gel (Fig 3.14).



- Lane 1** Gibco , DNA ladder 1 k.b.
- Lane 2** native pIND/LacZ plasmid, colony1
- Lane 3** native pIND/LacZ plasmid, colony2
- Lane 4** native pIND/LacZ plasmid, colony3
- Lane 5** native pIND/LacZ plasmid, colony4

Figure 3.14 1% agarose gel electrophoresis of native pIND/POB1, 7.0 kb band.

The presence of the targeted gene LacZ in the pIND recombinant plasmid was confirmed by performing a restriction enzyme digestion (Fig 3.15).



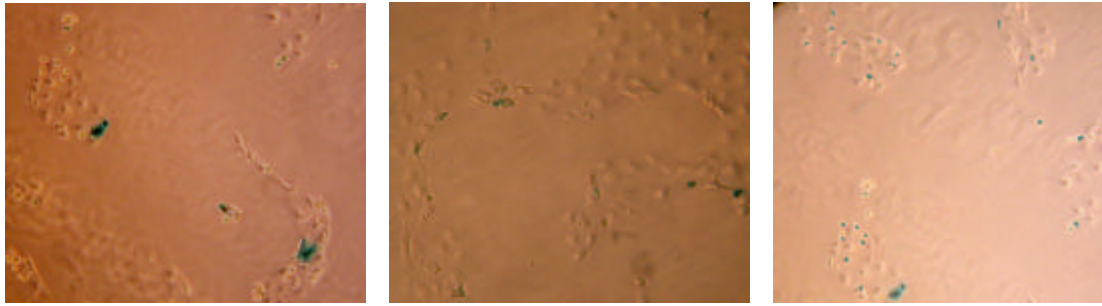
- Lane 1** Gibco , DNA ladder 1 k.b.
- Lane 2** pIND/LacZ plasmid digested with NheI and XhoI, colony1
- Lane 3** pIND/LacZ plasmid digested with NheI and XhoI, colony2
- Lane 4** pIND/LacZ plasmid digested with NheI and XhoI, colony3
- Lane 5** pIND/LacZ plasmid digested with NheI and XhoI, colony4

Figure 3.15 1% agarose gel electrophoresis of pIND/LacZ plasmid digested with NheI and XhoI, where 5.0 kb band represents pIND plasmid and 2.0 kb band represents the LacZ gene.

All four colonies selected from agar plate were positive for pIND/LacZ recombinant plasmid.

### *3.3.2 Co-transfection of pVgRXR stably transfected NSCLC H358 with pIND/LacZ*

Cell density during the log phase was determined by counting trypan blue excluding cells in a hemocytometer. 200,000 cells were seeded into each well of 12-well microtiter plates. For each clone four wells were used in order to standardize condition for the optimum concentration of ponasteron A, which induces protein expression. When the cells reached 90% confluence, co-transfection with pIND/LacZ was performed using a Lipofectamine 2000 kit (Invitrogen) (DNA: lipofectamine ratio was 1: 1). On the next day, the complexes were removed and the cells were washed twice with PBS. Then, each clone was treated with ponasteron A at four concentrations (2, 5, 10, and 50 µg/ml). After 48 hours, the β-galactosidase assay was performed according to the manufacturer's (Invitrogen) procedure. Briefly, cells were fixed with a fixative solution for 10 min at room temperature. After rinsing with PBS, the cells were incubated in a staining solution at 37 °C in a CO<sub>2</sub> incubator for two hours with occasional rocking. Next, the cell transfection was checked under a microscope for blue color development (Fig 3.16).



A.

B.

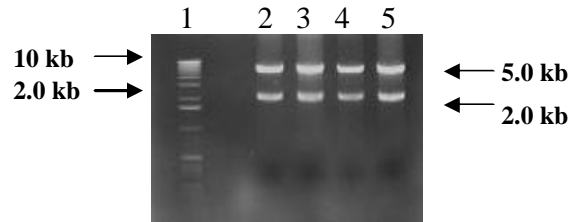
C.

Figure 3.16 Microscopic image of transient co-transfection of pVgRXX transfected NSCLC H358 cells with pIND/LacZ after  $\beta$ -Galactosidase staining. Panel A, B, C demonstrate three different clones.

Out of 20 clones, only 3 clones with optimal LacZ expression were chosen for transient co-transfection with pIND/POB1.

### 3.3.3 Polymerase chain reaction of POB1

The pcDNA/POB1 construct was subjected to restriction enzyme digestion in order to obtain a POB1 template for PCR amplification. The 2.0 kb band of the POB1 gene was cut and purified from the low melting gel using a Qiagen purification kit. The figure below (Fig 3.17) shows pcDNA/POB1 digested with two endonucleases: KpnI and XhoI:



**Lane 1** Gibco , DNA ladder 1 k.b.

**Lane 2** pcDNA/POB1 plasmid digested with KpnI and XhoI, colony1

**Lane 3** pcDNA/POB1 plasmid digested with KpnI and XhoI, colony2

**Lane 4** pcDNA/POB1 plasmid digested with KpnI and XhoI, colony3

**Lane 5** pcDNA/POB1 plasmid digested with KpnI and XhoI, colony3

Figure 3.17 1% agarose gel of pcDNA/POB1 recombinant plasmid, digested with KpnI and XhoI. 5.0 kb band represents a vector, 2.0 kb band POB1 gene.

Two primers were designed to introduce the Nhe I restriction site (underlined) immediately upstream of the initiator codon and the His-Xho I site (underlined) immediately downstream of the stop codon of the POB1 open reading frame

- *POB1-NheI forward primer:*

5' GGC GCT AGC ATGGA GGCGGCAGCGGC 3',

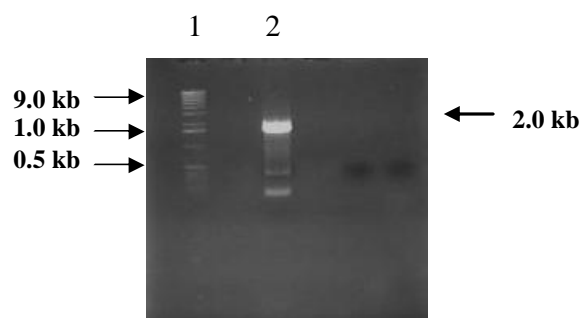
T<sub>m</sub> = 87 °C

- *POB1-XhoI reverse primer:*

5' CCG CTC GAG CAC CAT CAT CAT CAT CAT TCA CAA CAC AGT 3'

T<sub>m</sub> = 88 °C

The PCR amplification was performed under the incubation conditions described in the methods chapter. The specificity of the PCR amplification was confirmed by running the PCR product on agarose gel (Fig 3.18)

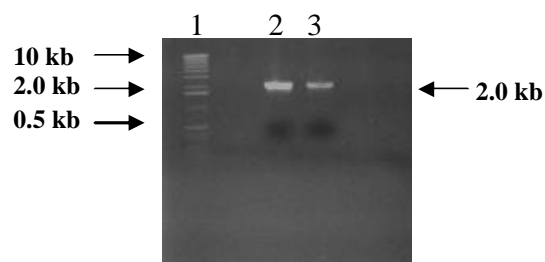


**Lane 1** Gibco , DNA ladder 1 k.b.

**Lane 2** PCR product, 2.0 kb POB1 gene

Figure 3.18 1 % agarose gel of PCR product, POB1 gene, which is represented by 2.0 kb band.

Then, the PCR product was purified from a low melting gel, and after confirmation of the POB1 sequence by sequence analysis, the gene was subjected to overnight restriction enzyme digestion with NheI and XhoI (Fig 3.19).



**Lane 1** Gibco , DNA ladder 1 k.b.

**Lane 2** PCR product, POB1 gene digested with NheI and XhoI, elution 1

**Lane 2** PCR product, POB1 gene digested with NheI and XhoI, elution 2

Figure 3.19 1% agarose gel of digested PCR product, POB1 gene, with NheI and XhoI, 2.0 kb band represents POB1 gene.

Next, the cleaved PCR product was ligated into pIND vector previously digested with the same restriction enzymes. The ligation product was later expressed into the DH5a competent cells and plasmid DNA was purified from the overnight culture of a single colony using Qiagen DNA purification kit. Unfortunately, the ligation of POB1 to pIND was not successful. Although, the ligation kits, ligation conditions, as well as gene to plasmid ratio were varied, the POB1 gene could not be cloned into a pIND plasmid.

There are several possibilities to explain why the ligation was unsuccessful. First, the pIND plasmid had all the restriction enzyme sites cut off except NheI and XhoI, so we were unable to perform blunt ended digestion with PmeI or another staggered digestion with a different pair of enzymes. Moreover, the beginning of a POB1 sequence is established by a fifteen GCG codons which corresponds to 15



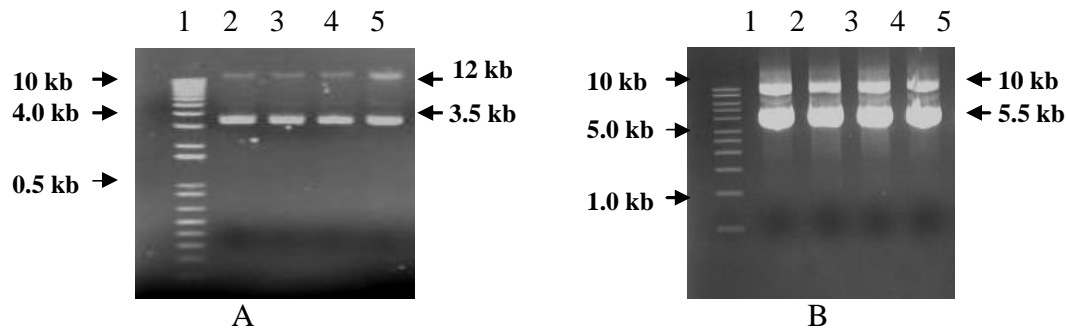
alanines. Thus, such nucleotide order might have been confusing for polymerase to amplify considering the fact that the forward primer is short because of elevated an melting temperature due to the high content of guanine. The POB1 reverse primer has a histidine tag attached to it in the form of 6 CAT codons at the beginning of the nucleotide fragment. Therefore, there are only 4 codons which recognize the POB1 sequence. Such limitations might have influenced the proper amplification of POB1 and explain difficulties in ligation into pIND plasmid.

After a few months of struggling, we decided to abandon creating an inducible plasmid system to express POB1 in cancer cells, and instead focused on using proteoliposomes with recombinant POB1 to deliver POB1 to cells.

### 3.4 Prokaryotic expression and purification of POB1 and POB1<sup>1-512</sup>

Full length POB1 cDNA as well as a cDNA encoding POB1<sup>1-512</sup> lacking RLIP76 binding site were used to create a His-tagged construct using basic molecular manipulation methods, described in the experimental section.

The digested PCR products with BamHI and XhoI were ligated into the prokaryotic expression vector pET30a(+) (Fig 3.20, Panel A and B) and the presence of the gene was confirmed by enzymatic digestion (Fig 3.21, Panel A and B).



**Lane 1** Gibco , DNA ladder 1 k.b.

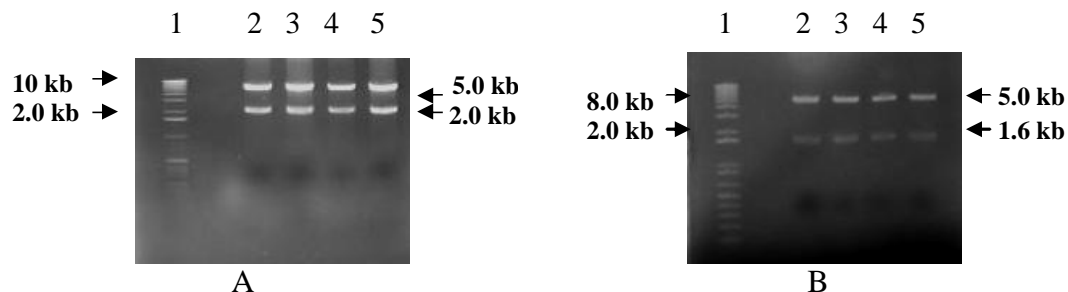
**Lane 2** native recombinant plasmid POB1/pET30 (A), and POB1<sup>1-512</sup>/pET30(B), colony 1

**Lane 3** native recombinant plasmid POB1/pET30 (A), and POB1<sup>1-512</sup>/pET30(B), colony 2

**Lane 3** native recombinant plasmid POB1/pET30 (A), and POB1<sup>1-512</sup>/pET30(B), colony 3

**Lane 5** native recombinant plasmid POB1/pET30 (A), and POB1<sup>1-512</sup>/pET30(B), colony 4

Figure 3.20 1% Agarose gel of native recombinant plasmid pET30a(+)/POB1 (Panel A), and pET30a(+)/POB1<sup>1-512</sup> (Panel B). Four colonies were screened for presence of targeted genes.



**Lane 1** Gibco , DNA ladder 1 k.b.

**Lane 2** plasmid POB1/pET30 (A), and POB1<sup>1-512</sup>/pET30(B) digested with BamHI and XhoI, colony 1

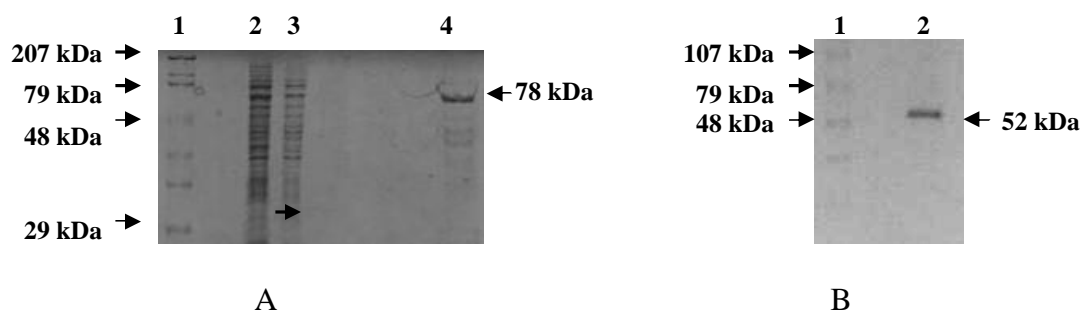
**Lane 3** plasmid POB1/pET30 (A), and POB1<sup>1-512</sup>/pET30(B) digested with BamHI and XhoI, colony 2

**Lane 4** plasmid POB1/pET30 (A), and POB1<sup>1-512</sup>/pET30(B) digested with BamHI and XhoI, colony 3

**Lane 5** plasmid POB1/pET30 (A), and POB1<sup>1-512</sup>/pET30(B) digested with BamHI and XhoI, colony 4

Figure 3.21 1% Agarose gel of recombinant plasmid pET30a(+)/POB1. (Panel A), and pET30a(+)/POB1<sup>1-512</sup> (Panel B) digested with two restriction endonucleases BamHI and XhoI. Vector is indicated by a 5 kb band, whereas full length POB1 by 2 kb and POB1<sup>1-512</sup> by 1.6 kb bands.

The recombinant plasmid containing full length POB1 or POB1 lacking RLIP76 binding site was transformed into the protein expression bacterial strain *E. coli* BL21, and corresponding proteins were purified by Ni-NTA affinity chromatography as described in the experimental section. SDS-PAGE confirmed the purity of these proteins which showed predominant bands at 78 kDa and 52 kDa for POB1 and POB1<sup>1-512</sup>, respectively (Fig. 3.22, Panel A and B)



**Lane 1** Standard protein marker

**Lane 2** Unabsorbed fraction

**Lane 3** First washing

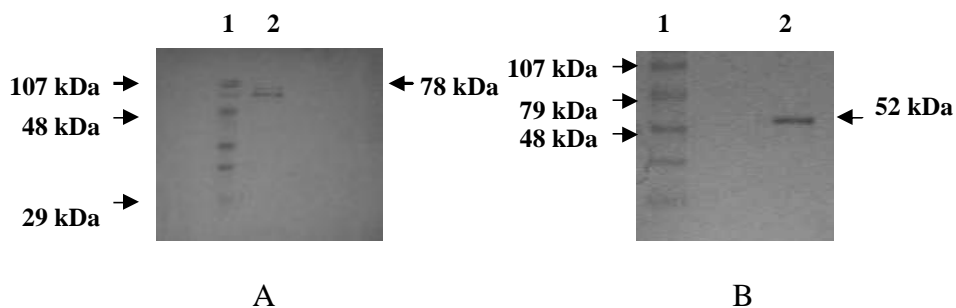
**Lane 4** 78 kDa band of purified POB1

**Lane 1** Standard protein marker

**Lane 2** 52 kDa band of purified POB1<sup>1-512</sup>

Figure 3.22 SDS-PAGE of Ni-NTA super flow resin purified recombinant POB1. (Panel A) and POB1<sup>1-512</sup> (Panel B). The 78 kDa band is a representation of full length POB1 (Panel A), the 52 kDa band shows purified POB1<sup>1-512</sup> (Panel B). SDS-PAGE was stained with Coomassie Brilliant Blue R250.

The proteins were recognized by anti-POB1 antibodies in Western blots. POB1 antibodies were raised in a rabbit against the 78 kDa band of recombinant POB1 as described in the methods section. Western blots were developed using horseradish peroxidase-conjugated goat-anti-rabbit-IgG as the secondary antibody and 4-chloro-1-naphthol as the chromogenic substrate (Fig.3.23 Panel A and B).



**Lane 1** Standard protein marker

**Lane 1** Standard protein marker

**Lane 2** 78 kDa band of purified POB1

**Lane 2** 52 kDa band of purified POB1<sup>1-512</sup>

Figure 3.23 Western Blot of purified recombinant POB1 (A) and POB1<sup>1-512</sup> (B). The 78 kDa band as well as the 52 kDa band were recognized by anti-POB1 IgG and are representation of full length POB1 (Panel A), and POB1<sup>1-512</sup> (Panel B), respectively.

For further studies, purified recombinant POB1 and POB1<sup>1-512</sup> were reconstituted into proteoliposomes as described in the methods section, and such delivery system was used to increase the level of POB1 in mammalian cells as well as to measure an inhibition of transport activity of RLIP76.

### 3.5 Doxorubicin and DNP-SG transport inhibition by POB1 in RLIP76 proteoliposomes

It has been demonstrated by Awasthi (Awasthi et al., 1994, 1998, 2000, 2001, 2003) that RLIP76 is capable of ATP-dependent transport of doxorubicin (DOX) and DNP-SG when reconstituted into proteoliposomes. In this experiment, 20 µg of purified RLIP76 was reconstituted into proteoliposomes along with different concentrations of POB1 or POB1<sup>1-512</sup> (0-80 µg). ATP-dependent transport of DOX as well as DNP-SG was measured in these proteoliposomes. The results presented in (Fig.3.24) show that Doxorubicin and DNP-SG transport activity of RLIP76 was inhibited in a

concentration-dependent manner by recombinant POB1, but not by POB1<sup>1-512</sup> or albumin.

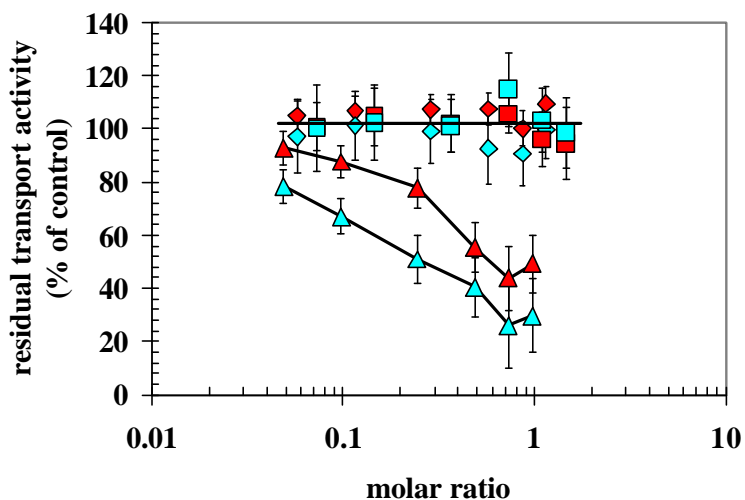


Figure 3.24 The transport activity of RLIP76 towards DOX (red symbols) and DNP-SG (blue symbols) measured in artificial liposomes reconstituted with purified recombinant RLIP76 along with varied amount of POB1 (triangles), POB1<sup>1-512</sup> (square) or bovine-serum albumin (diamond). (Yadav and Zajac 2005)

Note: Molar ratio: POB1/RLIP76

The result shows that there was 50% reduction in DOX transport and a 68% reduction in DNP-SG transport in proteoliposomes containing RLIP76 and POB1. This maximum inhibition was reached near a 1:1 molar ratio of POB1 to RLIP76. Increasing the amount of POB1 in liposomes did not change RLIP76 transport activity compared to a 1:1 ratio. These results suggest that maximal inhibition of RLIP76 catalyzed transport is achieved at a 1:1 stoichiometric binding of POB1 to RLIP76, and that inhibition is not complete.

### 3.6 DOX sensitivity assay in NSCLC H358 after augmentation of POB1 level

It has been shown that inhibition of ATP-dependent transport activity of RLIP76 by anti-RLIP76 IgG induces apoptosis in lung cancer cells and simultaneously increases a sensitivity of these cells to DOX. In this experiment we wanted to find out whether inhibition of the transport activity of RLIP76 with excess POB1 in cancer cells increases their sensitivity to DOX. POB1 and its deletion mutant POB1<sup>1-512</sup> were encapsulated in proteoliposomes, as described in the experimental section, and delivered to the cells followed by a MTT assay of DOX towards H358 cells (NSCLC). Cells were incubated for 12 hours with control liposomes or liposomes containing a varying amount of recombinant POB1 or POB1<sup>1-512</sup> (final concentration 10, 20, or 40 µg/ml) in order to determine which concentration of POB1 maximizes RLIP76 inhibition. After washing cells with PBS different concentration of DOX was added to the cells and IC<sub>50</sub> was measured by performing MTT assay, after 96 hours (Yadav et al., 2005).

The data shows that a POB1 concentration of 40 µg/ml sensitized the cells to DOX the most, compared to 20 or 10 µg/ml of protein. The IC<sub>50</sub> of DOX towards untreated NSCLC H358 was determined to be 0.7-0.9 µM (Awasthi et al., 1996). Our results provide evidence that treatment with POB1 liposomes increased the sensitivity of the H358 cells to DOX by about 2 fold, whereas POB1<sup>1-512</sup> had no significant effect on DOX-sensitivity (Fig 3.25).

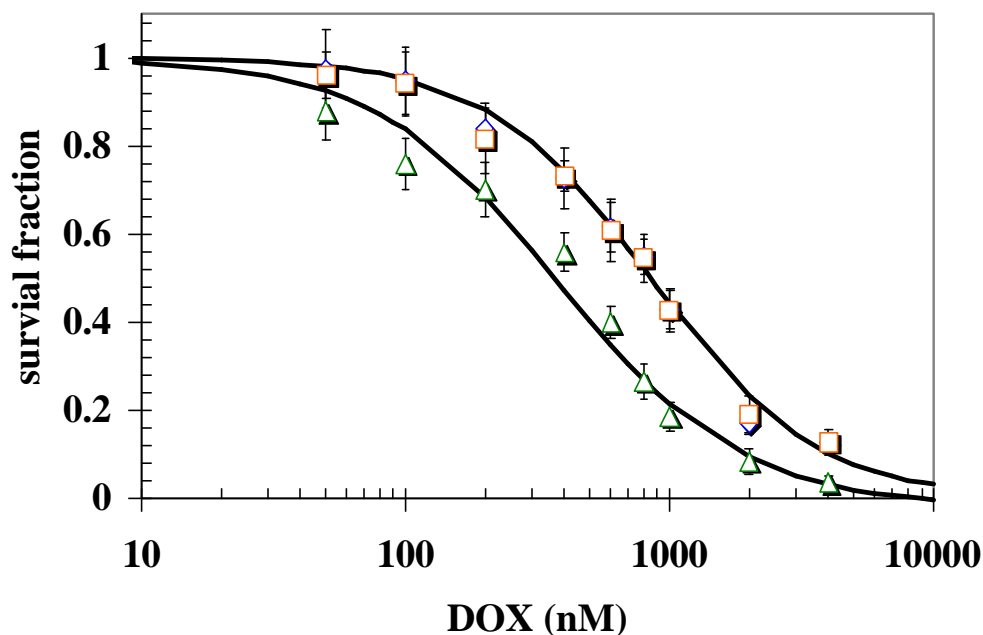


Figure 3.25 The effect of increased POB1 on DOX-cytotoxicity in NSCLC H358. IC<sub>50</sub> of DOX measured after incubating cells with proteoliposomes containing either POB1 (triangle), POB1<sup>1-512</sup> (square) or albumin (diamond) (Yadav and Zajac et al., 2005)

The fact that POB1<sup>1-512</sup>, lacking the RLIP76 binding site, does not change DOX IC<sub>50</sub> towards H358 cells indicates that binding to RLIP76 is necessary to inhibit its transport function. Excess of POB1 drastically reduces the ability of RLIP76 to undergo transmembrane movement, which in turn leads to an increased intracellular accumulation of drugs inside the cell and eventually affects the sensitivity of the cells to DOX. BSA did not have any effect on sensitivity of cells to DOX which reduces the possibility of a nonspecific binding effect on the observed parameters.

### 3.7 Apoptosis of cancer cells as a result of overexpression of POB1

During oxidative stress, heat shock, or UV radiation, cell membrane lipids undergo degradation which leads to formation of very toxic product 4-hydroxynonenal (4-HNE). It has been shown that low level of 4-HNE promote cell proliferation, whereas higher concentration induces cell apoptosis (Esterbauer et al., 1989; Ruef et al., 1998; Cheng et al., 1999). 4-HNE is a very reactive species. It can form DNA and protein adducts, create mutations on DNA, or alter protein functions, all which have tremendous consequences in proper cell homeostasis. Under the catalytic power of GSTs, 4-HNE is conjugated to glutathione (GS-HNE) and this compound is removed from the cell largely through RLIP76 modulated efflux (Awasthi et al., 2003; Singhal et al., 2003). Inhibition of RLIP76 mediated transport by anti-RLIP76 IgG has been shown to induce apoptosis in lung cancer cells, suggesting accumulation of the GS-HNE in cells (Singhal et al., 2003). Moreover, an increased GSH-HNE level inside the cell leads to inhibition of GSTs and impairs the ability of these enzymes to metabolize 4-HNE (Cheng et al., 1999; Cheng et al., 2001; Yang et al., 2003). Since our results showed the ATP-dependent transport activity of RLIP76 for DOX as well as DNP-SG, a GSH-conjugate, was inhibited by POB1 in a concentration dependent manner, we investigated whether augmenting the POB1 level inside the cell induced apoptosis. In order to test this hypothesis, H358 cells were incubated for 24 hours with equal amounts of proteoliposomes reconstituted with either 40 µg/ml of BSA, recombinant full length POB1 or POB1<sup>1-512</sup> protein. Then, a TUNEL assay (Promega Fluorescence) was carried out as described in the experimental section. The result shows that that the full length



POB1 caused apoptosis in cells (Fig. 3.28, Panel C) while the POB1<sup>1-512</sup> which did not inhibit transport properties of RLIP76, did not have any significant apoptotic effect (Fig. 3.26, Panel B).

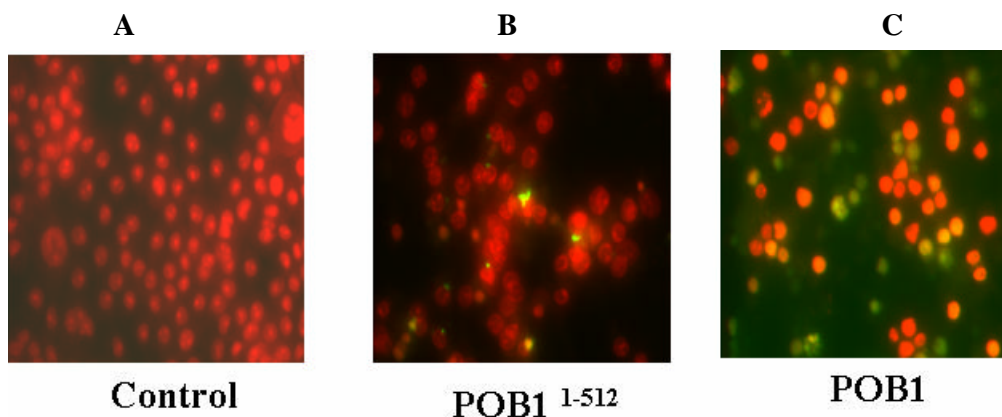


Figure 3.26 The effect of POB1-overloading on H358 cells apoptosis (TUNEL assay).

Apoptotic cells showed green fluorescence and characteristic cell shrinkage. Panel A – cells incubated with BSA, Panel B – cells incubated with POB1, Panel C – cells incubated with POB1<sup>1-512</sup>. Pictures taken at identical exposure at 400 x magnification using Zeiss LSM 510 META (Germany) laser scanning fluorescence microscope with filters 520 nm and >620 nm (Yadav and Zajac et. al., 2005)

These results are consistent with our previous studies showing that inhibition of RLIP76 results in an increased accumulation of glutathione-conjugates of endogenously generated toxicants such as 4-HNE, and culminates in apoptosis.

### 3.8 Accumulation and efflux of <sup>14</sup>C-DOX in H358 lung cancer cell treated with POB1

We have previously shown that transport of DOX and DNP-SG in proteoliposomes reconstituted with an equal molar ratio of POB1 to RLIP76 was decreased by about 50% and 68% respectively. We wanted to investigate a rate of DOX efflux from cells incubated with POB1 liposomes and quantitizef DOX accumulation in

such treated cells. We conducted drug-uptake by augmenting POB1 using proteoliposomes reconstituted with 40  $\mu\text{g/ml}$  of BSA (control), purified rec-POB1, or purified rec-POB1<sup>1-512</sup> added to intact H358 cells. Subsequently, cells were incubated with liposomes for 24 hours and after washing with PBS, 20  $\mu\text{l}$  of [<sup>14</sup>C]-DOX (final concentration 3.6 $\mu\text{M}$ , specific activity 8.5 x 10<sup>4</sup> cpm/nmol) was added and cells were incubated for varying times (5-30 min) at 37 °C. Then, the extracellular drug was washed off and cell-associated radioactivity was determined (Fig. 3.27).

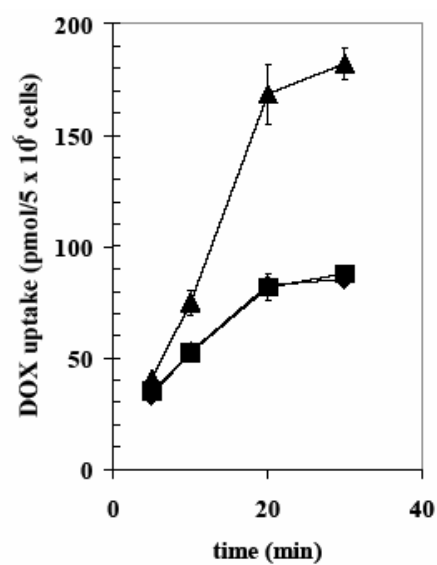


Figure 3.27 The cellular accumulation of DOX in H358 cells treated with 40  $\mu\text{g/ml}$  control liposomes (diamond), purified rec-POB1<sup>1-512</sup> liposomes (square), and purified rec-POB1 liposomes (triangle). The values of DOX uptake are presented in terms of pmol/1x 10<sup>6</sup> cells (Yadav and Zajac et al., 2005)

The results show (Fig. 3.29) that the total DOX accumulation was markedly increased in rec-POB1 liposomes treated cells. These results were consistent with reduced transport of DOX or DNPSG in rec-POB1 liposomes treated cells.

In the second experiment we measured the efflux of DOX from H358 cells treated with liposomes containing 40  $\mu\text{g/ml}$  of BSA (control), purified rec-POB1 or

purified rec-POB1<sup>1-512</sup> for 24 hours. Then, <sup>14</sup>C-DOX was added to the medium, and cells were loaded with DOX by incubating for after 60 min followed by collection of the pellet by centrifugation. Cells were resuspended in 1 ml drug-free medium, and 50  $\mu$ l of aliquots of external medium were taken every minute for radioactivity counting. Cell-associated drug concentration was calculated by back-addition and plotted with respect to time (Fig. 3.28).

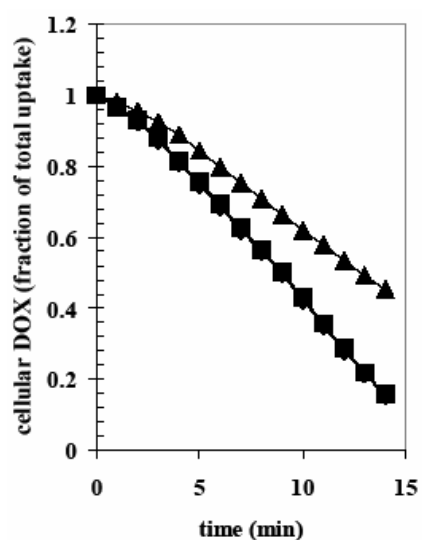


Figure 3.28 The back-added curves of cellular residual DOX vs. time in H358 cells treated with control liposomes (diamond), purified rec-POB1<sup>1-512</sup> liposomes (square), and purified rec-POB1 liposomes (triangle) and incubated with <sup>14</sup>C-DOX. (Yadav and Zajac et. al., 2005)

The data illustrates that the rate of doxorubicin loss from cells due to efflux was significantly lower for rec-POB1 liposome treated cells as compared with control cells and cells treated with POB1 lacking RLIP76 binding site. This experiment provided evidence that POB1 inhibited transport ability of RLIP76, demonstrated by decreased trans membrane movement of DOX.

### 3.9 Discussion

Lung cancer is the number one cause of cancer deaths among men and women in the United States. One of the keys to the prevention and cure of this disease is thorough understanding of the signaling mechanisms linked to RLIP76. RLIP76 is believed to be a novel potential target for cancer therapy. It is involved not only in a rate controlling step in phase III of the cell's detoxification but, also, it is a bridge linking signaling pathways crucial for survival, proliferation, and motility of cancer cells (Awasthi et al., 2003; Sharma et al., 2004; Jullien-Flores et al., 1995, 2000; Mirey et al., 2003; Quaroni et al., 1999; Awasthi et al., 2005). We have shown that several lung cancer cell lines exhibit increased sensitivity to anti-cancer drugs while treated with anti-RLIP76 IgG (Awasthi et al., 2003 II, III; Yadav et al., 2004; Stuckler et al., 2005). This immunoglobulin is able to suppress the ability of RLIP76 to transport xenobiotics from the cell. Therefore, the cancer treatment would be more effective and lower doses of medication are required to kill malignant cells. Our previous studies have shown that increased RLIP76-expression in response to stress or stable cell transfection is accompanied with an increased ability of cells to remove GS-HNE the metabolite of the potent pro-apoptotic lipid-derived alkenal, 4HNE (Cheng et al., 2001; Yang et al., 2003). In this model, RLIP76 functions as a defense against stress-induced apoptosis by regulation of intracellular 4-HNE, an obligate pro-apoptotic product of oxidant or radiant stress (Yadav et al., 2005).

RLIP76 has a coiled-coil region which is required for binding to POB1. These two proteins interact with each other resulting in a complex formation. When POB1 is

over-expressed in cancer cells, those cells become apoptotic. In contrast, when cells are supplied with POB1 with a deleted RLIP76 binding region, the apoptotic effect of this mutated protein is negligible. It is likely that apoptosis in prostate and lung cancer cells over expressing POB1 is due to the inhibition of RLIP76 mediated transport of GS-HNE. These findings appear to be consistent with a model in which intracellular accumulation of 4-HNE results in alkylation of DNA, apoptosis, and necrosis.

It appears that POB1 acts as a regulator of transport activity of RLIP76, which may be crucial for the maintenance of 4-HNE homeostasis in cells. It is known that when the 4-HNE level is high due to the presence of free radical damaged membrane lipids, cells undergo apoptosis (Esterbauer et al., 1996). In contrast, decreasing 4-HNE concentrations below the basal levels leads to differentiation and transformation of cells (Esterbauer et al., 1993). Thus, regulation of RLIP76 transport activity by POB1 may serve as an important role in carcinogenesis signaling. Our findings corroborate previous results of POB1 mediated apoptosis in prostate cancer cells and demonstrate that this mechanism of RLIP76-regulation is operative in lung cancer. We have shown for the first time that POB1 can regulate the transport function of RLIP76, which is consistent with our previous studies showing that inhibition of RLIP76 induces apoptosis in cancer cells through the accumulation of endogenously formed GSH-conjugates.

## CHAPTER 4

### THE ROLE OF RLIP76 IN A DEVELOPMENT OF INSULIN RESISTANCE

#### 4.1 Introduction

Oxidative stress has been implicated in a number of chronic diseases usually grouped under the umbrella of the age-related degenerative disorders, such as cancer (Valko et al., 2006), cataracts (Vinson, 2006) , glaucoma (Izzotti et al., 2006), Alzheimer's disease (Chauhan et al., 2006), heart diseases (Yung et al., 2006; Seddon et al., 2006; Heistad, 2006), male and female infertility (Agarwal et al., 2006), and neuromuscular dystrophies (Barber et al., 2006). Recently, it has been shown that reactive oxygen species contribute to insulin resistance, leading to the development of diabetes mellitus type 2 (Rudich et al., 1998; Ceriello, 1997; Tirosh et al., 1999; Hansen et al., 1999; Blair et al., 1999; Evans, 2003; Talior et al., 2003; Paolisso et al., 1996). Type 2 diabetes is the most prevalent and serious metabolic disease affecting people all over the world. Diabetes affects more than 230 million people worldwide and according to the World Health Organization it is estimated that the number of diabetic patients will increase by 50% within 20 years. The most emerging issue is the fact that diabetes and pre-diabetic conditions are diagnosed more often in young people and children, even though this disorder used to be considered a middle age and old subject disease. Lifestyles characterized by elevated stress, lack of physical activity, and high caloric

intake lead to obesity which plays a crucial role in development of a second type of diabetes. Type 2 diabetes develops when the cells do not respond fully to the action of insulin and are not able to use glucose from the bloodstream. This condition leads to an increased production of insulin by  $\beta$  cells in the pancreas in response to the high blood glucose level and low intracellular glucose. Hepatic cells respond by releasing more glucose to compensate the decreased uptake of glucose by peripheral tissue cells. Eventually, the pancreas becomes less efficient in insulin production which leads to insulin resistance and development of Type 2 diabetes (Kahn et al., 1989; Pessin et al., 2000). Hence, the hallmarks of Type 2 diabetes are pancreatic  $\beta$ -cell dysfunction and insulin resistance.

During oxidative stress  $\beta$ -cells are more susceptible to the damaging power of free radicals because they are low in free radical quenching enzymes such as catalase, glutathione peroxidase, and superoxide dismutase (Tiedge et al., 1997). It has been demonstrated that oxidative stress generated by a short exposure of  $\beta$ -cells to  $H_2O_2$  resulted in a decrease of insulin mRNA level and consequently the suppression of insulin secretion (Maechler et al., 1999). Moreover, exposure of  $\beta$ -cells to a high glucose concentration induced intracellular free radical content, causing the inhibition of insulin release (Sakai et al., 2003).

Multiple signaling mechanisms appear to operate under conditions of oxidative stress to induce insulin-resistance. Free radicals have been shown to activate a variety of cellular stress-sensitive pathways, which interfere with the insulin signaling pathway. ROS are responsible for activation of stress kinases, such as c-Jun N-terminal kinase,

p38, I kappaB kinase, and extracellular receptor kinase which leads to a down-regulation of the cellular response to insulin (Bloch-Damti et al., 2005). As a consequence, insulin reduces its ability to promote glucose uptake, and glycogen and protein synthesis. The mechanisms of down-regulation of insulin function in oxidized cells are complicated, and involve activation of TNF $\alpha$  which triggers increased Ser/Thr phosphorylation of insulin receptor and insulin receptor substrate-1 (IRS1) (Paz et al., 1997; Bloch-Damti et al., 2005; Hotamisligil, 2003; Evans et al., 2005). This reduces redistribution of IRS1 and phosphatidylinositol-kinase between the cytosol and microsomal fraction, reduction of protein kinase-B phosphorylation, and a resultant decreased rate of GLUT4 translocation to the plasma membrane (Hansen, 1999; Gual et al., 2003; Bloch-Damti et al., 2005). In addition, prolonged exposure to oxidative stress affects transcription of the glucose transporter GLUT4 through inhibition of nuclear protein binding to the insulin-responsive element in the GLUT4 promoter (Pessler et al., 2001). Moreover, during exposure to free radicals, protein kinase C and NF $\kappa$ B are activated, which causes an increase in NADPH oxidase activity (Dekker et al., 2000; Davidson-Moncada et al., 2002; Inoguchi et al., 2003; Frey et al., 2006). This enzyme catalyzes the production of superoxide anions by transferring electrons from NADPH and coupling these to molecular oxygen. This action amplifies the amount of harmful reactive oxygen molecules within a cell. An increased concentration of reactive molecules magnifies the activation of oxidative stress-induced insulin resistance. It has also been shown that administration of antioxidants such as vitamin E, alpha-lipoic acid, and N-acetylcysteine in oxidized cells of animal models of diabetes improved insulin



sensitivity (Evans et al., 2005; Bloch-Damti et al., 2005; Greene et al., 2001). Thus, oxidative stress appears to be a common factor in the development of insulin resistance.

To protect itself from the damaging result of reactive oxygen species formed from membrane lipids which underwent lipid peroxidation, cells have developed an inherent mechanism of detoxification defense. One of the most significant mechanism to combat chemical oxidative stress is the system of GSH-linked enzymes including Glutathione S-Transferases (GSTs), Glutathione Peroxidase (GPx) and Glutathione Reductase (GR). Our recent studies have shown that a rapid increase in cellular GSH-conjugate transporter RLIP76 is also a crucial GSH-linked defense (Cheng et al, 2001). Besides its transport function, RLIP76 is a signaling protein participating in signal transduction pathways of epidermal growth factor receptor and insulin receptor endocytosis. Receptor-mediated endocytosis is an essential mechanism for several important physiological processes taking place in eukaryotic cells. These include down regulation of cell surface receptors, degradation of the receptor and/or ligand, transport of essential nutrients and specific ligands, cell surface homeostasis and the activation of intracellular signal transduction cascades (Mellman, 1996; Pastan et al., 1981; Sorkin et al., 1993). There are several endocytic pathways that can mediate the internalization of receptors. The best-studied pathway is clathrin-dependent endocytosis (CDE), in which the protein clathrin, the major component of the endocytic vesicle coats, is recruited (Roth T.F., et al., 1964). However, there are multiple clathrin-independent endocytosis (CIE) pathways that generally depend on caveolae complexes, the cholesterol-rich membrane domains associated with the protein caveolin (McClain et al., 1988; Aguilar

et al., 2005). RLIP76 interacts with POB1 which is involved in clathrin-coated pit-mediated endocytosis of epidermal growth factor receptor and insulin receptor. Through activation of POB1 by binding to its C-terminal (Ikeda et al., 1998), RLIP76 creates a complex with three additional proteins EPS15, Epsin and AP2, which are directly involved in initiating the process of clathrin dependent endocytosis (Kariya et al., 2000). Moreover, RLIP76 contains a RhoGAP homology domain in its central region and exhibits GAP activity toward Rac1 and cdc42 (Julien-Flores et al., 1995; Feig et al., 1996), two proteins which are involved in a clathrin independent endocytotic pathway (Tkachenko et al., 2004; Sabharanjak et al., 2002; Mayor et al., 2004). An active form of RLIP76 causes the hydrolysis of GTP to GDP of cdc42 and Rac1 and this action turns an active form of these two proteins into an inactive form. Surprisingly, only the GDP bound form of cdc42 interacts with caveolin 1, which is a major constituent of caveolae (Rothberg et al., 1992; Scherer et al., 1996; Sargiacomo et al., 1995), the small invaginations of the cell surface which play an important role in cell surface signaling, endocytosis and intracellular cholesterol transport (Parton R.G., et al., 1996, Anderson R.C., 1998, Fujimoto T., et al., 1998). Consequently, RLIP76 should initiate caveolae dependent endocytosis by stimulating the change of cdc42-GTP to cdc42-GDP which can interact with caveolin.

Based on these findings, we hypothesized that RLIP76, through an interaction with POB1, is directly linked to endocytosis of insulin receptor and participates in the development of insulin resistance.

#### 4.2 Effect of RLIP76 on insulin and blood glucose level in mice

It has been shown that RLIP76 is involved in endocytosis of insulin receptor through an interaction with POB1 (Nakashima et al., 1999; Sugiyama et al, 2005; Yadav et al., 2005). Because endocytosis of insulin receptor is a crucial step in maintaining a proper insulin response to a high glucose level in blood, we decided to check the insulin and glucose level in RLIP76 knockout mice and WT mice with additional RLIP76 delivered in liposomes (intra peritoneal injections of 200 µg and 500 µg of RLIP76-liposomes).

Knockout mice were created by Lexicon genetics, and colonies of these mice were raised and segregated after genotyping from tail tissue (genotyping method described in the experimental section). Blood was collected by phlebotomy and subjected to automated analysis for plasma glucose and insulin levels (assay done by Endocrine Diagnostic Lab, Michigan State University, Dr. Kent R. Refsal and Ms. Susan Lombardini). The glucose level was expressed in mg/dL and insulin level in µU/ml. The values were calculated from triplicate determinations. The results show that in genetically modified mice the level of both insulin and glucose decreased with progressive RLIP76 loss (Fig. 4.1, 4.2) compared to control mice. In contrast, mice with augmented RLIP76 level (200 µg and 500 µg of RLIP76) demonstrate higher insulin and glucose levels compared to mice treated with control liposomes (Fig. 4.3, 4.4).

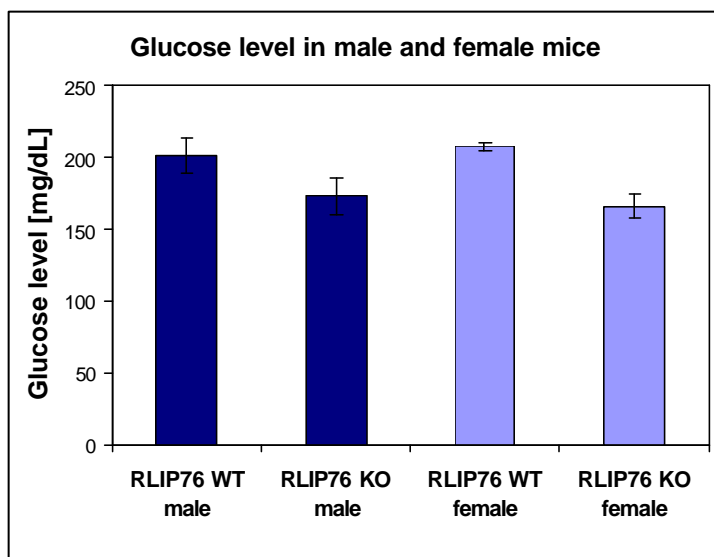


Figure 4.1 Blood glucose level in wild type (WT) and RLIP76 knockout mice (KO), male and female.

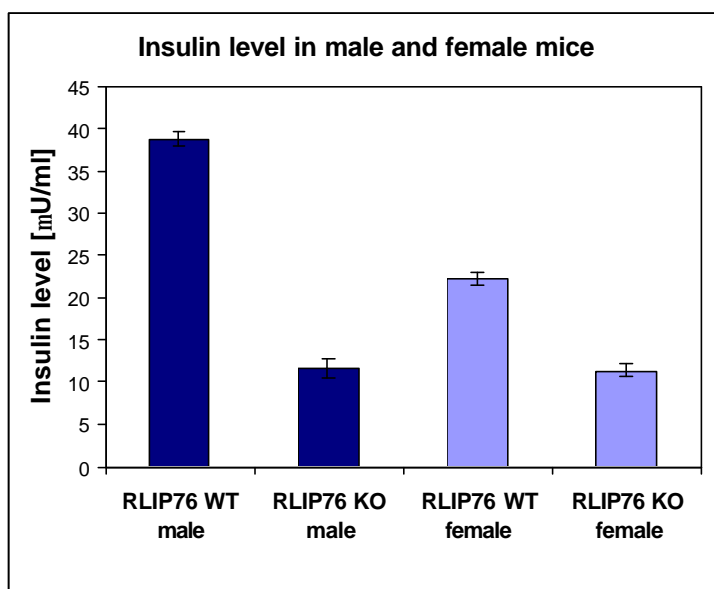


Figure 4.2 Insulin level in RLIP76 wild type (WT) and RLIP76 knockout (KO) mice, male and female

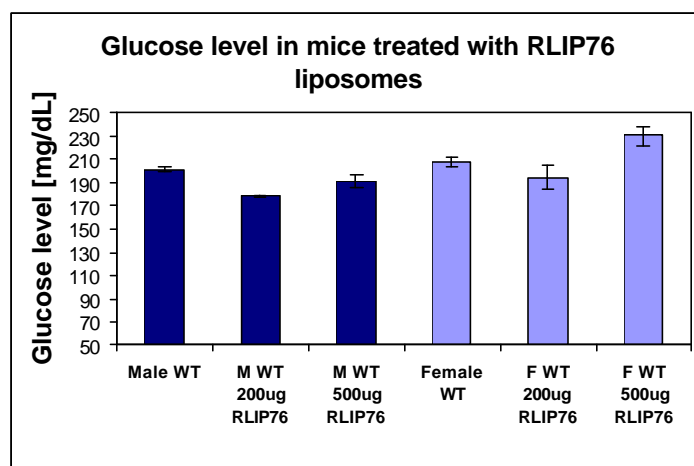


Figure 4.3 Blood glucose level in WT male and female, treated with 200 $\mu$ g and 500 $\mu$ g of RLIP76 encapsulated in liposomes

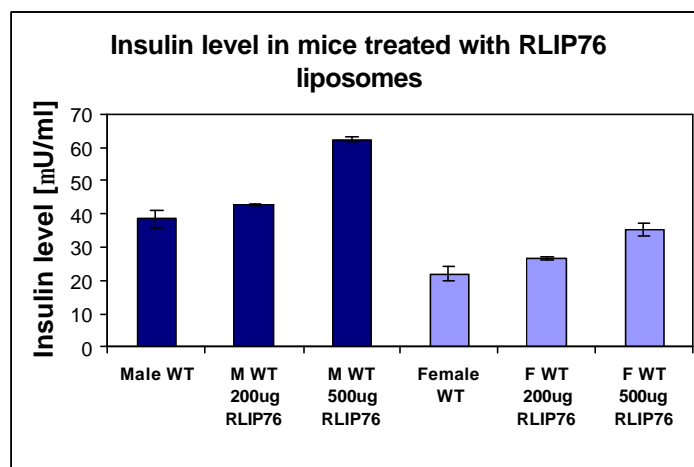
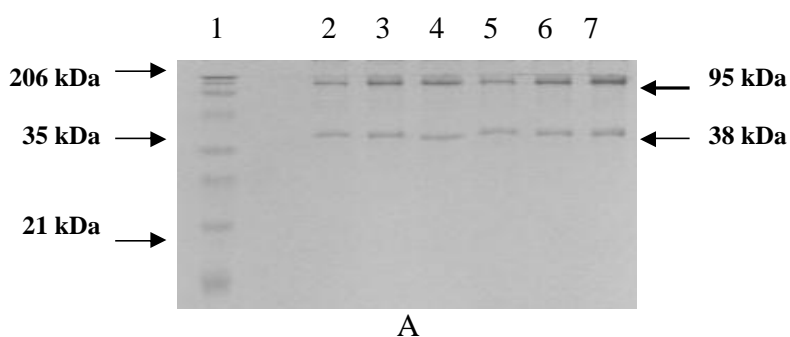


Figure 4.4 Insulin level in WT male and female, treated with 200 $\mu$ g and 500 $\mu$ g of RLIP76 encapsulated in liposomes

The levels of RLIP76 in the RLIP76 WT mice, which had delivered recombinant protein in proteoliposomes, was confirmed by comparing the results of a Western blot analysis from liver and heart of mice with and without proteoliposomes (Fig. 4.5, Panel A and B). The proteoliposomes containing 200  $\mu\text{g}$  and 500  $\mu\text{g}$  of RLIP76 and control liposomes were injected into the peritoneum of male and female mice. After 48 hours, the mice were sacrificed with  $\text{CO}_2$ , and two types of tissues, heart and liver, were collected for analysis.



**Lane 1** Protein marker

**Lane 2** male liver treated with control liposomes

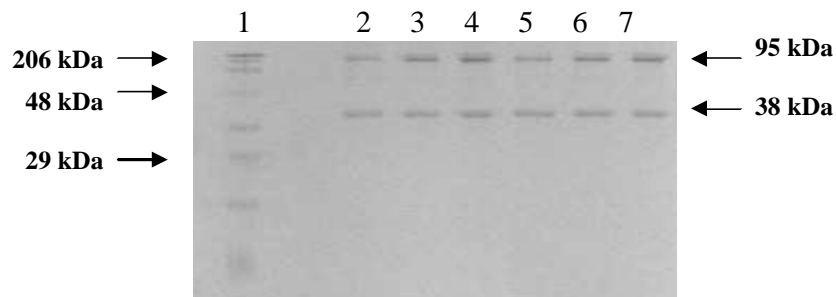
**Lane 3** male liver treated with 200  $\mu\text{g}$  RLIP76 liposomes

**Lane 4** male liver treated with 500  $\mu\text{g}$  RLIP76 liposomes

**Lane 5** male heart treated with control liposomes

**Lane 6** male heart treated with 200  $\mu\text{g}$  RLIP76 liposomes

**Lane 7** male heart treated with 500  $\mu\text{g}$  RLIP76 liposomes



B

**Lane 1** Protein marker

**Lane 2** female liver treated with control liposomes

**Lane 3** female liver treated with 200  $\mu$ g RLIP76 liposomes

**Lane 4** female liver treated with 500  $\mu$ g RLIP76 liposomes

**Lane 5** female heart treated with control liposomes

**Lane 6** female heart treated with 200  $\mu$ g RLIP76 liposomes

**Lane 7** female heart treated with 500  $\mu$ g RLIP76 liposomes

Figure 4.5 Western blot of 100  $\mu$ g of crude membrane fraction of male liver and heart. (Panel A) and female liver and heart (Panel B) after RLIP76 liposomal treatment. Membranes were developed using anti-RLIP76 IgG.

In order to obtain the whole picture about efficiency of delivering RLIP76 in proteoliposomes into mice tissues, the densitometry scans of developed bands on a western blot membrane were performed. The densitometry fold values of RLIP76 expression in the two tissues examined with respect to gender are presented in Fig. 4.6 and 4.7.

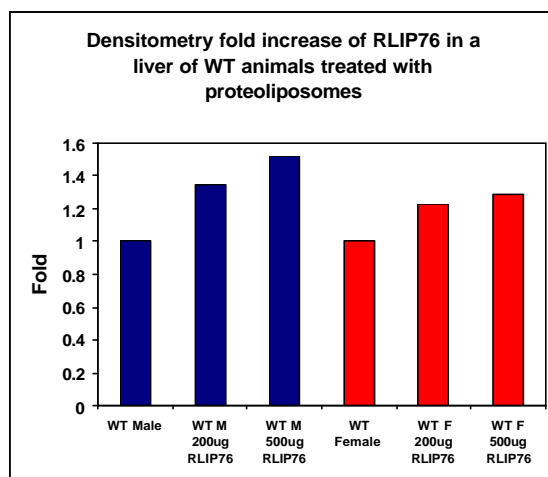


Figure 4.6 Densitometry scans of Western blots of 100 µg of crude membrane fraction of WT male and female liver treated with RLIP76 liposomes.

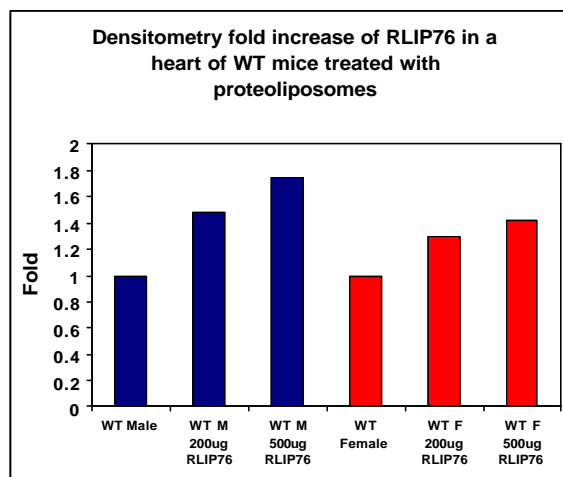


Figure 4.7 Densitometry scans of Western blots of 100 µg of crude membrane fraction of WT male and female heart, treated with RLIP76 liposomes.

The significant difference in the insulin and glucose levels between RLIP76

knockout animals and animals over expressing this protein led to the conclusion that RLIP76 may be involved in mediating insulin-resistance. The results demonstrated a five fold decrease in insulin level in mice lacking RLIP76 compared to mice with augmented RLIP76 levels. The concept of insulin resistance is relatively simple, but its



precise quantification is more complicated. Insulin resistance occurs when the normal amount of insulin secreted by the pancreas is not able to enter cells and activate the glucose transporter GLUT4. To maintain a normal blood glucose, the pancreas secretes additional insulin but insulin resistance hampers the response of peripheral tissue cells to higher levels of insulin. As a consequence, glucose accumulates in the blood, resulting in high blood glucose (hyperglycemia) or Type 2 diabetes. The relationship between glucose and insulin is quite complex and involves the interaction of many metabolic and regulatory factors, particularly the balance in action of insulin and glucagons as well as other gluconeogenic stimuli such as glucocorticoids. Because of inconsistencies in results from any single insulin resistance test, three tests were administer to ensure a reproducible and reliable index of insulin resistance: HOMA, QUICKI, and glucose to insulin ratio. The relationship between these three tests determines if insulin resistance has developed.

***Homeostatic model assessment (HOMA)***. HOMA has been widely employed in clinical research to assess insulin sensitivity since 1985 (Matthews et al., 1985)

The index was calculated using the following formula:

$$HOMA = \frac{I * G}{22.5}$$

Insulin values were expressed in  $\mu$ U/ml, whereas glucose in mmol/L

***Quantitative insulin sensitivity check index (QUICKI)***. Like HOMA, QUICKI can be applied to normoglycemic and hyperglycemic patients. This new mathematical

index was proposed by Katz (Katz et al., 2000) for assessing insulin sensitivity. It is derived by calculating the inverse of the sum of logarithmically expressed values of glucose and insulin:

$$QUICKI = \frac{1}{\log I + \log G}$$

The insulin values were expressed in  $\mu\text{U/mL}$ , whereas glucose values in  $\text{mg/dL}$ .

**Glucose/insulin ratio (G/I ratio).** The G/I ratio has become very popular since its first description in 1998 as an accurate index of insulin sensitivity (Legro et al., 1998). The ratio of glucose to insulin is easily calculated, with lower values representing higher degrees of insulin resistance.

From studies performed by other investigators, it is clear that HOMA and Insulin level values increase while the QUICKI and G/I ratio decreases in the insulin-resistant patients compared to control (McAuley et al., 2001; Quon, 2001; Monzillo et al., 2003). These insulin sensitivity tests were carried out on RLIP76 knockout mice and wild type mice treated with liposomes containing RLIP76. The results are displayed in Fig. 4.8-4.10 for knockout and Fig. 4.11-4.13 for RLIP76 augmented mice, respectively.

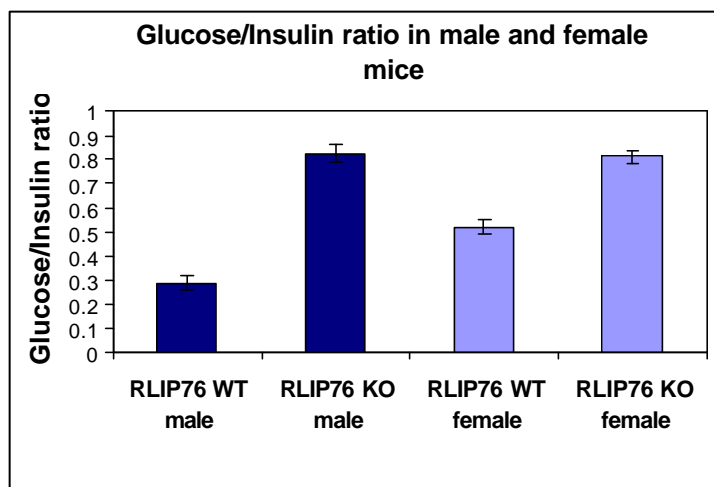


Figure 4.8 Blood glucose/Insulin ratio in WT and RLIP76 knockout mice, male and female

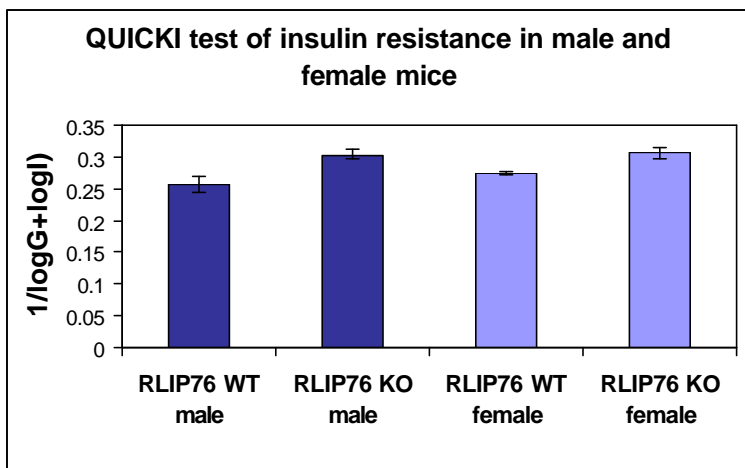


Figure 4.9 QUICKI test of insulin resistance in WT and RLIP76 knockout mice, male and female.

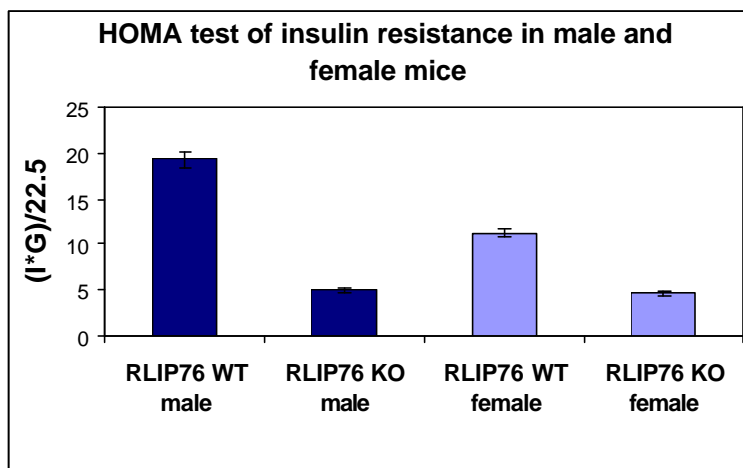


Figure 4.10 HOMA test of insulin resistance in WT and RLIP76 knockout mice, male and female.

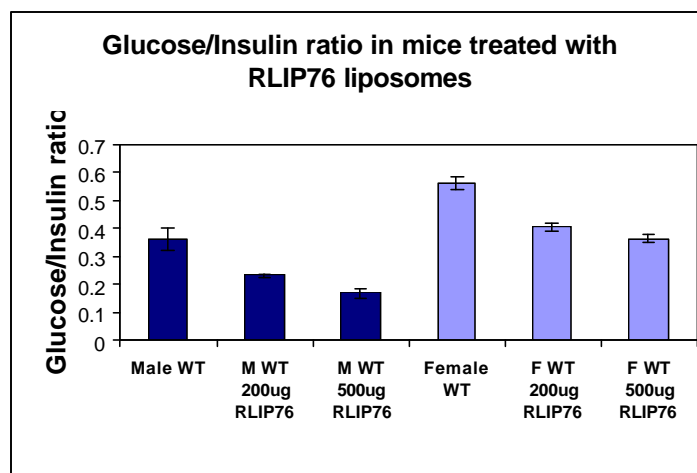


Figure 4.11 Blood Glucose/Insulin ratio in WT and RLIP knockout mice, male and female, treated with recombinant RLIP76 delivered in proteoliposomes.

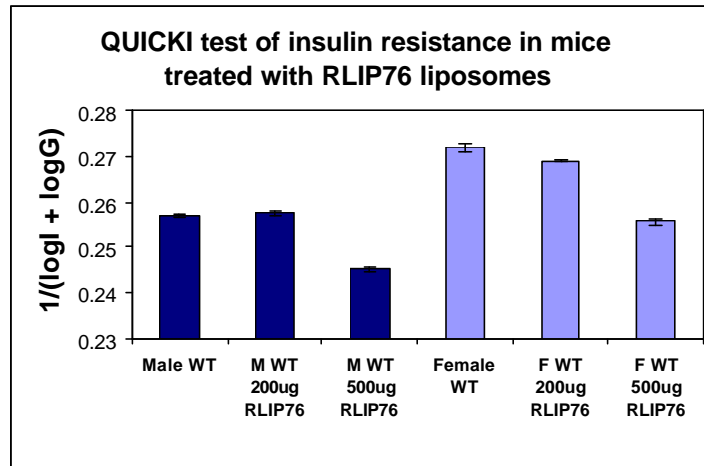


Figure 4.12 QUICKI test of insulin resistance in WT and RLIP knockout mice, male and female, treated with recombinant RLIP76 delivered in liposomes.

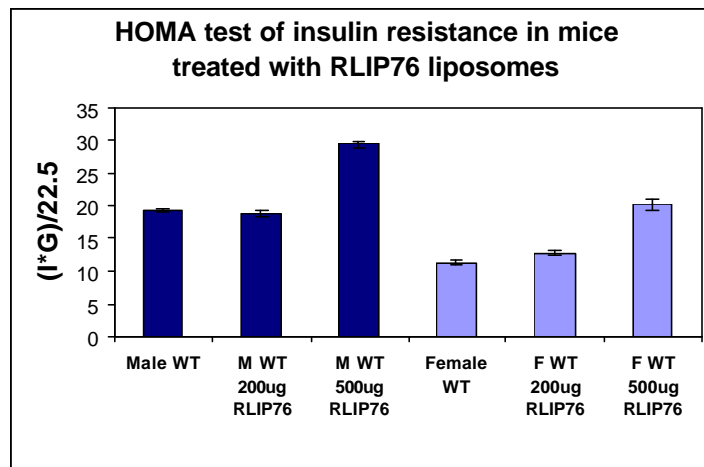


Figure 4.13 HOMA test of insulin resistance in WT and RLIP76 knockout mice, male and female, treated with recombinant RLIP76 delivered in liposomes.

The most remarkable finding is a progressive increase in HOMA and insulin values from animals with increasing RLIP76 in the following order: RLIP76 KO < RLIP76 WT < RLIP76 WT given 200  $\mu$ g RLIP76 < RLIP76 WT given 500  $\mu$ g RLIP76

(Fig.4.13, Fig 4.4). The glucose to insulin ratio, as well as the QUICKI test, showed an opposite pattern as expected (Fig. 4.11, Fig. 4.12): with an increasing amount of RLIP76 in animals, the values of G/I and QUICKI decreased. The effect of RLIP76 was demonstrable for both genders, though greater in male as compared with female mice. Since POB1 is an X-linked protein it can be speculated that this may be related to the different POB1 levels in males and females,.

These tests are a confirmation that along with the rising level of RLIP76 in animals, insulin resistance develops. Therefore, insulin resistance is observable in mice with distributed 200 µg and more significantly with 500 µg of RLIP76. In contrast, RLIP76 knockout mice did not show any sign of this disorder. Surprisingly, these mice exhibited increased sensitivity to insulin. The level of insulin is reduced to 1/3 in male and to 1/2 in female mice, whereas glucose level is diminished to about 1/2 compared with the control mice. The greater insulin-sensitivity of RLIP76 KO animals was readily apparent in the second animal experiment where RLIP76 KO and WT animals were treated with 0.05 U of insulin for two days, glucose level in the blood from a tail vein was measured every 30 minutes for 2 hours (Fig. 4.14, 4.15).

In KO animals, the first administration of insulin resulted in a significant decrease of a glucose level. However, the acute effects of insulin administration on blood glucose were quite similar in terms of percent reduction in blood glucose to WT animals (Fig. 4.14).

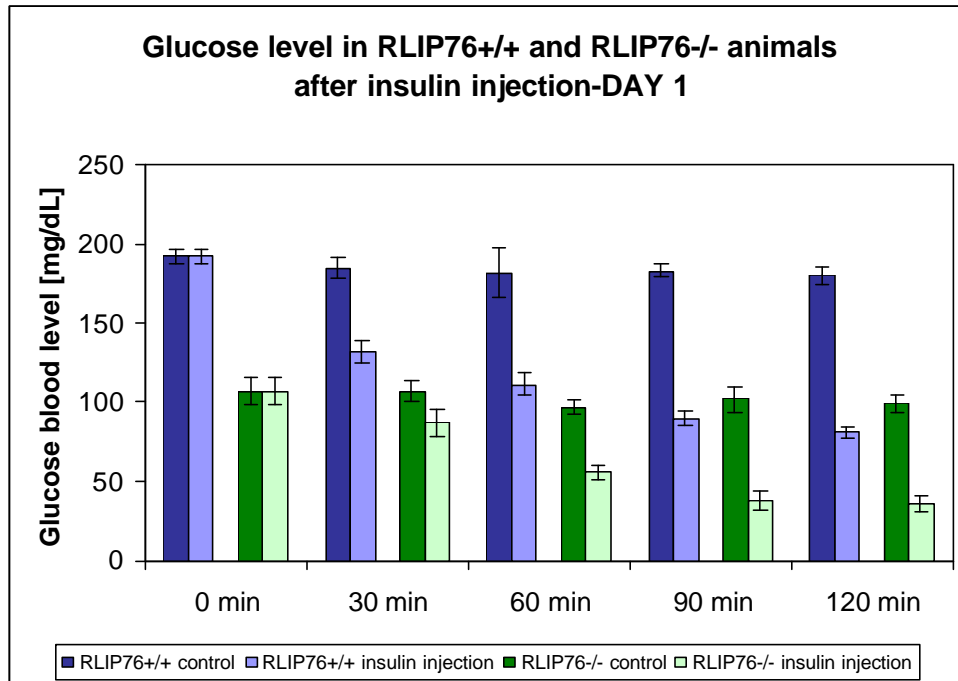


Figure 4.14 Blood glucose level in WT and RLIP76 knockout animals after administration of 0.02 U/ml of insulin.

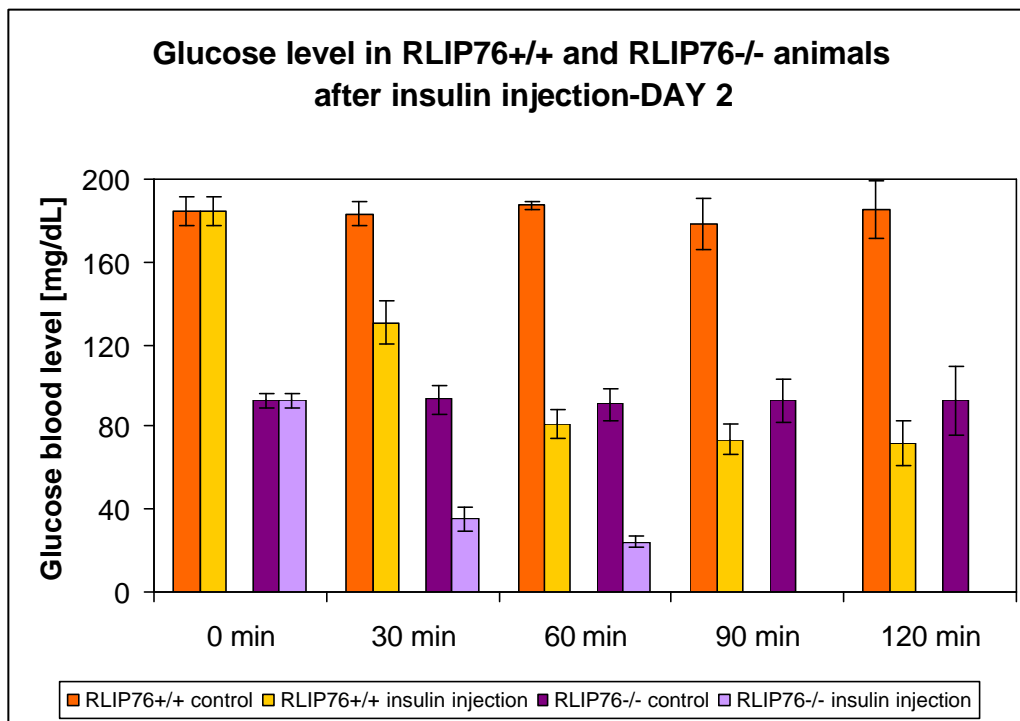


Figure 4.15 Blood glucose level in WT and RLIP76 knockout animals after second administration of 0.02U/ml of insulin.

A dramatic difference was noticed in insulin-sensitivity in the RLIP76 KO animals upon re-challenging with insulin on the second day (Fig. 4.15). Insulin induced hypoglycemia (low glucose level) was remarkably magnified in the RLIP76 KO animals and caused death within 90 min, whereas the WT animals has a response identical to that observed with the first dose. These findings demonstrated that the signaling effects of insulin are more prolonged in duration in the RLIP76 knockout animals, which led as to the conclusion that RLIP76 may participate in insulin signaling.

#### 4.3 Glucose level in WT and RLIP76 KO animals in response to hydrocortisone

Taking into consideration the unusual response to insulin, and ambient hypoglycemia in RLIP76 knockout mice, we decided to investigate whether there is any difference in the hyperglycemic response to glucocorticoids. Glucocorticoids are important hormones in the regulation of metabolic homeostasis. They are potent antagonists of insulin action and, when in excess, can induce insulin resistance and hyperglycemia (Andrews et al., 1999; Asensio et al., 2004; Liu et al., 2005). Glucocorticoids also exacerbate hyperglycemia through stimulation of hepatic gluconeogenesis, and a reduction of the ability of insulin to inhibit glucose production, both of which can magnify Type 2 diabetes (Rizza et al., 1982; Friedman et al., 1993). We studied the relationship between hydrocortisone and RLIP76 by comparing the acute hyperglycemic effects of a single high dose steroid injection between WT and RLIP76 KO animals. WT and RLIP76 KO animals were treated with 30 mg of



hydrocortisone and, after 120 minutes, the glucose level measurements were performed in triplicates from blood sample taken from a tail vein. The results are presented in Fig. 4.16.

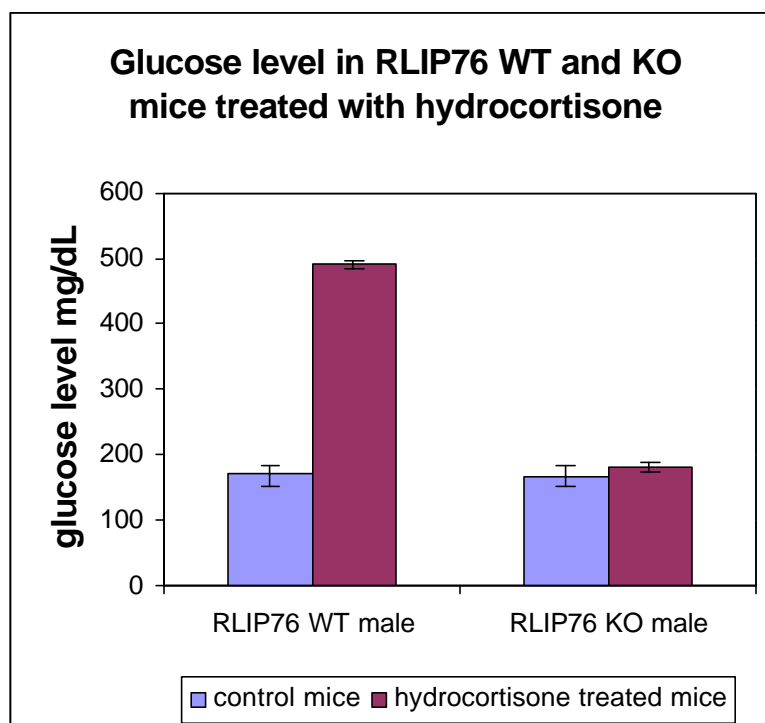


Figure 4.16 Blood glucose level in WT and RLIP76 knockout animals after IP administration of 30 mg of hydrocortisone

Acute exposure to glucocorticoids caused a remarkable increase of glucose level in WT animals, whereas RLIP76 KO mice did not show any significant response to the hormone.

The striking absence of glucocorticoid mediated hyperglycemia in RLIP76 KO animals provided strong evidence for the hypothesis that the glucocorticoids require RLIP76 for hyperglycemic effect to occur.

#### 4.4 Expression and activity of phosphoenol pyruvate carboxykinase and fructose 1,6 bis phosphatase in liver of WT and RLIP76 KO mice

Because glucocorticoid administration did not affect the glucose level in RLIP76 KO animals we reasoned that the lack of steroid induced hyperglycemia in these mice might be due to a decreased expression or inhibition of key gluconeogenic enzymes: glucose-6 phosphatase, fructose 1,6-bisphosphatase (FBPase) and phosphoenolpyruvate carboxykinase, which are increased in response to glucocorticoids (Garrett et al., 1999).

The glucocorticoid hormone, cortisol, enters the cytoplasm through the plasma membrane, where it binds to the high-affinity glucocorticoid receptor (GR). The resulting complex does not have the ability to bind DNA because its DNA binding domain is occupied by heat shock protein 90 (hsp90). Other proteins in this complex include heat shock protein 70 (hsp70) and FKBP52. Dissociation of the oligomeric complex yields the free cortisol-receptor subunit in the DNA-binding form. Then, the activated receptor forms a homodimer which enters the nuclear membrane through the nucleopore. Inside the nucleus, the receptor complex binds to specific DNA responsive elements (GRE) to activate transcription of many genes (Bruner et al., 1997; Drouin et al., 1992). One is a gene encoding phosphoenolpyruvate carboxykinase, a key enzyme of both gluconeogenesis and glycogenolysis. It plays a critical role in blood glucose homeostasis because it catalyses the rate limiting step in gluconeogenesis, the conversion of oxaloacetate to phosphoenolpyruvate. The gene encoding PEPCK contains two glucocorticoid response elements (Petersen et al., 1988), but its

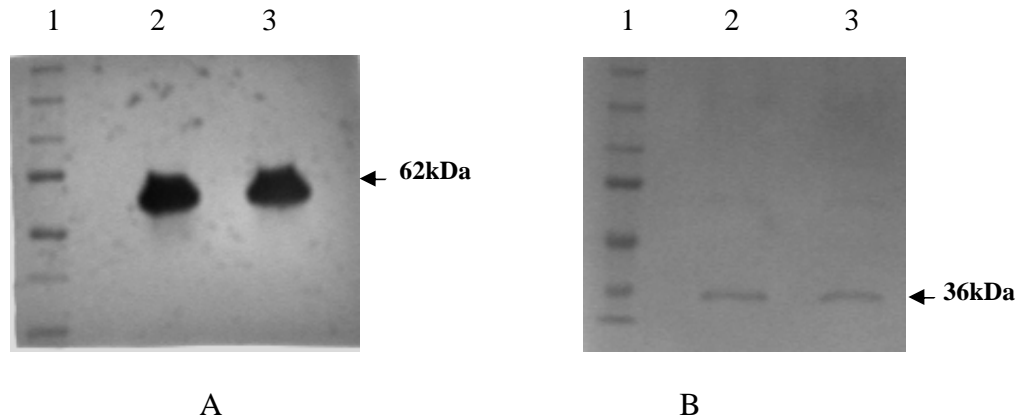
transcription is regulated not only by steroids but also by a variety of extracellular signaling molecules; positively by glucagons, retinoic acid, and cAMP and negatively by insulin and glucose (Sutherland, 1995; Barthel et al., 2003; Quinn et al., 2005; Cassuto et al., 2005). Insulin decreases the level of PEPCK mRNA in the liver and in hepatoma cells (Beale et al., 1984; Beale et al., 1986; Granner et al., 1983). On the other hand, glucocorticoids elevate PEPCK promoter activity mediated by a glucocorticoid response element and hepatocyte nuclear factor 1.

The second enzyme limiting gluconeogenesis process is Fructose 1,6-bisphosphatase (FBPase). It catalyses the reaction of splitting fructose 1,6-bisphosphate into fructose 6-phosphate and inorganic phosphate. FBPase is inhibited by AMP through affecting a turnover of bound substrate, but not the affinity for substrate (Marcus et al., 1987), and through competitive inhibition by fructose 2,6-bisphosphate (Barthel et al., 2003). Mutation of the FBPase gene leads to a deficiency of FBPase, which is associated with hypoglycemia (Matsuura et al., 2002)

Because of the crucial role these two enzymes play in hepatic glucose release, and a lack of response to glucocorticoids in KO mice, we investigated the expression of FBPase as well as phosphoenol-pyruvate carboxykinase in the liver of WT and RLIP76 knockout mice on the protein and gene level. In addition, the activities of these two enzymes were determined.

100 µg of crude liver fraction was subjected to SDS-PAGE followed by Western blot development with horseradish peroxidase. The results show that expressions of two

proteins, PEPCK and FBPase, in RLIP76 KO mice were not affected by a lack of RLIP76 (Fig. 4.17, Panel A and B).



1 – Protein marker Bio-Rad  
 2 – PEPCK (RLIP76 WT)  
 3 – PEPCK (RLIP76 KO)

1 – Protein marker Bio-Rad  
 2 – FBPase (RLIP76 WT)  
 3 – FBPase (RLIP76 KO)

Figure 4.17 Panel A: Western blot of PEPCK WT and KO from crude liver homogenate, Panel B: western blot of FBPase WT and KO from crude liver homogenate. 100  $\mu$ g of protein was loaded in both cases.

In order to confirm the equal expression of PEPCK and FBPase in WT and KO mice, the mRNA level of these two enzymes were tested. RNA was purified from the same liver samples (WT, KO), which were used for determination of protein expression followed by establishment of the expression of PEPCK and FBPase by RT-PCR.

The following primers were used to amplify PEPCK and FBPase genes:

- **PEPCK forward primer**

5' GAGTATATCCACATCTGCGATGGC 3'

T<sub>m</sub> = 54 °C, 50% GC

- **PEPCK reverse primer:**

5'GGCG AGT CTG TCA GTT CAA TAC CAA TC 3'

T<sub>m</sub> = 60 °C, 48% GC

- **FBPase forward primer**

5' GCT CAA CTC GAT GCT GAC TGC C 3'

T<sub>m</sub> = 59 °C, 59 % GC

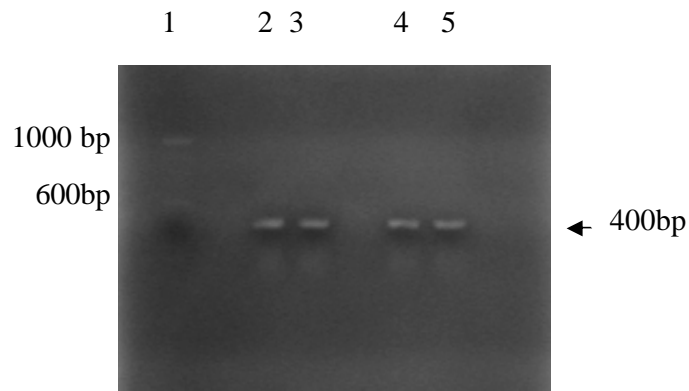
- **FBPase reverse primer**

5' ACC AGG GTT CGA CTA CCA TAC AGTG 3'

T<sub>m</sub> = 59 °C, 52% GC

RT-PCR was performed according to the procedure described in the experimental section.

The analysis of an 1% TAE agarose gel demonstrates that mRNA level of these two enzymes in mice liver remained the same after deleting the RLIP76 gene (Fig 4.18).



1 – Novagene DNA 100 bp ladder  
2 – PEPCK (RLIP76 WT)  
3 – PEPCK (RLIP76 KO)  
4 – FBPase (RLIP76 WT)  
5 – FBPase (RLIP76 KO)

Figure 4.18 RT-PCR of PEPCK and FBPase. 2 µg of DNA was loaded to each well

This finding indicates that the lack of RLIP76 did not appear to either increase or decrease expression of the key gluconeogenesis enzymes, PEPCK and FBPase. This observation left open the possibility that these enzymes were inhibited by soluble factors such as 4-HNE which may accumulate in cells of RLIP76 knockout animals.

The next step of investigation was establishing specific activities of these two enzymes in WT and RLIP76 KO liver tissues. The activity assay of PEPCK was based on the method of Opie and Newsholme (Opie and Newsholme, 1964), whereas FBPase assay was based on the method of Taketa and Pogell (Taketa and Pogell, 1968). The same samples of liver homogenate were used in both assays.

Results of these studies show that RLIP76 knockout did significantly reduce the activities of PEPCK and FBPase. Deletion of the RLIP76 gene causes a decrease in activity of these two enzymes (Fig. 4.19).

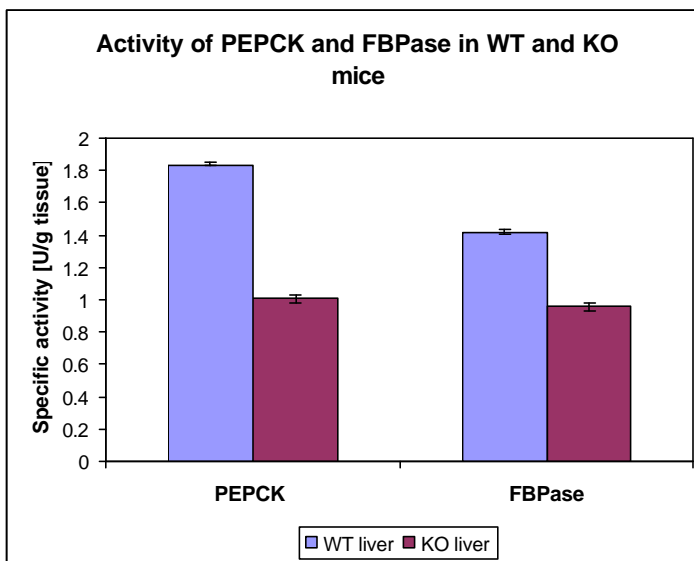


Figure 4.19 Specific activity of phosphoenolpyruvate carboxy kinase and fructose 1.6,- bisphosphatase from WT and RLIP76 KO mice liver.

Specific activity of PEPCK was decreased about 45% in KO mice compared to WT, whereas specific activity of FBPase was 33% lower in KO mice comparing to WT. Taken together, this discovery suggests an explanation for baseline hypoglycemia and lack of corticosteroid hyperglycemic response in RLIP76 KO animals. Since activities of both enzymes are diminished in RLIP76 KO animals, two crucial steps in gluconeogenesis are partially inhibited: formation of phosphoenol pyruvate and fructose 6-phosphate. Such action would slow the release of hepatic glucose to the bloodstream, even after administration of hydrocortisone. Based on these findings we concluded that a lack of response to cortisol in RLIP76 KO mice is at least partially due to decreased activities of the key glucogenic enzymes, PEPCK and FBPase.

#### 4.5 Mammalian cell transfection with pcDNA 3.1/RLIP76

Our observation in KO animals predicted that RLIP76 functions to antagonize insulin-signaling and suggested this should be demonstrable in cell culture as well. In this regard, although a normal hepatocyte and peripheral cell culture would be more ideal, we chose to study NSCLC and SCLC because we wanted to investigate the role of RLIP76 in insulin signaling and these cell lines express RLIP76 with higher activity than normal cells.

In order to see the effect of RLIP76 overexpression, two lung cancer cell lines NSCLC H358 and SCLC H1618 were chosen and stably transfected with pcDNA3.1 eukaryotic expression vector containing cloned RLIP76 gene cloned into it.

Cells lines over-expressing RLIP76 were used in further studies in order to see the effect of augmented RLIP76 on glucose uptake, expression of the insulin signaling proteins: foxo1 and akt1 and endocytosis of ligand-receptor complexes.

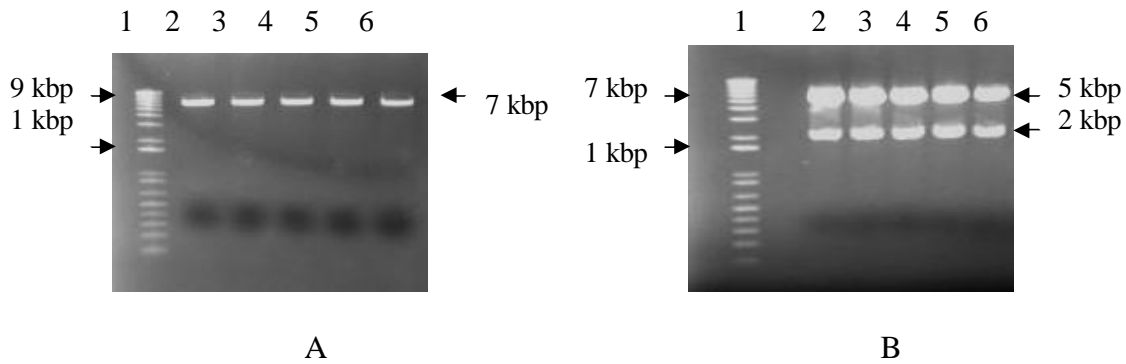
#### *4.5.1 Cloning of RLIP76 into the eukaryotic expression vector pcDNA3.1*

RLIP76 gene cloned into pcDNA3.1 was used for stable transfection of two lung cancer cell lines SCLC H1618 NSCLC H358 in order to see the effect of overexpression of this protein in in-vivo studies.

Digested RLIP76 gene with BamHI and XhoI restriction endonucleases was ligated into the eukaryotic expression vector pcDNA3.1 previously digested with the same two enzymes. The ligation mixture was used for *E. coli* DH5 $\alpha$  cell transformation and the recombinant plasmid was purified from 10 ml of bacterial culture in LB medium containing Ampicillin as a selective marker.

The purified recombinant plasmid was subjected again to enzymatic digestion with BamHI and XhoI in order to ensure the targeted gene was cloned into it (Fig. 4.20 Panel A and B).





Lane 1 1 kb DNA ladder (Novagene)  
 Lane 2 native pcDNA3.1/RLIP76 (colony 1)  
 Lane 3 native pcDNA3.1/RLIP76 (colony 2)  
 Lane 4 native pcDNA3.1/RLIP76 (colony 3)  
 Lane 5 native pcDNA3.1/RLIP76 (colony 4)  
 Lane 6 native pcDNA3.1/RLIP76 (colony 5)

Lane 1 1 kb DNA ladder (Novagene)  
 Lane 2 pcDNA3.1/ RLIP76 (colony 1) digested with BamHI and XhoI  
 Lane 3 pcDNA3.1/ RLIP76 (colony 2) digested with BamHI and XhoI  
 Lane 4 pcDNA3.1/ RLIP76 (colony 3) digested with BamHI and XhoI  
 Lane 4 pcDNA3.1/ RLIP76 (colony 3) digested with BamHI and XhoI  
 Lane 4 pcDNA3.1/ RLIP76 (colony 3) digested with BamHI and XhoI

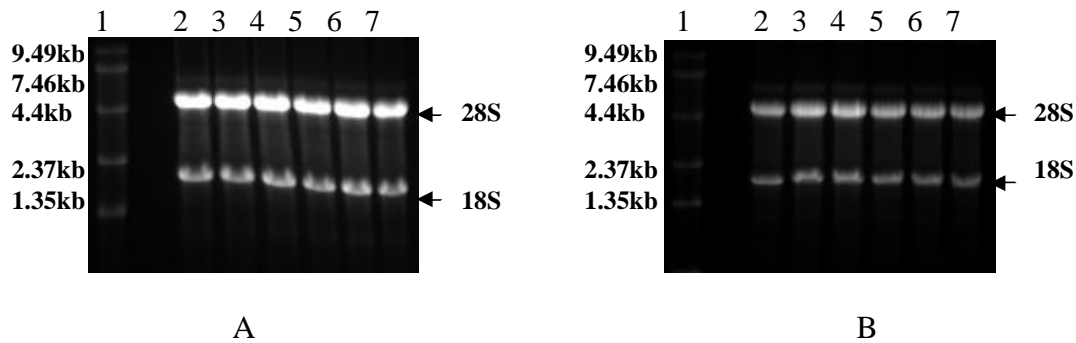
Figure 4.20 1% agarose gel DNA. Panel A represents native recombinant plasmid pcDNA with RLI76, Panel B represents pcDNA3.1/RLIP76 plasmid digested with BamHI and XhoI

The results showed that RLIP76 has been cloned into pcDNA3.1. and such form of recombinant plasmid can be used for transfection of human cancer cells lines using lipofectamine 2000 (Invitrogen).

Two human lung cancer cell lines, squamous carcinoma SCLC H1618 and bronchio alveolar NSCLC H358 were stably transfected with 0.4  $\mu$ g of eukaryotic expression vector pcDNA3.1 alone or with 0.4  $\mu$ g vector containing RLIP76 gene. The transfection described under experimental section was performed according to the manufacture protocol (Invitrogen). All cells were cultured at 37 °C in a humidified

atmosphere of 5 % CO<sub>2</sub> in RPMI-1640 medium supplemented with 10 % heat inactivated fetal bovine serum, and 1% P/S solution. Stable transfectants were selected in presence of 600 µg/ml of Genatamycin (G418) and were maintained in medium containing 300 µg/ml of G418. Single clonal stable transfectants was established by sequential dilution into a 96-well plate, such that only a single cell was seeded in each well. After reaching a log phase of growth, about 5 x 10<sup>6</sup> cells from each cell line were collected to check the level of expression of RLIP76. First, RNA was isolated by the TRIZOL method and RNA gel electrophoresis was carried out to check the quality of RNA and confirm the concentration of RNA previously quantified using a UV Spectrophotometer.

A two µg sample of RNA from H358 and H1618 was subjected to 1 % agarose gel electrophoresis in MOPS-formaldehyde buffer for 3 h at 70 V (Fig. 4.21. panel A and B).



**Lane 1** RNA ladder  
**Lane 2** H1618 control cells  
**Lane 3** H1618 cells transfected with pcDNA3.1  
**Lane 4** H1618 cells transfected with pcDNA3.1/RLIP76 – clone 1  
**Lane 5** H1618 cells transfected with pcDNA3.1/RLIP76 – clone 2  
**Lane 6** H1618 cells transfected with pcDNA3.1/RLIP76 – clone 3  
**Lane 7** H1618 cells transfected with pcDNA3.1/RLIP76 – clone 4

**Lane 1** RNA ladder  
**Lane 2** H358 control cells  
**Lane 3** H358 cells transfected with pcDNA3.1  
**Lane 4** H358 cells transfected with pcDNA3.1/RLIP76 – clone 1  
**Lane 5** H358 cells transfected with pcDNA3.1/RLIP76 – clone 2  
**Lane 6** H358 cells transfected with pcDNA3.1/RLIP76 – clone 3  
**Lane 7** H358 cells transfected with pcDNA3.1/RLIP76 – clone 4

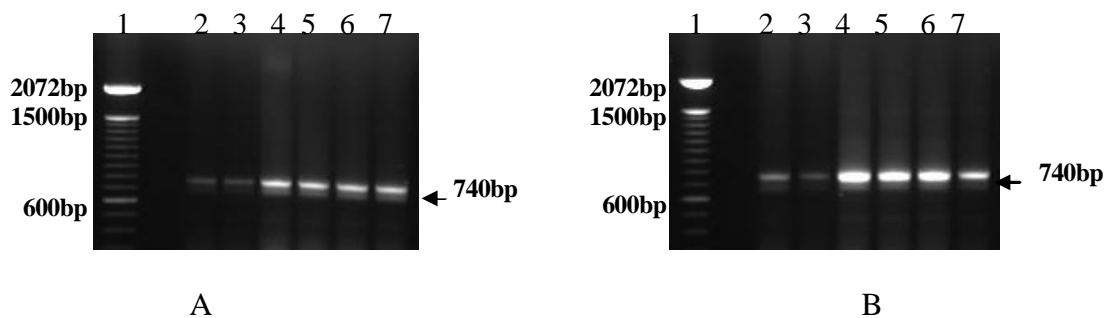
Figure 4.21 Gel electrophoresis of RNA isolated from SCLC H1618 (Panel A) and NSCLC H358 (Panel B) transfected with vector pcDNA3.1 alone and vector containing RLIP76 gene (4 stable clones from each cell line were isolated after transfection).

According to the agarose gel, the concentration of RNA was about 0.8  $\mu\text{g}/\mu\text{l}$  and 0.4  $\mu\text{g}/\mu\text{l}$  in H1618 and H358 cell lines respectively. To perform RT-PCR the same amount of RNA per each cell line needed to be used in the reaction mixture.

#### 4.5.2 RT-PCR analysis of RLIP76 mRNA

The expression of RLIP76 mRNA in lung cancer cell lines was evaluated by RT-PCR analysis (Fig. 4.22, Panel A and B) and fold induction of RLIP76 was confirmed by densitometry of the 740 bp band.

RT-PCR was carried out using RLIP76 gene-specific primers: 1228–1245 bp (upstream primer) and 1948–1968 bp (downstream primer). The results are shown below.



**Lane 1** DNA ladder 100 bp  
**Lane 2** H1618 control cells  
**Lane 3** H1618 cells transfected with pcDNA3.1  
**Lane 4** H1618 cells transfected with pcDNA3.1/RLIP76 – clone 1  
**Lane 5** H1618 cells transfected with pcDNA3.1/RLIP76 – clone 2  
**Lane 6** H1618 cells transfected with pcDNA3.1/RLIP76 – clone 3  
**Lane 7** H1618 cells transfected with pcDNA3.1/RLIP76 – clone 4

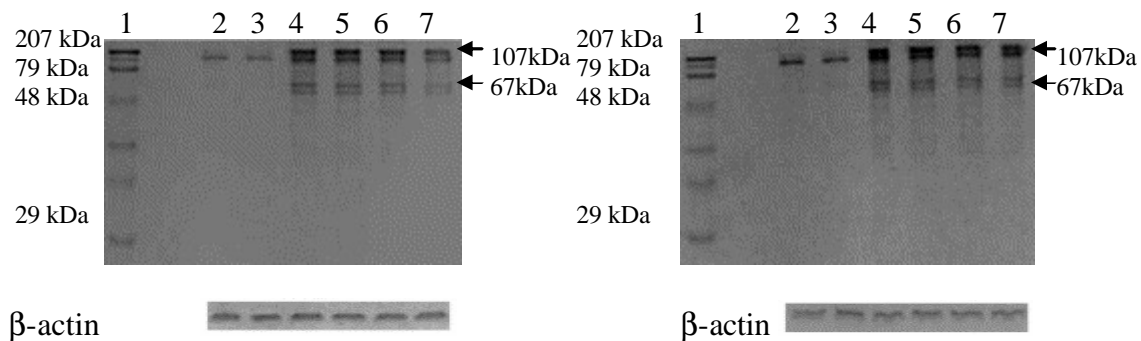
**Lane 1** DNA ladder 100 bp  
**Lane 2** H358 control cells  
**Lane 3** H358 cells transfected with pcDNA3.1  
**Lane 4** H358 cells transfected with pcDNA3.1/RLIP76 – clone 1  
**Lane 5** H358 cells transfected with pcDNA3.1/RLIP76 – clone 2  
**Lane 6** H358 cells transfected with pcDNA3.1/RLIP76 – clone 3  
**Lane 7** H358 cells transfected with pcDNA3.1/RLIP76 – clone 4

Figure 4.22 RT-PCR results of RLIP76 mRNA isolated from SCLC H1618 (Panel A) and NSCLC H358 (Panel B) transfected with vector pcDNA3.1 alone or vector containing RLIP76 gene (4 stable clones from each cell line were isolated after transfection).

During RT-PCR only RLIP76 mRNA was transcribed from total RNA isolated using the two RLIP76 specific primers. The final product of RT-PCR, RLIP76 DNA, was subjected to 1 % agarose gel and the intensity of the DNA bands visible under UV light was analyzed. According to the densitometry analysis there is 5 fold increase of band intensity of RLIP76 transfected cell lines H1618 and H358 compared to control and vector transfected cells. These results are evidence of a successfully performed cell transfection.

#### *4.5.3 Western Blot analysis of RLIP76 expression in cancer cell lines H1618 and H358*

Western blot analysis was performed to examine the level of protein expression in RLIP76 transfected cell lines H1618 and H358 (Fig. 4.23, Panel A and B). The 100 µg aliquots of protein were prepared from  $2 \times 10^6$  cell crude membrane extracts and applied to SDS-PAGE. Protein was detected by RLIP76 IgG on Western blots.



**A**

**Lane 1** Standard protein marker  
**Lane 2** H1618 control cells  
**Lane 3** H1618 cells transfected with pcDNA3.1  
**Lane 4** H1618 cells transfected with pcDNA3.1/RLIP76 – clone 1  
**Lane 5** H1618 cells transfected with pcDNA3.1/RLIP76 – clone 2  
**Lane 6** H1618 cells transfected with pcDNA3.1/RLIP76 – clone 3  
**Lane 7** H1618 cells transfected with pcDNA3.1/RLIP76 – clone 4

**B**

**Lane 1** Standard protein marker  
**Lane 2** H358 control cells  
**Lane 3** H358 cells transfected with pcDNA3.1  
**Lane 4** H358 cells transfected with pcDNA3.1/RLIP76 – clone 1  
**Lane 5** H358 cells transfected with pcDNA3.1/RLIP76 – clone 2  
**Lane 6** H358 cells transfected with pcDNA3.1/RLIP76 – clone 3  
**Lane 7** H358 cells transfected with pcDNA3.1/RLIP76 – clone 4

Figure 4.23 Transfection of RLIP76 in SCLC H1618 and NSCLC H358. Western Blot of RLIP76 expression in cancer cell lines H1618 (Panel A) and H358 (Panel B) transfected with pcDNA3.1 alone or pcDNA3.1 containing RLIP76.  $\beta$  Actin was used as an internal control (Singhal et al., 2005)

RLIP76 protein levels were increased in transfected clones of H1618 and H358 cell lines. Scanning densitometry analysis showed a higher expression level of RLIP76 in transfected cells compared to control which varied from 4.0 to 4.9 folds, and 3.1 to 3.8 folds in H1618 (Fig 4.24) and H358 (Fig 4.25), respectively.

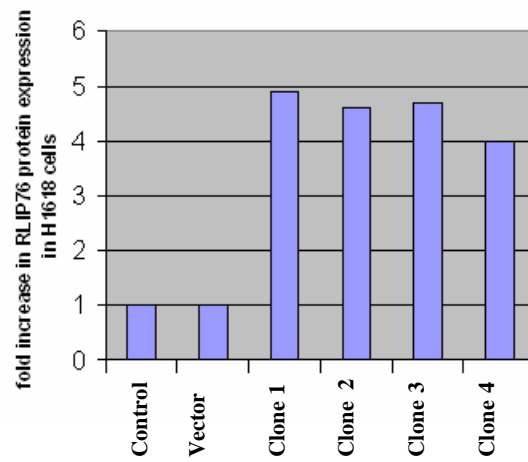


Figure 4.24 The graph is a representation of the level of expression of RLIP76 in H1618 cancer cell line after transfection with pcDNA3.1 alone or pcDNA3.1 containing RLIP76 gene.

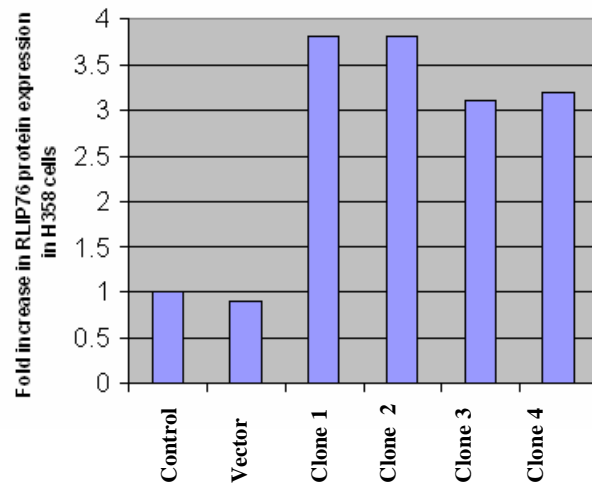


Figure 4.25 The graph is a representation of the level of expression of RLIP76 in H358 cancer cell line after transfection with pcDNA3.1 alone or pcDNA3.1 containing RLIP76 gene.

Taken together, the above experiments demonstrate that the cellular content of RLIP76 was augmented in H1618 or H358 by stable transfection.

#### 4.6 RLIP76 antagonizes glucose uptake by cells in culture

To explore the correlation of RLIP76 with glucose homeostasis, we investigated the relationship of insulin mediated glucose uptake and transport activity of RLIP76 in cultured human cell lines. Our previous studies have shown that the transport activity of RLIP76 is doubled in non-small cell lung cancer cells (NSCLC) as compared to small cell lung cancer cells (SCLC) (Awasthi et al., 2003). In addition, we studied glucose uptake in hepatoma cell line HepG2 expressing glucose carrier GLUT1, which in contrast to GLUT4 expressed by lung cancer cells (Ito et al., 1998) is insulin independent (Aloj et al., 1999; Younes et al., 1997) We thus used these cells as a model system for determining the relative effect of RLIP76 on glucose uptake upon stimulation with insulin. We also compared wild-type SCLC (H1618) and NSCLC (H358) cells with RLIP76-transfected cells that have a 2-3 fold over-expression of RLIP76 (Stuckler et al., 2005; Singhal et al., 2005). In addition, we examined the effect of anti-RLIP76 IgG inhibition on transport activity of RLIP76 (Yadav et al., 2005; Awasthi et al., 2003). Uptake of  $^{14}\text{C}$ -glucose into cells was determined at 30 min after incubation of cells in medium containing radiolabeled glucose, followed by rapid washing to remove extracellular glucose. The effects of insulin, and anti-RLIP76 antibody were determined by including these in the medium during the  $^{14}\text{C}$ -glucose incubation (Fig. 4.26, Fig. 4.27, Fig. 4.28).



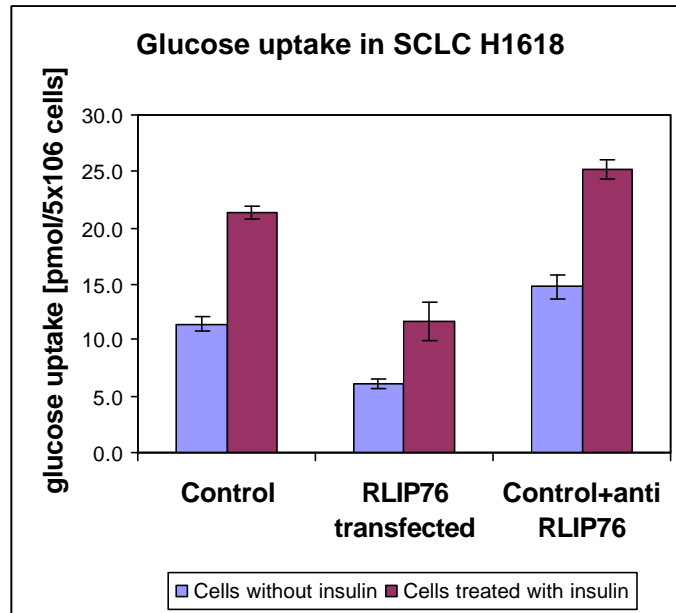


Figure 4.26 Effect of anti-RLIP76 IgG and insulin on glucose uptake in SCLC H1618.

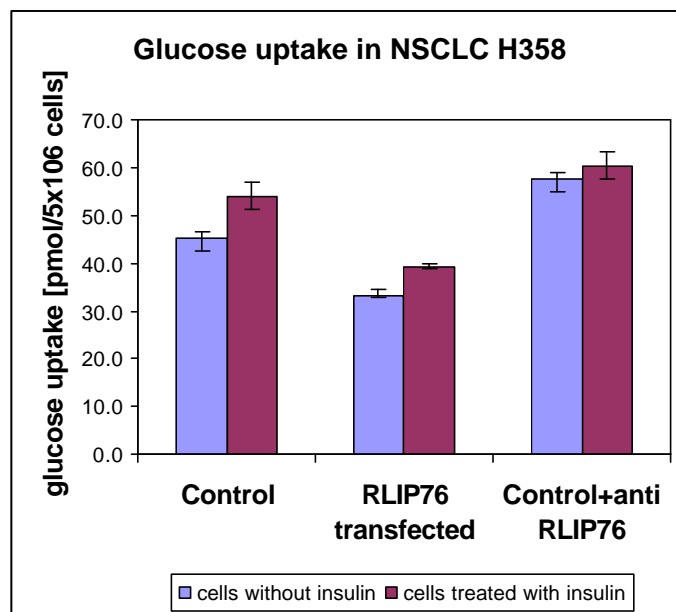


Figure 4.27 Effect of anti-RLIP76 IgG and insulin on glucose uptake in NSCLC H358

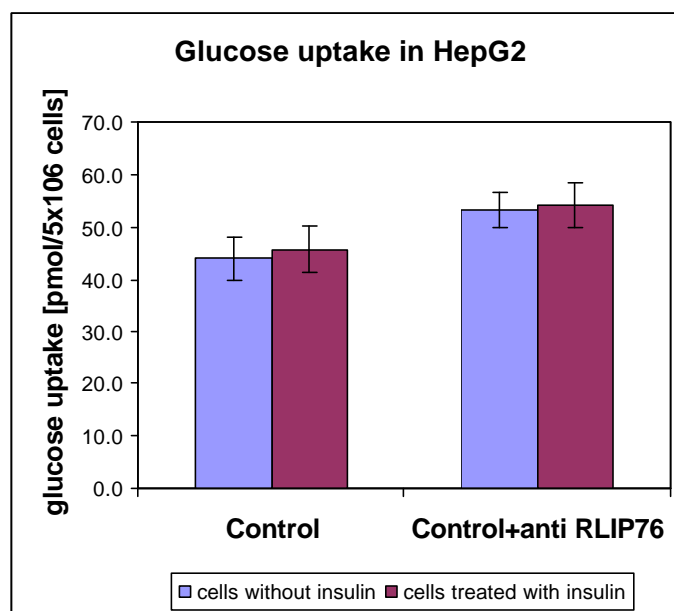


Figure 4.28 Effect of anti-RLIP76 IgG and insulin on glucose uptake in hepatoma cells HepG2.

The result showed that insulin-independent glucose uptake was several fold-greater in H358-NSCLC as compared with H1618-SCLC control cells. This is consistent with the known PET nature of NSCLC compared with SCLC. Augmenting RLIP76 level by stable transfection reduced glucose uptake significantly in both SCLC and NSCLC (Fig. 4.26, 4.27). As expected, insulin significantly increased glucose uptake (over 2-fold) in control SCLC (Fig. 4.26). However, in control NSCLC (Fig. 4.27), which have about a 2 fold higher RLIP76 transport activity as compared to SCLC, only a 20% increase in glucose uptake was observed, indicating an inverse relationship between RLIP76 activity and response to insulin. Expectedly, augmenting cellular RLIP76 by transfection resulted in decreased insulin-dependent glucose uptake in either SCLC or NSCLC, as predicted by our hypothesis.

Anti-RLIP76 antibodies have been shown previously to inhibit RLIP76 transport activity (Awasthi et al., 2003; Awasthi et al., 1994; Awasthi et al., 2003; Yadav et al., 2004). In order to further investigate a possible correlation of insulin responsiveness with RLIP76 transport activity, we studied the effects of anti-RLIP76 antibodies on insulin dependent glucose uptake. Treatment of cells with anti-RLIP76 antibodies caused an increase in glucose uptake in SCLC as well as NSCLC, both in the absence and presence of insulin, which is consistent with the idea that inhibition of transport function of RLIP76 augments insulin actions.

In hepatoma cell line HepG2, as expected, insulin did not have any effect on glucose uptake (Fig. 4.28). However, the RLIP76-inhibitor and anti-RLIP76 antibodies augmented glucose uptake in HepG2 cells. This effect was evident whether insulin was included in the medium or not. These findings confirmed previous reports of the insulin-insensitivity of HepG2 with respect to glucose uptake, and showed that blocking RLIP76 caused an insulin-independent increase in glucose uptake.

#### 4.7 Insulin signaling of Akt1 and FOXO1 in cancer cell lines

In order to further investigate the association of RLIP76 with glucose metabolism, we focused our studies on two crucial proteins involved in insulin signaling the forkhead transcription factor 1 (FOXO1) and protein kinase Akt. FOXO1 serves as one of the major substrates of Akt in response to insulin and growth factors (Lin et al., 1997; Ogg et al., 1997; Brunet et al., 1999; Greer et al., 2005). In the absence of insulin, FOXO1 is localized in the nucleus, where it causes upregulation of targeted genes (Biggs et al., 1999; Brunet et al., 1999; Takaishi et al., 1999). FOXO1 stimulates

expression of gluconeogenic genes, leading to hepatic glucose production and suppresses expression of genes involved in glycolysis (Zhang et al., 2006). It has been shown that transgenic mice expressing constitutively active FOXO1 in the liver had an elevated glucose level despite high insulin levels. Moreover, glucose tolerance was impaired in FOXO1 transgenic mice as compared to the WT (Zhang et al, 2006). On the other hand, expression of dominant negative FOXO1 mutant results in partial inhibition of glucose 6-phosphatase and phosphoenolpyruvate carboxykinase expression in primary cultures of mouse hepatocytes and kidney cells (Nakae et al., 2001; Barthel et al., 2003; Nakae et al., 2001). When insulin receptor is phosphorylated after insulin binding it triggers the recruitment and activation of phosphoinositide kinase (PI3K) which in turns activates the cascade of serine/threonine kinases such as Akt and SGK (Cantley, 2002). Phosphorylated Akt and SGK are translocated into a nucleus where they directly phosphorylate FOXO1 transcriptional factors (Alessi et al., 1997, Brunet et al., 2001, Nakae et al., 1999; Kops et al., 1999; Tang et al., 1999; Kops et al., 1999). Such action leads to a rapid relocalization of FOXO1 factors into the cytoplasm by chaperone molecules (Brunet et al. 2002; Rena et al., 2002). The sequestration of FOXO1 outside a nucleus inhibits the transcription of gluconeogenetic genes. On the other hand, phosphorylated Akt1 stimulates glucose uptake in muscles, fat and the liver by an initiation of a translocation of the glucose transporter (GLUT4) from cytoplasmic vesicles to the cell membrane (Bevan, 2001; Kido et al., 2001). These findings are evidence that FOXO1 and Akt1 are involved in insulin regulation of glucose metabolism.

To investigate the correlation of RLIP76 with FOXO1 and Akt1 we examine the expression of phosphorylated Akt1 at Ser 437 and the binding activity of FOXO1 in cell culture models. We studied two types of lung malignant cell lines control and RLIP76 transfected small cell lung cancer (H1618), and non-small cells lung cancer (H358) in which RLIP76 specific activity is higher due to differential PKC activity than in small cell lung cancer cells. In addition, we tested HepG2 hepatoma cells which has the highest expression of gluconeogenic and glycolytic enzymes (Lemaigre et al., 1994) and in addition the glucose transporter GLUT1 works on insulin insensitive pathway (Younes et al., 2000; Aloj et al., 1999; Medina et al, 2002).

Because these two proteins are stimulated (Akt1) or inhibited (FOXO1) by insulin, we determined their expression with or without respect to insulin.

Phospho-Akt1 was quantified in 50 µg of cell extract separated on a 12 % agarose gel followed by Western blot development with antibody against phospho-Akt1 (Ser 437). The expression level was determined by scanning densitometry (Fig. 4.32-4.34). FOXO1 DNA binding activity was examined using a TransAM FKHR colorimetric assay in which 50 µg of protein was subjected for each absorbance measurements at 450 nm using ELISA plates (Fig. 4.29-4.31).

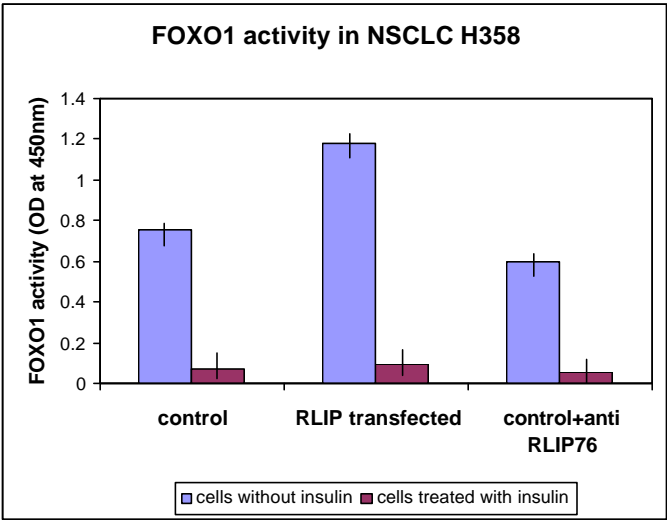


Figure 4.29 FOXO1 DNA binding activity in NSCLC H358

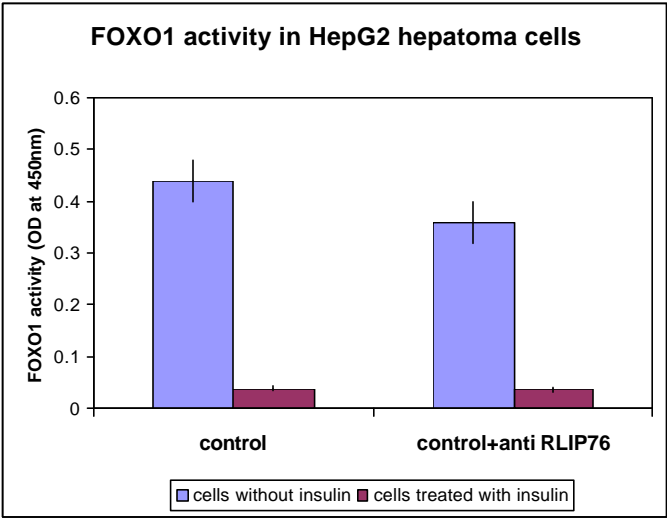


Figure 4.30 FOXO1 DNA binding activity in hepatoma HepG2 cell line

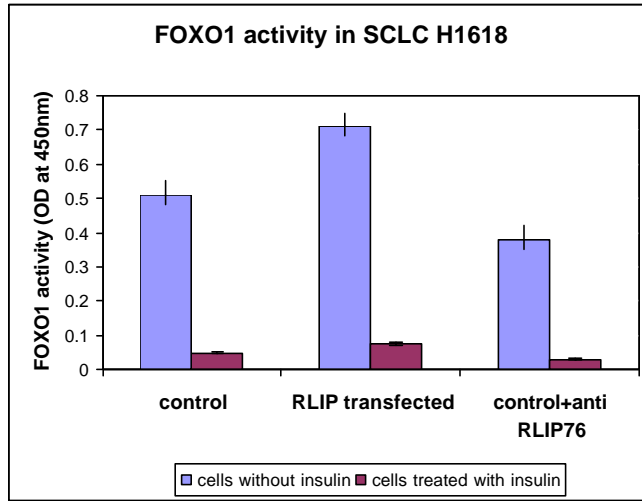


Figure 4.31 FOXO1 DNA binding activity in SCLC H1618

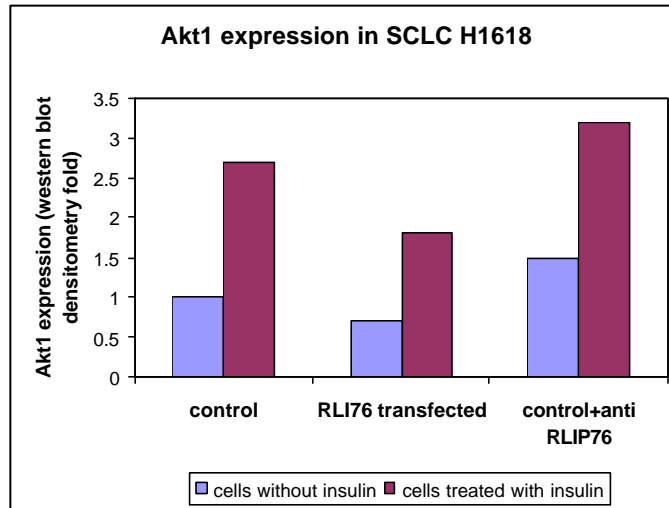


Figure 4.32 Phospho-Akt1 expression in SCLC H1618

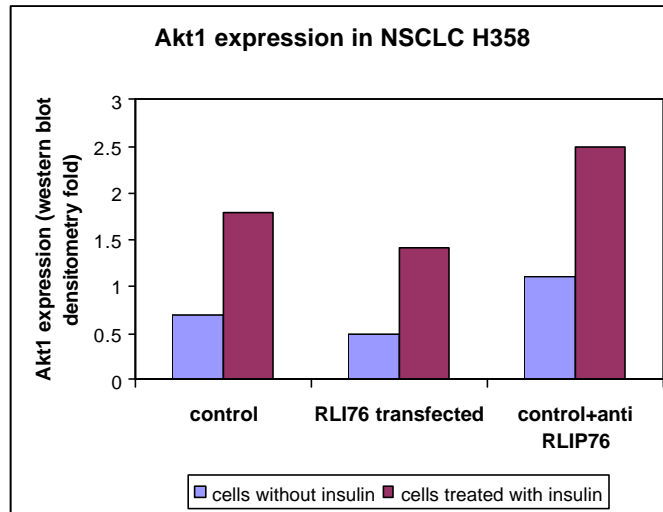


Figure 4.33 Phospho-Akt1 expression in NSCLC H358

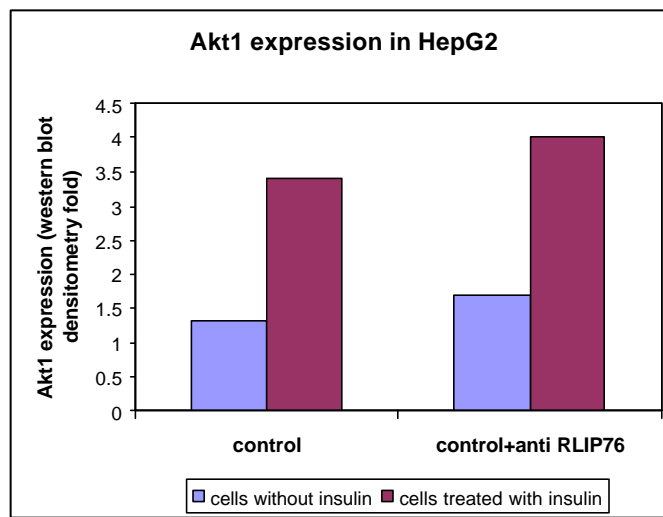


Figure 4.34 Phospho-Akt1 expression in HepG2 hepatoma cell line

The results are consistent with studies performed by other investigators. As expected, insulin markedly stimulates Akt1 phosphorylation in all three cell lines by 60%. In contrast, FOXO1 DNA binding activity was remarkably decreased (10 fold) after insulin treatment in investigated cells. Surprisingly, additional RLIP76 decreased



Akt1 expression by 30% in both transfected lung cancer cell lines, regardless of insulin treatment. On the other hand, FOXO1 activity was 25% higher in these RLIP76 transfected cells. Moreover, incubation cells with anti-RLIP76 IgG, which were shown to inhibit transport activity of RLIP76, resulted in a decrease in FOXO1 activity in NSCLC, SCLC and HepG2 cell lines, with and without insulin treatment. In contrast, anti-RLIP76 antibody increased expression of phospho-Akt1 in investigated cell lines without insulin in the following order: 50% in H1618, 36% in H358 and 23% in HepG2. Also when cells were incubated with insulin, RLIP76 IgG treatment caused an increase in Akt1 expression in H358 (28%), followed by H1618 (19%) and HepG2 (15%). In NSCLC, the level of phospho-Akt1 was slightly lower and FOXO1 slightly higher than that in SCLC. RLIP76 over-expression in NSCLC caused a significant decrease in phospho-Akt1 levels and an increase in FOXO1 activity, effects that are opposite to those caused by insulin.

Taken together, these findings indicate that RLIP76 antagonizes insulin-actions globally, affecting both glucose-uptake and other signals, as may be expected if it were operating at the level of the membrane, functioning to regulate the endocytosis of the insulin/insulin-receptor complex.

#### 4.8 Effect of RLIP76 on endocytosis of insulin-insulin receptor and EGF-epidermal growth factor receptor

To directly examine the relationship between RLIP76 and receptor-ligand pair endocytosis, we compared the uptake of rhodamine-labeled epidermal growth factor (EGF) in control and RLIP76-overexpressing H358 NSCLC transfected cells (Fig. 4.35). The internalization of EGF receptor was considerably quicker in RLIP76 over-

expressing cells compared to control. Interestingly, anti-RLIP76 antibodies markedly reduced EGF internalization. When cells were incubated with FITC-tagged insulin, similar findings were seen – a marked increase in the rate of endocytosis of FITC-insulin upon increased RLIP76 expression, and marked inhibition of this process by addition of anti-RLIP76 IgG (Fig. 4.36).

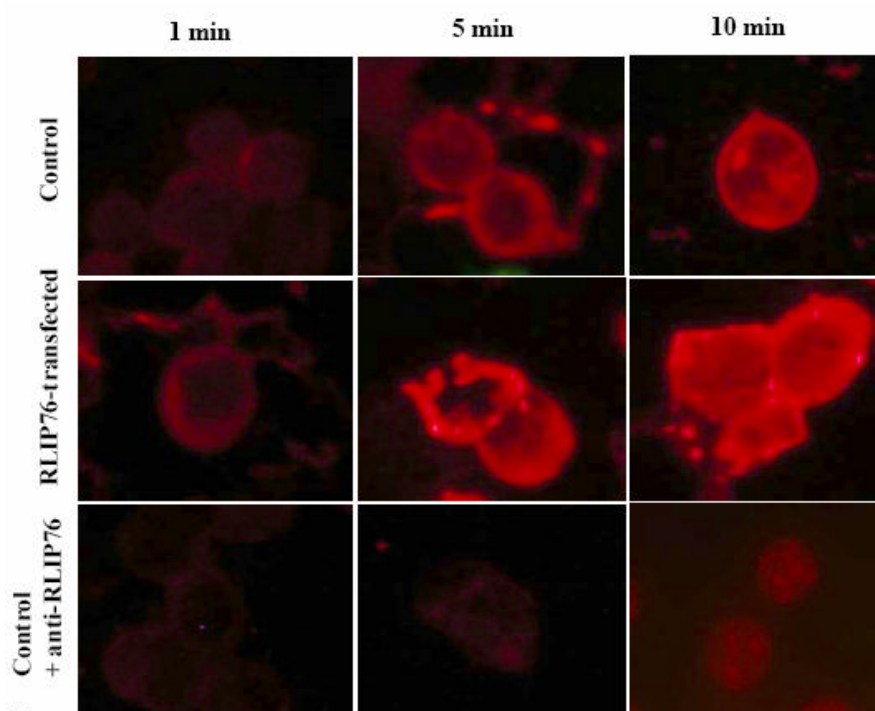


Figure 4.35 Effect of RLIP76 on EGF receptor internalization in NSCLC H358

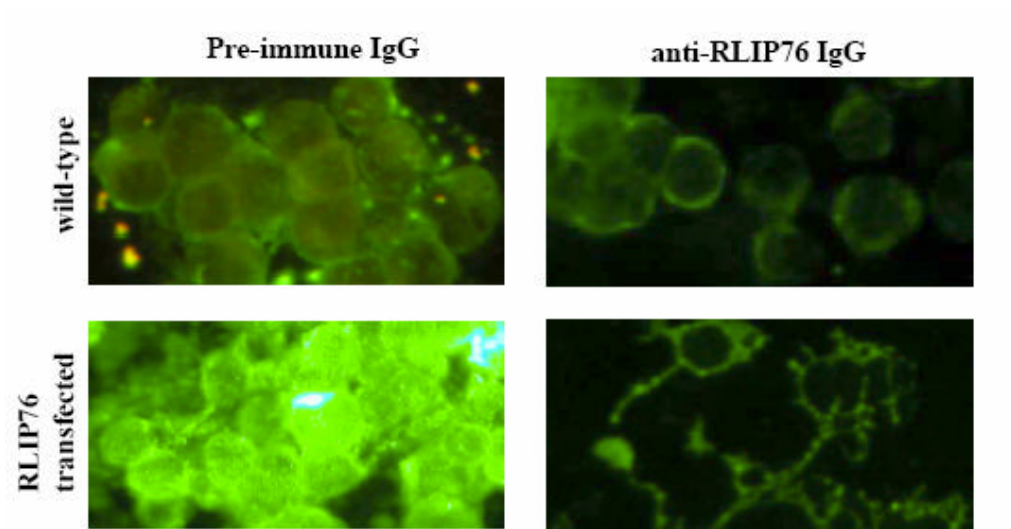


Figure 4.36 Effect of RLIP76 on insulin receptor internalization in NSCLC H358

In order to further explore the involvement of RLIP76 in clathrin mediated endocytosis of insulin receptor and epidermal growth factor receptor we studied mice embryonic fibroblasts cells isolated from WT and RLIP76 KO mice. It has been shown that RLIP76 is involved in clathrin dependent endocytosis through an interaction with POB1, EPS15, and Epsin (Ikeda et al., 1999; Nakishima et al., 1999; Yadav et al., 2005). Removal or negative mutation of EPS15 resulted in inhibition of clathrin dependent endocytosis (Confalonieri et al., 2000; Salcini et al., 2001; Sigismund et al., 2005). Based on these findings we decided to suppressed EPS15 with siRNA and investigate the contribution of RLIP76 in clathrin independent endocytosis in mice embryo fibroblast cells isolated from wild type mice (MEF – WT) and mice embryo fibroblast cells isolated from RLIP76 knockout mice (MEF – KO). The cells were incubated with rhodamine tagged EGF and FITC-tagged insulin for 10 minutes with or

without EPS15 siRNA, and the pictures were taken using a Zeiss LSM510 confocal laser microscopy at 400 x magnification (Fig., 4.37, 4.38).

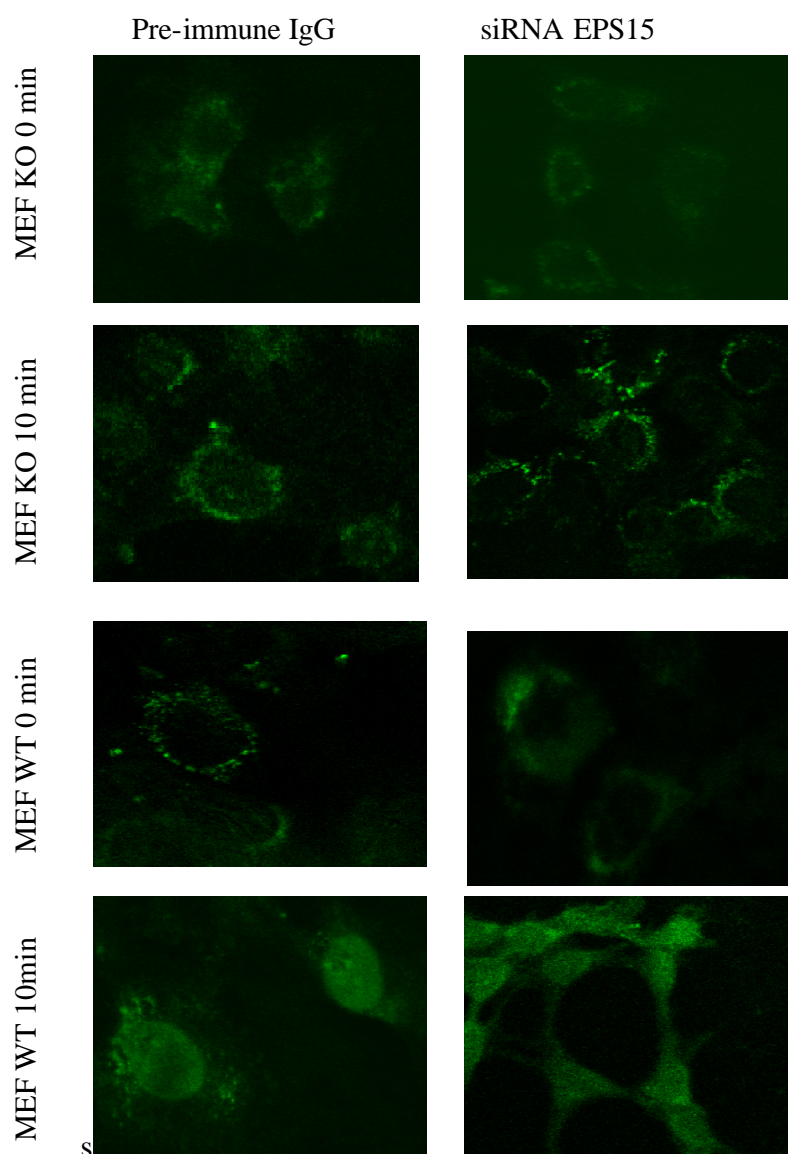


Figure 4.37 Effect of RLIP76 on clathrin mediated endocytosis of insulin receptor in MEF WT and MEF KO cells after suppression of EPS15 with siRNA.

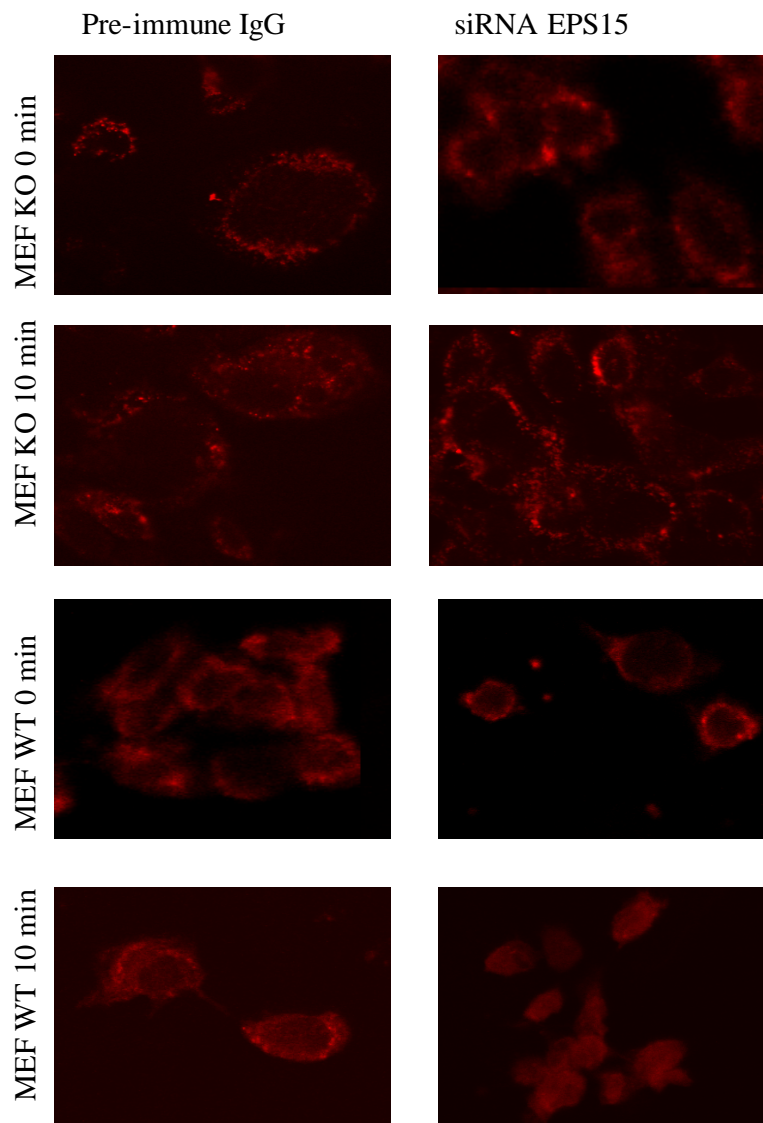


Figure 4.38 Effect of RLIP76 on clathrin mediated endocytosis of epidermal growth factor receptor in MEF WT and MEF KO cells after suppression of EPS15 with siRNA.

The results show that a lack of RLIP76 resulted in a remarkable decrease of clathrin mediated endocytosis of insulin receptor in MEF KO cells. As expected, treatment with EPS15 siRNA inhibited this process even more in MEF KO. This

finding confirmed our previous observation of endocytosis inhibition after suppressing RLIP76 with anti-RLIP76 IgG in NSCLC H358. However, the most significant finding was the discovery that after suppression of EPS15, the endocytosis of insulin receptor was still present in MEF WT. The same observation was noticed in the case of epidermal growth factor receptor. After inhibition of clathrin mediated endocytosis with EPS15 siRNA in MEF WT cells, the epidermal growth factor crossed the cell membrane through an alternative pathway distinct from the clathrin pit. In cells where the RLIP76 gene was deleted (MEF KO), endocytosis of epidermal growth factor, similarly to insulin, was dramatically decreased even after 10 minutes of incubation, as compared to MEF WT.

These findings are strong evidence for the crucial role of RLIP76 in clathrin dependent and independent receptor-ligand endocytosis. RLIP76, through interaction with POB1 and CDC42 may participate in both pathways and regulate glucose metabolism and growth rate. It is known that RLIP76 KO animals' growth rate is much slower comparing to the wild type. Even after reaching puberty, KO animals remain smaller than WT animals.

Taken together, our results are an indication that RLIP76 regulates the rate of endocytosis. Increasing cellular RLIP76 causes a marked increase in endocytosis of the rhodamine-tagged epidermal growth factor. On the other hand, blocking RLIP76 with antibodies or deletion of the RLIP76 gene (MEF KO) slows endocytosis remarkably.

A similar pattern is seen in the internalization of the insulin receptor. The process of endocytosis is also accelerated by augmented RLIP76 and decreased by the anti-RLIP76 IgG or gene deletion.

#### 4.9 Discussion

The role of free radicals in the development of hyperglycemia is suggested by many *in vitro* (Tesfamariam et al., 1992; Bast et al., 2002; Tesfamariam, 1992; Evans et al., 2003) and *in vivo* (Marfella et. al., 1994; Ting et al., 1996; Ceriello, 2000; Maddux et al., 2001, Griendling et al., Part I and II, 2003) studies, however the exact signaling mechanism responsible for it is has not yet been defined (Rosen et al., 2001; Ceriello et al., 2006).

High glucose concentration within the blood stream, as well as free fatty acids and their degradation products, are strongly implicated as chemical mechanisms of insulin resistance (Rosen et al., 2001; Evans et al., 2002; Ceriello et al., 2004; Fridlyand et al., 2004).

Another process which contributes to insulin resistance is perturbation of the clathrin coated pit mediated receptor-ligand pair endocytosis. In the absence of ligand, the IR normally resides at the plasma membrane. Upon insulin binding, the ligand–receptor complex is quickly translocated from the plasma membrane into the cytoplasm and internalized into endosomes within several minutes (Khan et al., 1989; Burgess et al., 1992). The acidic pH of the endosomes results in the dissociation of insulin from the insulin receptor and allows the degradation of insulin by endosomal acidic insulinase (Authier et al., 1994). The insulin receptor then undergoes dephosphorylation by protein

tyrosine phosphatases followed by recycling back to the cell membrane (King et al., 1990; Mooney et al., 1997; Cheng et al., 2002). However, under conditions of extended stimulation with saturating levels of insulin, a majority of the insulin receptors are transported to the endosomes and lysosomes for degradation (Doherty et al., 1990; Backer et al., 1990). This process leads to a reduction of active insulin receptors in the plasma membrane which results in insulin resistance (Hedo et al., 1985; Najjar et al., 2001).

Under conditions of oxidative stress, characterized by a serious imbalance between the production of reactive species and antioxidant defenses, one of the earliest responses is an induction of RLIP76. Its physiological transport substrates are glutathione conjugates with electrophiles such as leukotriene and 4-hydroxynonenal, a derivative of arachidonic acid. This transport function of RLIP76 is perhaps the reason of RLIP76 over-expression after exposure of cells to mild oxidative stress conditions. It may be reasonable to predict that induction of RLIP76 during stress should also affect the dynamics of its other functions, for example, ligand-receptor mediated endocytosis (Park et al., 1995; Ducluzeau et al., 2003). Therefore, based on results of our present studies, placed in context of the known transport functions of RLIP76 (Awasthi et al., 2003; Yadav et al., 2004; Yadav et al., 2005), and the involvement of RLIP76, POB1, and cdc42 in receptor-ligand endocytosis of insulin-insulin receptor and epidermal growth factor receptor (Nakashima et al., 1999; Morinaka et al., 1999; Cheng et al., 2006; Sabharanjak et al., 2002; Puri et al., 2001), we proposed a model which directly links oxidative stress, RLIP76 signaling, GSH-homeostasis and insulin resistance.



According to this model, induction of RLIP76 after oxidative stress results in acceleration of the rate of receptor/ligand complexes endocytosis, which leads to the increase in the degree of insulin receptor degradation. As a consequence, the number of active insulin receptors in the cell membrane is drastically reduced, contributing to a relative decrease in the effectiveness of ligands to initiate intracellular signaling. More specifically, such mechanism eventually would result in insulin resistance and development of Type 2 diabetes. On the other hand, inhibition or a decrease in the transport activity of RLIP76 would have the opposite effect of insulin-sensitization.

The proposed model and these postulates are strongly supported by present findings, both in an animal model, and in an isolated cell-culture model. In the animal studies, we showed for the first time that blood glucose and insulin levels are significantly perturbed in RLIP76 KO animals. Four tests providing an established index for insulin resistance: HOMA, QUICKI, Insulin level, and blood Glucose/Insulin ratio. The results of these tests strongly indicate that insulin resistance increases with increasing amounts of RLIP76 in studied animals. RLIP76 KO animals have the highest insulin sensitivity whereas RLIP76 WT animals treated with 200 µg or 500 µg of RLIP76 encapsulated in liposomes have developed an insulin resistance.

Because the signals generated by insulin and the insulin receptor itself are drastically diminished in augmented RLIP76 WT animals, we next examined the sensitivity of RLIP76 KO animals and RLIP76 WT animals to double insulin administration. Blood glucose dropped in both animal groups after injection of 0.02 U/ml of insulin, but after first 30 minutes in RLIP76 KO animals a 10 % decrease was

noticed whereas in RLIP76 WT it was more than 30%. After 120 minutes, blood glucose was quite similar in terms of percent reduction in blood glucose in both groups. A dramatic difference was apparent in insulin-sensitivity in the KO animals upon re-challenging with insulin on the second day. After the first 30 minutes from insulin injection glucose decreased by 70% in RLIP76 KO mice and 30% in RLIP76 WT animals. Insulin induced hypoglycemia was significantly magnified in the KO animals and caused death within 90 min, whereas the WT animals has a response identical to that observed with the first dose. These findings suggested certain signaling effects of insulin are more prolonged in duration in the RLIP76 KO animals.

In contrast to the insulin action which causes acute hypoglycemia we decided to investigate an effect of hydrocortisone which is known to cause hyperglycemia and insulin-resistance (Stewart, 1999; Marik et al., 2004; Almon et al., 2005). We studied the relationship between hydrocortisone and RLIP76 by comparing the acute hyperglycemic effects of a single high dose steroid injection between WT and KO animals. The results showed a lack of response to glucocorticoids in RLIP76 KO animals, and a restoration of the hyperglycemic effect in RLIP76 WT animals where glucose level increased by about 220%. This finding provides strong evidence for the affirmation that the glucocorticoids must signal acute hyperglycemic effects through RLIP76. Because administration of glucocorticoids in RLIP76 WT animals did not induce RLIP76 expression, we reasoned that the lack of steroid stimulated acute hyperglycemia in RLIP76 KO animals is more likely due to deficient hepatic glucose release. To pursue this line of reasoning, we compared specific activity and expression

of gluconeogenic regulatory enzymes, such as phosphoenol-pyruvate carboxy kinase (PEPCK) and fructose 1,6-bisphosphatase (FBPase), in hepatic tissues from RLIP76 KO and WT animals. RT-PCR and western blot analysis illustrate that these two enzymes expression was the same in both animal groups and was not affected by a lack of RLIP76 in KO animals. However, the activities of both enzymes were decreased in the KO animals by about 45 % and 33 % in PEPCK and FBPase, respectively, suggesting that RLIP76 participates in maintaining their activities on the optimal level.

Besides the animal studies, the mechanisms through which RLIP76 could increase insulin resistance were tested in cell culture models. We utilized this postulate in cultured cells using MEF cells from RLIP WT and RLIP76 KO animals. We also compared three types of malignant cells with decreasing transport ability of RLIP76: non-small cells lung cancer, small cell lung cancer (RLIP76 transfected, WT and WT treated with anti-RLIP76 IgG) as well as in HepG2 hepatoma cells (control and WT treated with antiRLIP76 IgG) which express a mutant form of RLIP76 with a 80 % lower specific activity for glutathione-conjugate transport. Signaling effects of insulin were examined with respect to glucose uptake, DNA binding activity of FOXO1 and phosphorylation of Akt1. Results of these studies were quite consistent with our model which predicts that cells with higher RLIP76 activity should display diminished insulin action and specific inhibition of RLIP76 by anti-RLIP76 IgG should increase insulin effects. Increasing the amount of RLIP76 in lung cancer cells decreased glucose uptake compared to the control, with or without insulin treatment. However, H358 cells which have a higher RLIP76 activity show a 4 fold higher rate of glucose translocation than

H1618. Surprisingly, HepG2 hepatoma control cells indicate quite the same amount of glucose uptake as control NSCLC H358. This can be explained by a presence of different glucose carriers in these cell lines (GLUT4 in lung cancer cells and GLUT1 in hepatoma cells), which have the capability of glucose transport through the cell membrane. As predicted in lung cancer cell lines, insulin increased glucose uptake, whereas in HepG2 cells there was not a significant effect, due to the insensitivity of GLUT1 to insulin. Inhibition of RLIP76 by anti-RLIP76 IgG resulted in increased glucose uptake in all studied cell lines.

In order to confirm these findings, we measured the activity of FOXO1 and Akt1, two proteins directly involved in insulin signaling. In all cell lines FOXO1 DNA binding activity was diminished after administration of insulin, whereas Akt1 phosphorylation was increased. Inhibition of RLIP76 resulted in inhibition of FOXO1 and activation of Akt1. Phosphorylated Akt1 is responsible for a translocation of the glucose transporter and an increase in glucose uptake, which is consistent with our previous studies. When FOXO1 DNA binding activity is reduced by anti-RLIP76 IgG, the gluconeogenesis process is halted, resulting in a low glucose level, as it was seen in RLIP76 KO animals.

The results are a confirmation that RLIP76 is actively involved in glucose metabolism and altering the amount of this protein leads to a perturbation in insulin signaling.

Because RLIP76 plays an integral role in clathrin dependent endocytosis via interaction with POB1, it is reasonable to suppose that greater RLIP76 expression

should increase the rate of endocytosis of ligand-receptor complexes. To directly examine this proposition, we compared endocytosis of rhodamine-labeled EGF or fluorescein-labeled insulin between WT and RLIP76 over-expressing NSCLC cells, and examined the effect of pre-exposure to anti-RLIP76 IgG. Moreover, we investigated the endocytosis of insulin and epidermal growth factor receptor in MEF cells isolated from RLIP76 KO and RLIP76 WT after suppression with siRNA EPS15, a protein directly involved in clathrin dependent internalization of the ligand-receptor pair. Results of these studies demonstrated that over-expression of RLIP76 increased the uptake rate of ligand/receptor complexes and anti-RLIP76 antibodies significantly abrogated this effect. The same pattern was noticed in MEF cells where endocytosis was dramatically reduced in RLIP76 KO cells comparing to RLIP76 WT cells.

In addition, suppressing EPS15 with siRNA did not have any effect on endocytosis of ligand-receptor complexes in MEF RLIP76 WT cells whereas in RLIP76 KO cells treated with siRNA, endocytosis was abrogated. This finding shows the existence of an alternative, clathrin independent endocytosis of insulin or EGF receptors, which RLIP76, through interaction with cdc42 (Jullien-Flores et al., 1995; Qiu et al., 1997; Cheng et al., 2001), participates in.

These studies show for the first time that RLIP76 plays a crucial role in glycemic control by regulating both steroid and insulin action. Oxidative stressors lead to a rapid over-expression of RLIP76 in the plasma membrane and increase in the specific activity as a result of phosphorylation mediated by activated PKC $\alpha$  (Yadav et al., 2004). Increased RLIP76 protein enhances the rate of endocytosis of the

insulin/insulin-receptor, antagonizing its degradation in lysosomes. This model is consistent with previous studies by others showing that insulin-resistance is associated with a decreased number of insulin-receptors in the plasma membrane (Moncada et al., 1986; Taylor et al., 1990; Zorad et al., 2003).

#### Publications

1. Yadav S, Zajac E, Singhal SS, Singhal J, Drake K, Awasthi YC, Awasthi S., POB1 over-expression inhibits RLIP76-mediated transport of glutathione-conjugates, drugs and promotes apoptosis.

Biochem Biophys Res Commun. 2005 Mar 25;328(4):1003-9.

2. Zajac E., Singhal S., Singhal J., Yadav S., and Awasthi S.,

Role of Ralbp1 in Regulation of Glycemic Control, manuscript in preparation

## Appendix A

### NUCLEOTIDE SEQUENCES OF INVESTIGATED GENES (NCBI sequence viewer)

## 1. Nucleotide sequence of POB1/REPS2

1 atggaggcgg cagcggcggc ggcggcggcg gcagcggcag cggcagcggc gggcgggggc  
61 tgtggtccg ggccgccgc gctgctgctg agcgagggcg agcagcagtg ctactccgag  
121 ctcttcgcg gctgtgccgg cgccgcgggc gggggccccg ggtctgggcc ccccgaggcc  
181 gccagagtcg cccccggcac ggccactgcg gccgccggcc cctgggctga cctgtttcgg  
241 gcatgcagc tgcccgcga gacgctgcac cagatcacag aactgtgtgg tgcaaagcgg  
301 gttggttatt ttggtccaac acagttttac attgcctga aattaattgc tgcagcacia  
361 tetggcctcc cggtacggat agagagtatt aaatgtgaat tgcctctgcc tgcctttatg  
421 atgtcaaaga atgatgtga gatacgattt gggaaccag ctgagctgca tggaaactag  
481 gttcagattc catatttaac tacagaaaaa aattcctca aaagaatgga cgatgaggat  
541 aaacaggaaa cacagtctcc cacgatgca ccctcgctt ccctcctc ttccccgct  
601 cattaccaga ggggtgccctt gagccatggc tacagcaaac tgcggagcag cgcagaacag  
661 atgcatccag caccttatga agctaggcag cccttgctc agcccgaggg atcctcatca  
721 gggggcccag gaaccaagcc ccttcggcat caggcttccc ttatccggtc cttttcagt  
781 gagagggaac tacaggataa cagcagttac cccgacgaac cctggaggat aacagaagaa  
841 cagcgcgagt actatgtaa tcagttccga tccctcagc cagaccaag ctctttcatt  
901 tcagtttctg tggccaagaa cttctcacc aaatcaaagc ttccattcc agaactctc  
961 tatatatggg agcttagtga tgctgactgt gatggagccc tgaccctgcc tgagttctgt  
1021 gctgcgtttc atctcattgt ggctcggag aacggctacc cattgcctga gggcctcct  
1081 ccaactctgc agccagaata cctgcaggca gcttttcta agcccaaag ggactgtcaa  
1141 ttatttgatt cttattctga gtcactccg gcaaatcaac aacctcgtga cttgaatcgg  
1201 atggagaaga catctgtaa agacatggct gacctcctg tcctaacca ggatgtaact



1261 agt gatgaca aacaagcttt gaaaagtact atcaatgaag ccttaccaa ggacgtgtct  
1321 gaggatccag caactccaa ggattccaac agtetcaaag caagaccaag atccagatct  
1381 tactctagca cctccataga agaggccatg aaaagggcg aggacctcc caccccgcca  
1441 cctcggccac agaaaacca ttccagagcc tctccttg atctgaataa agtctccag  
1501 cccagtgtgc cagctacaa gtcaggattg ttacccccac cacctgcgct cctccaaga  
1561 cctgtccat cacagtctga acaagtgtcg gaggccgagt tactcccaca gctgagcaga  
1621 gccccatcc aggetgcaga aagtagtcca gaaagaagg atgtactgta ttctcagcca  
1681 ccatcaaagc ccattcgtag gaaattcaga ccagaaaacc aagctacaga aaaccaagag  
1741 ccttccactg ctgcaagtgg gccagcttct gcggcaacca tgaaccgca tccaacagtc  
1801 caaaagcagt ctccaaca gaagaaggcc attcaaactg ctatccgcaa aaataagag  
1861 gcaaacgcag tgctggctcg gctgaacagt gagctccagc agcagctcaa ggaggttcat  
1921 caagaacgaa ttgattgga aaaccaattg gaacaacttc gtccggtcac tgtgttga

## 2. Nucleotide sequence of RLIP76

1 ggtcgcgchg cggcaggcac aggtgtaatg gataggtaac agagaagacc tcgtcccttc  
61 ctagtcaggg catcagcatg actgagtgtc tctgcccc caccagcagc cccagtgaac  
121 accgcagggt ggagcatggc agcgggctta cccggacccc cagctctgaa gagatcagcc  
181 ctactaagtt tctggattg taccgactg gcgagccctc acctcccat gacatcctcc  
241 atgagcctcc tgatgtagt tctgatgatg agaaagatca tgggaagaaa aaagggaaat  
301 ttaagaaaaa ggaaaagagg actgaaggct atgcagcctt tcaggaagat agctctggag  
361 atgaggcaga aagtccttct aaaatgaaga ggtccaaggg aatccatgtt tcaagaagc  
421 ccagcttttc taaaaagaag gaaaaggatt taaaataaa agagaaaccc aaagaagaaa  
481 agcataaaga agaaaagcac aaagaagaaa aacataaaga gaagaagtca aaagactga  
541 cagcagctga tgttgtaaa cagtggaagg aaaagaagaa aaagaaaaag ccaattcagg  
601 agccagaggt gcctcagatt gatgttcaa atctcaaacc catttttga attcctttgg  
661 ctgatgcagt agagaggacc atgatgtatg atggcattcg gctgccagcc gtttccgtg  
721 aatgtataga ttacgtagag aagtatggca tgaagtgtga aggcattctac agagtatcag  
781 gaattaaatc aaaggtgat gagctaaaag cagcctatga ccgggaggag tctacaaact  
841 tggagacta tgagcctaac actgtagcca gtttgctgaa gcagtattg cgagacctc  
901 cagagaattt gcttaccaaa gagcttatgc ccagattga agaggcttgt gggaggacca  
961 cggagactga gaaagtgcag gaattccagc gttfactcaa agaactgcca gaatgtaact  
1021 atcttctgat ttctggctc attgtgcaca tggaccatgt cattgcaaag gaactggaaa  
1081 caaaaatgaa tatacagaac atttctatag tgctcagccc aactgtgcag atcagcaatc  
1141 gagtctgta tgtgttttc acacatgtgc aagaactctt tggaaatgtg gtactaaagc  
1201 aagtgatgaa acctctgcca tggcttaaca tggccacgat gccacgctg ccagagaccc

1261 aggcgggcat caaggaggag atcaggagac aggagtttct tttgaattgt ttacatcgag  
1321 atctgcaggg tgggataaag gatttgctta aagaagaaag attatgggaa gtacaaagaa  
1381 tttgacagc cctcaaaaga aaactgagag aagctaaaag acaggagtgt gaaaccaaga  
1441 ttgcacaaga gatagccagt cttcaaaag aggatgttc caaagaagag atgaatgaa  
1501 atgaagaagt tataaatatt ctcttgctc aggagaatga gatcctgact gaacaggagg  
1561 agctctggc catggagcag tttctgcgc gccagattgc ctcagaaaa gaagagattg  
1621 aacgcctcag agctgagatt getgaaatc agagtcgcca gcagcacggc cgaagtgaga  
1681 ctgaggagta ctctccgag agcgagagcg agagtgagga tgaggaggag ctgcagatca  
1741 ttctggaaga cttacagaga cagaacgaag agctggaaat aaagaacaat catttgaatc  
1801 aagcaattca tgaggagcgc gaggccatca tcgagctgcg cgtgcagctg cggtgctcc  
1861 agatgcagcg agccaaggcc gagcagcagg cgcaggagga cgaggacct gagtggcgcg  
1921 ggggtgccgt ccagccgcc agagacggcg tccttgagcc aaaagcagct aaagagcagc  
1981 caaaggcagg caaggagccg gcaaagccat cgcccagcag ggataggaag gagacgtcca  
2041 tctgagcagc ctgcgtggcc gtctggagtc cgtgagactg aaaggaccg tgcatcttac  
2101 tgtaaccgg gggccaggcc ggctctctcg ctgtacatc tgtaaagggt tctctcttc  
2161 tcagactctt cctctgtcac acgtctgact cttcacgtc aggctcaggt tccatgggag  
2221 gacgaagcag tggacgcatt gtgggcttta gggacagatg agtttccag atagtgtcag  
2281 cttattttaa gattaatftt cttgttaac ttaaataac tattttaacc cttgagtggc  
2341 ttcttttaa accaaaaate gtcttcttt gctttttat cacagcagaa tcaggatctc  
2401 tttctcatc aaggggggaa ccacaccagg tcagcgtgc gcctgctgtg gccgccgca  
2461 gccacgcct ctgggatctc tggtagcgtc actcttgcct gtgcctcca cacctctcg  
2521 gtgcagatcc ctatggggga gctgcctcac gttctctgac tggtcagagc agcgcctggt

2581 ggggtgttccc tggcccactc tcctctctcc ttctgcagtt ctaaaccaca gtctataagc  
2641 ccgagtcacc aggacggcct gtctggccac agacaggggc tgcctgtgga gcctgcccac  
2701 cggccccccg cagtgcagtc cagcggggag gaggctgccc gttctgcca gttctcact  
2761 gcggggacca gcaaaggcct tctcactggg ttggtaaag gtagtcacct tggcctgggtg  
2821 catccacaga ggatgttgtt caaaccagaa atcttttaa cgactgacct tccttaaaaa  
2881 cagaatgact ccgattgctt gcttgggcta gaatgtacac gtctccttgc ctgaataagc  
2941 catatatatg ctcttaaaca aaagttgaa attatccata tcatctcagt gaacctactg  
3001 gtggactccc aattgacaag attgagcaat agaaaaaat tccttctt tgaatgatag  
3061 ctgtgattca cccacccca tttcttgtt tctggccat ccgatgagac ggatgctctg  
3121 atgctctgag gcttctggga ggctgggccc tggaggcaac gtgctgcagg cgcactctgt  
3181 cagagtgaac agcaccgca gacaggccag gctcgtggct cggaagaca accccacaca  
3241 cactcaaggg gtcgaaaaca aaccacac gagggctctc acctccttct ctaggtagt  
3301 atttatttc agcacctgtt tgatgcagtt ttaatectc tacctattgc actgttga  
3361 ctcgttgcc attattgat tttgtacga aaaaagctt tgtatagaa atcagcatac  
3421 tatttttta aatctggaga gaagatattc tggtagtga aagtatggc ggggtcaga  
3481 tataaatgt caaatgcctt cttgctgtcc tgcggtctc agtacgttca cttatagct  
3541 getggcaata tcgaaggctt ctttttgtt tgtgtaaact ctaatttcta tcaaggtgc  
3601 atggattttt aaaattagta ttcattaca aatgtctcag cattggtaa ctaattttg  
3661 ccaggacat tattgatcaa gcaataaat tcaacagcca tttgggaaa agaaaagctt  
3721 ctagttttt tgtagacatt cttctgtga ggagattgag tactctgcag ctggcgagga  
3781 gttggtgag gcattcttc aaggccaagg gggaacacag tgtttgtt ccagctcact  
3841 ttgtaccct cacctctgca gacacgggga gaacccgga cccctggcat gcatgctggc

3901 ggcggcatgc ctccttcca caagcccatg ctgctgcaga gggagcctgt gttgcaaaa

3961 cccagtggac tgggctgggt ctgctgtctg agcagctcct ggctccgggtg ggaactgcac

4021 acaagtccac tggcctggct tggccccagg cattgcaatt gacagacatt tgcatttcat

4081 acggtaaag aggactcagc acagccaacc ataacagca tgtctgggat agactggtct

4141 agaataaaaa tgaagtttcc atgctttgt ttgctttaa aattccacaa ttaaaatate

4201 tgcattgaa agcttaaaaa aaaaaaaaaa

//

### 3. Nucleotide sequence of PEPCK

1 acagttggcc ttcctctgg gaacacaccc tcggtcaaca ggggaaatcc ggcaaggcgc  
61 tcagcgatct ctgatccaga cttccaaaa ggaagaaagg tggcaccaga gttctgcct  
121 ctctccacac cattgcaatt atgcctctc agctgcataa cggctcggac ttcttgcca  
181 aggttatcca gggcagcctc gacagcctgc cccaggcagt gaggaagttc gtggaaggca  
241 atgctcagct gtgccagccg gagtatatcc acatctgcga tggctccgag gaggagtacg  
301 ggcagttgct ggccacatg caggaggagg gtgtcatccg caagctgaag aaatatgaca  
361 actgttgget ggetctcact gaccctcgag atgtggccag gatcgaaagc aagacagtca  
421 tcataccca agagcagaga gacacagtgc ccatcccaa aactggcctc agccagctgg  
481 gccgctggat gtcggaagag gactttgaga aagcattcaa cgccaggttc ccagggtgca  
541 tgaaggccg caccatgat gtcatccat tcagcatggg gccactgggc tcgccgctgg  
601 ccaagattgg tattgaactg acagactcgc cctatgtggt ggccagcatg cggatcatga  
661 ctccgatggg catatctgtg ctggaggccc tgggagatgg ggagttcadc aagtgcctgc  
721 actctgtggg gtgccctctc ccttaaaaa agcctttggt caacaactgg gcctgcaacc  
781 ctgagctgac cctgatgcc cacctcccgg accgcagaga gatcatctcc tttggaagcg  
841 gatatggtgg gaactcacta ctccggaaga aatgctttgc gttgcggatc gccagccgct  
901 tggctaagga ggaagggtgg ctggcggagc atatgctgat cctgggcata actaaccgcc  
961 aaggcaagaa gaaatacctg gccgcagcct tcctagtgc ctgtgggaag actaacttgg  
1021 ccatgatgaa cccagcctg cccgggtgga aggtcgaatg tgtggcgat gacattgcct  
1081 ggatgaagtt tgatgcccaa ggcaacttaa gggctatcaa cccagaaaac gggtttttg  
1141 gaggttgctc tggcacctca gtgaagacia atccaatgc cattaaaacc atccagaaa  
1201 acaccatctt caccaactg gccgagacta gcgatggggg tgtttactgg gaaggcatcg

1261 atgagccgct ggccccggga gtcacatca cctcctgaa gaacaaggag tggagaccgc  
1321 aggacgcgga accatgtgcc catcccaact cgagattctg caccctgcc agccagtgcc  
1381 ccattattga cctgcctgg gaatctccag aaggagtacc cattgagggt atcatctttg  
1441 gtggccgtag acctgaaggt gtcccccttg tctatgaagc ctcagctgg cagcatgggg  
1501 tgtttgtagg agcagccatg agatctgagg ccacagctgc tgcagaacac aagggaaga  
1561 tcatcatgca cgacccttt gccatgcgac cttcttcgg ctacaactc ggcaatacc  
1621 tggcccactg getgagcatg gccaccgcc cagcagcaa gttgccaag atctccatg  
1681 tcaactggtt ccggaaggac aaagatggca agttcctctg gccaggcttt ggcgagaact  
1741 cccgggtgct ggagtggatg ttcgggcgga tgaagggga agacagcgc aagctcacg  
1801 ccatcggeta catccetaag gaaaacgct tgaacctgaa aggctgggg ggcgtcaacg  
1861 tggaggagct gtttggatc ttaaggagt tctgggagaa ggaggtggag gagatcgaca  
1921 ggtatctgga ggaccagtc aacaccgacc tcccttacga aattgagagg gagctccgag  
1981 ccctgaaaca gagaatcagc cagatgtaa tccaatggg ggcgtctga gagtcccc  
2041 ttccactca cagcatcgct gagatctagg agaaagccag cctgctccag cttgagata  
2101 gggcacaat cgtgagtaga tcagaaaagc acctttaat agtcagttga gtagcacaga  
2161 gaacaggcta ggggcaaata agattgggag gggaaatcac cgcatagtct ctgaagttg  
2221 cattgacac caatgggggt tttgttcca ctcaaggtc actcaggaat ccagttctc  
2281 acgttagctg tagcagtag ctaaatgca cagaaacat actgagctg tatatatgtg  
2341 tgtgaacgtg tctctgtgtg agcatgtgtg tgtgtgtgtg tgtgtgtgtg tgtgtgtgtg  
2401 tgtgtgtgtg tgtacatgcc tgtctgtccc attgtccaca gtatatata aaccttggg  
2461 gaaaaatctt gggcaaattt gtactgtaa ctgagagtc atgtgcttt gttgtagta  
2521 tgtatgttta aattattttt atacaccgcc ctfaccttc ttacataat tgaaattgtg  
2581 atccgacca cttctggga aaaaattac aaaataaa

#### 4. Nucleotide sequence of FBPase

1 ttgggatctc atttgcaaa tgacggacag aagccccctt gagacagaca tgctgacct  
61 gaccggttac gttatggaaa agggggcgaca ggccaaagg accggagaac tcaccagct  
121 gctcaactcg atgctgactg ccatcaaagc catctctcc gcagtgcgca aggccggcct  
181 ggccaacctg tatgggattt cggggagcgt gaatgtgaca ggagatgagg tgaagaaact  
241 ggacgtgctg tccaactccc tggcatcaa catgcttcag tcctctaca gcacctgtg  
301 gctcgtctcc gaagagaata aagaggcggg gatcacagcc caggagagga gggggaaata  
361 tgggtttgc ttgaccctc tggatggat tcaaacatt gactgcctgg cctccatcg  
421 aactatatt gctattaca gaaagaccac ggaggacgag cctctgaga aggatgcct  
481 gcagcctggc cgcaacatcg tggctgcggg ttatgactg tatgtagtc gaacctggt  
541 tgctcttcc acaggacaag gattggatct gttcatgctg gaccggctc ttggagaatt  
601 cgtgctagt gaaaaagatg tccggattaa gaagaaagg aaaatttta gcctcaacga  
661 gggctatgcc aagtatttg atgctgctac tgctgagtat gtacagaaaa agaaattccc  
721 cgaggatggc agtgagcctt atggagccag gtacgtgggt tccatggtgg ctgatgtgca  
781 tcgaccttg gtctatggag gaatcttcat gtaccagcc aaccagaaga gtctaatgg  
841 caagtcceg ctcctgatg aatgcaatcc tgtggcctat atcatgagc aagcaggagg  
901 tatggcaacc acaggeaccc agccagtact ggatgtgaaa cctgagagta ttcaccagcg  
961 agtccccctc attctgggtc ccctgaggat gtgcaagagt atctcagctg tgtgcagaga  
1021 aaccaggcag gcaggtagt agcctgaacc catgagccc cttcccttg tctttgtaa  
1081 ttgaaaaact agatgaatga gctatggaga tgggaggaaa ggcaaagaag tcaagtgaca  
1141 caggtcacgg tcagaacagc gccctgctgc taaggacagg gttagaagcc aggggtaaag  
1201 aaagatacag tctttggact aaaataaaaa tatgaatctg aa



## REFERENCES

- (1) Agarwal A; Gupta S; Sikka S *Curr. Opin. Obstet. Gynecol.* **2006**, *18*, 325-332.
- (2) Aguilar RC; Wendland B *Proc. Natl. Acad. Sci. U. S. A.* **2005**, *102*, 2679-2680.
- (3) Alessi DR; Deak M; Casamayor A; Caudwell FB; Morrice N; Norman DG; Gaffney P; Reese CB; MacDougall CN; Harbison D; Ashworth A; Bownes M *Curr. Biol.* **1997**, *7*, 776-789.
- (4) Allen, J. D.; Brinkhuis, R. F.; Wijnholds, J.; Schinkel, A. H. *Cancer Res.* **1999**, *59*, 4237-4241.
- (5) Allikmets, R.; Gerrard, B.; Hutchinson, A.; Dean, M. *Hum. Mol. Genet.* **1996**, *5*, 1649-1655.
- (6) Almon RR; Lai W; DuBois DC; Jusko WJ *Am. J. Physiol. Endocrinol. Metab.* **2005**, *289*, E870-82.
- (7) Aloj L; Caraco C; Jagoda E; Eckelman WC; Neumann RD *Cancer Res.* **1999**, *59*, 4709-4714.
- (8) Ambudkar, S. V.; Dey, S.; Hrycyna, C. A.; Ramachandra, M.; Pastan, I.; Gottesman, M. M. *Annu. Rev. Pharmacol. Toxicol.* **1999**, *39*, 361-398.
- (9) Ambudkar, S. V.; Kim, I. W.; Sauna, Z. E. *Eur. J. Pharm. Sci.* **2006**, *27*, 392-400.
- (10) Anderson RG *Annu. Rev. Biochem.* **1998**, *67*, 199-225.
- (11) Audrezet, M. P.; Chen, J. M.; Ragueneas, O.; Chuzhanova, N.; Giteau, K.; Le Marechal, C.; Quere, I.; Cooper, D. N.; Ferec, C. *Hum. Mutat.* **2004**, *23*, 343-357.
- (12) Authier F; Rachubinski RA; Posner BI; Bergeron JJ *J. Biol. Chem.* **1994**, *269*, 3010-3016.

- (13) Awasthi YC; Garg HS; Dao DD; Partridge CA; Srivastava SK *Blood* **1981**, *58*, 733-738.
- (14) Awasthi, S.; Cheng, J.; Singhal, S. S.; Saini, M. K.; Pandya, U.; Pikula, S.; Bandorowicz-Pikula, J.; Singh, S. V.; Zimniak, P.; Awasthi, Y. C. *Biochemistry* **2000**, *39*, 9327-9334.
- (15) Awasthi, S.; Sharma, R.; Singhal, S. S.; Zimniak, P.; Awasthi, Y. C. *Drug Metab. Dispos.* **2002**, *30*, 1300-1310.
- (16) Awasthi, S.; Singhal, S. S.; Pandya, U.; Gopal, S.; Zimniak, P.; Singh, S. V.; Awasthi, Y. C. *Toxicol. Appl. Pharmacol.* **1999**, *155*, 215-226.
- (17) Awasthi, S.; Singhal, S. S.; Pikula, S.; Piper, J. T.; Srivastava, S. K.; Torman, R. T.; Bandorowicz-Pikula, J.; Lin, J. T.; Singh, S. V.; Zimniak, P.; Awasthi, Y. C. *Biochemistry* **1998**, *37*, 5239-5248.
- (18) Awasthi, S.; Singhal, S. S.; Singhal, J.; Cheng, J.; Zimniak, P.; Awasthi, Y. C. *Int. J. Oncol.* **2003**, *22*, 713-720.
- (19) Awasthi, S.; Singhal, S. S.; Singhal, J.; Yang, Y.; Zimniak, P.; Awasthi, Y. C. *Int. J. Oncol.* **2003**, *22*, 721-732.
- (20) Awasthi, S.; Singhal, S. S.; Srivastava, S. K.; Zimniak, P.; Bajpai, K. K.; Saxena, M.; Sharma, R.; Ziller, S. A., 3rd; Frenkel, E. P.; Singh, S. V. *J. Clin. Invest.* **1994**, *93*, 958-965.
- (21) Awasthi, S.; Singhal, S. S.; Yadav, S.; Singhal, J.; Drake, K.; Nadkar, A.; Zajac, E.; Wickramarachchi, D.; Rowe, N.; Yacoub, A.; Boor, P.; Dwivedi, S.; Dent, P.; Jarman, W. E.; John, B.; Awasthi, Y. C. *Cancer Res.* **2005**, *65*, 6022-6028.
- (22) Ayala JE; Streeper RS; Desgrosellier JS; Durham SK; Suwanichkul A; Svitek CA; Goldman JK; Barr FG; Powell DR; O'Brien RM *Diabetes* **1999**, *48*, 1885-1889.
- (23) Backer JM; Kahn CR; Cahill DA; Ullrich A; White MF *J. Biol. Chem.* **1990**, *265*, 16450-16454.
- (24) Bakos, E.; Evers, R.; Szakacs, G.; Tusnady, G. E.; Welker, E.; Szabo, K.; de Haas, M.; van Deemter, L.; Borst, P.; Varadi, A.; Sarkadi, B. *J. Biol. Chem.* **1998**, *273*, 32167-32175.

- (25) Barber SC; Mead RJ; Shaw PJ *Biochim. Biophys. Acta* **2006**.
- (26) Barthel A; Schmoll D *Am. J. Physiol. Endocrinol. Metab.* **2003**, 285, E685-92.
- (27) Bast A; Wolf G; Oberbaumer I; Walther R *Diabetologia* **2002**, 45, 867-876.
- (28) Beale E; Andreone T; Koch S; Granner M; Granner D *Diabetes* **1984**, 33, 328-332.
- (29) Beale EG; Koch SR; Brotherton AF; Sheorain VS; Granner DK *Diabetes* **1986**, 35, 546-549.
- (30) Bevan P J. *Cell. Sci.* **2001**, 114, 1429-1430.
- (31) Biggs WH 3rd; Meisenhelder J; Hunter T; Cavenee WK; Arden KC *Proc. Natl. Acad. Sci. U. S. A.* **1999**, 96, 7421-7426.
- (32) Blair AS; Hajduch E; Litherland GJ; Hundal HS *J. Biol. Chem.* **1999**, 274, 36293-36299.
- (33) Bloch-Damti A; Bashan N *Antioxid. Redox Signal.* **2005**, 7, 1553-1567.
- (34) Borst, P.; Elferink, R. O. *Annu. Rev. Biochem.* **2002**, 71, 537-592.
- (35) Borst, P.; Evers, R.; Kool, M.; Wijnholds, J. *J. Natl. Cancer Inst.* **2000**, 92, 1295-1302.
- (36) Boyer, T. D. *Hepatology* **1989**, 9, 486-496.
- (37) Bradford, M. M. *Anal. Biochem.* **1976**, 72, 248-254.
- (38) Broxterman, H. J.; Heijn, M.; Lankelma, J. *J. Natl. Cancer Inst.* **1996**, 88, 466-468.
- (39) Bruggemann, E. P.; Currier, S. J.; Gottesman, M. M.; Pastan, I. *J. Biol. Chem.* **1992**, 267, 21020-21026.
- (40) Bruggemann, M.; Teale, C.; Clark, M.; Bindon, C.; Waldmann, H. *J. Immunol.* **1989**, 142, 3145-3150.
- (41) Bruner KL; Derfoul A; Robertson NM; Guerriero G; Fernandes-Alnemri T; Alnemri ES; Litwack G *Recept. Signal Transduct.* **1997**, 7, 85-98.
- (42) Brunet A; Bonni A; Zigmond MJ; Lin MZ; Juo P; Hu LS; Anderson MJ; Arden KC; Blenis J; Greenberg ME *Cell* **1999**, 96, 857-868.

- (43) Burgess JW; Wada I; Ling N; Khan MN; Bergeron JJ; Posner BI *J. Biol. Chem.* **1992**, *267*, 10077-10086.
- (44) Campbell, J. D.; Koike, K.; Moreau, C.; Sansom, M. S.; Deeley, R. G.; Cole, S. P. *J. Biol. Chem.* **2004**, *279*, 463-468.
- (45) Cantley LC *Science* **2002**, *296*, 1655-1657.
- (46) Cantor, S. B.; Urano, T.; Feig, L. A. *Mol. Cell. Biol.* **1995**, *15*, 4578-4584.
- (47) Cassuto H; Kochan K; Chakravarty K; Cohen H; Blum B; Olswang Y; Hakimi P; Xu C; Massillon D; Hanson RW; Reshef L *J. Biol. Chem.* **2005**, *280*, 33873-33884.
- (48) Ceriello A *Endocr. Pract.* **2006**, *12 Suppl 1*, 60-62.
- (49) Ceriello A *Metabolism* **2000**, *49*, 27-29.
- (50) Ceriello A *Diabet. Med.* **1997**, *14 Suppl 3*, S45-9.
- (51) Ceriello A; Hanefeld M; Leiter L; Monnier L; Moses A; Owens D; Tajima N; Tuomilehto J *Arch. Intern. Med.* **2004**, *164*, 2090-2095.
- (52) Chauhan V; Chauhan A *Pathophysiology* **2006**, *13*, 195-208.
- (53) Cheng A; Dube N; Gu F; Tremblay ML *Eur. J. Biochem.* **2002**, *269*, 1050-1059.
- (54) Cheng JZ; Sharma R; Yang Y; Singhal SS; Sharma A; Saini MK; Singh SV; Zimniak P; Awasthi S; Awasthi YC *J. Biol. Chem.* **2001**, *276*, 41213-41223.
- (55) Cheng JZ; Singhal SS; Saini M; Singhal J; Piper JT; Van Kuijk FJ; Zimniak P; Awasthi YC; Awasthi S *Arch. Biochem. Biophys.* **1999**, *372*, 29-36.
- (56) Cheng JZ; Singhal SS; Sharma A; Saini M; Yang Y; Awasthi S; Zimniak P; Awasthi YC *Arch. Biochem. Biophys.* **2001**, *392*, 197-207.
- (57) Chien Y; White MA *EMBO Rep.* **2003**, *4*, 800-806.
- (58) Chugani, D. C.; Kедersha, N. L.; Rome, L. H. *J. Neurosci.* **1991**, *11*, 256-268.
- (59) Cole, S. P.; Bhardwaj, G.; Gerlach, J. H.; Mackie, J. E.; Grant, C. E.; Almquist, K. C.; Stewart, A. J.; Kurz, E. U.; Duncan, A. M.; Deeley, R. G. *Science* **1992**, *258*, 1650-1654.

- (60) Confalonieri S; Di Fiore PP *FEBS Lett.* **2002**, *513*, 24-29.
- (61) Confalonieri S; Salcini AE; Puri C; Tacchetti C; Di Fiore PP *J. Cell Biol.* **2000**, *150*, 905-912.
- (62) Daitoku H; Yamagata K; Matsuzaki H; Hatta M; Fukamizu A *Diabetes* **2003**, *52*, 642-649.
- (63) Dalhoff, K.; Buus Jensen, K.; Enghusen Poulsen, H. *Methods Enzymol.* **2005**, *400*, 618-627.
- (64) Darendeliler, F.; Fournet, J. C.; Bas, F.; Junien, C.; Gross, M. S.; Bundak, R.; Saka, N.; Gunoz, H. *J. Pediatr. Endocrinol. Metab.* **2002**, *15*, 993-1000.
- (65) David Josephy, P.; Peter Guengerich, F.; Miners, J. O. *Drug Metab. Rev.* **2005**, *37*, 575-580.
- (66) Davidson-Moncada JK; Lopez-Lluch G; Segal AW; Dekker LV *Biochem. J.* **2002**, *363*, 95-103.
- (67) Dean, M.; Annilo, T. *Annu. Rev. Genomics Hum. Genet.* **2005**, *6*, 123-142.
- (68) Dean, M.; Rzhetsky, A.; Allikmets, R. *Genome Res.* **2001**, *11*, 1156-1166.
- (69) Deeley, R. G.; Cole, S. P. *FEBS Lett.* **2006**, *580*, 1103-1111.
- (70) Dekker LV; Leitges M; Altschuler G; Mistry N; McDermott A; Roes J; Segal AW *Biochem. J.* **2000**, *347 Pt 1*, 285-289.
- (71) Dingemans, A. M.; van Ark-Otte, J.; van der Valk, P.; Apolinario, R. M.; Scheper, R. J.; Postmus, P. E.; Giaccone, G. *Ann. Oncol.* **1996**, *7*, 625-630.
- (72) Doherty JJ 2nd; Kay DG; Lai WH; Posner BI; Bergeron JJ *J. Cell Biol.* **1990**, *110*, 35-42.
- (73) Douglas, K. T. *Adv. Enzymol. Relat. Areas Mol. Biol.* **1987**, *59*, 103-167.
- (74) Doyle, L. A.; Ross, D. D. *Oncogene* **2003**, *22*, 7340-7358.
- (75) Doyle, L. A.; Yang, W.; Abruzzo, L. V.; Kroghmann, T.; Gao, Y.; Rishi, A. K.; Ross, D. D. *Proc. Natl. Acad. Sci. U. S. A.* **1998**, *95*, 15665-15670.

- (76) Drouin J; Sun YL; Tremblay S; Lavender P; Schmidt TJ; de Lean A; Nemer M  
*Mol. Endocrinol.* **1992**, *6*, 1299-1309.
- (77) Ducluzeau PH; Cousin P; Malvoisin E; Bornet H; Vidal H; Laville M; Pugeat M J.  
*Clin. Endocrinol. Metab.* **2003**, *88*, 3626-3631.
- (78) Ecker, G. F.; Csaszar, E.; Kopp, S.; Plagens, B.; Holzer, W.; Ernst, W.; Chiba, P.  
*Mol. Pharmacol.* **2002**, *61*, 637-648.
- (79) Ejendal, K. F.; Hrycyna, C. A. *Curr. Protein Pept. Sci.* **2002**, *3*, 503-511.
- (80) Esterbauer H *Am. J. Clin. Nutr.* **1993**, *57*, 779S-785S; discussion 785S-786S.
- (81) Esterbauer H; Ramos P *Rev. Physiol. Biochem. Pharmacol.* **1996**, *127*, 31-64.
- (82) Esterbauer H; Zollner H *Free Radic. Biol. Med.* **1989**, *7*, 197-203.
- (83) Evans JL; Goldfine ID; Maddux BA; Grodsky GM *Diabetes* **2003**, *52*, 1-8.
- (84) Evans JL; Goldfine ID; Maddux BA; Grodsky GM *Endocr. Rev.* **2002**, *23*, 599-622.
- (85) Evans JL; Maddux BA; Goldfine ID *Antioxid. Redox Signal.* **2005**, *7*, 1040-1052.
- (86) Evers, R.; Cnubben, N. H.; Wijnholds, J.; van Deemter, L.; van Bladeren, P. J.; Borst, P. *FEBS Lett.* **1997**, *419*, 112-116.
- (87) Farrell, G. C. *Pharmacol. Ther.* **1987**, *35*, 375-404.
- (88) Feig LA; Urano T; Cantor S *Trends Biochem. Sci.* **1996**, *21*, 438-441.
- (89) Feldmann, D.; Laroze, F.; Troadec, C.; Clement, A.; Tournier, G.; Couderc, R.  
*Hum. Mutat.* **2001**, *17*, 356.
- (90) Frey RS; Gao X; Javaid K; Siddiqui SS; Rahman A; Malik AB *J. Biol. Chem.*  
**2006**, *281*, 16128-16138.
- (91) Fridlyand LE; Philipson LH *Diabetes* **2004**, *53*, 1942-1948.
- (92) Fujimoto T; Hagiwara H; Aoki T; Kogo H; Nomura R *J. Electron. Microsc.*  
*(Tokyo)* **1998**, *47*, 451-460.

- (93) Gille H; Downward J In *Multiple ras effector pathways contribute to G(1) cell cycle progression*. 1999; Vol. 274, pp 22033-22040.
- (94) Goi T; Shipitsin M; Lu Z; Foster DA; Klinz SG; Feig LA *EMBO J*. **2000**, *19*, 623-630.
- (95) Gottesman, M. M. *Annu. Rev. Med.* **2002**, *53*, 615-627.
- (96) Gottesman, M. M.; Ambudkar, S. V. *J. Bioenerg. Biomembr.* **2001**, *33*, 453-458.
- (97) Gottesman, M. M.; Pastan, I.; Ambudkar, S. V. *Curr. Opin. Genet. Dev.* **1996**, *6*, 610-617.
- (98) Graf, G. A.; Yu, L.; Li, W. P.; Gerard, R.; Tuma, P. L.; Cohen, J. C.; Hobbs, H. H. *J. Biol. Chem.* **2003**, *278*, 48275-48282.
- (99) Graham GG; Chinwah P; Kennedy M; Wade DN *Med. J. Aust.* **1980**, *2*, 124-130.
- (100) Granner D; Andreone T; Sasaki K; Beale E *Nature* **1983**, *305*, 549-551.
- (101) Greene EL; Nelson BA; Robinson KA; Buse MG *Metabolism* **2001**, *50*, 1063-1069.
- (102) Greer EL; Brunet A *Oncogene* **2005**, *24*, 7410-7425.
- (103) Griendling KK; FitzGerald GA *Circulation* **2003**, *108*, 2034-2040.
- (104) Gual P; Le Marchand-Brustel Y; Tanti J *Diabetes Metab.* **2003**, *29*, 566-575.
- (105) Habig, W. H.; Pabst, M. J.; Jakoby, W. B. *J. Biol. Chem.* **1974**, *249*, 7130-7139.
- (106) Haimeur, A.; Conseil, G.; Deeley, R. G.; Cole, S. P. *Curr. Drug Metab.* **2004**, *5*, 21-53.
- (107) Hall RK; Yamasaki T; Kucera T; Waltner-Law M; O'Brien R; Granner DK *J. Biol. Chem.* **2000**, *275*, 30169-30175.
- (108) Hansen LL; Ikeda Y; Olsen GS; Busch AK; Mosthaf L *J. Biol. Chem.* **1999**, *274*, 25078-25084.
- (109) Hayes, J. D.; Flanagan, J. U.; Jowsey, I. R. *Annu. Rev. Pharmacol. Toxicol.* **2005**, *45*, 51-88.

- (110) Hayes, J. D.; Pulford, D. J. *Crit. Rev. Biochem. Mol. Biol.* **1995**, *30*, 445-600.
- (111) Hayes, J. D.; Strange, R. C. *Free Radic. Res.* **1995**, *22*, 193-207.
- (112) Hazlehurst, L. A.; Foley, N. E.; Gleason-Guzman, M. C.; Hacker, M. P.; Cress, A. E.; Greenberger, L. W.; De Jong, M. C.; Dalton, W. S. *Cancer Res.* **1999**, *59*, 1021-1028.
- (113) Hedro JA; Moncada VY; Taylor SI *J. Clin. Invest.* **1985**, *76*, 2355-2361.
- (114) Heistad DD *Arterioscler. Thromb. Vasc. Biol.* **2006**, *26*, 689-695.
- (115) Henry DO; Moskalenko SA; Kaur KJ; Fu M; Pestell RG; Camonis JH; White MA *Mol. Cell. Biol.* **2000**, *20*, 8084-8092.
- (116) Higgins, C. F. *Res. Microbiol.* **2001**, *152*, 205-210.
- (117) Higgins, C. F.; Linton, K. J. *Nat. Struct. Mol. Biol.* **2004**, *11*, 918-926.
- (118) Higgins, C. F.; Linton, K. J. *Science* **2001**, *293*, 1782-1784.
- (119) Hinchman, C. A.; Ballatori, N. *J. Toxicol. Environ. Health* **1994**, *41*, 387-409.
- (120) Holland, I. B.; Blight, M. A. *J. Mol. Biol.* **1999**, *293*, 381-399.
- (121) Honjo, Y.; Hrycyna, C. A.; Yan, Q. W.; Medina-Perez, W. Y.; Robey, R. W.; van de Laar, A.; Litman, T.; Dean, M.; Bates, S. E. *Cancer Res.* **2001**, *61*, 6635-6639.
- (122) Hotamisligil GS *Int. J. Obes. Relat. Metab. Disord.* **2003**, *27 Suppl 3*, S53-5.
- (123) Hu, X.; Plomp, A.; Gorgels, T.; Brink, J. T.; Loves, W.; Mannens, M.; de Jong, P. T.; Bergen, A. A. *Genet. Test.* **2004**, *8*, 292-300.
- (124) Hu, Y.; Mivechi, N. F. *J. Biol. Chem.* **2003**, *278*, 17299-17306.
- (125) Huffman, K. E.; Corey, D. R. *Biochemistry* **2005**, *44*, 2253-2261.
- (126) Igarashi T; Tomihari N; Ohmori S; Ueno K; Kitagawa H; Satoh T *Biochem. Int.* **1986**, *13*, 641-648.
- (127) Ikeda, M.; Ishida, O.; Hinoi, T.; Kishida, S.; Kikuchi, A. *J. Biol. Chem.* **1998**, *273*, 814-821.



- (128) Inoguchi T; Sonta T; Tsubouchi H; Etoh T; Kakimoto M; Sonoda N; Sato N; Sekiguchi N; Kobayashi K; Sumimoto H; Utsumi H; Nawata H. *J. Biol. Chem* **2003**; 14, 227-32.
- (129) Ishikawa, T. *Trends Biochem. Sci.* **1992**, 17, 463-468.
- (130) Ito T; Noguchi Y; Satoh S; Hayashi H; Inayama Y; Kitamura H *Mod. Pathol.* **1998**, 11, 437-443.
- (131) Ito, K.; Olsen, S. L.; Qiu, W.; Deeley, R. G.; Cole, S. P. *J. Biol. Chem.* **2001**, 276, 15616-15624.
- (132) Izquierdo, M. A.; van der Zee, A. G.; Vermorken, J. B.; van der Valk, P.; Belien, J. A.; Giaccone, G.; Scheffer, G. L.; Flens, M. J.; Pinedo, H. M.; Kenemans, P. *J. Natl. Cancer Inst.* **1995**, 87, 1230-1237.
- (133) Izzotti A; Bagnis A; Sacca SC *Mutat. Res.* **2006**, 612, 105-114.
- (134) Jedlitschky, G.; Leier, I.; Buchholz, U.; Barnouin, K.; Kurz, G.; Keppler, D. *Cancer Res.* **1996**, 56, 988-994.
- (135) Jedlitschky, G.; Leier, I.; Buchholz, U.; Center, M.; Keppler, D. *Cancer Res.* **1994**, 54, 4833-4836.
- (136) Juliano, R. L.; Ling, V. *Biochim. Biophys. Acta* **1976**, 455, 152-162.
- (137) Jullien-Flores, V.; Dorseuil, O.; Romero, F.; Letourneur, F.; Saragosti, S.; Berger, R.; Tavitian, A.; Gacon, G.; Camonis, J. H. *J. Biol. Chem.* **1995**, 270, 22473-22477.
- (138) Jullien-Flores, V.; Mahe, Y.; Mirey, G.; Leprince, C.; Meunier-Bisceuil, B.; Sorkin, A.; Camonis, J. H. *J. Cell. Sci.* **2000**, 113 ( Pt 16), 2837-2844.
- (139) Kahn CR; Goldstein BJ *Science* **1989**, 245, 13.
- (140) Kariya K; Koyama S; Nakashima S; Oshiro T; Morinaka K; Kikuchi A *J. Biol. Chem.* **2000**, 275, 18399-18406.
- (141) Katz A; Nambi SS; Mather K; Baron AD; Follmann DA; Sullivan G; Quon MJ *J. Clin. Endocrinol. Metab.* **2000**, 85, 2402-2410.

- (142) Kedersha, N. L.; Hill, D. F.; Kronquist, K. E.; Rome, L. H. *J. Cell Biol.* **1986**, *103*, 287-297.
- (143) Kedersha, N. L.; Miquel, M. C.; Bittner, D.; Rome, L. H. *J. Cell Biol.* **1990**, *110*, 895-901.
- (144) Kerb, R.; Hoffmeyer, S.; Brinkmann, U. *Pharmacogenomics* **2001**, *2*, 51-64.
- (145) Khan MN; Baquiran G; Brule C; Burgess J; Foster B; Bergeron JJ; Posner BI *J. Biol. Chem.* **1989**, *264*, 12931-12940.
- (146) Kickhoefer, V. A.; Vasu, S. K.; Rome, L. H. *Trends Cell Biol.* **1996**, *6*, 174-178.
- (147) Kido Y; Nakae J; Accili D *J. Clin. Endocrinol. Metab.* **2001**, *86*, 972-979.
- (148) King MJ; Sale GJ *Biochem. J.* **1990**, *266*, 251-259.
- (149) Kipp, H.; Arias, I. M. *Annu. Rev. Physiol.* **2002**, *64*, 595-608.
- (150) Klucken, J.; Buchler, C.; Orso, E.; Kaminski, W. E.; Porsch-Ozcurumez, M.; Liebisch, G.; Kapinsky, M.; Diederich, W.; Drobnik, W.; Dean, M.; Allikmets, R.; Schmitz, G. *Proc. Natl. Acad. Sci. U. S. A.* **2000**, *97*, 817-822.
- (151) Koike, K.; Oleschuk, C. J.; Haimeur, A.; Olsen, S. L.; Deeley, R. G.; Cole, S. P. *J. Biol. Chem.* **2002**, *277*, 49495-49503.
- (152) Kong, L. B.; Siva, A. C.; Rome, L. H.; Stewart, P. L. *Structure* **1999**, *7*, 371-379.
- (153) Kops GJ; Burgering BM *J. Mol. Med.* **1999**, *77*, 656-665.
- (154) Kops GJ; Dansen TB; Polderman PE; Saarloos I; Wirtz KW; Coffey PJ; Huang TT; Bos JL; Medema RH; Burgering BM *Nature* **2002**, *419*, 316-321.
- (155) Kops GJ; de Ruyter ND; De Vries-Smits AM; Powell DR; Bos JL; Burgering BM *Nature* **1999**, *398*, 630-634.
- (156) Koshiba S; Kigawa T; Iwahara J; Kikuchi A; Yokoyama S *FEBS Lett.* **1999**, *442*, 138-142.
- (157) Kozma, R.; Ahmed, S.; Best, A.; Lim, L. *Mol. Cell. Biol.* **1995**, *15*, 1942-1952.
- (158) Krishna, D. R.; Klotz, U. *Clin. Pharmacokinet.* **1994**, *26*, 144-160.

- (159) Krishnamurthy, P.; Schuetz, J. D. *Annu. Rev. Pharmacol. Toxicol.* **2006**, *46*, 381-410.
- (160) Kruh, G. D.; Gaughan, K. T.; Godwin, A.; Chan, A. *J. Natl. Cancer Inst.* **1995**, *87*, 1256-1258.
- (161) Kuwano, M.; Toh, S.; Uchiumi, T.; Takano, H.; Kohno, K.; Wada, M. *Anticancer Drug Des.* **1999**, *14*, 123-131.
- (162) LaBelle, E. F.; Singh, S. V.; Ahmad, H.; Wronski, L.; Srivastava, S. K.; Awasthi, Y. C. *FEBS Lett.* **1988**, *228*, 53-56.
- (163) Langheim, S.; Yu, L.; von Bergmann, K.; Lutjohann, D.; Xu, F.; Hobbs, H. H.; Cohen, J. C. *J. Lipid Res.* **2005**, *46*, 1732-1738.
- (164) Lebreton, S.; Boissel, L.; Iouzalén, N.; Moreau, J. *Mech. Dev.* **2004**, *121*, 1481-1494.
- (165) Lechner, A.; Leech, C. A.; Abraham, E. J.; Nolan, A. L.; Habener, J. F. *Biochem. Biophys. Res. Commun.* **2002**, *293*, 670-674.
- (166) Legro RS; Finegood D; Dunaif A. *Biochem. Biophys. Res. Commun.* **1998**; *83*, 2694-2698.
- (167) Leier, I.; Jedlitschky, G.; Buchholz, U.; Center, M.; Cole, S. P.; Deeley, R. G.; Keppler, D. *Biochem. J.* **1996**, *314 ( Pt 2)*, 433-437.
- (168) Lemaigre FP; Rousseau GG. *Toxicology* **1994**; *303*, 1-14.
- (169) Leslie, E. M.; Deeley, R. G.; Cole, S. P. *Toxicology* **2001**, *167*, 3-23.
- (170) Lin K; Dorman JB; Rodan A; Kenyon C *Science* **1997**, *278*, 1319-1322.
- (171) List, A. F.; Spier, C. S.; Grogan, T. M.; Johnson, C.; Roe, D. J.; Greer, J. P.; Wolff, S. N.; Broxterman, H. J.; Scheffer, G. L.; Scheper, R. J.; Dalton, W. S. *Blood* **1996**, *87*, 2464-2469.
- (172) Loe, D. W.; Deeley, R. G.; Cole, S. P. *Cancer Res.* **1998**, *58*, 5130-5136.
- (173) Loo, T. W.; Clarke, D. M. *J. Biol. Chem.* **2001**, *276*, 36877-36880.
- (174) Lugo, M. R.; Sharom, F. J. *Biochemistry* **2005**, *44*, 643-655.

- (175) Luo JQ; Liu X; Frankel P; Rotunda T; Ramos M; Flom J; Jiang H; Feig LA; Morris AJ; Kahn RA; Foster DA *Proc. Natl. Acad. Sci. U. S. A.* **1998**, *95*, 3632-3637.
- (176) Machida, I.; Wakusawa, S.; Sanae, F.; Hayashi, H.; Kusakabe, A.; Ninomiya, H.; Yano, M.; Yoshioka, K. *J. Gastroenterol.* **2005**, *40*, 366-370.
- (177) Maddux BA; See W; Lawrence JC Jr; Goldfine AL; Goldfine ID; Evans JL *Diabetes* **2001**, *50*, 404-410.
- (178) Maechler P; Jornot L; Wollheim CB *J. Biol. Chem.* **1999**, *274*, 27905-27913.
- (179) Maliepaard, M.; van Gastelen, M. A.; de Jong, L. A.; Pluim, D.; van Waardenburg, R. C.; Ruevekamp-Helmers, M. C.; Floot, B. G.; Schellens, J. H. *Cancer Res.* **1999**, *59*, 4559-4563.
- (180) Mao, Q.; Unadkat, J. D. *AAPS J.* **2005**, *7*, E118-33.
- (181) Marcus F; Rittenhouse J; Gontero B; Harrsch PB *Arch. Biol. Med. Exp. (Santiago)* **1987**, *20*, 371-378.
- (182) Marfella R; Giugliano D; Cozzolino D; Di Maro G; Giunta R; Rossi F *Diabetes Care* **1994**, *17*, 161-162.
- (183) Marik PE; Raghavan M *Intensive Care Med.* **2004**, *30*, 748-756.
- (184) Martin, C. M.; Meeson, A. P.; Robertson, S. M.; Hawke, T. J.; Richardson, J. A.; Bates, S.; Goetsch, S. C.; Gallardo, T. D.; Garry, D. J. *Dev. Biol.* **2004**, *265*, 262-275.
- (185) Matsuura T; Chinen Y; Arashiro R; Katsuren K; Tamura T; Hyakuna N; Ohta T *Mol. Genet. Metab.* **2002**, *76*, 207-210.
- (186) Matsuzaki, T.; Hanai, S.; Kishi, H.; Liu, Z.; Bao, Y.; Kikuchi, A.; Tsuchida, K.; Sugino, H. *J. Biol. Chem.* **2002**, *277*, 19008-19018.
- (187) Matthews DR; Hosker JP; Rudenski AS; Naylor BA; Treacher DF; Turner RC *Diabetologia* **1985**, *28*, 412-419.
- (188) Mayor S; Riezman H *Nat. Rev. Mol. Cell Biol.* **2004**, *5*, 110-120.

- (189) McAuley KA; Williams SM; Mann JJ; Walker RJ; Lewis-Barned NJ; Temple LA; Duncan AW *Diabetes Care* **2001**, *24*, 460-464.
- (190) McClain DA; Olefsky JM *Diabetes* **1988**, *37*, 806-815.
- (191) McGinniss, M. J.; Chen, C.; Redman, J. B.; Buller, A.; Quan, F.; Peng, M.; Giusti, R.; Hantash, F. M.; Huang, D.; Sun, W.; Strom, C. M. *Hum. Genet.* **2005**, *118*, 331-338.
- (192) McIlwain, C. C.; Townsend, D. M.; Tew, K. D. *Oncogene* **2006**, *25*, 1639-1648.
- (193) Medina RA; Owen GI *Biol. Res.* **2002**, *35*, 9-26.
- (194) Mellman I *Annu. Rev. Cell Dev. Biol.* **1996**, *12*, 575-625.
- (195) Mirey G; Balakireva M; L'Hoste S; Rosse C; Voegelings S; Camonis J *Mol. Cell. Biol.* **2003**, *23*, 1112-1124.
- (196) Miyake, K.; Mickley, L.; Litman, T.; Zhan, Z.; Robey, R.; Cristensen, B.; Brangi, M.; Greenberger, L.; Dean, M.; Fojo, T.; Bates, S. E. *Cancer Res.* **1999**, *59*, 8-13.
- (197) Moncada VY; Hedro JA; Serrano-Rios M; Taylor SI *Diabetes* **1986**, *35*, 802-807.
- (198) Monzillo LU; Hamdy O *Nutr. Rev.* **2003**, *61*, 397-412.
- (199) Mooney RA; Kulas DT; Bleyer LA; Novak JS *Biochem. Biophys. Res. Commun.* **1997**, *235*, 709-712.
- (200) Mor-Cohen, R.; Zivelin, A.; Rosenberg, N.; Shani, M.; Muallem, S.; Seligsohn, U. *J. Biol. Chem.* **2001**, *276*, 36923-36930.
- (201) Morinaka K; Koyama S; Nakashima S; Hinoi T; Okawa K; Iwamatsu A; Kikuchi A *Oncogene* **1999**, *18*, 5915-5922.
- (202) Muller, M.; Meijer, C.; Zaman, G. J.; Borst, P.; Scheper, R. J.; Mulder, N. H.; de Vries, E. G.; Jansen, P. L. *Proc. Natl. Acad. Sci. U. S. A.* **1994**, *91*, 13033-13037.
- (203) Nakae J; Accili D *J. Pediatr. Endocrinol. Metab.* **1999**, *12 Suppl 3*, 721-731.
- (204) Nakae J; Kitamura T; Ogawa W; Kasuga M; Accili D *Biochemistry* **2001**, *40*, 11768-11776.
- (205) Nakae J; Kitamura T; Silver DL; Accili D *J. Clin. Invest.* **2001**, *108*, 1359-1367.

- (206) Nakashima, S.; Morinaka, K.; Koyama, S.; Ikeda, M.; Kishida, M.; Okawa, K.; Iwamatsu, A.; Kishida, S.; Kikuchi, A. *EMBO J.* **1999**, *18*, 3629-3642.
- (207) Nakatomi, K.; Yoshikawa, M.; Oka, M.; Ikegami, Y.; Hayasaka, S.; Sano, K.; Shiozawa, K.; Kawabata, S.; Soda, H.; Ishikawa, T.; Tanabe, S.; Kohno, S. *Biochem. Biophys. Res. Commun.* **2001**, *288*, 827-832.
- (208) Nemoto S; Finkel T *Science* **2002**, *295*, 2450-2452.
- (209) Nies, A. T.; Jedlitschky, G.; Konig, J.; Herold-Mende, C.; Steiner, H. H.; Schmitt, H. P.; Keppler, D. *Neuroscience* **2004**, *129*, 349-360.
- (210) Ogg, S.; Paradis, S.; Gottlieb, S.; Patterson, G. I.; Lee, L.; Tissenbaum, H. A.; Ruvkun, G. *Nature* **1997**, *389*, 994-99.
- (211) Ohta, Y.; Suzuki, N.; Nakamura, S.; Hartwig, J. H.; Stossel, T. P. *Proc. Natl. Acad. Sci. U. S. A.* **1999**, *96*, 2122-2128.
- (212) Oosterhoff JK; Penninkhof F; Brinkmann AO; Anton Grootegoed J; Blok LJ *Oncogene* **2003**, *12*, 2920-2925.
- (213) Opie LH; Newsholme EA *Biochem. J.* **1967**, *103*, 391-399.
- (214) Oshiro T; Koyama S; Sugiyama S; Kondo A; Onodera Y; Asahara T; Sabe H; Kikuchi A *J. Biol. Chem.* **2002**, *277*, 38618-38626.
- (215) Paolisso G; Giugliano D *Diabetologia* **1996**, *39*, 357-363.
- (216) Park, S. H.; Weinberg, R. A. *Oncogene* **1995**, *11*, 2349-2355.
- (217) Parton RG *Curr. Opin. Cell Biol.* **1996**, *8*, 542-548.
- (218) Pastan IH; Willingham MC *Annu. Rev. Physiol.* **1981**, *43*, 239-250.
- (219) Paz K; Hemi R; LeRoith D; Karasik A; Elhanany E; Kanety H; Zick Y *J. Biol. Chem.* **1997**, *272*, 29911-29918.
- (220) Penninkhof F; Grootegoed JA; Blok LJ *Oncogene* **2004**, *23*, 5607-5615.
- (221) Pessin JE; Saltiel AR *J. Clin. Invest.* **2000**, *106*, 165-169.
- (222) Pessler D; Rudich A; Bashan N *Diabetologia* **2001**, *44*, 2156-2164.

- (223) Petersen DD; Magnuson MA; Granner DK *Mol. Cell. Biol.* **1988**, 8, 96-104.
- (224) Pleban, K.; Kopp, S.; Csaszar, E.; Peer, M.; Hrebicek, T.; Rizzi, A.; Ecker, G. F.; Chiba, P. *Mol. Pharmacol.* **2005**, 67, 365-374.
- (225) Puri V; Watanabe R; Singh RD; Dominguez M; Brown JC; Wheatley CL; Marks DL; Pagano RE *J. Cell Biol.* **2001**, 154, 535-547.
- (226) Qiu RG; Abo A; McCormick F; Symons M *Mol. Cell. Biol.* **1997**, 17, 3449-3458.
- (227) Quaroni A; Paul EC *J. Cell. Sci.* **1999**, 112 ( Pt 5), 707-718.
- (228) Quinn PG; Yeagley D *Curr. Drug Targets Immune Endocr Metabol. Disord.* **2005**, 5, 423-437.
- (229) Quon MJ *J. Clin. Endocrinol. Metab.* **2001**, 86, 4615-4617.
- (230) Ren, X. Q.; Furukawa, T.; Aoki, S.; Sumizawa, T.; Haraguchi, M.; Che, X. F.; Kobayashi, M.; Akiyama, S. *Br. J. Pharmacol.* **2003**, 138, 1553-1561.
- (231) Rena G; Woods YL; Prescott AR; Pegg M; Unterman TG; Williams MR; Cohen P *EMBO J.* **2002**, 21, 2263-2271.
- (232) Renes, J.; de Vries, E. G.; Jansen, P. L.; Muller, M. *Drug Resist Updat* **2000**, 3, 289-302.
- (233) Renes, J.; de Vries, E. G.; Nienhuis, E. F.; Jansen, P. L.; Muller, M. *Br. J. Pharmacol.* **1999**, 126, 681-688.
- (234) Reuther GW; Der CJ *Curr. Opin. Cell Biol.* **2000**, 12, 157-165.
- (235) Rosen P; Nawroth PP; King G; Moller W; Tritschler HJ; Packer L *Diabetes Metab. Res. Rev.* **2001**, 17, 189-212.
- (236) Rosse, C.; L'Hoste, S.; Offner, N.; Picard, A.; Camonis, J. *J. Biol. Chem.* **2003**, 278, 30597-30604.
- (237) Roth T.F.; Porter K.R. *J. Cell Biol.* **1964**, 20, 313-332.
- (238) Rothberg JM; Artavanis-Tsakonas S *J. Mol. Biol.* **1992**, 227, 367-370.
- (239) Rothberg KG; Heuser JE; Donzell WC; Ying YS; Glenney JR; Anderson RG *Cell* **1992**, 68, 673-682.

- (240) Rudich A; Tirosh A; Potashnik R; Hemi R; Kanety H; Bashan N *Diabetes* **1998**, *47*, 1562-1569.
- (241) Ruef J; Rao GN; Li F; Bode C; Patterson C; Bhatnagar A; Runge MS *Circulation* **1998**, *97*, 1071-1078.
- (242) Sabharanjak S; Sharma P; Parton RG; Mayor S *Dev. Cell.* **2002**, *2*, 411-423.
- (243) Sakai K; Matsumoto K; Nishikawa T; Suefuji M; Nakamaru K; Hirashima Y; Kawashima J; Shirotani T; Ichinose K; Brownlee M; Araki E *Biochem. Biophys. Res. Commun.* **2003**, *300*, 216-222.
- (244) Salcini AE; Confalonieri S; Doria M; Santolini E; Tassi E; Minenkova O; Cesareni G; Pelicci PG; Di Fiore PP *Genes Dev.* **1997**, *11*, 2239-2249.
- (245) Salcini AE; Hilliard MA; Croce A; Arbucci S; Luzzi P; Tacchetti C; Daniell L; De Camilli P; Pelicci PG; Di Fiore PP; Bazzicalupo P *Nat. Cell Biol.* **2001**, *3*, 755-760.
- (246) Sargiacomo M; Scherer PE; Tang Z; Kubler E; Song KS; Sanders MC; Lisanti MP *Proc. Natl. Acad. Sci. U. S. A.* **1995**, *92*, 9407-9411.
- (247) Sauna, Z. E.; Ambudkar, S. V. *J. Biol. Chem.* **2001**, *276*, 11653-11661.
- (248) Sauna, Z. E.; Peng, X. H.; Nandigama, K.; Tekle, S.; Ambudkar, S. V. *Mol. Pharmacol.* **2004**, *65*, 675-684.
- (249) Saxena, M.; Singhal, S. S.; Awasthi, S.; Singh, S. V.; Labelle, E. F.; Zimniak, P.; Awasthi, Y. C. *Arch. Biochem. Biophys.* **1992**, *298*, 231-237.
- (250) Schadendorf, D.; Makki, A.; Stahr, C.; van Dyck, A.; Wanner, R.; Scheffer, G. L.; Flens, M. J.; Scheper, R.; Henz, B. M. *Am. J. Pathol.* **1995**, *147*, 1545-1552.
- (251) Scheffer, G. L.; Wijngaard, P. L.; Flens, M. J.; Izquierdo, M. A.; Slovak, M. L.; Pinedo, H. M.; Meijer, C. J.; Clevers, H. C.; Scheper, R. J. *Nat. Med.* **1995**, *1*, 578-582.
- (252) Scheper, R. J.; Broxterman, H. J.; Scheffer, G. L.; Kaaijk, P.; Dalton, W. S.; van Heijningen, T. H.; van Kalken, C. K.; Slovak, M. L.; de Vries, E. G.; van der Valk, P. *Cancer Res.* **1993**, *53*, 1475-1479.



- (253) Scherer PE; Lewis RY; Volonte D; Engelman JA; Galbiati F; Couet J; Kohtz DS; van Donselaar E; Peters P; Lisanti MP *J. Biol. Chem.* **1997**, *272*, 29337-29346.
- (254) Schinkel, A. H.; Wagenaar, E.; van Deemter, L.; Mol, C. A.; Borst, P. *J. Clin. Invest.* **1995**, *96*, 1698-1705.
- (255) Schmoll D; Walker KS; Alessi DR; Grempler R; Burchell A; Guo S; Walther R; Unterman TG *J. Biol. Chem.* **2000**, *275*, 36324-36333.
- (256) Schulz, V.; Hendig, D.; Schillinger, M.; Exner, M.; Domanovits, H.; Raith, M.; Szliska, C.; Kleesiek, K.; Gotting, C. *J. Vasc. Res.* **2005**, *42*, 424-432.
- (257) Schulz, V.; Hendig, D.; Szliska, C.; Gotting, C.; Kleesiek, K. *Hum. Biol.* **2005**, *77*, 367-384.
- (258) Seddon M; Looi YH; Shah AM *Heart* **2006**.
- (259) Sharma, R.; Awasthi, Y. C.; Yang, Y.; Sharma, A.; Singhal, S. S.; Awasthi, S. *Curr. Cancer. Drug Targets* **2003**, *3*, 89-107.
- (260) Sharma, R.; Gupta, S.; Ahmad, H.; Ansari, G. A.; Awasthi, Y. C. *Toxicol. Appl. Pharmacol.* **1990**, *104*, 421-428.
- (261) Sharma, R.; Gupta, S.; Singh, S. V.; Medh, R. D.; Ahmad, H.; LaBelle, E. F.; Awasthi, Y. C. *Biochem. Biophys. Res. Commun.* **1990**, *171*, 155-161.
- (262) Sharma, R.; Singhal, S. S.; Cheng, J.; Yang, Y.; Sharma, A.; Zimniak, P.; Awasthi, S.; Awasthi, Y. C. *Arch. Biochem. Biophys.* **2001**, *391*, 171-179.
- (263) Sharma, R.; Singhal, S. S.; Wickramarachchi, D.; Awasthi, Y. C.; Awasthi, S. *Int. J. Cancer* **2004**, *112*, 934-942.
- (264) Shimamoto, Y.; Sumizawa, T.; Haraguchi, M.; Gotanda, T.; Jueng, H. C.; Furukawa, T.; Sakata, R.; Akiyama, S. *Oncol. Rep.* **2006**, *15*, 645-652.
- (265) Shimano, K.; Satake, M.; Okaya, A.; Kitanaka, J.; Kitanaka, N.; Takemura, M.; Sakagami, M.; Terada, N.; Tsujimura, T. *Am. J. Pathol.* **2003**, *163*, 3-9.
- (266) Sigismund S; Woelk T; Puri C; Maspero E; Tacchetti C; Transidico P; Di Fiore PP; Polo S *Proc. Natl. Acad. Sci. U. S. A.* **2005**, *102*, 2760-2765.
- (267) Singhal, S. S.; Awasthi, Y. C.; Awasthi, S. *Cancer Res.* **2006**, *66*, 2354-2360.

- (268) Singhal, S. S.; Saxena, M.; Ahmad, H.; Awasthi, Y. C. *Biochim. Biophys. Acta* **1992**, *1116*, 137-146.
- (269) Singhal, S. S.; Sharma, R.; Gupta, S.; Ahmad, H.; Zimniak, P.; Radomska, A.; Lester, R.; Awasthi, Y. C. *FEBS Lett.* **1991**, *281*, 255-257.
- (270) Singhal, S. S.; Singhal, J.; Sharma, R.; Singh, S. V.; Zimniak, P.; Awasthi, Y. C.; Awasthi, S. *Int. J. Oncol.* **2003**, *22*, 365-375.
- (271) Singhal, S. S.; Yadav, S.; Singhal, J.; Zajac, E.; Awasthi, Y. C.; Awasthi, S. *Biochem. Pharmacol.* **2005**, *70*, 481-488.
- (272) Situ, D.; Haimeur, A.; Conseil, G.; Sparks, K. E.; Zhang, D.; Deeley, R. G.; Cole, S. P. J. *Biol. Chem.* **2004**, *279*, 38871-38880.
- (273) Sorkin A; Waters CM *Bioessays* **1993**, *15*, 375-382.
- (274) Steiner E; Holzmann K; Elbling L; Micksche M; Berger W In *Cellular functions of vaults and their involvement in multidrug resistance*. 2006; Vol. 7, pp 923-934.
- (275) Stewart PM *Lancet* **1999**, *353*, 1341-1347.
- (276) Stuckler, D.; Singhal, J.; Singhal, S. S.; Yadav, S.; Awasthi, Y. C.; Awasthi, S. *Cancer Res.* **2005**, *65*, 991-998.
- (277) Sugiyama S; Kishida S; Chayama K; Koyama S; Kikuchi A *J. Biochem. (Tokyo)* **2005**, *137*, 355-364.
- (278) Sutherland C; O'Brien RM; Granner DK *J. Biol. Chem.* **1995**, *270*, 15501-15506.
- (279) Szakacs, G.; Annereau, J. P.; Lababidi, S.; Shankavaram, U.; Arciello, A.; Bussey, K. J.; Reinhold, W.; Guo, Y.; Kruh, G. D.; Reimers, M.; Weinstein, J. N.; Gottesman, M. M. *Cancer. Cell.* **2004**, *6*, 129-137.
- (280) Takaishi H; Konishi H; Matsuzaki H; Ono Y; Shirai Y; Saito N; Kitamura T; Ogawa W; Kasuga M; Kikkawa U; Nishizuka Y *Proc. Natl. Acad. Sci. U. S. A.* **1999**, *96*, 11836-11841.
- (281) Taketa K.; Pogell B.M. *J. Biol. Chem.* **1965**, *240*, 651-662.
- (282) Talior I; Yarkoni M; Bashan N; Eldar-Finkelman H *Am. J. Physiol. Endocrinol. Metab.* **2003**, *285*, E295-302.

- (283) Tamaki, T.; Akatsuka, A.; Ando, K.; Nakamura, Y.; Matsuzawa, H.; Hotta, T.; Roy, R. R.; Edgerton, V. R. *J. Cell Biol.* **2002**, *157*, 571-577.
- (284) Tang ED; Nunez G; Barr FG; Guan KL *J. Biol. Chem.* **1999**, *274*, 16741-16746.
- (285) Taylor SI; Kadowaki T; Kadowaki H; Accili D; Cama A; McKeon C *Diabetes Care* **1990**, *13*, 257-279.
- (286) Tesfamariam B; Cohen RA *Am. J. Physiol.* **1992**, *262*, H1915-9.
- (287) Tesfamariam B; Cohen RA *Am. J. Physiol.* **1992**, *263*, H321-6.
- (288) Thiebaut, F.; Tsuruo, T.; Hamada, H.; Gottesman, M. M.; Pastan, I.; Willingham, M. C. *Proc. Natl. Acad. Sci. U. S. A.* **1987**, *84*, 7735-7738.
- (289) Tian X; Rusanescu G; Hou W; Schaffhausen B; Feig LA *EMBO J.* **2002**, *21*, 1327-1338.
- (290) Tiedge M; Lortz S; Drinkgern J; Lenzen S *Diabetes* **1997**, *46*, 1733-1742.
- (291) Ting HH; Timimi FK; Boles KS; Creager SJ; Ganz P; Creager MA *J. Clin. Invest.* **1996**, *97*, 22-28.
- (292) Tirosh A; Potashnik R; Bashan N; Rudich A *J. Biol. Chem.* **1999**, *274*, 10595-10602.
- (293) Tkachenko E; Lutgens E; Stan RV; Simons M *J. Cell. Sci.* **2004**, *117*, 3189-3199.
- (294) Towbin, H.; Staehelin, T.; Gordon, J. *Proc. Natl. Acad. Sci. U. S. A.* **1979**, *76*, 4350-4354.
- (295) Tran Y; Benbatoul K; Gorse K; Rempel S; Futreal A; Green M; Newsham I *Oncogene* **1998**, *17*, 3499-3505.
- (296) Urano T; Emkey R; Feig LA *EMBO J.* **1996**, *15*, 810-816.
- (297) Valko M; Rhodes CJ; Moncol J; Izakovic M; Mazur M *Chem. Biol. Interact.* **2006**, *160*, 1-40.
- (298) van Zon, A.; Mossink, M. H.; Scheper, R. J.; Sonneveld, P.; Wiemer, E. A. *Cell Mol. Life Sci.* **2003**, *60*, 1828-1837.

- (299) van Zon, A.; Mossink, M. H.; Schoester, M.; Houtsmuller, A. B.; Scheffer, G. L.; Scheper, R. J.; Sonneveld, P.; Wiemer, E. A. *J. Cell. Sci.* **2003**, *116*, 4391-4400.
- (300) van Zon, A.; Mossink, M. H.; Schoester, M.; Scheper, R. J.; Sonneveld, P.; Wiemer, E. A. *Cancer Res.* **2004**, *64*, 4887-4892.
- (301) Vinson JA *Pathophysiology* **2006**, *13*, 151-162.
- (302) Williams R. Tecwyn In *Detoxication Mechanisms*; J.Wiley & Sons, New York, N.Y. (1959),; .
- (303) Wolthuis, R. M.; Zwartkruis, F.; Moen, T. C.; Bos, J. L. *Curr. Biol.* **1998**, *8*, 471-474.
- (304) Wong WT; Schumacher C; Salcini AE; Romano A; Castagnino P; Pelicci PG; Di Fiore P *Proc. Natl. Acad. Sci. U. S. A.* **1995**, *92*, 9530-9534.
- (305) Yadav, S.; Singhal, S. S.; Singhal, J.; Wickramarachchi, D.; Knutson, E.; Albrecht, T. B.; Awasthi, Y. C.; Awasthi, S. *Biochemistry* **2004**, *43*, 16243-16253.
- (306) Yadav, S.; Zajac, E.; Singhal, S. S.; Singhal, J.; Drake, K.; Awasthi, Y. C.; Awasthi, S. *Biochem. Biophys. Res. Commun.* **2005**, *328*, 1003-1009.
- (307) Yan, Z.; Caldwell, G. W. *Curr. Top. Med. Chem.* **2001**, *1*, 403-425.
- (308) Yang Y; Sharma A; Sharma R; Patrick B; Singhal SS; Zimniak P; Awasthi S; Awasthi YC *J. Biol. Chem.* **2003**, *278*, 41380-41388.
- (309) Yang, C. H.; Schneider, E.; Kuo, M. L.; Volk, E. L.; Rocchi, E.; Chen, Y. C. *Biochem. Pharmacol.* **2000**, *60*, 831-837.
- (310) Yasuda, S.; Narumiya, S. *Methods Enzymol.* **2006**, *406*, 656-665.
- (311) Yoshikawa, M.; Ikegami, Y.; Hayasaka, S.; Ishii, K.; Ito, A.; Sano, K.; Suzuki, T.; Togawa, T.; Yoshida, H.; Soda, H.; Oka, M.; Kohno, S.; Sawada, S.; Ishikawa, T.; Tanabe, S. *Int. J. Cancer* **2004**, *110*, 921-927.
- (312) Younes M; Brown RW; Stephenson M; Gondo M; Cagle PT *Cancer* **1997**, *80*, 1046-1051.

- (313) Younes M; Lechago J; Chakraborty S; Ostrowski M; Bridges M; Meriano F; Solcher D; Barroso A; Whitman D; Schwartz J; Johnson C; Schmulen AC; Verm R; Balsaver A; Carlson N; Ertant A *Scand. J. Gastroenterol.* **2000**, *35*, 131-137.
- (314) Yu, L.; Hammer, R. E.; Li-Hawkins, J.; Von Bergmann, K.; Lutjohann, D.; Cohen, J. C.; Hobbs, H. H. *Proc. Natl. Acad. Sci. U. S. A.* **2002**, *99*, 16237-16242.
- (315) Yu, L.; Li-Hawkins, J.; Hammer, R. E.; Berge, K. E.; Horton, J. D.; Cohen, J. C.; Hobbs, H. H. *J. Clin. Invest.* **2002**, *110*, 671-680.
- (316) Yung LM; Leung FP; Yao X; Chen ZY; Huang Y *Cardiovasc. Hematol. Disord. Drug Targets* **2006**, *6*, 1-19.
- (317) Zhang W; Patil S; Chauhan B; Guo S; Powell DR; Le J; Klotsas A; Matika R; Xiao X; Franks R; Heidenreich KA; Sajan MP; Farese RV; Stolz DB; Tso P; Koo SH; Montminy M; Unterman TG *J. Biol. Chem.* **2006**, *281*, 10105-10117.
- (318) Zhang, D. W.; Cole, S. P.; Deeley, R. G. *J. Biol. Chem.* **2002**, *277*, 20934-20941.
- (319) Zhou, S.; Schuetz, J. D.; Bunting, K. D.; Colapietro, A. M.; Sampath, J.; Morris, J. J.; Lagutina, I.; Grosveld, G. C.; Osawa, M.; Nakauchi, H.; Sorrentino, B. P. *Nat. Med.* **2001**, *7*, 1028-1034.
- (320) Zorad S; Jezova D; Szabova L; Macho L; Tybitanclova K *Gen. Physiol. Biophys.* **2003**, *22*, 557-560.

## BIOGRAPHICAL INFORMATION

Ewa Zajac was born in Poland on December 25<sup>th</sup> 1974, and obtained her Master Degree in polymer chemistry from the Department of Chemistry at the University of Technology in Krakow in 1998. As a graduate student, she worked under supervision of Dr. Sanjay Awasthi on new functions of RLIP76. She obtained her Ph.D in fall 2006.